Engineering Library
NOV 19 1929

UNITED STATES DEPARTMENT OF COMMERCE

BUREAU OF STANDARDS JOURNAL OF RESEARCH

Vol. 3 NOVEMBER, 1929 No. 5

CONTENTS

RP. No.	TITLE AND AUTHOR	Page
112.	Optica heterogeneity of a fused quartz disk. L. W. Tilton and A. Q. Tool	619
113.	Data on ultra-violet solar radiation and the solarization of window materials. W. W. Coblentz and R. Stair	629
114.	Progress report on investigation of fire-clay bricks and the clays used in their preparation. R. A. Heindl and W. L. Pendergast	691
115.	The first spectrum of xenon. William F. Meggers, T. L. deBruin, and C. J. Humphreys	731
116.	The arc spectrum of arsenic. William F. Meggers and T. L. deBruin	765
117.	Metallographic polishing. I. Automatic metallographic polishing machine. S. Epstein and John P. Buckley	783
118.	Correcting engine tests for humidity. Donald B. Brooks	795
119.	Analysis of diaphragm system for the X-ray standard ionization chamber. Lauriston S. Taylor	807

BUREAU OF STANDARDS JOURNAL OF RESEARCH

CONTENTS OF RECENT NUMBERS

June, 1929 (Vol. 2, No. 6)

RP67. Experimental production of roofing felts. Merle B. Shaw, George W. Bicking, and O. G. Strieter. Price 5 cents.

RP68. Bearing bronzes with and without zinc. H. J. French and E. M. Staples. Price 15 cents.

RP69. Critical study of methods of measuring the bulk of paper. F. T. Carson. Price 10 cents.

RP70. Some observations of short-period radio fading. T. Parkinson. Price 5 cents.

RP71. Determination of the source and the means of prevention of stones in glass. Herbert Insley. Price 5 cents.

RP72. The spotting of plated or finished metals. W. P. Barrows. Price 10 cents.

RP73. The arc spectrum of chlorine and its structure. C. C. Kiess and T. L. deBruin. Price 5 cents.

RP74. Potential differences across the boundaries between solutions of mixed univalent chlorides. Edgar Reynolds Smith. Price 5 cents.

RP75. The accurate determination of the gasoline content of natural gas and the analytical separation of natural gases by isothermal fractional distillation. Martin Shepherd. Price 15 cents.

RP76. Relation of radio wave propagation to disturbances in terrestrial magnetism. Ivy Jane Wymore. Price 5 cents.

July, 1929 (Vol. 3, No. 1)

RP77. A course-shift indicator for the double-modulation type radiobeacon. H. Diamond and F. W. Dunmore.

RP78. Relative visibility of luminous flashes from neon lamps and from incandescent lamps with and without red filters. F. Chapin Breckenridge and J. E. Nolan.

RP79. A crystalline difructose anhydride from hydrolyzed inulin. Richard F. Jackson and Sylvia M. Goergen.

RP80. Fastness of dyed fabrics to dry cleaning. A. S. Eichlin.

RP81. Note on a mercury spark gap for instantaneous photography. L. F. Curtiss.

RP82. Improvements in the preparation of aldonic acids. C. S. Hudson and H. S. Isbell.

RP83. Note on the ratio of the electromagnetic to the electrostatic unit of electricity as compared to the velocity of light. Harvey L. Curtis.

RP84. Bunsen flames of unusual structure. Francis A. Smith and S. F. Pickering.

RP85. A study of sheathing papers. F. T. Carson and F. V. Worthington.

Research papers are available as separates for purchase from the Superintendent of Documents United States Government Printing Office, Washington, D. C.

[Continued on page 3 of cover]

UNITED STATES DEPARTMENT OF COMMERCE
R. P. LAMONT, Secretary
BUREAU OF STANDARDS
GEORGE K. BURGESS, Director

BUREAU OF STANDARDS JOURNAL OF RESEARCH

November, 1929
Vol. 3, No. 5

UNITED STATES
GOVERNMENT PRINTING OFFICE
WASHINGTON : 1929

For sale by the Superintendent of Documents, Washington, D.C. - - Price $2.75 Per Year on Subscription

For a partial list of previous research papers appearing in Volumes 2 and 3, BUREAU OF STANDARDS JOURNAL OF RESEARCH, see pages 2 and 3 of the cover

OPTICAL HETEROGENEITY OF A FUSED QUARTZ DISK

By L. W. Tilton and A. Q. Tool

ABSTRACT

In preparing a refractive index standard of fused quartz, having the form of a 60° prism, it was considered advisable to investigate carefully the optical density of this glass since appreciable variations might be present because of nonuniform heat treatment or other factors. With this in view the standard, together with nine small auxiliary prisms, was cut from a disk 52 mm in diameter and 13 mm thick. The indices of these prisms were measured, for five different wave lengths, to an accuracy of a few units in the sixth decimal place. As a result, the standard is adjudged uniform within the limits of $\pm 4 \times 10^{-6}$ in its index of refraction. The optical heterogeneity distribution found within the whole disk is in accord with the hypothesis that the variations are caused mainly by temperature gradients which exist during the annealing or which change during the cooling procedures.

CONTENTS

	Page
I. Relative variations in certain properties of fused and crystalline quartz	619
II. Requirements for prismatic standards of refractive index	622
III. Preparation of an index standard and the auxiliary prisms	623
IV. The index data and their interpretation	624

I. RELATIVE VARIATIONS IN CERTAIN PROPERTIES OF FUSED AND CRYSTALLINE QUARTZ

Quantitative data showing that the refractivity and certain other properties of optical glass are affected by the character of the annealing have been obtained by Tool and others.[1] Although no such definite information concerning fused quartz (or quartz glass) appears to be available, both Dorsey[2] and Merritt[3] have observed a difference between the thermal dilations of quenched and annealed samples. Merritt has also reported that in a specimen of fused quartz a change in size occurred when it was held at a constant temperature slightly above 1,020° C. From these results it may be inferred that differences occurring in the rates of cooling which are employed for this material

[1] A. Q. Tool and E. E. Hill, Trans. Soc. Glass Tech., **9**, pp. 185-207; 1925. A. Q. Tool, L. W. Tilton, and E. E. Hill, Meeting Opt. Soc. Am., Ithaca, N. Y.; 1925 (abstract in J. Opt. Soc. Am. and Rev. Sci. Inst., **13**, pp. 490-491; 1926). Fritz Eckert, Trans. Soc. Glass Tech., **9**, pp. 267-272; 1925; Zeitschr. f. Tech Phys., **7**, pp. 282-287; 1926. A. A. Lebedeff, Revue d'Optique, **5**, pp. 1-30; 1926; Die Glas Industrie, **35**, pp. 6-9; 1927.

[2] H. G. Dorsey, Phys. Rev. **30**, pp. 271-272; 1910.

[3] G. E. Merritt, J. Am. Ceram. Soc., **7**, pp. 803-808; 1924. See also R. B. Sosman, The Properties of Silica, pp. 408-411 (New York); 1927.

may also produce appreciable changes in the optical density. Furthermore, if the cooling is sufficiently rapid it may cause this property to vary within a single piece of the glass. If the properties of transparent fused quartz are affected by cooling rates to an appreciable degree, wider variations in such properties should be found among samples of the glass than among the crystals from which it is made. Concerning density this relative magnitude of their variations certainly obtains, for according to figures given by Sosman,[4] who has critically examined the numerous published data, the definitely established variations in density for various samples of this glass having optical quality are approximately ten times as large as the corresponding variations for specimens of crystalline quartz.

Additional evidence of the same nature is afforded by an inspection of the measurements of refractive indices. In this case, Sosman[5] concludes from the published data that the variations in the refractive index of clear crystalline quartz of optical grade are certainly as large as 2 and possibly amount to 10 units in the fifth decimal place. In fused quartz of optical quality there is, on the other hand, some indication that such interspecimen variations may reach 300×10^{-5}. The latter figure, however, is subject to question. It depends on several measurements, but only three or four of them appear of sufficiently high accuracy to yield convincing results and these show a much smaller total variation. For the purpose of a further critical comparison, some of these values are given in Table 1, together with results both for the disk, which is the chief subject of discussion in this paper, and for another sample previously measured. This restricted list of values shows a difference in index of approximately 20×10^{-5} when either one of the latter two samples is compared with the fused quartz used by Trommsdorff or with that measured by Gifford. This spread is considerably larger than that hitherto found among precisely measured samples, and it brings the interspecimen variation for fused quartz to a value which, as in the case of density determinations, is ten or more times as great as that reliably established for crystals of quartz.

[4] R. B. Sosman, The Properties of Silica, p. 305 (New York); 1927.
[5] R. B. Sosman, The Properties of Silica, p. 616 (New York); 1927.

TABLE 1.—*Variations in index and dispersion of fused quartz glass*

Observer	Conditions of measurement	Measured values			Computed values $t=20.0°$ C., air at 20° C		
		n_D	$(n_F-n_C)\times10^5$	ν	n_D $\lambda=5893$	$(n_F-n_C)\times10^5$	ν
H. Trommsdorff	$\lambda=5890$ A, $t=15°$ C. (?)	1.45843	677	67.71	1.45847	677	67.7
Dr. Riedel	?	1.45848	677	67.8	----------	----------	----------
J. W. Gifford and W. A. Shenstone.	$\lambda=5893$ A, $t=15°$ C.						
	I. Simple prism	1.458477	675.0	67.92	1.458526	675.3	67.90
	II. Compound prism	1.458483	----------	----------	1.458532	----------	----------
L. W. Tilton and A. Q. Tool (Table 2 of this paper).	$\lambda=5893$ A, $t=25.0°$C (Corrections to 760 mm. pressure).	1.458808	675.9	67.88	1.458759	675.6	67.90
L. W. Tilton (unpublished data previously obtained on entirely different sample).	$\lambda=5893$ A (Corrections to 760 mm. pressure).						
	I. Min. dev. method. $t=25.0°$ C.	1.458765	----------	----------	1.458716	----------	----------
	II. Wollaston method $t=29.6°$ C.	1.458815	----------	----------	1.458720	----------	----------

NOTE.—These variations in the optical density of different samples of fused quartz glass are approximately ten times as large as the corresponding variations which are known to exist among different samples of crystalline quartz from which such glass is made. This is regarded as an indication that fused quartz may be optically sensitive to heat treatment. The Trommsdorff measurements (Inaug. Diss. (Jena); 1901. Or, see Physikal. Zeitschr., **2**, pp. 576–578; 1901) were made on a sample from a Jena melt. The temperature mentioned here for his data is that given by Landolt-Börnstein (Physikalisch-Chemische Tabellen (5), Suppl. **1**, p. 485 (Berlin); 1927). Riedel also worked on a Jena melt of quartz glass (see M. Herschkowitsch, Zeitschr. Physikal. Chem., **46**, pp. 408–414; 1903). Gifford and Shenstone (Proc. Royal Soc., London, **73**, pp. 201–208; 1904), however, measured prisms which were made by melting together many fine rods of "vitreous silica." Of the two samples measured at this bureau, at least one was produced by the General Electric Co., Lynn, Mass. The temperature coefficients of relative index which were used in obtaining all of the computed values of this table are those which have been determined for the standard prism (No. 54 of Table 2), viz, +9.7, +9.9, and $+10.3\times10^{-6}$ per 1° C., for the C, D, and F lines, respectively. Direct measurements at 20.0° C. yielded for the last sample listed in this table an index of 1.458715, a value in excellent agreement with the computed result of 1.458716. To the check measurements on this sample by the Wollaston method, no irradiation corrections have yet been applied. (See J. Guild and A. Barbara Dale, Trans. Opt. Soc., London, **22**, p. 151; 1920–21. Or Nat. Phys. Laboratory, Collected Researches, **17**, p. 23; 1922.)

The facts cited above show that in any investigation of the degree of optical homogeneity of quartz glass, it is pertinent to remember the possibility that heterogeneities may be introduced by nonuniform heat treatments of the material during its production, and more especially in the period during which it is in the annealing range. They also indicate that when seeking an especially uniform optical component of this glass it may be advisable to consider the possibility of improving the uniformity of the medium by annealing it under such conditions that temperature gradients may be made as small as required. While this method of treatment has been successfully used for an optical glass,[6] it is realized, in suggesting its extension to fused quartz glass, that great caution will be necessary in the choice of annealing temperatures and periods, and also cooling rates, because of the latter material's tendency to devitrify and, in some cases, to develop discolored regions or filmlike imperfections.

[6] L. W. Tilton, A. N. Finn, and A. Q. Tool, B. S. Sci. Papers, **22** (No. 572), pp. 719–736; 1928.

II. REQUIREMENTS FOR PRISMATIC STANDARDS OF REFRACTIVE INDEX

The refractivity measurements herein reported were made in connection with the preparation of a sample of fused quartz as a refractive index standard for testing refractometers. It is customary for such purposes to prepare standard test pieces having the form of plates or slabs with dimensions approximating 4 by 12 by 25 mm. One face and one end of such a plate are so polished that the face is optically plane and that the end intersects it at an angle of 90°, forming an unbroken edge.

The indices of such plates may be determined on a calibrated refractometer, but their form is not favorable for the use of other methods by which more accurate determinations may be readily made. Accordingly, to permit accurate index measurements by the minimum-deviation method, index standards have in a number of instances been prepared in the form of 60° prisms with their refracting edges so modified[7] (see fig. 1) that one face of such a prism may be applied to the blocks (prisms) of refractometers for testing and calibrating these instruments.

For a test piece of this sort it is preferable, and at times necessary, to attain an accuracy of a few units in the sixth decimal place of the index measurements leading to standardization. This provides only a small factor of safety because with a Pulfrich refractometer a calibration accurate to the fifth place[8] may under certain conditions be required, and even instruments of the Abbe type are sometimes made so that fifth decimal place index readings may be obtained by estimating tenths of a scale division. In determining the effective indices of such test prisms to the requisite degree of accuracy it is obvious that a lack of optical homogeneity may be a serious matter, since only a very thin layer near the contact surface is employed when the piece is used in testing a refractometer whereas approximately its entire volume is involved when the indices are determined spectrometrically.

Current opinion concerning the optical homogeneity within samples of fused quartz is, moreover, not reassuring. It is well known that many specimens show very irregular and peculiar patterns[9] when they are examined either in polarized light or by the "method of striæ" (Foucault Töpler knife-edge test); hence, it is generally considered

[7] Test specimens of this form were originally employed in the refractometric laboratory of this bureau by G. E. Merritt.

[8] J. Guild, Proc. Phys. Soc. London, **30**, pp. 157–189; 1918. Or see Nat. Phys. Laboratory, Collected Researches, **14**, pp. 273–300; 1920.

[9] In some cases these patterns indicate a coarse reticulated structure which is probably similar to that observed by Petit (Carnegie Institution of Washington, Yearbook No. 27, p. 147; 1927–28). It is along the interfaces forming this structure that many of the above noted discolored regions develop during certain heat treatments of this material.

that quartz glass is unsuitable for making high-grade optical components. Quite aside from the question of the presence of a very fine grained structure[10] which is somewhat inimical to best definition but of little or no consequence in the instance under discussion, there is the important possibility of the existence of a grosser type of heterogeneity. In this connection it may also be noted that Buisson[11] has presented evidence that quartz itself, when examined over distances of 5 cm within the limits of a single sample, may vary in index by 5 to 8 units of the sixth decimal place, and is therefore not a homogeneous body with perfectly defined properties.

In view of these facts and considering also that relatively small chemical or physicochemical differences may produce optical heterogeneity affecting the fifth decimal place of index, it seemed quite unwise, in making a test prism of fused quartz, to neglect possible nonuniformities and to rely entirely on the assumption that minimum deviation measurements of index are characteristic of a thin layer at the prism's testing surface. Consequently, in preparing the index standard now to be described it was decided to subject the surrounding portions of the material to a rigorous test of its optical uniformity.

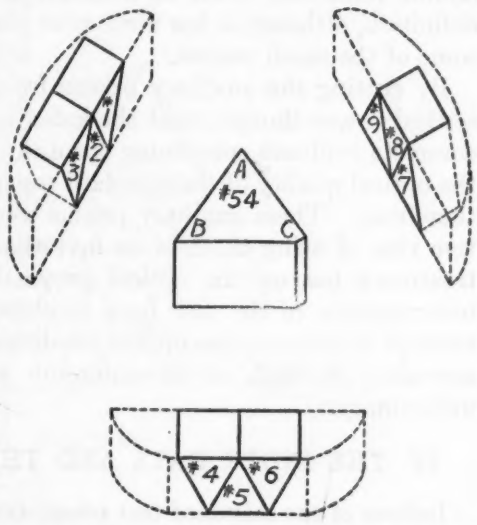

FIGURE 1.—*Relative locations of 60° prisms in disk*

A standard test prism was cut from the center of a disk 52 mm in diameter and 13 mm thick. Nine auxiliary prisms were used in testing the homogeneity of the remaining portions of the disk.

III. PREPARATION OF AN INDEX STANDARD AND THE AUXILIARY PRISMS

The standard test prism was cut from the center of a 13 mm thick disk sawed from a cylinder 52 mm in diameter. From each of the three peripheral segments of the disk, three auxiliary prisms were cut, as shown in Figure 1. Each group of three prisms thus consists of that portion of the material which had been adjacent to one of the faces of the test prism. To the prisms were assigned numbers, and

[10] Lord Rayleigh, Proc. Opt. Convention, pt. 1, pp. 41–46; 1926. L. C. Martin and B. K. Johnson, J. Sci. Inst., 5, p. 338; 1928.

[11] H. Buisson, Compt. Rend., 142, pp. 881–883; 1906.

their outlines and relative positions were indicated on the disk and also recorded on diagrams before any saw cuts were made. The refracting faces of the resulting standard test prism are 12 by 25 and those of the auxiliary prisms 10 by 13 mm, the smaller dimension being in all cases the height. These surfaces,[12] with one or two exceptions, were plane to approximately one-tenth wave length and they formed refracting angles of approximately 60°.

When finished, very few seeds or bubbles were observed, but some double refraction could be detected in these prisms. All gave fair definition, although a few striæ were observed in the standard and in some of the small prisms.

By cutting the auxiliary prisms from the disk in the manner described it was thought that the index measurements would give such complete evidence concerning the disk's degree of heterogeneity that the optical quality of the standard test prism might be safely inferred therefrom. These auxiliary prisms were made, also, with the tentative idea of using them in an investigation of the effect which heat treatment has on the optical properties of fused silica. Had the heterogeneity of the disk been so objectionable as to necessitate an attempt to improve the optical condition of the standard by carefully annealing it, such an investigation would have been a required preliminary.

IV. THE INDEX DATA AND THEIR INTERPRETATION

Indices of the standard test prism were measured for the C, F, and G′ lines of hydrogen and for a mean of the D lines of sodium [13] because it is customary to calibrate Pulfrich refractometers for these wave lengths. For added information on the dispersion of a medium in the range of short visible wave lengths, it is often desirable to use the mercury lines, $\lambda = 4358$ and $\lambda = 4047$ A, and since the conditions and purposes controlling this investigation make it desirable to employ a fairly large number of observations, all of the above lines were included for measuring all prisms, except that the relatively faint G′ line was used only in making measurements on the standard.

The measurements of the indices were made on a spectrometer, by use of the minimum deviation method, while the prisms were immersed in a stirred air bath inclosed in a constant temperature prism housing held at 25.0° C. Corrections were made so that the results correspond to a standard air pressure of 760 mm of mercury and to zero millimeters of absolute humidity. The measurements, of prism angles in particular, were carried out with all the precautions

[12] The prisms were made by E. L. Robinson, of the optical glass shop.

[13] Although a refractometer determination with sodium light is somewhat indefinite and subject to a relatively large personal error unless there is resolution of these lines (see footnote 8, p. 622), it seems in practice that such settings are usually made in the absence of resolution and correspond to some wave length intermediate between D_1 and D_2.

which experience has shown to be consistent with probable errors of a few units in the sixth decimal place of index.[14] In the case of deviation measurements it should be noted that accidental errors made in determining individual indices have little effect in the final analysis of the results because the comparisons between prisms are based on their indices for five wave lengths. It is believed that the combined effect of all errors, whether systematic or accidental, does

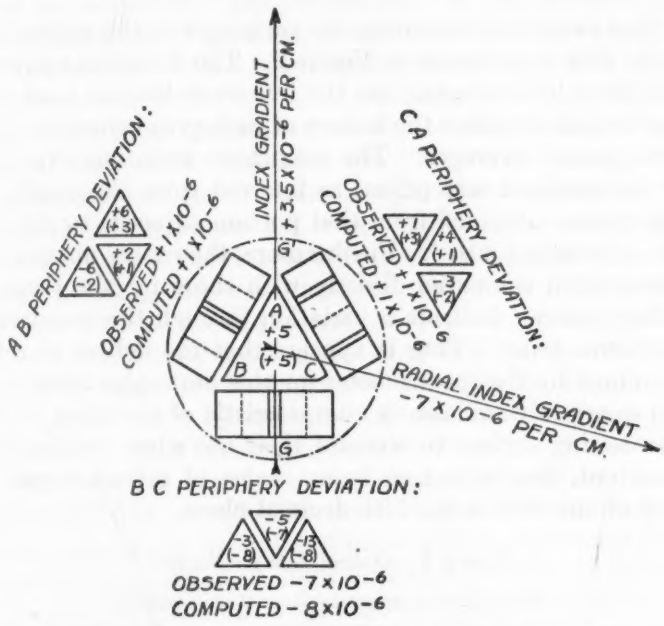

FIGURE 2.—*Observed and computed deviations in index*

The auxiliary prisms are shown in horizontal and also in vertical projection. The values are given in units of the sixth decimal place of index of refraction, and are averages for the five wave lengths which were used. The computed deviations, given in parentheses, are based on the average measured indices, the relative positions of the prisms, and the assumption that uniform index gradients exist as shown by the arrows.

not enter into any index deviation recorded in Figure 2 to an extent greater than $\pm 3 \times 10^{-6}$.

The results of all observations are included in Table 2; that is, none of the data was rejected. Furthermore, no smoothing of values was attempted, although in some instances it may for certain other purposes be advisable. In the few cases where extra observations were made, these determinations were given only equal weight with those which had preceded. The results for the auxiliary prisms, given separately for each wave length, are averages, each of which represents one of the three peripheral groups corresponding to the

[14] For a discussion of some of the goniometrical requirements in index measurements to this degree of accuracy, see L. W. Tilton, B. S. Jour. Research, 2 (RP64), pp. 909–930; 1929.

three faces of the test prism. This averaging was done because the small size of these prisms made it impossible to reach in any other manner the high degree of precision desired for each wave length unless measurements were repeated to a burdensome extent. The general averages used in determining the individual deviations were obtained by giving equal weights to the measured values of the indices of the central prism and to those of each group of three auxiliary prisms.

The final evidence concerning the variations in the optical density within the disk is presented in Figure 2. The deviations shown there were obtained by averaging, for the five wave lengths used throughout, the deviations which the indices of each prism show as compared with the general averages. The maximum variation over the face CA of the standard test prism, as inferred from the results on the auxiliary prisms obtained from that portion adjacent to this surface, is of the order of $\pm 4 \times 10^{-6}$. Furthermore, the results obtained on the test prism when compared directly with those for the three groups of auxiliary prisms, indicate a variation through the standard which is of the same order. Thus it appears that the indices of refraction as determined by the spectrometer for this particular standard prism of fused quartz are sufficiently characteristic of the layer of material near the testing surface to warrant their use when calibrating, with this standard, the refractive index scales of refractometers to an accuracy of one unit in the fifth decimal place.

TABLE 2.—*Optical data for the disk*

(25.0° C., 760 mm air pressure, 0 mm absolute humidity)

Prism No. and disk location	Indices of refraction					Dispersion	
	n_C λ=6563 A	n_D λ=5893 A	n_F λ=4861 A	n_g λ=4358 A	n_Δ λ=4047 A	$(n_F - n_C) \times 10^6$	$\frac{1}{2}(n_g + n_\Delta) \times 10^6$ minus $\frac{1}{2}(n_C + n_F) \times 10^6$
54 center	1.456778	1.458816	1.463534	1.467105	1.470030	6,756	10,770
1, 2, 3, AB periphery	1.456772	1.458811	1.463533	1.467102	1.470026	6,761	10,773
4, 5, 6, BC periphery	1.456764	1.458800	1.463524	1.467094	1.470020	6,760	10,773
7, 8, 9, CA periphery	1.456773	1.458807	1.463533	1.467102	1.470028	6,760	10,773
General average	1.456772	1.458808	1.463531	1.467101	1.470026	6,759	10,773

NOTE.—The indices tabulated under n_D correspond to settings made on the unresolved sodium doublet. The standard test prism, No. 54, was also measured for the G' line λ=4340 A, with a resulting index of 1.467254. Note that the center of the disk has not only a higher index, but also a lower dispersion than the peripheral portions.

The data give no evidence of a variation in index in a direction parallel to the axis of the disk. Prisms numbered 1, 3, 4, 6, and 8 were cut from a level slightly higher (see fig. 1) than that of prisms numbered 2, 5, 7, and 9, but the general average excess index of the second of these groups is only 1×10^{-6}. Furthermore, separate

measurements were made on the upper and lower halves [15] of the central prism and the resulting index difference between them was only 1×10^{-6}, the larger value corresponding this time to the upper half of the disk.

There is, however, in a plane perpendicular to the axis of the disk, evidence of a slight optical density gradient in the general direction of the dotted arrow, GG', shown in Figure 2, and the average change in index is $+3.5\times10^{-6}$ per centimeter. If, in addition, an outwardly directed radial gradient of -7×10^{-6} per centimeter is considered as superposed, then it is found that the experimentally determined deviations for individual prisms agree, within the limits of $\pm5\times10^{-6}$, with those computed from the average index on the simple assumption that these uniform gradients existed. Such limits are nearly in accord with the estimated errors, whereas from the observed deviations shown in Figure 2 it is not apparent at a glance that the results of the index measurements can have such precision. Neglecting other possible causes of nonuniformities in the material, an explanation of these index gradients is that they occur because the central and the exterior portions of the cylinder were cooled through the annealing range at different rates and likewise because the sides G and G' were cooled differently. In other words, the assumption that the index of fused quartz varies with different heat treatments is thus confirmed by the fact that, in this disk, the distribution of the heterogeneity is in accord with predictions which could have been made from the known behavior of other glasses, including those containing large proportions of silica. Even after this analysis of the data, however, the conclusion that the test prism is uniform in index to $\pm4\times10^{-6}$ seems to require little or no revision.

As shown in Table 2, there is, also, in addition to these index changes, a slight but probably not fortuitous difference between the partial dispersions of the central portion, as represented by the large prism, and the dispersions of the peripheral regions of the disk. Although the central prism has the higher index, its dispersion is lower. This result has not been accepted without careful review of the data. An association of index and dispersion changes in opposite senses in a given glass is a phenomenon which the authors have observed to a more pronounced degree when investigating other glasses and one which they have in some cases definitely connected with character of heat treatment.

Concerning heterogeneities localized in minute volumes, no conclusive evidence was obtained in this investigation, and it is not known whether in the case of these prisms the slight observed scattering of light was caused by fine structure or by the observed striæ.

[15] The lower half contained no definitely discernible striæ, gave somewhat better definition than the upper half, and appeared noticeably better when examined by the Foucault-Töppler knife-edge test.

Obviously, from the results on this single disk, no definite statements should be made regarding the probable uniformity of other pieces of fused quartz. This specimen was, however, a random sample, not one carefully selected, and it does not appear markedly different under the knife-edge test from some of several other samples which have been examined. Therefore, in addition to yielding the desired particular information, this study as a whole indicates that it is possible at present to obtain fused quartz of optical quality which, at least in so far as the grosser type of heterogeneity is concerned, is sufficiently uniform for use in the production of small optical components of a good grade provided the light path does not greatly exceed a centimeter.[16]

Large components for systems requiring the best definition are desirable, however, not only for certain special purposes, such as replacing the less durable fluor crown glass employed in certain objectives,[17] but also for more general use as a substitute for crystalline quartz, particularly in photography of portions of the ultra-violet region. Under present conditions such components can only be used when a certain amount of scattered light and birefringence can be tolerated.

Although it seems unnecessary to anneal the test prism whose optical condition has been studied, it is quite possible that much larger variations in index are present in other, and especially in larger pieces of this material. Consequently, attention is directed to the desirability of thoroughly studying the problems of fusing and carefully annealing optical quartz glass. Certain difficulties would undoubtedly be encountered but such an investigation should yield valuable information if, as shown to be probable, the properties of this material are, in fact, dependent to some extent on variations in its heat treatment.

WASHINGTON, May, 1929.

---

[16] For this distance it seems that a one-fourth wave length phase difference would not be introduced by heterogeneities of less than ±0.000007 in index. (L. W. Tilton, A. N. Finn, and A. Q. Tool, B. S. Sci. Papers, 23 (No. 572), p. 720; 1928.)

[17] D. R. P. No. 242.170, Mar. 21, 1910; Brevet français No. 476.882, Mar. 4, 1911, Carl Zeiss.

DATA ON ULTRA-VIOLET SOLAR RADIATION AND THE SOLARIZATION OF WINDOW MATERIALS

By W. W. Coblentz and R. Stair

ABSTRACT

In this paper the following topics are discussed:

1. The variation of ultra-violet solar radiation, available for therapeutic purposes, as dependent upon the time of the day, the season of the year, the altitude and geographic latitude of the station, the pollution of the atmosphere by smoke, etc.

By four methods of attack, data are presented on the amount of ultra-violet solar radiation, used in the treatment of rickets, shut out by common window glass. It is shown that on the clearest days, at the noon hour in summer, at sea-level stations, in the latitude of Washington (38° 56′) the amount of ultra-violet solar radiation useful for prevenenting rickets amounts to less than 0.3 per cent of the total incident solar rays, or less than about 0.004 g cal./cm²/min., decreasing to an imperceptible value at unsrise and during cloudy weather.

2. The newly developed window glasses and glass substitutes for transmitting the short wave length ultra-violet solar radiation that is obstructed by common window glass, and their use on different sides (north, south) of a solarium. References are cited showing the futility of using a small window exposed to the north sky for therapeutic purposes.

Data are given showing that, with variation of the angle of incidence of the solar rays from normal upon a solarium, during the year and during the day, the amount transmitted through the glass varies (decreases) by about 20 per cent, as the result of variation in reflection from the surface, and an increase in the optical path of the rays through the glass. This is considered of minor importance in comparison with the question of keeping the glass clean and free from dust, which may reduce the transmission of these rays by 30 to 40 per cent.

Data are given on heavy, double-thickness (one-fourth inch, 6 mm) wired glass showing that the transmission of such material at 302 mμ, after complete solarization, amounts to only 3 to 5 per cent, which is probably too low for therapeutic use. Hence, a glass of single thickness, with a wire mesh under it for safety from breakage, is recommended for solarium roofs.

3. The decrease in transmission of short wave length ultra-violet radiation which occurs in the newly developed glasses and glass substitutes as a result of exposure to the ultra-violet radiation from artificial sources and from the sun.

Data are presented on the decrease in transmission of Corex, Helioglass, Vitaglass, Celoglass, and a number of less commonly known glasses which occurs on exposure to the mercury arc, to the carbon arc with and without a glass chimney, and to the sun at high altitudes and at sea level.

It is shown that these glasses, in thicknesses of 2.3 mm (marketed prior to February 1, 1929) may be divided into six groups, according to their transmissive properties at 302 mμ after solarization: (*a*) Common window glass and Quartzlite having a transmission less than 1 per cent; (*b*) Vitaglass, Sanalux and Renovic, transmission about 25 per cent; (*c*) Holviglass, Sunlit, and Sendlinger's ultra-violet glass, transmission 35 to 40 per cent; (*d*) Helioglass, Uviol-Jena, and Neuglas, transmission 45 to 50 per cent; (*e*) Corex-D glass, transmission 60 to 65 per cent; and (*f*) Corex-G981FF[2] and Quartz glass, 80 to 90 per cent.

CONTENTS

	Page
I. Introduction	631
1. Concerning methods of making the observations	632
II. Some determinations of the ultra-violet solar radiation shut out by common window glass	633
III. Effect of solarization upon the ultra-violet transmission of window glasses	643
1. Methods of photochemical stabilization	646
2. Effect of temperature upon the solarization of window glasses	646
3. Rejuvenation of glasses	647
4. Vitaglass	648
(*a*) Effect of sunlight	648
(*b*) Effect of artificial light	651
(*c*) Infra-red transmission	653
5. Helioglass	656
(*a*) Effect of artificial light	656
(*b*) Effect of sunlight	657
6. Corex-A glass	660
(*a*) Effect of sunlight	660
(*b*) Effect of artificial light	661
7. Corex-G981FF [2]	661
8. Corex-D glass	662
9. Ultra-violet filters	663
10. Quartz glass	663
11. Locke glass	663
12. Quartzlite glass	664
13. Window glass and bottle glass	665
14. Holviglass	666
15. Sunlit	666
16. Neuglas	666
17. Uviol-Jena	667
18. Ultra-violet glass	667
19. Miscellaneous new glasses	667
20. Discussion of results on solarization	668
IV. Effect of solarization upon the ultra-violet transmission of substitutes for window glass	672
1. Flexoglass	672
2. Celoglass	674
(*a*) Accelerated aging under artificial light	676
(*b*) Exposure to sunlight	677
(*c*) Exposure to weather	677
3. Cellophane	680
4. Pollopas, aldur, gelatin	680
5. Tracing cloth	681
V. Concerning the use of windows	681
VI. Summary	686
VII. References	687

I. INTRODUCTION

It is well known that common window glass shuts out completely the ultra-violet rays in sunlight of wave lengths less than about 310 mμ. Biologists have found that these ultra-violet rays, which are shut out by common window glass, have a special healing value in preventing rickets, whence the name "antirachitic rays." Data will be cited presently showing that, in sunlight, this spectral range of antirachitic activity is only about 5 to 10 mμ in width, and has its maximum activity at about 302 mμ. Hence, in this paper the physical designation "302-region" is used in place of the biological designations "antirachitic rays," "vital rays," etc., used by various writers.

Some years ago special window glasses were put on the market for transmitting the short wave length ultra-violet rays of the solar spectrum, shut out by common window glass. Early in the spring of 1927, reports came to this bureau that these glasses appeared to be losing their transparency as the result of "solarization," which is the designation of the photochemical reaction most of these glasses undergo on exposure to sunlight.

Owing to the importance of this question to the public, an investigation was instituted and a preliminary report issued (1).[1]

Since then several reports have been prepared (2) summarizing the information available on the properties of light sources and window materials used for therapeutic purposes; also the correlation between the biological data and the physical measurements, etc. The reader is referred to these papers for extensive information not given in the present communication, which deals primarily with the decrease in transmission of ultra-violet radiation that occurs in these newly developed window materials as the result of exposure to ultra-violet radiation from artificial sources and from the sun.

At the present time much attention is being given to the development of window materials for transmitting the short wave length ultra-violet rays of the sun, for the purpose of preventing rickets. In fact, the development of new glasses is so rapid that this paper can not claim completeness of discussion of this subject.

On the other hand, because of the variability of sunlight and, hence, the difficulty of standardizing its intensity, attention is being given to the use of artificial sources, especially the carbon arc and the quartz mercury arc lamp. However, since the shortest ultra-violet rays, emitted by these artificial sources of radiation, appear to be unsuitable for the activation of foods (3), etc., it is considered desirable in such cases to cover the arc with a screen which transmits only wave lengths longer than about 290 mμ; that is to say, the wave lengths which occur in sunlight.

[1] Figures in parentheses here and throughout the text indicate references given at the end of this paper.

In view of this situation, the data presented in this paper are to be considered from two viewpoints: (*a*) The applicability of these glasses as window material of high transparency for transmitting the short wave length ultra-violet rays of the solar spectrum, and (*b*) similarly as filters for use with artificial sources to obstruct the ultra-violet rays of wave lengths less than about 290 mμ which are found to be destructive (3) to vitamin D, the active principle that is recognized by biologists as having a beneficial effect in preventing rickets. The information presented will be useful also to those who have purchased special window glasses and desire to know the probable transparency of these glasses after solarization.

1. CONCERNING THE METHODS OF MAKING THE OBSERVATIONS

In the present investigation the methods of determining the spectral transmissions are essentially the same as those used in previous work. The ultra-violet transmissions were determined by means of a quartz spectroradiometer (4) of high light gathering power and a portable vacuum thermopile (5) of bismuth-silver, connected with an ironclad galvanometer (6).

The source of radiation was a quartz mercury arc lamp which has numerous intense emission lines (notably at 280, 297, 302, 313, 334, and 365 mμ) conveniently distributed throughout the ultra-violet. It has but little infra-red and visible radiation to diffuse over the ultra-violet spectrum. The presence of scattered, long wave-length radiation is a serious matter when making transmission measurements amounting to less than 1 per cent in the spectral region of wave lengths less than 302 mμ, an intense emission line in the mercury arc. To eliminate completely the effect of diffuse radiation of long wave lengths a shutter of clear window glass was used when making measurements at wave lengths less than 302 mμ, and a shutter of red glass (Noviol C would be better) for measurements in the spectral region of 313 to 436 mμ.

The infra-red measurements were made with a mirror spectroradiometer and the above-mentioned portable vacuum thermopile.

In the present investigation the transmission of numerous samples of various kinds of window glass was determined throughout the whole ultra-violet spectrum. In the meantime there was a marked increase in the demand for transmission measurements on newly developed window glasses, before and after solarization. The necessity, therefore, arose to simplify the methods of testing the transmissions. In this connection it is of interest to note that biological researches show that the strong emission line at 313 mμ has only a slight (7) or a doubtful (8) value in preventing rickets and that ultra-violet rays of longer wave lengths have no antirachitic effect, while radiation of wave lengths 297 to 302 mμ have a marked

antirachitic potency. Since, as will be noticed presently, in the wintertime the short wave-length limit of solar radiation is about 305 mμ, it appears that the spectral range of ultra-violet solar radiation, useful for therapeutic purposes in preventing rickets, is only about 5 to 10 mμ in width.

From these biological data and from the similarity of the transmissions of all of these new window glasses in the spectral range from 280 to 365 mμ we have concluded that the efficiency of a window glass for transmitting the short wave length ultra-violet solar rays, which have a therapeutic value in preventing rickets, may be determined by confining the measurements to the wave length at 302 mμ. Hence, the recent measurements reported upon in this paper have been made almost entirely on the emission lines at 297 and 302 mμ, and it is intended to make future measurements and specifications solely on the emission lines of mercury at 302 mμ.

There appears to be a tendency among some distributors of these ultra-violet transmitting window glasses to include 320 mμ or even longer wave lengths of the ultra-violet in the spectral range of therapeutic activity. However, the inclusion of ultra-violet of wave lengths 320 mμ or longer leads to an incorrect appraisal as it gives a higher average transmission than seems warranted when it is recognized that the greatest therapeutic activity occurs in the 302-range of wave lengths shut out by common window glass. Furthermore, since different samples of common window glass transmit from 2 to 20 per cent at 320 mμ, there is no special reason for including this wave length in the specification of these ultra-violet transmitting glasses. The real value of these special glasses is owing to their superiority for transmitting the solar rays in the spectral region of 302 mμ. If the rays at 320 mμ (which have a relatively high intensity—five to ten times that at 302 mμ) had a special healing value, there would be no need of using special ultra-violet transmitting glass instead of selecting the least greenish tinted (as viewed edgewise, for example W–2, fig. 2) samples of common window glass, which would serve the purpose just as well, at a considerable saving in cost.

II. SOME DETERMINATIONS OF THE ULTRA-VIOLET SOLAR RADIATION SHUT OUT BY COMMON WINDOW GLASS

Much of the discussion of the need of special window glasses for transmitting the 302-range of wave lengths of ultra-violet solar radiation is based upon the observation that common window glass shuts out these rays, which have the property of preventing rickets (49). Hence, in connection with the present investigation of the optical properties of the newly developed window glasses for transmitting

the 302-range of wave lengths of ultra-violet solar radiation the question arose as to the total amount of these rays, of wave lengths less than about 310 $m\mu$, that is absorbed by common window glass. This information will be useful in obtaining an estimate of the threshold value of ultra-violet radiation that will be effective for therapeutic purposes. It will be useful also in connection with the specification of the unit of dosage in heliotherapy, discussed in a previous paper (9).

It has been suggested that the unit of dosage be called the "Finsen," in honor of the pioneer in ultra-violet light therapy. The energy value of the unit of dosage may be any convenient, arbitrarily assigned number. Hence, if we define the Finsen Unit as having an intensity (radiant flux density) of 0.001 g cal./cm^2/min., whether of ultra-violet or infra-red radiation, then 1 F. U. = 0.001 g cal./cm^2/min.—1 millicalory/cm^2 per minute. The most convenient number in ergs is 1,000 ergs/cm^2 per second.

The problem of the physiologist is to determine how many units are needed for a single dose. The problem of the physicist is to determine the intensity (the radiant flux density) of the so-called vitalizing or biologically active rays in a given source of ultra-violet radiation, whether the sun, or at a standard distance from an artificial source; also to devise instruments and methods for measuring the radiation stimulus to be used in phototherapy.

The use of such a unit will be simple. For example, suppose that the physicist finds that the ultra-violet solar intensity = 4 F. U. and the physiologist finds that 20 F. U. are required to produce an erythema. Then it will require an exposure of ($20 \div 4 =$) 5 minutes in order to produce the desired result.

The problem of accurately determining the amount of ultra-violet solar radiation, in the 302-range of wave lengths, shut out by common window glass, and thus obtaining a measure of the amount involved in therapeutic work, is extremely difficult because the magnitude involved is only a few thousandths of the total incident solar radiation. Hence, owing to atmospheric conditions, it is practically impossible to obtain reliable measurements at sea-level stations except at rare intervals, on perfectly clear days, when for short periods (of 5 to 15 minutes) measurements can be repeated to 0.3 to 0.5 per cent. The average of a large number (20 to 30) of such observations appears to be sufficiently precise to obtain an estimate of the amount of short wave length ultra-violet solar radiation shut out by common window glass.

Our measurements were made with direct sunlight as a source, during the noon hours of especially clear days from April to December, 1927, and early in the year, 1929. On these days we were in telephone communication with I. F. Hand, of the United States Weather Bureau, who gave us the solar radiation intensities, Q at the time of

our observations. On clear days, for air mass $m=1$, the solar intensity at Washington ranges from $Q=1.23$ to 1.4 g cal./cm²/min.

Owing to the great variability in the transparency of common window glasses in the ultra-violet, and to the fact that the decrease in spectral transmission is not sharply defined, the spectral range and the total amount of ultra-violet absorbed varies greatly from sample to sample. Hence, after an examination of a large number of samples, we selected a sample (W–10, fig. 2) which represents about the average that is found in the market. This sample is practically opaque at 310 mμ (tr. = 0.3 per cent at 313 mμ) and transmits about 8 per cent at 320 mμ.

In the present paper the magnitude of the short wave length ultra-violet component of solar radiation which is shut out by common window glass is derived by several methods which will now be discussed.

Method I.—By calculation from the solar spectral energy curve. In this method the intensities (the relative energies) at different wave lengths are multiplied by the corresponding spectral transmission of the window glass and the areas under the two curves are integrated. The main difficulty lies in determining the solar spectral energy distribution, especially in the extreme ultra-violet. The published data are taken from a smooth spectral energy curve, whereas the bolometrically observed spectral energy curve is deeply indented. Furthermore, the few determinations extant of the ultra-violet spectral energy distribution of the sun differ greatly, depending upon the method of observation. For example, the results obtained by Fabry and Buisson (53) by a photographic comparison of the spectrum of the sun with that of the crater of a carbon arc differ greatly from their earlier photographic measurements (54). In turn all of these data differ greatly from the spectrobolometric measurements obtained by Abbot and Fowle, which are much higher at 300 mμ. Hence, for the purpose of the present calculations the most reliable spectrobolometric data of Fabry and Buisson are combined with those of Abbot and Fowle (summarized in the Smithsonian Physical Tables, Fowle, 7th rev. ed.) forming a curve which terminates (10) practically at about 295 mμ, which is in agreement with other observations for sea-level stations. For Washington (practically sea level) the intensities of the solar radiation of wave lengths 295 to 450 mμ is 0.13 g cal., or 10 per cent of the total incident radiation of all wave lengths, for air mass $m=1$. The solar spectral energy curve at Washington for air mass, $m=1$, coincides practically with the energy curve at Mount Wilson for $m=2$.

By multiplying the solar spectral radiation intensities by the spectral transmission of the window glass, at the different wave lengths as already mentioned, it is found that for the purposes of the

present calculation the glass becomes practically opaque to wave lengths at about 320 mμ. The area of the curve extending from 295 to 320 mμ (that is, the ultra-violet component between these two wave lengths) relative to the area from 295 to 450 mμ is 0.012 (1.2 per cent); and since the area between the wave lengths 295 to 450 mμ is 10 per cent of all wave lengths (see preceding paragraph) the ultra-violet component between 295 and 320 mμ is 0.12 per cent (=0.15 per cent if we use only the Smithsonian data) of the total incident solar radiation.

On this same basis, the ultra-violet component between 295 and 310 mμ (which is one-third the area between 295 and 320 mμ) is 0.04 per cent (0.05 per cent if we use only the Smithsonian data) of the total incident solar radiation at sea level, or about 0.0005 g cal./cm ^{2}/min. Pettit (47) has recently calculated a value of about 0.001 g cal./cm ^{2}/min.

Method II.—By direct measurements of wide spectral bands of solar radiation using a spectropyrheliometer (11) in which the total solar radiation of wave lengths extending from 300 to 389 mμ, on the clearest days, was about 2.2 per cent of the total incident radiation (Q=1.35 g cal. on September 25, 1919). The calculated value on the above-described spectral energy curve is 3.0 per cent of the total, which is in good agreement with the observed value of 2.2 per cent.

Using this spectropyrheliometer, the ultra-violet component of solar radiation of wave lengths less than 300 mμ was found to be less than 2 per cent of the radiation between 300 to 389 mμ or less than ($0.022 \times 0.02 =$) 0.00044 of the total incident solar radiation (September 24, 1919, Q=1.31 g cal.). On this basis the ultra-violet of wave lengths of less than 310 mμ would be about three times this value or about 0.0012 (0.12 per cent) of the total incident solar radiation.

Method III.—By isolating the ultra-violet component from the total incident solar radiation (of wave lengths less than 1,400 mμ) by using the standard sample of window glass as a screen. This method was used in measuring the spectral component radiation from stars (12) and from artificial sources (13) of radiation.

This method of observation consisted in exposing a copper-constantan thermocouple (covered with a cell of water 1 cm in thickness, with windows of quartz, to eliminate the infra-red of wave lengths longer than 1,400 mμ) to the sun and noting the decreases in the galvanometer deflections when increasing amounts of the ultra-violet were shut out (*a*) by one sample then (*b*) by two samples of the same kind of glass. The combination of two samples was used in order to obtain a correction factor for the ultra-violet rays of wave lengths longer than about 310 mμ, partly absorbed by this sample of window glass.

For example, when using quartz or Corex-A glass, which have practically no absorption in the ultra-violet of wave lengths longer than 295 mμ, the second sample transmitted 91.8 per cent of the total solar radiation (of wave lengths less than 1,400 mμ which is the long wave-length limit of the water cell) which had passed through the first sample. This is in agreement with the value calculated from reflection data. From similar observations on the sample W–4 (and of W–10, fig. 2) of common window glass which was used as a standard (14), it was found that the second sample transmitted 85.3 to 85.7 per cent (average 85.5 per cent during the season) of the solar radiation that had passed the first sample. The value calculated from the above-mentioned solar spectral energy transmitted through the water cell is 85.4 per cent.

As shown in Figure 2, (W–4) sample No. 4, of common window glass becomes practically opaque at about 310 mμ. Hence, the transmission factor 85.5 per cent may be used to correct for the solar radiation, of wave lengths 310 to 1,400 mμ, absorbed and reflected by the glass screen, and thus obtain the amount of ultra-violet, principally of wave lengths shorter than about 310 mμ, which is absorbed by this glass.

Measurements of this type gave values of ultra-violet solar radiation, shut out by common window glass, ranging from 1.5 per cent (15) of the total incident radiation of all wave lengths in May and June when the air mass was $m=1$, to 0.8 or 0.9 per cent in December when the air mass was $m=2$. Evidently this sample of window glass shut out ultra-violet of longer wave lengths than those having a therapeutic value. For, as just mentioned, ultra-violet radiation of wave lengths 297 to 302 mμ are claimed to be the most potent in preventing rickets; also that during the winter (air mass larger than $m=2$) these wave lengths are almost completely absorbed by the atmosphere. Hence, in the wintertime the amount of ultra-violet, of wave lengths 297 to 302 mμ, shut out by this sample of glass should have been 0 per cent instead of 0.8 to 0.9 per cent of the total incident radiation. From this it appears that the above-mentioned correction for absorption by window glass is probably too low when considered in terms of biological activity and that, in the latitude of Washington (38.9°), during the noon hours of the clearest days in May and June (air-mass $m=1$) the amount of activating radiation in the 302-region of sunlight, shut out by common window glass, is the difference between the values observed in the summer and in the winter. This is of the order of $(1.5-0.9=)$ 0.6 per cent of the total incident solar radiation, or about 0.007 g cal./cm^2/min. This, of course, would represent the upper limit on the clearest days which are few in number. The so-called average value would be much less, say, 0.001 g cal./cm^2/min., and more likely even lower than this value.

While it has recently been shown biologically that, during the winter months in Washington, solar radiation contains some short wave length ultra-violet radiation that is beneficial in preventing rickets, it is evident that, of the above-mentioned 0.9 per cent, the greatest part is of wave lengths at about 313 mμ, which are the least active, and that only a small part of this 0.9 per cent consists of wave lengths at 302 mμ which are the most active in preventing rickets.

This value of 0.9 per cent for an air mass, $m=2$, is substantiated by measurements made in the early forenoon, in summer. Hence, the above value, 0.6 per cent, as obtained by this method, is probably a fair estimate of the amount of the most potent of the activating rays in ultra-violet solar radiation shut out by common window glass.

Method IV.—By isolating the ultra-violet part of the solar spectrum by means of a screen and determining the amount of this shut out by common window glass. For a filter we used a plate of ultra-violet transmitting glass, Corning *G*986*A* which, for a thickness of 3 mm, has a transparent band, *A*, at 250 to 440 mμ with a high transmission (about 85 per cent) of the incident short wave length ultra-violet solar rays at 295 to 350 mμ. Unfortunately it does not completely absorb all of the infra-red rays. (Fig. 10.) However, when used in conjunction with the screen of water (cell 1 cm thickness) the total infra-red solar radiation of wave lengths extending from 600 to 1,400 mμ (band *B*) as determined experimentally by isolating this region with a screen of Schott's (16) red glass (No. 4512) is only about three times that of the ultra-violet band, *A*, at 295 to 440 mμ in summer and about four times this amount in winter.

From two closely agreeing measurements (Apr. 27 and May 2, 1927) it was found that this combination filter consisting of a water cell and a certain sample of Corning glass, *G*986*A*, transmitted 8.37 per cent of the total incident radiation. Of this amount about 30 per cent (or about 2.5 per cent of the total) was located in the ultra-violet band transmitted by this glass screen. This is in good agreement with the calculated value of 2.3 per cent of the total incident radiation in the band *A* (295 to 440 mμ).

From this it will be noticed that this method has a distinct advantage over the preceding method in that the ultra-violet component shut out by window glass is greatly magnified relative to the total radiation measured—amounting to 5 per cent, or more, of the total as compared with 1.5 per cent of the total by the preceding method.

By isolating the infra-red band *B* (λ600 to 1,400 mμ) by temporarily inserting a sample of Schott's red glass, it was found that our standard sample of common window glass transmitted 82 per cent of the incident radiation for air mass $m=2.4$ (January 7 and 8, 1929). This is in as good agreement with the calculated value (80.5 per cent) as can be expected in view of the fact that the latter is

based upon a smooth solar spectral energy curve, whereas the energy distribution in this part of the spectrum is deeply indented by absorption bands of (atmospheric) water vapor.

A further test of the reliability of this method was obtained (on January 7 and 8, 1929) by observing the transmission of our standard sample of window glass for both bands of radiation A and B (tr. = 79.6 per cent) and for the infra-red band B, (tr. = 82 per cent) from which, by taking into consideration that the observed intensity of B is about four times A, it follows that this sample transmitted 70 per cent of the ultra-violet in the band, A, at 295 to 440 mμ. This is in as good agreement with the calculated value (68 to 69.5 per cent) as can be expected in view of the uncertainty of the spectral energy distribution of the sun in the region of 295 to 310 mμ, especially when the altitude of the sun is low, air mass $m = 2.4$.

By making measurements (a) with one piece of our standard of window glass and (b) with two pieces of this window glass interposed (see Method III) it was found that at the noon hour on June 8, 1927 (sky hazy, $Q = 0.9$ g cal.), the amount of short wave length (less than about 310 mμ) ultra-violet rays shut out by common window glass was 3.2 per cent of the radiation transmitted through this filter or ($0.032 \times 0.0837 =$) 0.27 per cent of the total incident solar radiation.

This is in good agreement with the value obtained by calibrating the galvanometer deflection by exposing the thermopile to a standard of radiation and then noting the deflection corresponding to the amount of short wave length ultra-violet solar radiation shut out by our sample of window glass. Since the thermopile intercepted radiation from about 35° of the sky, which contains relatively more of the short wave length ultra-violet rays than direct sunlight, the amount of ultra-violet radiation shut out by common window glass, as determined by Methods III and IV, is slightly higher than would be obtained by not including part of the sky in the solar radiation measurement. In practice, however, the patient would be exposed to the sky as well as the sun, and, since these values are upper limits anyway, it would be illusory to attempt refinements in the measurements.

On two very clear days (June 27 and 29, 1927) the amount of short wave length ultra-violet rays shut out by common window glass was about 6 per cent of the radiation transmitted by the filter, or 0.48 and 0.50 per cent (air mass $m = 1$; intensity $Q = 1.4$ and 1.3 g cal.), respectively, of the total incident solar radiation.

On two clear days in the winter, at the noon hour, when the air mass was $m = 2.4$, the amount of ultra-violet shut out by our sample of common window glass was 0.07 and 0.096 per cent, respectively. (Fig. 1.) It is relevant to cite the following data: January 7, 1929; dust low; fleeting clouds; $Q = 1.14$ g cal.; conditions somewhat below

the average. January 8, 1929; clear cold, $Q = 1.33$ g cal.; March 7, high winds, fewest dust particles for two years; $Q = 1.398$ g cal. at 12 m; atmospheric conditions somewhat above the average for January and March.

It is interesting to note that this screen method is very sensitive to small variations in intensity of the short wave length ultra-violet solar radiation which enabled us to record rapid changes in the transparency of the atmosphere, as for example on March 8, 1929. (Fig. 1.)

Assuming, as in the preceding method, that this sample of window glass shuts out ultra-violet solar radiation of longer wave lengths than are effective for therapeutic purposes, then the difference between the observed summer and winter values represents more nearly

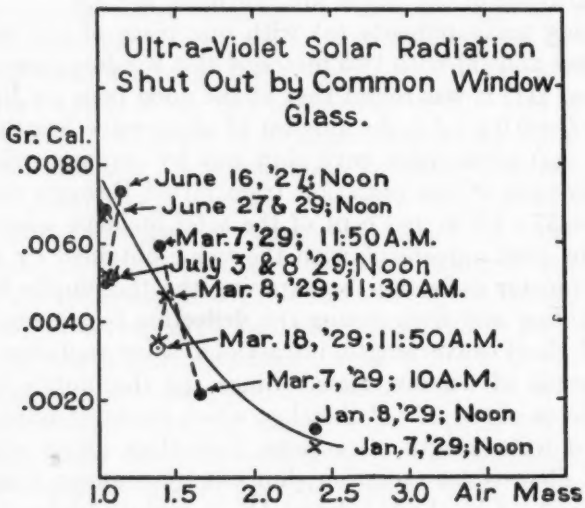

FIGURE 1

the magnitude of the most potent ultra-violet rays available in sunlight at the noon hours on the clearest days in summer. This amounts to about 0.4 per cent of the total incident radiation or about 0.005 g cal./cm ^{2}/min., and is easily reduced to a much smaller value by dust and smoke.

As already mentioned, recent biological tests made by Fleming (51) by exposing rats to the sun in Washington, and by Russell and Massengale (52) by exposing chicks to the sun, in New Brunswick, N. J. (lat. 40.5° N.), show that during the winter months of January, February, and March there is sufficient ultra-violet radiation present in sunlight to produce an antirachitic effect. Hence, at least part of the above-observed values of 0.07 to 0.09 per cent, no doubt, includes ultra-violet wave lengths having an antirachitic action. However, it

does not modify our conclusions, whether or not we deduct this value from our data observed (for air mass $m=1$) in the summer time.

In Method III, the amount of ultra-violet shut out by the window glass was about 1 to 2 per cent of the amount transmitted by the water cell, which transmitted about 75 per cent of the total incident radiation.

In Method IV, the amount of ultra-violet shut out was about 6 per cent of the total measured, which latter, however, was only about 8.4 per cent of the total incident solar radiation. As a result, a higher sensitivity was required and there was a much greater fluctuation in the single readings. Hence, this method was used only on a few days when the sky appeared free from clouds of water vapor (as viewed through Noviweld glasses) and there was no strong wind. However, the disturbances by the wind could be remedied by using a vacuum thermopile. In spite of the greater fluctuation in the individual readings, it is the opinion of the writers that the data obtained by Method IV are the most reliable. Hence, even though it may not be possible to find a means for eliminating the infra-red rays between 600 and 1,400 mμ, this screen method appears promising as an approximate method for isolating the ultra-violet radiation of wave lengths less than 310 mμ. For this purpose two sheets of optical glass[2] (practically free from iron and hence free from the absorption band at 1,000 mμ) should be used instead of the samples of common window glass used in the present investigation, in which the information desired was for another purpose.

It is to be emphasized that high accuracy can not be expected. However, in the absence of any quantitative data, of this type, at least a beginning has been made. The exact value of the amount of ultra-violet shut out depends greatly upon the sample of window glass selected. For example, the sample of window glass, W–2 (fig. 2) which was exceptionally transparent (tr. = 3.4 per cent at 313 mμ) shut out only 0.28 per cent of the total or 0.003 g cal.) of the short wave length ultra-violet as compared with the standard, W–10 (tr. = 0.3 per cent at 313 mμ) which on the same day, shut out 0.48 per cent of the total, or 0.0053 g cal./ cm^2/min. This, however, was an exceptional sample whereas the object is to provide data on the so-called average window glass. In connection with these measurements, reference may be made to the estimates recently published by Doctor Clark (48) who used the rate of blackening of zinc sulphide as a method of measuring ultra-violet radiation, and recorded a variation in intensity of solar radiation, between 290 and 310 mμ, which ranged from about 500 ergs in winter to about 4,000 ergs in summer, in Baltimore. This is in good agreement with our values which range from 600 ergs in winter to 5,000 ergs in summer.

[2] A barium flint glass (nd 1.605) made at the Bureau of Standards has recently been found satisfactory for this purpose.

TABLE 1.—*Summary of estimates of the ultra-violet component radiation between the wave lengths 295 and 310 mμ relative to the total incident solar radiation of all wave lengths, at sea level, at Washington, D. C., air mass m=1*

	How obtained	Per cent
Method I	By calculation from the solar spectral energy curve	0.04
Method II	By using the spectropyrheliometer data of Coblentz and Kahler (9)	.12
Method III	By isolating the short wave length ultra-violet component by means of a sample of common window glass.	.60
Method IV	By isolating the ultra-violet part of the solar spectrum by means of a filter of Corning G986A glass and determining the amount shut out by common window glass.	.40
	Mean	.3

A comparison of these four methods of determining the amount of short wave length ultra-violet solar radiation shut out by common window glass shows that the values obtained by direct measurement (0.4 per cent) are about three to sixteen times larger than the values calculated from the probable spectral energy distribution which is admittedly in doubt for sea-level stations.

The values obtained by these different methods are so discordant that the conclusion to be drawn is that even on the clearest days at the noon hour, in summer, the total amount of ultra-violet solar radiation of wave lengths less than 310 mμ, which has a therapeutic effect in preventing rickets, is extremely small, at the most amounting to only about 0.3 per cent of the total incident solar radiation (or about 0.004 g cal.) and more likely only one-tenth of this value at sea-level stations. The value on cloudy days, at sunrise and at sunset, and in high latitudes would be very much smaller.

In conclusion, it is to be emphasized that the amount of ultra-violet shut out by common window glass will depend upon the sample examined. We have selected what appeared to be an average sample, and have found that it shuts out short wave length ultra-violet radiation amounting to about 0.4 per cent of the total incident solar radiation. But this sample may have shut out ultra-violet of a greater range of wave lengths than is effective for therapeutic purposes. As already noted a more transparent sample would shut out short wave length ultra-violet amounting to less than the above-estimated value of 0.4 per cent of the total incident radiation and yet might not show any difference in a therapeutic efficiency test.

As already mentioned, all this interest in special window glasses is based upon the observation that common window glass shuts out ultra-violet rays having a therapeutic value, especially in preventing rickets (23). In this connection it is relevant to cite recent tests by Bethke and Kennard (49) made at Wooster, Ohio (lat. 40° 45′ N.; altitude about 800 feet), between March 18 and May 27, 1926. These experiments covered the period between the first and tenth week of the life of the chick. The season was already sufficiently

advanced to insure the presence of an appreciable amount of ultra-violet vitalizing rays. The chicks that were exposed to direct sunlight, or sunlight filtered through a glass substitute that transmitted an appreciable amount of the vitalizing rays, did not develop rickets, whereas those that were exposed to the solar rays filtered through common window glass developed rickets.

It should be emphasized that these measurements of the amount of ultra-violet light shut out by window glass were made only on the clearest days which, at sea-level stations, are few in number. Hence, the numerical values represent the approximate upper limit that may be expected. The so-called average value, which would be much lower, will depend upon the condition of the sun (sun spots) the altitude and the latitude of the station and the almost infinite variety of air pollution and weather conditions that are encountered at different seasons of the year and during different years.

The whole discussion indicates the importance of having an artificial source of ultra-violet radiation (and a unit of dosage that is correlated with ultra-violet similar to solar radiation) that can be controlled, which is not possible with solar radiation.

III. EFFECT OF SOLARIZATION UPON THE ULTRA-VIOLET TRANSMISSION OF WINDOW GLASSES

In view of the fact that improvements may be expected in the transmissive properties of all of these glasses, it is to be emphasized that the present data on Helioglass and Vitaglass are based upon an examination of melts that were marketed prior to February 1, 1929.

Under this caption data are given on the transmissive properties of window glasses in the ultra-violet, visible and infra-red spectrum, and particularly on the decrease in transmission of ultra-violet radiation through these glasses as the result of photochemical stabilization by exposure to artificial sources of radiation and to the sun. A comparison of the ultra-violet transmission of various glasses, after solarization, is illustrated in Figure 15.

In Figure 2 is shown the ultra-violet spectral transmission of various window glasses when new. From this illustration it appears that, as regards their spectral transmissions, these glasses fall into three distinct groups: (*a*) Quartzlite and common window glass which transmit little or no ultra-violet in the region of 297 to 310 mμ; (*b*) Vitaglass, Helioglass, and Holviglass which transmit considerable radiation at 302 mμ; and (*c*) Corex-D, and quartz glass which transmit over 85 per cent at 302 mμ (for "single strength" glass, thickness = 0.09 inch = 2.3 mm. B. S. Circular No. 164).

By means of these spectral transmission curves an estimate of the relative transmissions of these various glasses, for the ultra-violet rays which are shut out by common window glass, may be obtained

by reading from the curves the values of the transmission at 302 mμ—the wave length of an intense mercury line, of convenient value for

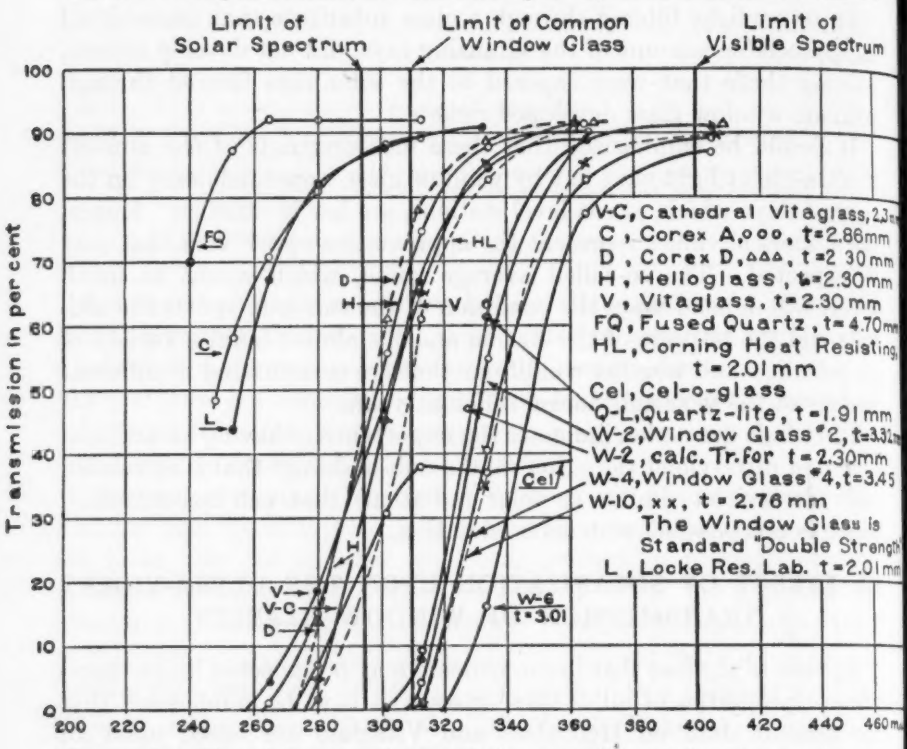

FIGURE 2.—*Ultra-violet spectral transmission of various window glasses when new*

making such tests. Table 2 gives the average transmission values (37) for this wave length.

TABLE 2.—*Transmission of various glasses at 302 mμ, when new and after photochemical stabilization by exposure at a distance of 15 cm from a quartz mercury arc for 10 hours*

Trade name	Number of samples tested	Average thickness	Average transmission	
			New	After exposure
		mm	*Per cent*	*Per cent*
Quartz glass	1	4.7	92	92
Corex-D	15	2.3	61	59
Neuglas	12	2.3	63	49
Uviol-Jena	14	2.3	58	43
Helioglass (Vioray) [1]	24	2.3	58	40
Sunlit ultra-violet health glass	9	2.3	65	39
Vitaglass	19	2.3	48	23
Cel-o-glass [2]	5	[3] 1	30	[4] .5
Quartzlite	16	1.9	.5	0
Common window glass	14	3.3	0	0

[1] Vioray is the foreign trade name of Helioglass.
[2] This consists of a fine wire screen whose interstices are covered with cellulose acetate. The value of 30 per cent includes practically all the rays diffusely transmitted.
[3] About.
[4] About 0.2 per cent for $t=2.3$ mm.

The foregoing data are completely verified numerically in a recent paper by Goodman and Anderson (38) who placed Quartzlite in Class I with window glass which, according to their observations had no measurable transmission for ultra-violet radiation of wave lengths 293 to 310 mμ, while Helioglass (Vioray) and Vitaglass are placed in Class II with a transmission of 56 and 48 per cent, respectively.

Unfortunately, as stated elsewhere in this paper, in most of these glasses the long wave length side of the ultra-violet absorption band coincides closely with the spectral region of activating rays, at 297 to 302 mμ, and, hence, a slight variation in thickness produces a great change in transmission of these rays; for example, for glasses having a transmission of 40 to 50 per cent (at, say, 302 mμ, $t = 2.3$ mm) a varia-

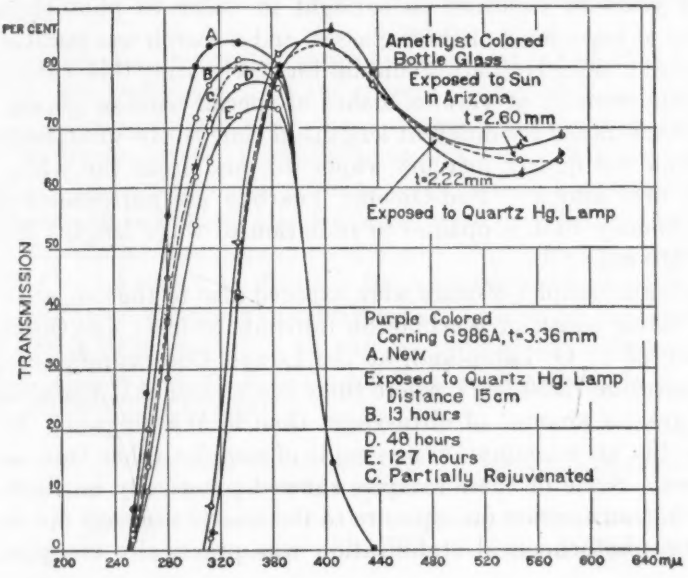

FIGURE 3

tion in thickness of 0.1 mm produces a change in transmission of 1.2 per cent. Since these glasses are handblown, a variation of 0.5 mm (or 6 per cent in transmission) is frequently found in a single sheet of window glass.

As is well known, certain kinds of glass (for example, bottle glass, fig. 3) containing iron as an impurity, which have been decolorized by means of selenium or manganese, undergo a photochemical change and exhibit an amethyst color when exposed to solar radiation, especially after exposure to the intense sunshine in the desert regions of our Western States.

A further illustration is the familiar amethyst color developed in glass globes which inclose carbon arcs used in street lighting. Evidently the material which produces this discoloration is variable in its

chemical stability under the action of light. For example, we have observed an occasional gas lamp, containing a Welsbach mantle, in which the larger outer glass inclosure had a conspicuous amethyst color while the small glass chimney, which formed the immediate surrounding of the mantle, showed no color.

1. METHODS OF PHOTOCHEMICAL STABILIZATION

Early in this investigation it was observed that these special window glasses underwent a photochemical reaction, and decreased in transmission, especially in the short wave length ultra-violet, after exposure to sunlight and to artificial sources emitting ultra-violet radiation. It was then surmised that it would probably require several years of exposure to sunlight in order to photochemically stabilize at least some of these glasses, and a search was instituted for a source of artificial radiation suitable for accelerating this stabilization. Duplicate samples of various makes of special window glasses were, therefore, exposed for different lengths of time to the unfiltered radiation from the quartz mercury vapor arc and from the white flame carbon arc; also a ("Fad-Ometer") carbon arc surrounded with a glass chimney that is opaque to radiation of wave lengths less than about 320 mμ.

Duplicate samples of glass were exposed also to the sun, at an angle of 45° facing south in Washington (altitude 50 feet), and through the courtesy of C. O. Lampland, at the Lowell Observatory, Flagstaff, Ariz. (altitude 7,250 feet), where there is a clearer sky, more sunshine and a greater amount of ultra-violet than in Washington. In addition to this, an examination was made of samples taken from hospital windows. Some of these samples showed practically no further decrease in transmission on exposure to the quartz mercury arc showing that the photochemical stabilization was practically complete.

2. EFFECT OF TEMPERATURE UPON THE SOLARIZATION OF WINDOW GLASSES

The solarization of ultra-violet transmitting window glasses is essentially a problem in photochemistry which is a function (*a*) of the temperature, (*b*) of the absorptive properties of the material for ultra-violet radiation, (*c*) of the presence of a material (for example, ferrous iron (39) as an impurity) which reacts to ultra-violet rays; and (*d*) the source of radiation.

Solarization is commonly attributed to the presence of iron in the glass. We have found that (soda-lime) glasses, which were prepared under the direction of F. C. Flint, of the Hazel-Atlass Glass Co., from chemically-pure (iron-free) material, in receptacles that could not contaminate the material with iron, do not solarize on exposure to ultra-violet radiation of wave lengths 250 to 350 mμ

which are absorbed by the glass. On the other hand, as will be noticed on a subsequent page, we have found that Corex-A glass, which contains iron as an impurity and is transparent to radiation of wave lengths longer than 302 mμ does not solarize on exposure to the sun, but decreases rapidly in transmission on exposure to ultra-violet radiation of wave lengths 250 to 280 mμ which are absorbed by this glass.

It is to be expected that the solarization will continue so long as any of the chemically active material remains uncombined. This is evident from the fact that after the glass has practically ceased to decrease in transmission, because the activitating rays can not penetrate the entire layer of glass, the solarization is renewed on turning the under (previously unexposed) side of the glass toward the source of radiation.

In our solarization tests during the summer and fall of 1927 it was found that the transmission of the glasses decreased to a constant value. The following summer these glasses underwent a further decrease in transmission on exposure to the sun. This seemed to be owing to the increased temperature. To test this question duplicate samples of Helioglass and Vitaglass were exposed to the mercury arc, the one at a temperature of about 70° C. and the other at about 15° C. As shown in Table 3 the samples at the higher temperature decreased the most in transmission, as is to be expected for a small rise in temperature. As will be noticed on a subsequent page these glasses can be rejuvenated by heating them to a temperature of 200° C. or higher.

TABLE 3.—*Effect of temperature on the solarization of window glasses exposed to the mercury arc*

Transmission of—	New	Exposed 1 hour	Exposed 11 hours
Helioglass (t=1.71 mm):	*Per cent*	*Per cent*	*Per cent*
Cool	56.0	46.4	42.0
Hot	56.0	43.0	38.2
Vitaglass (t=2.5 mm):			
Cool	42.5	26.5	20.0
Hot	42.5	24.8	18.3

3. REJUVENATION OF GLASSES

As is to be expected, the photochemical action produced by the ultra-violet rays can be reversed by heat treatment. The rate of recovery, of course, depends upon the temperature to which the glass is heated (40). There seems to be no measurable recovery in transmitting power of the solarized glass on standing in the dark, at room temperatures.

In Figure 6 is shown a series of photochemical aging and rejuvenation curves of Vitaglass in which the process was repeated through several cycles, with no perceptible fatigue or permanent change in chemical composition of the material, which would be evidenced by a change in the transmission curve. Further experiments on rejuvenation are depicted in Figure 11—Corex-*A*.

4. VITAGLASS

Of the various new glasses now obtainable for therapeutic purposes, Vitaglass has been on the market the longest. Hence, concerning this glass, we have been able to obtain the most information regarding solarization. This glass has been marketed in the smooth and in the "cathedral" finish. Apparently there is a difference in the chemical composition of these two types of glasses. This is apparent from the transmission curves, Figure 2 (V=smooth finish, and V–C=cathedral surface, polished before examination) and also from the color as viewed edgewise, under which conditions the cathedral finish (at least the kind first marketed) shows but little color, while the smooth finish has a decidedly greenish-yellow tinge and an appreciably lower transmission in the violet. This probably explains the confusing results obtained by various observers.

(a) EFFECT OF SUNLIGHT

As shown in Figure 2 the transmission of a polished sample of cathedral Vitaglass (V–C) is decidedly lower than the smooth Vitaglass (V) in the region of 280 mμ when new. But the chemical constituents of the glass used in the cathedral finish seem to be less affected by sunlight. For example, the dotted curves in Figure 4 show the transmission of a (polished) sample of cathedral-finish Vitaglass (V–C in fig. 2; thickness 2.3 mm) that had been in use for two years in an animal house. The upper dotted curve gives the transmission at the edge of the glass which had been covered with putty, and, hence, not exposed directly to light.

The transmission of ultra-violet of wave lengths 290 to 310 mμ through this unpolished sample (which was very soiled when received) was only 22 per cent before washing and 58 per cent after washing, an increase of 36 per cent, showing the importance of keeping the windows clean in order to maintain a high transmission.

A further exposure of this (polished) sample of cathedral Vitaglass (fig. 4) to the sun, in Washington from March 7 to May 7, 1928 (about nine weeks) decreased the transmission at 302 mμ by less than 1 per cent. An additional exposure of 10 hours to the quartz mercury arc changed the transmission at 302 mμ from 42 per cent (fig. 4) to 36 per cent, showing that solarization was about complete before exposure to the mercury arc.

On the other hand, a sample of the smooth finished Vitaglass (tinged bluish white as viewed edgewise) which had been in a hospital window in Rhode Island for a year, was found to have a transmission of only 25 per cent at 302 mμ (for thickness, $t=2.3$ mm). Further exposure to the quartz mercury arc reduced the transmission but little, showing that solarization was practically complete.

In the present investigation, the samples of glass were exposed continuously, day and night, at an angle of 45° facing south. Our tests show that the greatest decrease in the transmission of the greenish-yellow tinged (as viewed edgewise) Vitaglass occurs during the first two or three weeks of exposure to direct sunlight. This is illustrated by the full line curves in Figure 4, which show the de-

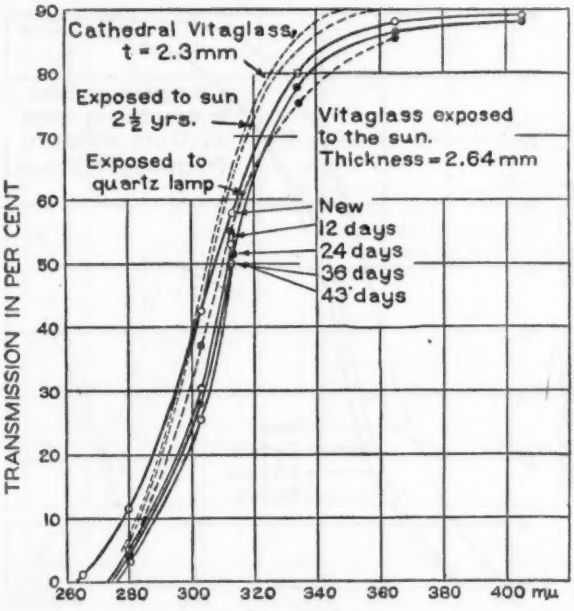

FIGURE 4

crease in transmission of a sample of greenish-yellow tinged Vitaglass that was exposed to the sun, in Washington, during the months of August and September, 1927. Fortunately, this occurred at a time when there was but little cloudy weather, the first 24 days being practically cloudless. The greatest decrease in transmission occurred during the first 12 days of exposure. After an exposure of 36 to 43 days the transmission of this sample did not decrease perceptibly. This is a typical example of the change in transmission that occurs in Vitaglass as a result of solarization. In the upper part of Figure 6 is depicted the decrease in transmission of this sample of glass at 302 mμ which shows that the greatest change in transmission occurs during the first few weeks' exposure to the sun.

The transmission of Vitaglass after solarization by exposure to the sun is about 25 per cent at 302 mμ, although an occasional sample is found that transmits 35 per cent while others transmit only 17 per cent after seven months' exposure to the sun, showing the great variation in purity that occurs in different melts. These data are summarized in Tables 4, 5, 6, and 7, and illustrated in Figure 15.

In another test, a sample of Vitaglass ($t=2.35$ mm) was exposed directly to the sun, between 9 a. m. and 3 p. m. for a total of 123 hours, during the months of June, July, and August, 1927, which decreased the transmission from 47 to 32 per cent at 302 mμ. (Fig. 6.)

Even the weak intensity of the light from the north sky in winter decreases the transmission of Vitaglass. A sample ($t=2.6$ mm) that

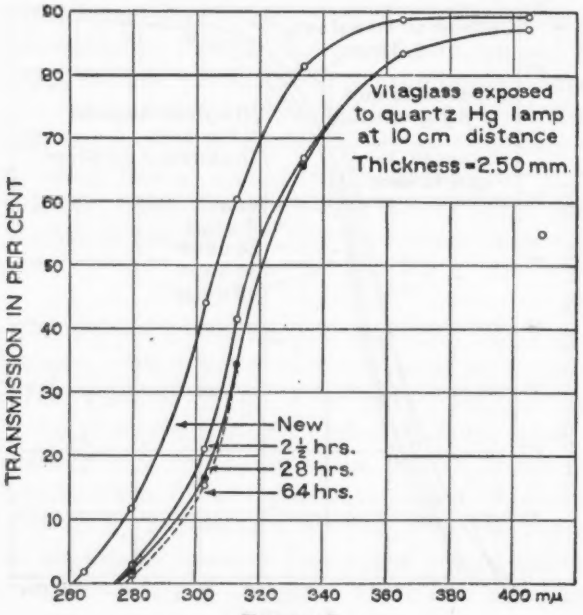

FIGURE 5

was placed about 3 m above the ground on the north side of a long, 4-story building, decreased in transmission from 45 to 39 per cent at 302 mμ after an exposure of one month (December, 1927), and to 31 per cent by a year (December, 1928).

The solarization data obtained at the higher altitude, at Flagstaff, Ariz., are interesting in showing that after prolonged exposure the average transmission of the glasses (see Table 5) is practically the same as that obtained at Washington. A typical example of the change in transmission after an exposure to the sun for about eight weeks (March 12 to May 7, 1928) is shown in Figure 8. The average transmission of two samples for wave length 302 mμ after exposure to the sun from March to May at Flagstaff, Ariz., was 21.4 per cent

(t=2.55 mm) and the transmission of duplicate samples exposed at the same time in Washington was 22.2 per cent. The results as a whole show that this type of Vitaglass solarizes very quickly. This is further verified by the tests with artificial radiation.

(b) EFFECT OF ARTIFICIAL LIGHT

The effect of ultra-violet light from artificial sources of radiation is practically the same as that of sunlight upon the ultra-violet transmission of Vitaglass; the only difference being the rate of change, which is more rapid with the quartz mercury arc than with the sun.

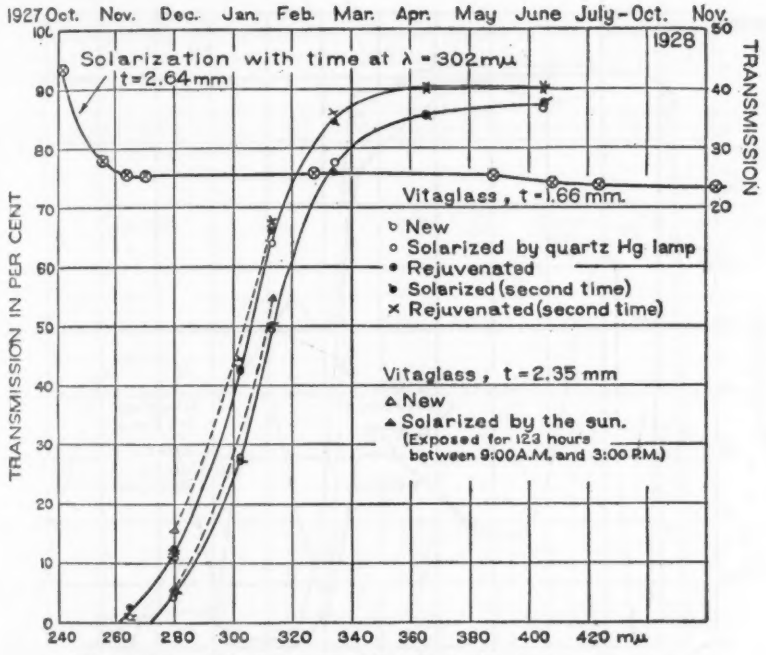

FIGURE 6.—*Solarization of Vitaglass with time, upper curve*

The carbon arc (including the "Fad-Ometer," dye-fading carbon arc which is surrounded with a glass chimney that is opaque to ultra-violet radiation of wave lengths less than 310 mμ, see fig. 12 and Table 6) also decreases the ultra-violet transmission of this glass; for example, two samples of Vitaglass (Table 7, t=2.3 mm) which transmitted 34.6 and 40.3 per cent, respectively, at 302 mμ when new, decreased in transmission to 19 and 23 per cent, respectively, after an exposure of 300 hours to a white flame carbon arc, and to 18 and 20 per cent, respectively, on a further exposure of 10 hours to the mercury lamp.

As shown in Figure 5, exposure of Vitaglass to ultra-violet radiation from the quartz mercury arc produces practically the same kind of photochemical action as sunlight, the only difference being the time

involved. In other respects these two sets of transmission curves (obtained on two samples cut from the same sheet of glass, figs. 4 and 5) are practically superposable. The average transmission of Vitaglass at 302 mμ after complete photochemical stabilization by exposure to the mercury arc is about 23 per cent for a thickness of 2.3 mm. (See Table 2.)

As is well known, different melts of glass vary in purity and, hence, in transmission of ultra-violet radiation. Samples of Vitaglass of the most recent importation (January, 1929) had a transmission of about 62 per cent (for $t=2.3$ mm, samples 1j to 3j, Table 4) when

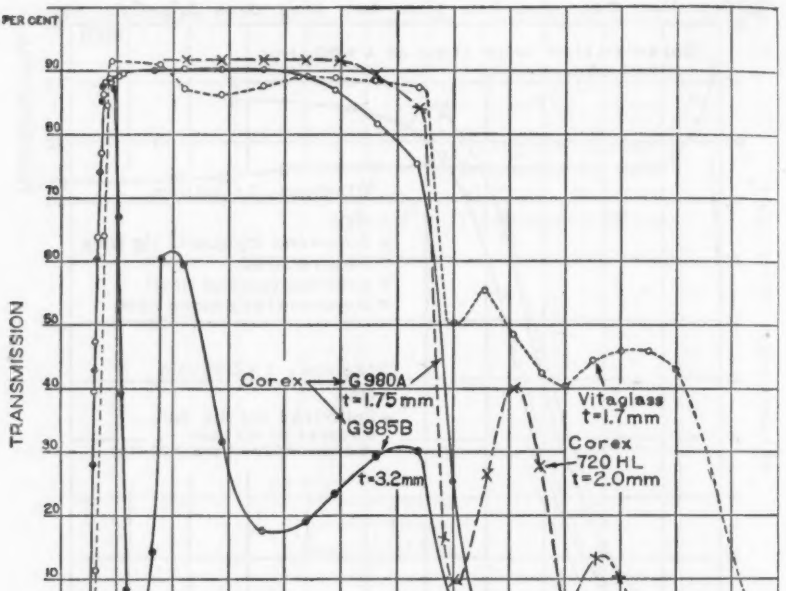

FIGURE 7.—*Infra-red transmission of window glasses*

new and about 30 per cent after complete stabilization under the mercury arc.

It is relevant to add that the transmission of Vitaglass appears to undergo a somewhat greater decrease in the region of 320 to 380 mμ as a result of exposure to the quartz mercury arc than to the sun. However, this part of the ultra-violet spectrum is not known to have special vitalizing properties. Hence, the question of the method of solarization is relatively unimportant, especially so when it is known that glasses can be made which have a higher transmission after the most severe photochemical stabilization by the mercury arc than some of the most transparent samples now obtainable, when new. This is

the most severe test that can be applied and manufacturers may well be proud of their ability to produce a glass that withstands this test.

(c) INFRA-RED TRANSMISSION

The complete spectral transmission curve of Vitaglass is depicted in Figure 7 from which it may be seen that its transmission in the infra-red is much the same as common window glass having the same thickness. (Fig. 14.) The relatively high transmission beyond 4,000 mμ is unimportant because the infra-red solar radiation of wave lengths longer that 4,000 mμ is less than 0.5 per cent of the total incident solar radiation.

TABLE 4.—*Decrease in transmission of window glasses at wave length 302 mμ on exposure to the Sun in Washington (except Helioglass No. 2a and Corex-A, which were at Flagstaff, Ariz., and 1m which was on Long Island)*

[The exposure of 258 days extended from February to November 15. The shortest exposures (89 days) extended from August 17 to November 15, 1928. Duplicate samples were exposed to the mercury arc.]

Sample	Thickness	Transmission when new	Transmission after exposure to sun	Time exposed	Transmission after exposure to mercury lamp for 10 hours
Vitaglass:	*mm*	*Per cent*	*Per cent*	*Days*	*Per cent*
2a	2.65	----------	24.1	425	16.3
2a	*2.65*	----------	*23.3*	*654*	----------
1b	2.43	44.6	27.5	395	18.6
1b	*2.43*	*44.6*	*26.7*	*624*	----------
1m	2.01	----------	26.5	365	21.8
1v	2.50	51.9	34.8	258	----------
1v	*2.50*	*51.9*	*32.6*	*487*	----------
1h	2.55	40.5	20.9	258	18.5
1h	*2.55*	*40.5*	*19.6*	*487*	----------
2h	2.55	39.3	20.8	216	18.3
1p	3.35	55.5	35.4	239	20.2
1j	2.30	62.4	----------	----------	30.3
2j	1.98	65.3	----------	----------	34.3
3j	2.26	61.1	----------	----------	29.8
Helioglass:					
1	2.55	57.3	50.7	258	----------
1	*2.55*	*57.3*	*48.5*	*487*	----------
2a	2.32	59.0	52.9	238	----------
1h	*1.75*	*61.3*	*48.9*	*445*	----------
2h	1.70	56.0	45.8	231	38.2
2p	2.55	51.9	42.7	258	----------
4a	1.99	61.7	52.7	251	----------
3h	2.20	56.3	45.1	261	35.2
5h	2.60	50.6	37.2	231	27.9
5h	*2.60*	*50.6*	*35.0*	*460*	----------
6h	2.20	58.2	46.4	231	42.4
6h	*2.20*	*58.2*	*45.8*	*460*	----------
7h	2.00	58.0	46.2	231	36.7
7h	*2.00*	*58.0*	*43.7*	*460*	----------
9h	1.90	58.6	47.1	107	34.2
9h	*1.90*	*58.6*	*45.8*	*336*	----------
10b	1.88	58.5	47.8	107	37.1
11h	1.77	45.0	36.4	89	28.0
12h	1.95	42.5	33.7	89	25.5
15h	1.81	43.4	35.1	89	26.6
16h	1.93	43.4	33.8	89	27.2
17h	2.60	69.1	----------	----------	48.0
18h	2.60	67.4	----------	----------	45.7
1k	2.25	66.9	----------	----------	42.1
2k	2.27	65.9	----------	----------	48.8
3k	2.25	62.9	----------	----------	49.3
4k	2.25	67.0	----------	----------	50.0

TABLE 4.—*Decrease in transmission of window glasses at wave length 302 mμ on exposure to the sun in Washington (except Helioglass No. 2a and Corex-A, which were at Flagstaff, Ariz., and 1m which was on Long Island)*—Continued

Sample	Thickness	Transmission when new	Transmission after exposure to sun	Time exposed	Transmission after exposure to mercury lamp for 10 hours
	mm	*Per cent*	*Per cent*	*Days*	*Per cent*
Ultravit:					
1	2.07	50.5	34.7	189	27.5
2	2.05	62.3	47.0	89	37.6
Holviglass:					
1	2.47	39.2	35.5	174	31.2
1	*2.47*	*39.2*	*35.0*	*403*	
2	2.40	41.1	37.4	124	
2	*2.40*	*41.1*	*37.0*	*353*	
Bretlet:					
1	2.66	52.0	38.8	216	
2	2.71	41.0	25.5	216	15.8
Sanalux:					
1	2.59	44.8	22.6	251	17.3
2	2.14	51.0	29.0	251	21.2
Ultra-violet glass (Sendlinger's U. G.):					
1	2.10	57.3	53.0	117	49.8
2	2.42	42.0			31.4
3	2.41	40.0			29.0
4	2.71	48.3			39.0
5	2.50	40.0			29.2
6	2.07	52.8			41.0
7	3.30	32.6			20.1
Locke:					
189	2.93	85.0			51.0
193	2.45	86.0			64.0
9RF	3.22	86.9	83.5	239	
133P	2.62	88.3	84.0	239	
Renovic	1.70	38.5	32.9	174	31.9
Sunlit:					
M	2.30	64.6			36.4
2	1.92	65.0	46.0	72	38.2
2	*1.92*	*65.0*	*45.1*	*301*	
3	1.88	65.3	47.0	72	38.6
3	*1.88*	*65.3*	*44.5*	*301*	
8	2.00	63.8			
9	2.27	51.5			41.0
26	1.88	75.4			49.1
27	1.87	74.6			48.8
30	1.91	73.7			48.0
32	2.08	71.7			46.2
Neuglas:					
1	2.50	58.5	52.3	182	43.7
1	*2.50*	*58.5*	*51.9*	*411*	
A	2.44	64.7			50.9
B	2.33	62.8			49.9
D	2.58	60.0			47.8
E	2.30	61.7	58.7	91	51.0
F	2.32	65.1	56.0	91	47.1
G	1.98	65.4			54.7
H	2.47	59.2			47.0
K	2.24	65.9			49.6
L	2.05	65.6			48.6
M	2.38	63.0			41.7
N	2.42	61.8	59.5	91	46.8
Uviol-Jena:					
1	1.89	50.6	41.9	239	
1	*1.89*	*50.6*	*40.4*	*468*	
2	1.97	49.5	45.8	182	30.1
2	*1.97*	*49.5*	*43.4*	*411*	
11A	2.03	59.3	53.4	91	45.9
11B	2.02	60.4			41.0
11C	2.02	61.0	54.5	91	42.8
11D	2.02	60.2			43.1
B3	1.90	62.5			44.1
A66	1.95	64.0			43.5
A68	2.06	63.2	56.7	91	44.1
A73	1.93	64.0			44.2
A88	2.00	62.8			42.2
A100	2.22	57.9			42.6

TABLE 4.—*Decrease in transmission of window glasses at wave length 302 mμ on exposure to the sun in Washington (except Helioglass No. 2a and Corex-A, which were at Flagstaff, Ariz., and 1m which was on Long Island)*—Continued

Sample	Thickness	Transmission when new	Transmission after exposure to sun	Time exposed	Transmission after exposure to mercury lamp for 10 hours
Triol-Jena—Continued.	*mm*	*Per cent*	*Per cent*	*Days*	*Per cent*
52A	2.00	69.8			52.1
52B	2.03	70.3			50.0
52C	2.02	71.5			50.7
52D	2.02	69.5			51.8
Corex-A	2.95	88.0	82.3	238	
Corex G981FF[2]:					
1	2.01	81.3	78.7	157	70.1
2	4.00	73.2	69.1	157	
Corex-D:					
1p	2.00	65.0			
1g	1.97	61.1			[1] 57.5
2g	1.97	60.9			[1] 58.6
3g	1.97	69.7			[1] 61.2
1t	1.99	61.4			60.4
2t	1.99	63.7			62.9
3t	1.99	63.5			62.9
4t	1.99	63.2			62.6
5t	1.99	63.1			61.7
6t	1.99	64.8			63.2
7t	1.99	64.5			62.0
8t	1.99	66.1			64.6
9t	1.99	64.8			64.0
10t	1.99	61.4			60.3
11t	1.99	66.5			
12t	1.99	65.0			

[1] These 3 samples were exposed for 30 hours at a distance of 15 cm from a quartz mercury arc lamp.

TABLE 5.—*Transmission of duplicate samples of window glasses at wave length 302 mμ before and after exposure to the sun at Flagstaff, Ariz., and in Washington, D. C., and after exposure to the mercury lamp at a distance of 10 cm*

Sample	Thickness	Transmission, new	Exposed in Arizona		Exposed in Washington, D. C.		Exposed to mercury lamp for 10 hours
			Transmission	Time exposed	Transmission	Time exposed	
Vitaglass:	*mm*	*Per cent*	*Per cent*	*Days*	*Per cent*	*Days*	*Per cent*
1b	2.55	40.5	20.0	238	20.9	258	18.5
1h	*2.55*	*40.5*			*19.6*	*437*	
2b	2.55	39.3	19.8	238	20.8	216	18.3
1p	3.35	58.5	34.0	209	35.4	239	20.2
Helioglass:							
1h	1.75	61.3	48.8	215	50.5	216	
1h	*1.75*	*61.3*			*48.9*	*445*	
2b	2.42	50.4	44.3	238	43.2	440	39.5
3h	2.20	56.3	43.5	215	45.1	216	35.2
4h	2.76	49.3	37.4	215	36.5	216	
8h	2.60	50.8	38.6	215	36.9	216	31.5
Locke:							
9RF	3.22	86.9	85.6	209	83.5	239	
133P	2.62	88.3	88.9	209	84.0	239	
Triol:							
1	1.89	50.6	42.8	209	43.9	239	

5. HELIOGLASS

This glass appeared on the market late in 1927 when intense sunshine was no longer available. Furthermore, since the transmission curves of Helioglass and Vitaglass are so closely the same, and since these glasses appeared to be of somewhat similar composition, it seemed fair to make the first comparisons of solarization of these two kinds of glass by accelerating the decrease in transmission by means of the quartz mercury arc lamp, which procedure is vindicated by our recent sunlight tests.

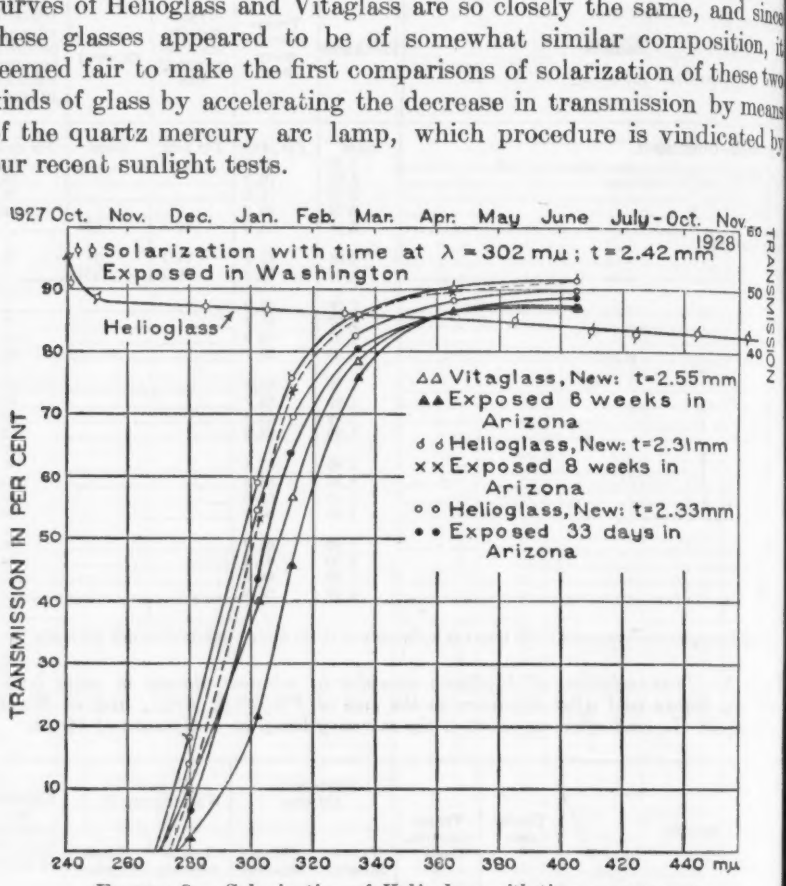

FIGURE 8.—*Solarization of Helioglass with time, upper curve*

The above-described tests on Vitaglass, when using the mercury arc, also the carbon arc with a chimney (see Table 6), solarization by exposure to the north sky, rejuvenation, etc., were made also on Helioglass. Hence, it is unnecessary to give further detailed descriptions.

(a) EFFECT OF ARTIFICAL LIGHT

In Figure 9, is shown the effect of exposure of the sample of Helioglass for 72 hours at a distance of 10 cm from the mercury arc lamp.

The data now on hand seem to indicate that on exposure to the quartz mercury arc, Helioglass does not decrease in transmission quite so rapidly as Vitaglass; also, that after complete photochemical

stabilization the transmission in the region of 320 to 380 mμ is not as low as observed in Vitaglass.

As might be expected the various shipments of Vitaglass and Helioglass, representing melts of different batches of the same kind of material, differ greatly in transmission. (See Tables 4 and 5.) For example, several samples marked Helioglass (Table 4, 11h to 16h), which had a slightly yellowish tint when viewed edgewise, transmitted less than 30 per cent at 302 mμ after stabilization under the mercury lamp.

However, as viewed edgewise, Helioglass is usually colorless, "water white," and the transmission of such samples, after degeneration under the mercury lamp, ranges from 38 to 42 per cent (Table 4,

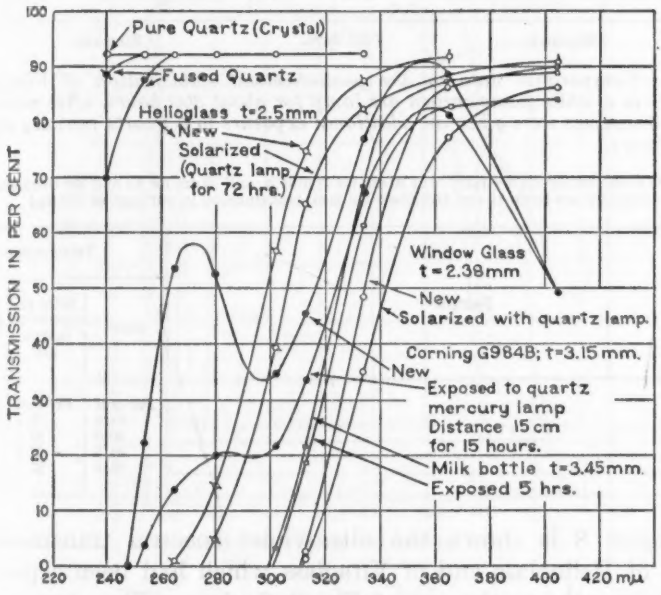

FIGURE 9

6h, and 7h), while the most recent shipment tested (Table 4, 17h, and 18h, January, 1929) had a transmission of 48 per cent, or 51 per cent for a thickness of 2.3 mm. This is a decided improvement in the quality of this glass. However, the transmission of the general run of Helioglass, at 302 mμ, after complete photochemical stabilization by the mercury arc appears to be between 35 and 40 per cent for a thickness of 2.3 mm. (Tables 2, 4, and 7.)

(b) EFFECT OF SUNLIGHT

Our investigations show that, on exposure to the sun, Helioglass does not solarize and decrease so low in transmission as Vitaglass (11). This is in agreement with the observations on the accelerated stabilization under the mercury arc.

TABLE 6.—*Comparative data on the transmission (at 302 mμ) of duplicate samples of Vitaglass and Helioglass after exposure to the Fad-Ometer, to the mercury arc (distance 10 cm), and to the sun*

Sample	Thickness	Transmission when new	Transmission after exposure to Fad-Ometer carbon arc (glass chimney)		Transmission after exposure to sun	Transmission after exposure of 10 hours to mercury lamp
			1,500 hours at 15 inches	3,000 hours at 15 inches		
Vitaglass:	*mm*	*Per cent*	*Per cent*	*Per cent*	*Per cent*	*Per cent*
1d	2.23	47.4	37.9	37.7	[1] 30.3	21.1
2h	2.55	39.3	30.4	----	[2] 20.8	18.1
Helioglass:						
3a	2.02	57.7	52.5	51.4	----	----
5h	2.60	50.6	41.6	----	[3] 37.2	27.1

[1] 395 days. [2] 216 days. [3] 231 days.

TABLE 7.—*Comparative data on the photochemical stabilization of Vitaglass by exposure to a white flame carbon arc lamp for about 300 hours, after which treatment the samples were given an additional exposure to a quartz mercury arc lamp for 10 hours*

[The distance from the carbon arc lamp was 20 cm for 1t and 2t, and 30 cm for 1b and 2b; distance from the mercury arc lamp 15 cm; thickness 2.3 mm; transmission in per cent at 302 mμ]

Sample	Transmission		
	New	After exposure to carbon arc	After exposure to mercury arc
	Per cent	*Per cent*	*Per cent*
1t	34.6	19.2	17.6
1b	40.3	23.1	20.4
2t	44.2	23.2	22.1
2b	49.8	27.3	22.6

In Figure 8 is shown the ultra-violet spectral transmission of samples of Helioglass and of Vitaglass which had been exposed (at 45° facing south) to the sun at Flagstaff, Ariz. The average transmission of two samples of Helioglass for wave length 302 mμ after exposure at Flagstaff for about eight weeks (March 12 to May 7, 1928, see fig. 8) is 49.4 per cent ($t=2.35$ mm) as compared with 23.8 per cent (21.4 per cent for $t=2.55$ mm) for two samples of Vitaglass similarly exposed to the sun.

In Figure 8 the circles and dots (o o o, . . .) show the average transmission of four samples of Helioglass that were exposed to the sun for 33 days (April 4 to May 7, 1928) at Flagstaff, Ariz. These four samples seemed to decrease more in transmission than the preceding two samples which were exposed for eight weeks, the average transmission of the four samples at 302 mμ being 43.7 per cent ($t=2.33$ mm) while duplicates of these four samples, after being exposed in Washington for 25 days (April 12 to May 7, 1928), transmitted

44.5 per cent. The difference in the amount of solarization at Flagstaff and at Washington is no doubt to be ascribed to the greater amount of ultra-violet radiation at the higher altitude. However, as already noted, after prolonged exposure there is practically no difference in the solarization at the two stations.

From the slope of the curve in the upper part of Figure 8 which shows the decrease in transmission at 302 mμ with time, it appears that the solarizarion of Helioglass after 13 months' exposure is still incomplete. Hence, it can not be stated definitely what the average

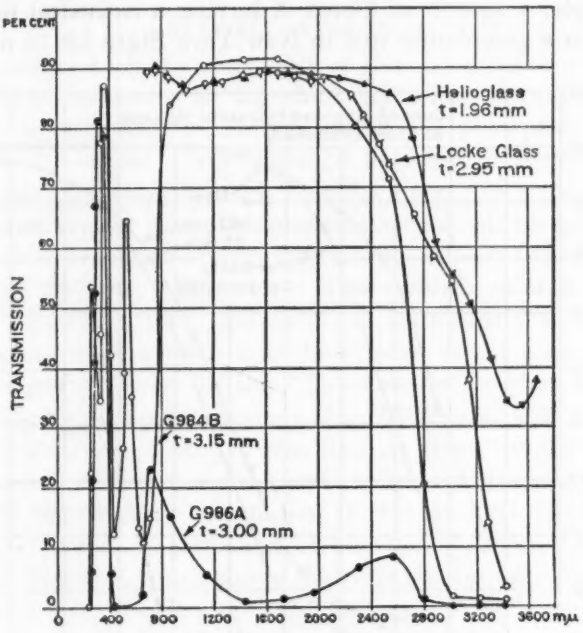

FIGURE 10.—*Infra-red transmission*

transmission will be after complete solarization. However, extrapolation of the exposure time curve in the upper part of Figure 8 indicates a transmission of about 40 per cent after complete solarization of this sample. Further exposure of this sample to the mercury arc reduced the transmission from 43 to 39.5 per cent, which is in agreement with the extrapolated value. (See also Table 4.)

The infra-red transmission of Helioglass (extending to 3,600 mμ) is illustrated in Figure 10, which shows that, for the same thickness, it is similar to that of common window glass. The ultra-violet transmission of the solarized material is depicted in Figure 15.

6. COREX-A GLASS

The trade name of the glasses for transmitting ultra-violet radiation, made by the Corning Glass Works, is Corex. There are several distinct types of this glass, Corex-A, Corex-B, etc., depending upon the chemical composition and its intended use.

(a) EFFECT OF SUNLIGHT

The glass called Corex-A (Corning G980A) appears to undergo no appreciable change in transmission when exposed to solar radiation. For example, a sample of Corex–A having a cathedral finish which had been in a greenhouse roof in New York State for 14 months was

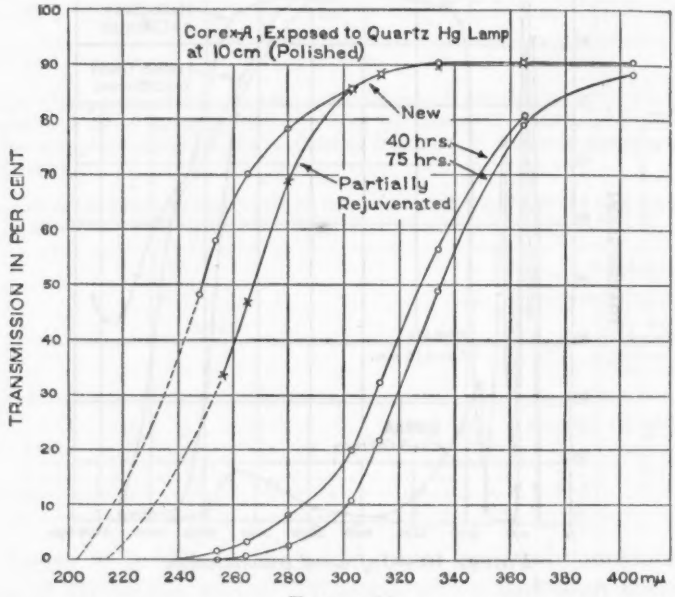

FIGURE 11

found to have, as nearly as could be measured on that kind of surface (which had been roughened by moisture), the same transmission as a new sample. It was then polished plane and found to have a transmission of 89.5 per cent at 302 mμ, while the average transmission of several new samples, as given in Table 1, is 89 per cent.

As already mentioned, the constancy in the transmission is probably owing to the fact that this glass absorbs but little (transmission = 91 per cent for the most homogeneous samples) in the spectral range of solar radiation. Similar results were obtained at higher altitudes, hence, included shorter wave lengths of ultra-violet solar rays. For example, a sample of Corex-A ($t = 4.5$ mm) after an exposure of about six weeks (February 28 to April 10, 1928) at the Desert Lab-

oratory, Tucson, Ariz. (elevation 2,360 feet), had a transmission of 87 per cent at 302 mμ, which value would have been still higher if allowance had been made for scattering of the rays by the very noticeable inhomogeneity of the glass. Another sample exposed at Flagstaff, Ariz. (elevation 7,250), from March to November, 1928, (238 days) transmitted 83 per cent at 302 mμ, as compared with 88 per cent when new, the lower value being due mainly to the diffusing effect of the roughened surface of the glass. From the results at hand it is evident that it will require a very prolonged exposure to the sun in order to affect the transmission.

(b) EFFECT OF ARTIFICIAL LIGHT

In contrast with the constancy of the transmission under exposure to sunlight, exposure to the short wave-length radiation from the quartz mercury arc (at 250 mμ where the absorption begins to be appreciable) causes a very marked decrease in the transmission of ultra-violet radiation through Corex-A glass. As a result of exposure to the mercury arc lamp, this glass takes on a reddish color and greatly decreases in transmission throughout the ultra-violet of wave lengths less than 360 mμ. (Fig. 11.) This reddish color is most intense at the exposed surface, and decreases in intensity with the distance from the exposed surface into the interior of the glass.

Prolonged exposure to the "Fad-Ometer" carbon arc which was surrounded with a glass chimney (Fig. 12) that absorbed all the rays of wave lengths less than 310 mμ, had no effect upon the ultra-violet transmission of Corex-A glass, as is to be expected since this material seems to be perfectly transparent in this spectral region.

The infra-red transmission of Corex-A (G980A, $t = 1.75$ mm) is given in Figure 7, which shows that this glass is very opaque to radiation of wave lengths longer than 3,200 mμ. A homogeneous sample 2 mm in thickness should, therefore, prove useful as a screen in astronomical radiometry (42) in addition to the quartz which is opaque to wave lengths greater than about 4,100 mμ, and the screen of Pollopas, (43) which in thicknesses of 10 mm is opaque to radiation of wave lengths greater than 1,600 mμ.

7. COREX GLASS, G981FF[2]

Through the courtesy of the Corning Glass Works, we have been able to test an experimental sample of window glass which has a high transmission at 302 mμ and is resistant to weathering and to solarization. The sample examined had a transmission of 78.7 per cent ($t = 2.01$ mm) after an exposure of five months (June to November, 1928) as compared with 81.3 per cent when new. The stability in transmission under the mercury arc is equally favorable.

A comparison of the ultra-violet transmission of this solarized sample Corex G981FF[2] with other glasses is illustrated in Figure 15.

8. COREX-D GLASS

The Corning glasses which are designed to have a sharp cut-off at about 290 mμ are designated Corex-D. One of these new heat resisting, ultra-violet transmitting glasses, G720HL (fig. 2, HL) was found to change but little in transmission on exposure to the quartz mercury arc. Hence, this promises to be a useful filter, to be placed over lamps emitting excessive amounts of ultra-violet of wave lengths less than about 290 mμ. The infra-red transmission of this glass is given in Figure 7.

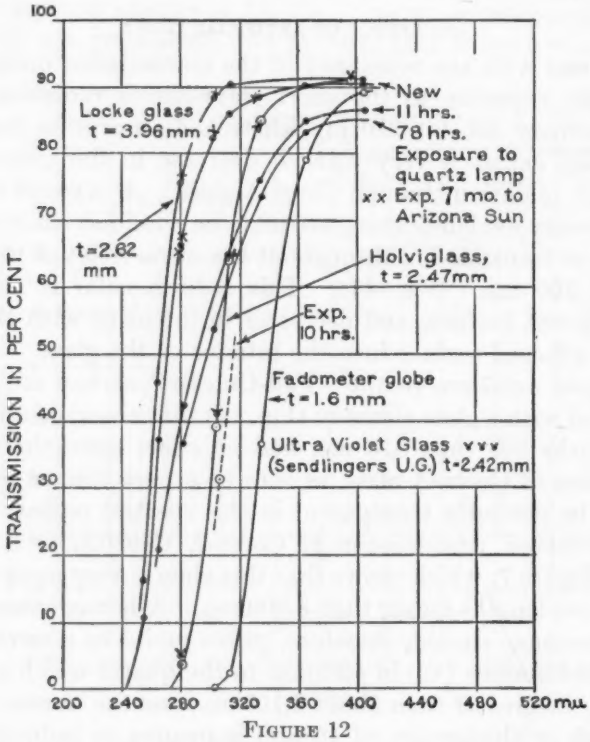

FIGURE 12

In Figure 2 is shown the average transmission curve of three samples of Corex-D glass. These samples represent three melts, on a commercial basis, extending over a period of about two months and appear to be representative of what may be expected of this type of glass produced on a commercial scale. Further data on a dozen samples of different melts, observed at 302 mμ, are given in Table 4.

In Figure 15 is shown the spectral transmission of the average of these three samples of Corex-D after exposure to the radiation from a quartz mercury arc lamp, at a distance of about 15 cm for about 30 hours. From this curve and Tables 2 and 4 it may be noticed

that this glass decreases but little in transmission on exposure to the ultra-violet rays, the transmission after prolonged exposure being 60 per cent at 302 mμ as compared with 61 per cent ($t=2.3$ mm) when new. It may be noted also that while this glass is intended primarily for windows of carbon arc lamps, its transmission at 302 mμ (fig. 15) exceeds that of solarized Vitaglass and Helioglass, and is useful also for windows in solariums.

9. ULTRA-VIOLET FILTERS

In addition to the colorless screens, it is of interest to record some observations of the variation in transmission of a dark purple-colored glass filter, Corning G986A, illustrated in Figure 3 (see also a light purple-colored screen, G985B, in fig. 7) and a greenish-colored glass G984B, depicted in Figure 9. The infra-red transmissions of these two glasses are given in Figure 10.

No doubt the time will come when new glasses will be on the market which will not change in transmission. In the meantime it will be necessary to take into consideration possible changes in the short wave length ultra-violet transmission of the foregoing screens when used for isolating radiation stimuli in biological and photochemical and allied investigations.

10. QUARTZ GLASS

We have tested several transparent homogeneous samples of fused quartz for solarization and have found that even samples which show strong absorption (fig. 9) and fluorescence, did not decrease more than 2 per cent in transmission, at 240 and 254 mμ on exposure to the quartz mercury arc for 110 hours (44).

11. LOCKE GLASS

This is an experimental glass of interest because of its high transmission throughout the ultra-violet. (Fig. 12, $t=2.62$ and 3.96 mm.) Even after prolonged exposure to the quartz mercury arc, the transmission remains higher than that of some of the unsolarized glasses now obtainable. Whether this same condition would obtain when the glass is made on a commercial scale, remains to be determined. As shown by the crosses (xxx) in Figure 12, this glass did not solarize on exposure to the sun for seven and one-half months (March 24 to November 5, 1928) at Flagstaff, Ariz. The sample exposed in Washington during this same period showed a small decrease (4 per cent) in transmission; but this was owing to a deterioration of this surface by moisture. The infra-red transmission of this glass, to 3,600 mμ, is given in Figure 10.

12. QUARTZLITE GLASS

In view of the increase in transmission which was supposed to occur on exposure of Quartzlite glass to ultra-violet radiation, tests were made to determine the effect of irradiation. In Figure 13, curve *A* gives the results of an exposure of 10 hours to an iron arc; curve *B*, 5½ hours to a quartz mercury arc; and curve *C*, 20 days to a "Fad-Ometer" carbon arc, which was covered with a glass chimney that absorbed all the ultra-violet of wave lengths less than 310 mμ. (See transmission curve in fig. 12.)

As shown in this illustration (curves *A* and *B*) the ultra-violet rays of wave lengths less than 310 mμ produce a small decrease in trans-

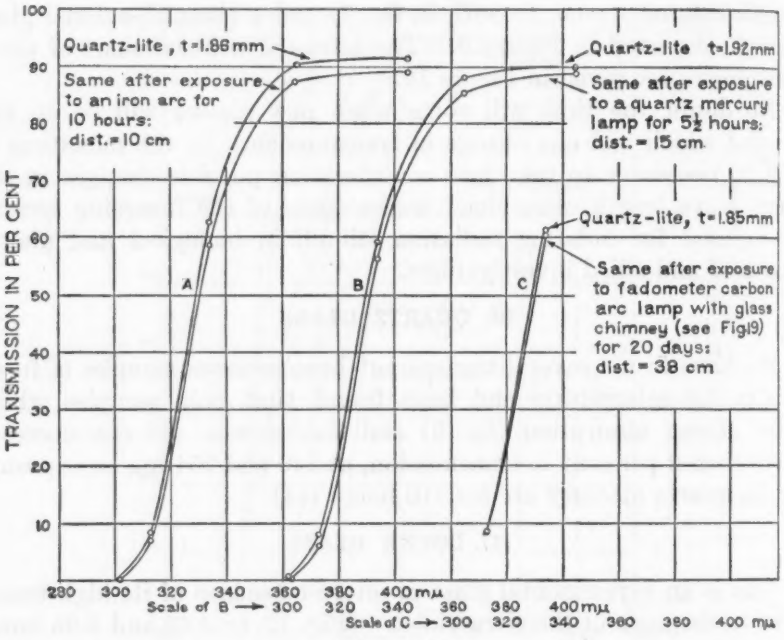
TRANSMISSION IN PER CENT
100
90
80
70
60
50
40
30
20
10
Quartz-lite, t=1.88mm
Same after exposure to an iron arc for 10 hours: dist.=10 cm
Quartz-lite t=1.92mm
Same after exposure to a quartz mercury lamp for 5½ hours: dist.=15 cm
Quartz-lite, t=1.85mm
Same after exposure to fadometer carbon arc lamp with glass chimney (see Fig.9) for 20 days: dist.=38 cm
A
B
C
290 300 320 340 360 380 400mμ
Scale of B → 300 320 340 360 380 400mμ
Scale of C → 300 320 340 360 380 400 mμ

FIGURE 13

mission through this glass. The ultra-violet rays of wave lengths less than 302 mμ do not penetrate deeply into it and the photochemical action is mainly in the production of a greenish-brown color at the surface of the glass. The color is best observed by viewing the interior of the glass by looking at it edgewise, at a grazing angle of emergence of the rays.

The results of these tests show that exposure of this glass to ultra-violet rays from artificial sources does not increase its transmission, but, under certain conditions the transmission is appreciably decreased. Exposure to the sun does not appear to change the transmission appreciably.

The infra-red transmission of Quartzlite is illustrated in Figure 14 from which it may be seen that, for the same thickness, its transparency does not differ appreciably from that of common window glass.

13. WINDOW GLASS AND BOTTLE GLASS

Common window glass which is not decolorized decreases a little in transmission in the ultra-violet on exposure to the quartz mercury arc lamp. (Fig. 9.)

Common window glass and bottle glass differ only in composition to the extent that in the latter the greenish color, which is caused by the presence of iron as an impurity, is removed by some decolorizer;

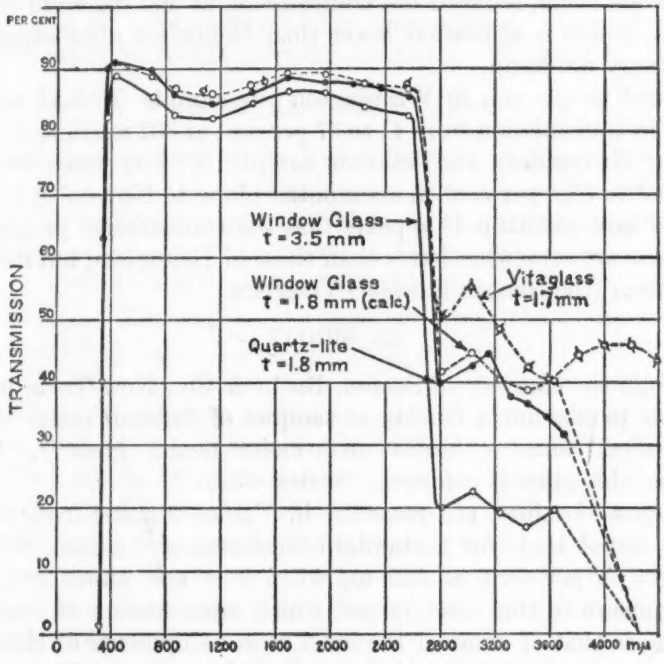

FIGURE 14.—*Infra-red transmission of window glasses*

for example, manganese or selenium. The effect of ultra-violet solar radiation in producing an amethyst color in a bottle glass, which presumably was decolorized with manganese, is shown in Figure 3 which gives the transmission curves of two fragments (ground and polished to a thickness of 2.22 and 2.60 mm, respectively) of a flat-walled glass bottle, picked up some years ago on the mesa at Flagstaff, Ariz. The material had a deep amethyst color, and as shown in the dotted curve (ooo) in Figure 3, the amethyst color of the thicker sample was still further increased by exposure to the quartz mercury arc lamp.

In Figure 9 is shown the spectral transmission of a polished piece of glass from a milk bottle which was probably decolorized with

selenium. Exposure to the mercury arc seemed to affect only the surface which became yellowish-brown as viewed edgewise. This lowers the transmission throughout the visible and the ultra-violet spectrum.

14. HOLVIGLASS

This glass is a recent production, made by the Holophane Co. (Ltd.), London. The sample examined ($t=2.47$ mm, fig. 12) had a transmission almost identical with that of the sample of cathedral Vitaglass ($t=2.3$ mm) illustrated in Figure 2.

An exposure of 10 hours, at a distance of 15 cm from a quartz mercury arc lamp, reduced the transmission at 302 mμ from 39 to 31 per cent, which is somewhat lower than Helioglass after exposure to the mercury arc lamp.

Exposed to the sun in Washington one sample ($t=2.41$ mm) decreased in transmission from 41 to 37 per cent at 302 mμ in four months (July to November) and another sample ($t=2.47$ mm) decreased from 39.2 to 35.5 per cent in six months (June to November). From the data now available it appears that the transmissive properties of Holviglass are somewhat lower than those of Helioglass, but decidedly higher than (the smooth finished) Vitaglass.

15. SUNLIT

Through the courtesy of Semon, Bache & Co., New York, we have been able to examine a number of samples of different melts of a new glass, called Sunlit ("Sunlit ultra-violet health glass"). Viewed edgewise, this glass is colorless, "water white."

The data obtained are recorded in Tables 2 and 4 from which it may be noted that, for a standard thickness of 2.3 mm, this glass transmits 65 per cent at 302 mμ when new and about 39 per cent after exposure to the mercury arc, which transmission is practically the same as that of some of the most recent shipments of Helioglass.

16. NEUGLAS

Through the courtesy of the Vitrea Co. (Inc.), New York, we have been able to examine a number of samples of different melts of a newly developed glass called Neuglas (from the Neue Glasindustr. Gesellsch. Weisswasser, O. L.).

The ultra-violet spectral transmission curve of this (unsolarized) material coincides almost exactly with that of the sample of Corex-D, depicted in Figure 2, the transmission being a trifle lower in the region of 313 to 334 mμ

The transmission of Neuglas at 302 mμ decreases considerably more than that of Corex-D on exposure to the ultra-violet radiation from the quartz mercury arc. As shown in Table 2, the average transmission of the samples of Neuglas examined by us (thickness = 2.3 mm)

is about 63 per cent when new, and decreases to about 49 per cent after exposure of 10 hours to the quartz mercury arc lamp.

17. UVIOL-JENA

Through the courtesy of the Fish-Schurman Corporation, New York, we have obtained data on a number of melts of a new glass called Uviol-Jena.

The transmission curve of this glass coincides closely with that of Helioglass. The transmission at 302 mμ (for $t=2.3$ mm) averages about 58 per cent when new and 43 per cent after exposure to the quartz mercury arc lamp. (Table 2.) The latest importations 52A to 52D have an appreciably higher transmission, averaging 50 per cent after exposure to the mercury arc lamp. (Table 4.)

18. ULTRA-VIOLET GLASS

Through the courtesy of the Ultra-Violet Glass Corporation, New York, we have been able to examine a number of samples of different melts of "Ultra-Violet Glass, U. G." made by the Sendlinger Optical Glass Works, Germany. As shown in Figure 12 the transmission of this glass ($t=2.42$ mm) is identical with the sample of Holviglass just described. Exposed to the mercury lamp the transmission at 302 mμ decreased from 42 per cent to 31 per cent.

A sample from an earlier melt had a much higher transmission, amounting to 57 per cent at 302 mμ ($t=2.1$ mm) which decreased to 49 per cent after exposure to the mercury arc. Exposed to the sun in Washington for four months (July to November) the transmission decreased from 57 to 53 per cent. If this record can be maintained, after the process has been standardized, it will mark a real improvement in glasses for transmitting ultra-violet radiation. Samples of more recent manufacture, however, showed an appreciably lower transmission.

Through the courtesy of the Ultra-Violet Glass Sales Co., Chicago, Ill., we are able to include some measurements on several recently imported samples (Nos. 4, 5, 6, 7, Table 4) of this glass.

19. MISCELLANEOUS NEW GLASSES

As mentioned in the beginning of this paper, progress in the development of new glasses is so rapid that information can be given only on those kinds that are being actively marketed in this country.

Through the courtesy of importers, especially the Hobbs Manufacturing Co., London, Ontario, Canada, we have been able to obtain data on a number of newly developed ultra-violet transmitting glasses of English, French, and German manufacture.

In all of these glasses, as already observed in Helioglass and Vitaglass, the long wave length side of the absorption band extends into

the region of 334 mμ, with transmissions of only 40 to 50 per cent at 302 mμ when new, and 30 per cent down to 20 per cent, or even lower, after complete solarization. None of these glasses have the ideal transmission characteristics of quartz glass, Corex-A, and the Locke glass which have a high transmission at 302 mμ even after solarization.

We have examined at least one sample of each of the following glasses:

Renovic	St. Gobain, Chauney & Cirey, Paris.
Bretlet	Robert Baus, Nuremberg.
Ultravitglas (Sun Ray)	Schmidt's. Gebr. Hirsch & Co., Kunzendorf.
Sanalux	Semon, Bache & Co., New York, N. Y.

All of these glasses with the exception of Bretlet and Renovic have ultra-violet transmission curves similar to that of Helioglass (fig. 2) and, when new, they have a transmission of 5 to 15 per cent at 280 mμ, 45 to 55 per cent at 302 m, and 90 to 92 per cent at 365 mμ.

Exposed to the sun or to the quartz mercury arc, these glasses decrease in transmission, and, after complete stabilization by exposure to the quartz mercury lamp, the transmission at 302 mμ ranges from about 20 per cent for Bretlet and Sanalux, and about 30 per cent for Renovic. More samples of each kind of glass will, of course, be required in order to establish average values. The Neuglas and Sendlinger's Ultra-Violet glass show a distinct advance in the attempts to improve the ultra-violet transparency of window glass. Improvements are also being made in products from the older formulas, as, for example, Helioglass, of which the latest sample examined (in January, 1929) had a transmission of 51 per cent after complete photochemical stabilization by exposure to the quartz mercury arc.

20. DISCUSSION OF RESULTS ON SOLARIZATION

In the foregoing pages data are given on the decrease in transmission of ultra-violet radiation through window glasses and substitutes for window glasses as the result of some undetermined photochemical action on exposure to the sun, and to artificial sources or radiation.

The sources used were the sun, which does not contain appreciable radiation of wave lengths less than about 295 mμ; the carbon arc (without, and with a glass chimney which is opaque to wave lengths less than 310 mμ) which has a fairly continuous spectrum of ultra-violet radiation; and the mercury arc in which the ultra-violet radiation is confined principally to a number of strong emission bands at 254 to 365 mμ. All of these sources lower the transmission of these glasses and glass substitutes, the unfiltered radiation from the artificial sources apparently causing a somewhat greater decrease in transmis-

sion than sunlight. This, however, may be owing to the fact that some of these window glasses solarize but slowly and may not have attained a minimum transmission in the time (one year) allotted for making the test. For example, owing to a prolonged delay in sending the foregoing paper to the printer advantage was taken of this status to include further measurements on the solarization of window glasses that has occurred from November 15, 1928, to July 2, 1929 (an additional exposure of 229 days) when the last measurements were made on glasses which are being exposed to the sun in Washington. A still greater change in transmission would be expected during this same length of time if the exposure had been made in the summer months.

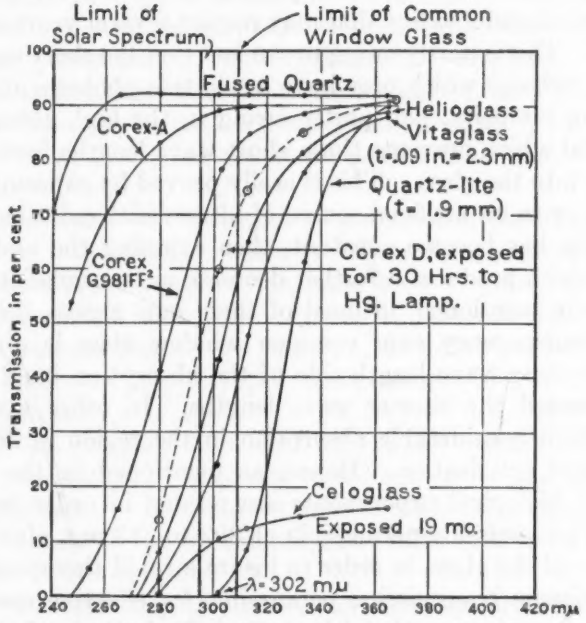

FIGURE 15.—*Ultra-violet transmission of various window glasses after exposure to the sun for 12 months (thickness, t=0.09 inch=2.3 mm)*

These new data, which were obtained on Vitaglass, Helioglass, etc., are indicated, by italics in Tables 4 and 5. All these glasses show a further decrease in transmission, which approaches closely the values obtained by exposure to the mercury arc lamp. (See Table 4, Vitaglass 1h; Helioglass, 5h, 7h; Holviglass, 1; and Sunlit, 3.)

From this it appears that in the course of a few years the photochemical stabilization by solarization will be fairly complete, when the transmission will differ but little from that resulting from exposure to the quartz mercury or carbon arc lamp. This is, of course, in agreement with the observations already described on a sample of Vitaglass which was taken from a hospital window after a year's

use. On further exposure to the mercury arc lamp the transmission of the sample decreased but little showing that the photochemical stabilization by exposure to sunlight was practically complete. It shows also that the photochemical stabilization by exposure to the sun is practically the same as that produced by the accelerated stabilization by exposure to the unfiltered radiation from the mercury, or the white flame carbon arc lamp, provided that sufficient time is given for the sun's rays to complete the photochemical reaction.

In other words, the photochemical reactions, produced by these three sources of ultra-violet radiation, are brought about by such a wide range of wave lengths that the carbon and the quartz mercury arcs may be used to bring to completion, in a relatively few hours, a photochemical stabilization that may require several years of exposure to the sun. This is partly owing to the fact that the short wave lengths (less than 290 mμ) which may have a selective photochemical action, are weak in intensity, and partly owing to the high absorptivity of the material which prevents these short wave lengths from penetrating deeply into the glass. This is easily proved by exposing the glass to the sun or to an artificial source of ultra-violet radiation until the transmission has become constant, then exposing the under side of the glass which produces a further decrease in transmission.

As already mentioned, in most of these new glasses the improvement in transparency over common window glass is obtained by shifting the long wave length side of the absorption band at 290 to 310 mμ toward the shorter wave lengths. In other words, these glasses exhibit considerable absorption in the region of 302 mμ, especially after solarization. Hence, as mentioned in the preceding report (45) biological experiments are needed in order to establish the lowest transmission permissible at 302 to 313 mμ, after complete solarization of the glass, in order to insure a rapid therapeutic action.

The minimum transmission permissible for effective results manifestly will depend upon the altitude and the latitude of the station. Evidently the most transparent glass available will be required in our northern latitudes where the activating rays are of low intensity, while in localities where sunshine is abundant a glass having a lower transmission may prove satisfactory. The first requirement is therefore a source (or locality in the case of sunlight) having sufficient ultra-violet to prevent rickets; the second requirement is a satisfactory glass to transmit these rays; and the third requirement is proper care of the glass, to keep it clean. It requires but little dust and dirt to reduce the transmission by 40 to 50 per cent. For example, two samples of glass which had been used as windows in an animal house for three months, and which transmitted 17 and 24 per cent, respectively, at 302 mμ before washing increased in trans-

mission to 28 and 40 per cent, respectively, after washing, showing the importance of keeping the windows clean.

The reaction is evidently photochemical involving the presence of a chemically unstable material (especially ferrous iron) as an impurity (46). It is therefore to be expected that different sources may produce different photochemical reactions (at least different amounts of the same kind of reaction), which will continue so long as there is material present that will undergo a photochemical change and so long as the opacity has not increased sufficiently to prevent the rays of various wave lengths from penetrating into the material. As just mentioned, this is easily observed by exposing first one side then both sides of a piece of glass to the arc lamp or to the sun, or by exposing two superposed pieces of glass (say Vitaglass or Helioglass) of single thickness, which is practically equivalent to a piece of glass of double thickness. It is then observed that the transmission of the lower piece (which corresponds practically to the lower half of the thick piece) has decreased far less than that of the upper piece.

That the amount of this impurity and, hence, the amount of depreciation in transmission, varies greatly is shown by the fact that samples of different melts of the same kind of glass, having practically the same thickness, differ greatly in transmission. (Table 4, Helioglass, sample No. 12, $t=1.95$ mm, tr.$=42.5$ per cent; sample No. 4, $t=1.99$ mm, tr.$=61.7$ per cent; sample No. 7, $t=2.00$ mm, tr.$=58$ per cent.)

Our tests on Vitaglass show that after what appears to be a fairly complete solarization by exposure to the sun, when the transmission at 302 mμ is down to 20 to 25 per cent an additional exposure to the mercury arc reduces the transmission but little further—18 to 22 per cent. (See Tables 4, 5, and 7.)

In the case of Helioglass (and other recently introduced glasses which solarize but slowly) we have not yet had samples exposed to the sun for a sufficient length of time to make certain that solarization was complete. Extrapolation of the upper curve in Figure 8 indicates a probable minimum transmission of 38 to 40 per cent, whereas, an exposure to the mercury arc reduces the transmission to 39 per cent. From the data given in Table 4 it may be noticed that the unfiltered radiation from the mercury arc reduces the transmission to a value between 35 and 40 per cent, which is about 8 per cent lower than that resulting from exposure to the sun, which from Figure 8 is probably not the minimum.

In the case of the Corex-D and several other newly developed glasses the minimum transmission at 302 mμ, after photochemical stabilization by exposure to the mercury arc, is decidedly higher than that of Vitaglass and Helioglass. After taking into consideration

the great variation in the transmission, at 302 mμ, of various melts of the same kind of glass it seems misleading to make close comparisons in transmissions. Hence, whether we solarize these glasses by exposure to the sun or obtain the photochemical stabilization by exposure to an artificial source of radiation (the mercury arc) containing ultra-violet rays of wave lengths not present in sunlight, the same relative transmissions are obtained. The data presented show also that it is possible to make a glass that will not decrease appreciably in transmission on exposure to the mercury arc or the sun.

It is to be noted that as the result of solarization, the transmission decreases to a permanent value, which, in some of these glasses, is only about one-half the transmission when new. In some of these glasses the transmission, after solarization, is higher than that of the unsolarized earlier products, showing the progress that is being made in the production of glasses having a high transmission of ultra-violet radiation.

In conclusion, it may be stated that, owing to the slowness of some of these glasses in coming to photochemical equilibrium on exposure to the sun, it will require several years to determine whether the accelerated test is too severe. However, the outstanding difference in transmission between the samples of glass subjected to the accelerated test and the duplicate samples which were exposed to the sun is too small to take into consideration. Moreover, all the various makes of glass are comparable on the same basis, whether by accelerated aging with the mercury arc, the carbon arc, or by solarization by exposure to sunlight when the latter exposure is sufficiently prolonged.

IV. EFFECT OF SOLARIZATION UPON THE ULTRA-VIOLET TRANSMISSION OF SUBSTITUTES FOR WINDOW GLASS

Under this caption are given data on the spectral transmission of substitutes for window glass, especially windows for transmitting ultra-violet solar radiation into animal inclosures, hothouses, cold-frames, solariums, etc. Only one material, Celoglass, was extensively investigated for resistance to ultra-violet radiation and the weather.

1. FLEXOGLASS

This material (sometimes called glass cloth) consists of a loosely woven cotton cloth (cheesecloth, millinette) which is impregnated with paraffin. The amount of paraffin on the cloth is variable. Hence, the discussion of the optical properties is applicable only in a general way to this material.

Owing to internal reflection among the fibers of the Flexoglass the loss by reflection to the outer surface, facing the sun, is high. As a

result, the total amount of radiation transmitted to the interior of the inclosure is rather low. By placing the sample directly over the thermopile receiver it was found that about 35 per cent of the incident ultra-violet light from a quartz mercury arc (filtered through Corex-G. 986A) was diffusely transmitted. This value increased as the material softened and became more translucent when it became heated—a property that is observed when the cloth is exposed to the sun.

In Figure 16 is given the spectral transmission of the radiation traversing linearly through the cloth which was placed over the entrance slit of the spectrometer. This reduces the total intensity by a greater amount than would be observed when the sample is placed over the thermopile at the exit slit (29). But the latter procedure is subject to errors from heating of the material by the absorbed radiation (which material then radiates to the thermopile) and by diffuse light

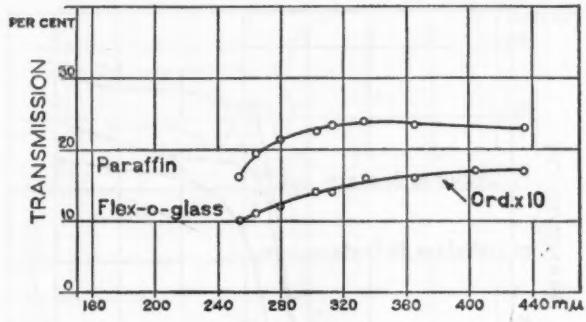

FIGURE 16

from the adjacent part of the spectrum which passes through the exit slit and falls upon the thermopile.

As shown in Figure 16, a thin layer of solid paraffin (between two plates of quartz) is uniformly transparent throughout the ultra-violet part of the spectrum which is of interest in therapeutic work. A similar uniform but much lower transmission (fig. 16) was observed through (the interstices of) the Flexoglass cloth.

Whether the amount of ultra-violet solar radiation transmitted by this material is sufficient for therapeutic purposes, especially in the winter when these activating rays are most needed, is a problem in biology that will require further investigation. The tests already made (30) seem to show that the transmission of the activating solar radiation is too low to be useful therapeutically and that because of its tendency to soften in the sun, and hence, retain dust, this material is to be considered primarily only as an inexpensive temporary protection for use in animal husbandry in winter.

2. CELOGLASS

The material sold under this trade name consists of a film (of variable thickness) of cellulose acetate on a wire mesh. The solvents of cellulose commonly used are acetone, ethyl lactate, and triphenyl phosphate.

In the material now on the market the wire mesh obstructs about 30 per cent of the incident light. Hence, not taking into account absorption and internal reflection in the cellulose film, the maximum amount that can be transmitted through Celoglass (cellulose acetate) is only about 60 per cent of the incident solar radiation. In the visible, and in the long wave length ultra-violet, where there is but little selective absorption, the observed transmission is fairly uniform, amounting to about 35 to 45 per cent at 400 mμ, depending upon the thickness of the film. The difference between the observed (35 to

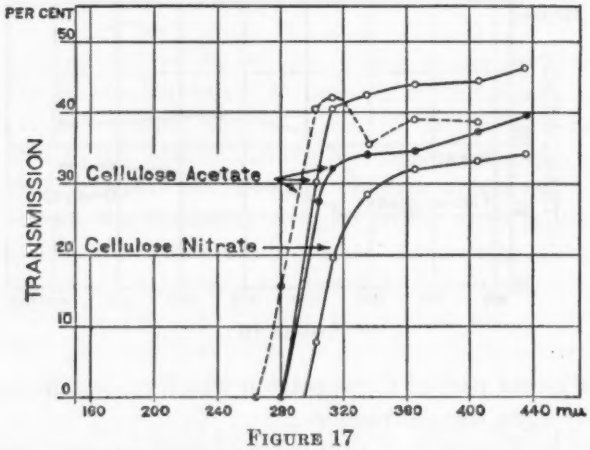

FIGURE 17

45 per cent) and the calculated value (60 per cent) is to be ascribed to absorption and diffusion of the light.

The cellulose material examined was the nitrate and the acetate. The cellulose nitrate was brittle and as shown in Figure 17, even when new, it was practically opaque to wave lengths less than 300 mμ. The cellulose acetate was less brittle and it was transparent to 280 mμ in the ultra-violet. In a previous paper (31) we have given the transmission of thin homogeneous films of pure cellulose (viscose rayon) and cellulose acetate (celanese rayon). In that paper it is shown that pure cellulose has a high transmission throughout the ultra-violet to 250 mμ. (Fig. 18.)

As shown in Figures 17 to 23, when new, Celoglass (cellulose acetate film) transmits, rectilinearly, 25 to 35 per cent at 302 mμ, and, hence, an average of about 25 per cent of the total incident vitalizing ultra-

violet solar rays which are absorbed by window glass. This average value of 25 per cent refers to the rays that are not deviated from their original direction in passing through the material. The total amount passing through the Celoglass, including the (scattered, diffused) rays deviated from their incident path would be about 5 per cent higher, or an average transmission of 30 per cent at 302 mμ. (See Table 2.) This was determined by the screen method described in B. S. Jour. Research (RP6), 1, p. 105; 1928; in which the wave lengths of about 365 mμ were isolated by means of a filter of Corning glass, G586J. In this manner it was established that the total amount

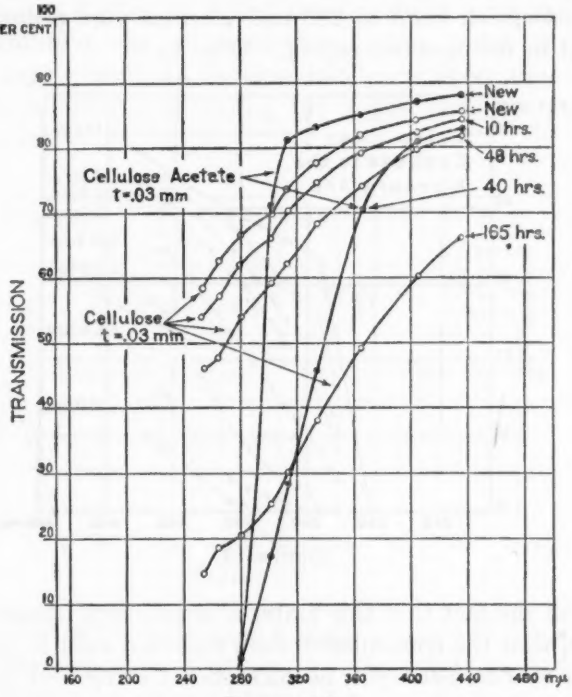

FIGURE 18

of radiation transmitted diffusely through Celoglass (average of five samples) was 52 per cent, whereas only 40 per cent of the rays of wave lengths 365 mμ were transmitted directly into the spectrometer.

As shown elsewhere (29) in cases where great optical homogeneity and freedom from scattering of the light is not essential, the amount of vitalizing rays transmitted by this material (at least when new) is sufficient to have a beneficial effect in animal husbandry. However, the transparency is greatly decreased by the deposition of dust, and, hence, the length of time that a given sample of this material can be used on animal houses will depend upon the prevalence or absence of dust.

We have found considerable variation in ultra-violet transmission of different samples of this material, when new; also a difference in their behavior when exposed to sunlight and to artificial light.

Early in this investigation it was found that there is a marked difference in the aging of Celoglass depending upon the method of acceleration, whether (*a*) by exposure to artificial light, (*b*) by exposure to direct sunlight, or (*c*) by exposure to the weather, day and night, either under the eaves of a building or directly in the open.

In the sunlight tests it was observed that, when first exposed, some of the samples increased somewhat in transparency at 280 mμ. This is, no doubt, owing to the evaporation of the solvents which have a strong absorption band at 280 mμ, whereas pure cellulose is fairly transparent in this spectral region. (Fig. 18.)

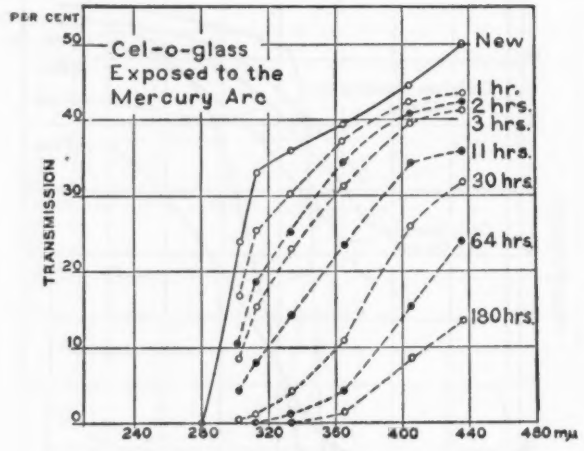

FIGURE 19

In view of the fact that this material is not very homogeneous it is to be noted that the transmission data recorded refer to the rays that entered the spectrometer slit, no correction having been made for the loss by scattering.

(a) ACCELERATED AGING UNDER ARTIFICIAL LIGHT

As just mentioned the accelerated aging of Celoglass, by exposure to the quartz mercury arc, which is strong in ultra-violet rays not present in solar radiation, is different from the photochemical aging that results from exposure of this material to sunlight. These short wave length ultra-violet rays produce a rapid photochemical change in the cellulose compound so that an exposure of a few hours reduces the ultra-violet transmission to practically zero, and, hence, the material is but little better than common window glass, although to the eye the color developed is barely perceptible. On further exposure

the cellulose is tinged a yellowish brown. This change in transmission is illustrated in Figure 19 which is interesting in showing the rapid decrease in transmission in the short wave lengths, whereas in the long wave lengths the decrease in transmission with age is less rapid. This effect is practically the same for the cellulose nitrate and cellulose acetate films on the wire mesh and is in agreement with previous observations (32) of the effect of ultra-violet light upon films of cellulose.

(b) EXPOSURE TO SUNLIGHT

In this test the samples were mounted side by side on a block of wood and exposed at normal incidence to the solar rays between the hours of 9 a. m. and 4.30 p. m. during the months of April to October, 1927. The mounting was adjusted several times a day in order to maintain the rays closely at vertical incidence upon the samples. During cloudy weather and during the night these samples were kept in the laboratory.

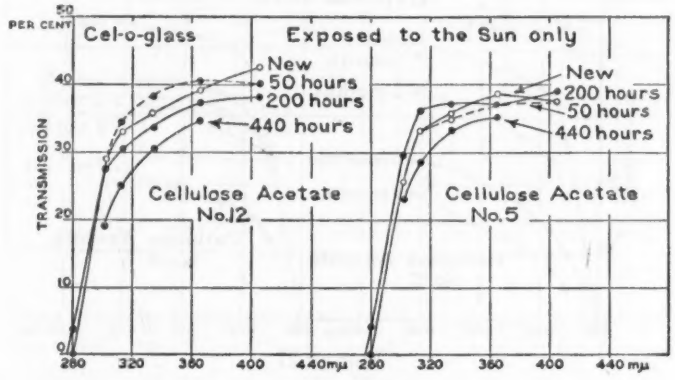

FIGURE 20

As shown in Figure 20, aside from a slight increase in transparency at 280 mμ, on first exposure, which is no doubt owing to evaporation of the solvent, exposure to sunlight has only a slow action in decreasing the transparency of (Celoglass) cellulose acetate. It is interesting to note that after 200 hours' exposure of the Celoglass to sunlight the accelerated aging under the mercury arc continued in the same manner as on samples which had not been seasoned in the sun.

(c) EXPOSURE TO THE WEATHER

The effect of varying weather conditions upon the transparency of Celoglass is clearly illustrated in Figure 21 which shows the change in transmission of two samples (Nos. 5 and 9) of cellulose acetate exposed side by side continuously day and night at an angle of 45°, facing south, from April 1 to December, 1927. From this illustration and Figure 20 it may be seen that sample No. 5, which was not

greatly affected by sunshine, decreased continuously in spectral transmission when exposed to the weather day and night, and, hence, probably became valueless for transmitting ultra-violet therapeutic rays after nine months' usage. In contrast with this is sample No. 9 (also a cellulose acetate) which changed but little in ultra-violet transmission during the first five months of exposure to the weather. This, however, was an unusual sample which, on first exposure to the mercury arc lamp, decreased in transmission to a constant value, at which level it remained even after prolonged exposure to the lamp.

On further exposure to the weather this sample showed a marked decrease in transmission, probably owing to accumulation of dust and smoke, which increased in the fall and winter months.

In Figure 22 is shown the effect of aging upon a Celoglass sample No. 6 which was exposed continuously and simultaneously with samples Nos. 5 and 9 (fig. 21), but in another part of the city which

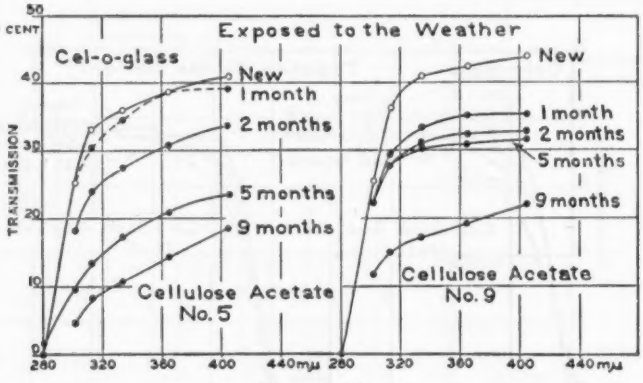

FIGURE 21

was free from dust, smoke, etc. In this case, after three months' exposure, the transparency of sample No. 6 at 280 mμ was actually higher than when new, although there was a decrease in transmission in the longer wave lengths. The explanation given to us by a competent authority is that the whitish (powdery) film which forms on the surface of the cellulose acetate when exposed to the weather is blown away by the wind, thus decreasing the thickness of the film. This probably accounts for the fact that after an exposure for nine months to the weather this sample was full of holes.

In addition to the decrease in thickness, we have to consider also the evaporation of the solvents (fig. 20), which have a high absorption for wave lengths less than 300 mμ.

In contrast with the samples (fig. 20) which were exposed only to the sun, in Figure 23, sample No. 3 shows the effect of exposing the material in a locality free from dust, in the south window of a large building with overhanging eaves and window frames so that but little,

if any, rain fell upon the Celoglass. In this sample the transmission changed but slowly after being exposed two months, and even after nine months, judging from biological tests (29) the transmission (23 per cent at 302 mμ) is still sufficiently high to be useful for therapeutic purposes. After an exposure through 2 summers (19 months) the transmission at 302 mμ was 10 per cent. From this it may be seen that when used on the side of a building having a wide overhanging roof the deterioration of Celoglass by the weather is greatly retarded.

In Figure 22 is shown the spectral transmission curves of new and of old samples of cellulose nitrate which had been exposed to the weather and then submitted to us for examination. The cellulose nitrate, especially after esposure to the weather for two months, does not appear to transmit sufficient ultra-violet (see fig. 17 for another sample) to be of interest therapeutically, and hence need not be discussed.

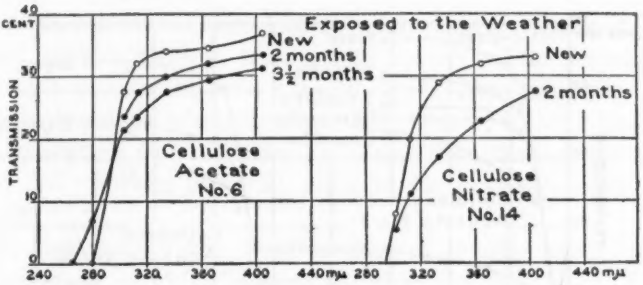

FIGURE 22

In Figure 23 the Celoglass sample No. 13 is of interest because sample No. 13–C, which had been out in the weather for four months, and had become covered with dirt, was more opaque than the fairly clean sample, No. 13–B (said to have been taken from the same roll as No. 13–A) which had been exposed for two years. While this may seem anomalous it is easily explained on the basis of the presence or absence of dust and smoke in the atmosphere and of the amount of protection from overhanging eaves, etc., as we have found by actual test.

From the foregoing tests, on material placed out of doors only on clear days it is shown that direct sunlight has only a slow effect upon the aging of Celoglass. On the other hand, the combined effect of sunlight and the varying atmospheric conditions (also dust) have a marked effect in decreasing the ultra-violet transmission of (Celoglass) cellulose acetate. As a result, the transmission of ultra-violet solar radiation of short wave lengths is greatly decreased (fig. 15) and in some cases the material probably becomes valueless for therapeutic purposes.

In view of the fact that it is recognized that summer weather deteriorates this material, it is recommended to be used in poultry houses, etc., during the winter months, and removed during the summer months.

3. CELLOPHANE

As shown in Figure 18 pure cellulose (viscose rayon, cellophane, protectoid) is highly transparent throughout the ultra-violet. Recently Pfund (33) has proposed the substitution of cellophane in place of the usual window glass. For this purpose he suggested using large sheets of the material which are to be mounted between two pieces of wire mesh.

Our tests show that cellophane undergoes a large shrinkage (8 to 12 per cent) on exposure to the weather for a few months. Hence, it will be necessary to provide for this decrease in size, if it is to be used in frames as described by Pfund.

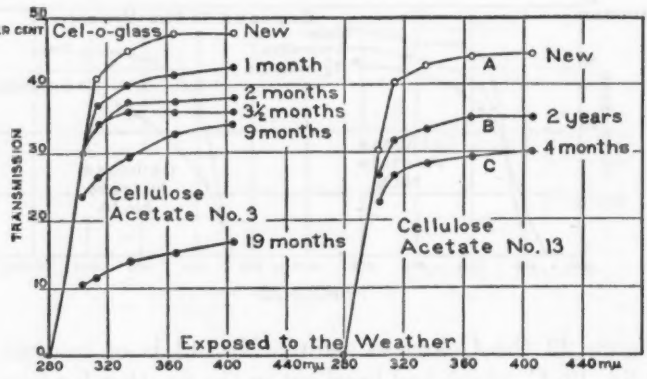

FIGURE 23

Cellophane appears to solarize, but slowly, on exposure to the weather. In fact, owing to evaporation of the solvent or plasticiser the transmission may actually increase during the first few weeks of exposure; for example, one sample, 0.14 mm in thickness, that was exposed from July to October, 1928, shrank about 12 per cent in length and increased in transmission from an initial value of 38 to a final value of 58 per cent at 302 mμ.

4. POLLOPAS, ALDUR, GELATIN

The newly discovered condensation products of formaldehyde and urea (trade names Pollopas, Aldur) when entirely colorless have a high transmission throughout the ultra-violet (34). However, a slight brownish discoloration introduced in the preparation of the material, or as the result of solarization, greatly reduces the transmission in the ultra-violet.

The sample of Aldur examined by us had a fairly high transmission (about 32 per cent for $t=2.5$ mm, surface uneven) at 302 mμ.

Recently Crist (35) published data on a sample of Aldur (36) 3 mm in thickness, which transmitted about 66 per cent at 302 mμ. Exposure to the mercury arc for 18 hours reduced the transmission at 254 mμ from 48 to 40 per cent.

Recently we have tested the transmission of a film of a gelatin product, mounted on a wire mesh, similar to Celoglass. The material examined had a transmission similar to that of cellophane (fig. 18) with a characteristic absorption band at 280 mμ with a high transmission at 250 mμ. Whether gelatin has any weathering qualities was not determined.

5. TRACING CLOTH

In view of the publicity given to the discovery that ordinary tracing cloth transmits short wave length ultra-violet radiation, tests were made on this material.

Tracing cloth consists of thin, loosely woven fabric of linen or cotton impregnated with a soluble, transparent starch. The drawback in the use of such a material, as a window, is the high solubility of the sizing, which dissolves when touched with water, leaving the cloth in a rough condition which is then no better than that of other thin, bleached, loosely woven material, such as, for example, nainsook or balloon cloth.

We have determined the transmission of tracing cloth by the methods described in B. S. Research Paper No. 6 (vol. 1, p. 105; 1928), and find that the total ultra-violet of wave lengths 250 to 310 mμ diffusely transmitted through a new sample of tracing cloth amounted to 25.9 per cent before wetting the glossy surface, and 14.2 per cent after removing the sizing and drying the cloth. In the publication just cited (B. S. Research Paper No. 6, Table 1) are recorded the ultra-violet transmissions of a sample of balloon fabric (tr.=21 per cent), of batiste (tr.=16 per cent) and of nainsook (tr.=31 per cent) showing that tracing cloth is not superior to other fabrics for use as a window for transmitting ultra-violet radiation.

V. CONCERNING THE USE OF WINDOWS

In a foregoing caption it was deduced that for air mass $m=1$, the amount of short wave length ultra-violet solar radiation that has the property of preventing rickets amounts, at the most, to perhaps about 0.004 g cal./cm^2/min.

This is an appreciable amount when considered in terms of full sunlight at the noon hour in summer. Within a properly constructed solarium, glazed with the most transparent material obtainable (quartz glass), about 90 per cent of the 302-region of ultra-violet

solar radiation (or about 0.0036 g cal.) would be transmitted in the summer and, owing to the greater air mass ($m=2.5$) traversed, less than 10 per cent of this value (less than 0.00036 g cal.) would be available in winter. (Fig. 1.)

The question of the amount of skylight and sunlight that can enter through a vertical opening (a window of a house) is important to the house owner. In this connection the curves published by Kimball and Hand (17) showing the amount of sunlight and daylight coming through a vertical opening (a window), on all sides of a house, at different hours of the day and different seasons of the year, are especially instructive and worthy of study by architects and heliotherapists.

From our direct measurements, supplemented by the photometric measurements of Kimball and Hand, we deduce that, in the wintertime (December), the maximum amount of short wave length ultra-violet solar radiation that can enter a vertical opening (a window glazed with quartz glass) facing south would be less than 0.00036 g cal./cm²/min., and through a north window it would be less than 0.0001 g cal./cm²/min., decreasing, of course, to an imperceptible amount at sunrise and at sunset. For, as shown by Pettit, (18), at Mount Wilson, it is only during the five or six hours through the middle of the day that an appreciable amount of these activating rays is transmitted through the atmosphere. He has photographed the solar spectrum down to 293 mμ (47).

In this connection, it is relevant to cite some of our direct measurements on the ultra-violet radiation from the north sky, which were made by Method IV (but using a 12-junction Bi-Ag thermopile) described in a preceding caption. On an exceptionally clear, cloudless day (March 18, 1929, see fig. 1) at the noon hour the short wave length ultra-violet from (85° of) the north sky, amounted to 0.00029 g cal./cm²/min., as compared with 0.0033 g cal./cm²/min. from the direct solar radiation, or about one twenty-fifth of the short wave length ultra-violet in June. (Fig. 1.)

The shortest wave length observed in December by Dorno (19) at Davos, Switzerland (elevation 5,300 feet), was at about 308 mμ. He found that the short wave length ultra-violet solar radiation at midday in July, as measured with a cadmium photoelectric cell, was ten times greater than in January—in agreement with the thermocouple measurements in Figure 1. The advantage of the thermocouple over the photoelectric cell is in the ease with which it can be calibrated to obtain the measurements in absolute value.

Recent investigations by Bundesen (20) and his collaborators show that in our smoke-laden cities but little ultra-violet radiation of wave lengths less than 297 mμ is transmitted to the earth's surface in

summer, while in the three winter months the shortest wave length transmitted was at about 303.5 mμ.

Owing to the difficulties in preventing fogging of the photographic plate on long exposures, it is difficult to photograph the extreme limit of the solar spectrum. However, sufficient data appear to be at hand to show that even at the noon hour in winter but little, if any, ultra-violet solar radiation of wave lengths less than about 305 mμ is transmitted to the earth's surface, especially in large industrial cities.

If, in addition to atmospheric absorption, the rays must pass through a glass which transmits only 25 to 30 per cent of these rays (or less than about 0.0001 g cal. through a north window) the intensity appears to be close to the threshold value for therapeutic purposes. This conclusion follows from the observations of Tisdall and Brown (21), who obtained practically no healing effects from the light of the sky at a distance of 3 feet or more from an average-sized window, under conditions similar to those found in the average home.

Their observations, which were made in August, show that in the latitude of Toronto (43.6°) the light of the sky shining through an ordinary-sized window, whether glazed with special glass or covered with ordinary fly screen, had practically no effect in preventing rickets in animals except immediately adjacent to the window (that is, an exposure to the whole sky), and that in order to obtain real benefit it is necessary to receive the direct rays from the sun. Furthermore, they found (22) that, while during the winter months (December, January, and February) the ultra-violet rays produced a slight, but definite antirachitic effect (which was only about one-eighth as great as in April and May), the use of special window glasses in that locality during the winter months is probably of little value. As is to be expected, their work shows that in order to obtain a useful antirachitic effect from sky shine (that is, solar rays reflected from the sky and clouds) approximately equal to that of the direct rays of the sun, it is necessary to construct a solarium of special glass which will admit rays from a large part of the sky.

The most recent and important data, which, no doubt, will settle the question of placing windows of special glass on the north side of school and office buildings, were published by Clark (23). The observations were made in a large room on the seventh floor with a north exposure. During perfectly clear days, at noon, in March and April, when the illumination from the hemisphere of north sky incident upon the window sill was approximately 400 foot candles (in good agreement with the measurements of Kimball and Hand, already mentioned), the illumination in the center of the room, 5 m from the window was 10 foot candles. The conclusion was that if the room were equipped with ultra-violet-transmitting glass windows, a child,

located in the center of the room, would have to sit there for 20 hours in order to obtain as much untra-violet radiation as it would receive in two minutes out of doors in sunlight at the noon hour. In May, it would be necessary to sit there for 15 hours in order to get the equivalent of two minutes of direct noon sunlight. But since only during five to six hours at midday an appreciable amount of ultra-violet is transmitted through the atmosphere, it would be necessary to sit for three days to obtain the benefit of two minutes of direct noon sunlight. The usefulness of such glasses in solariums is admitted, but Doctor Clark states that a better solution of the problem is to get out of the schoolroom and the office at the noon hour.

Further evidence supporting these conclusions was recently published by Eddy (24) who found that, in order to prevent rickets, the animals under test had to be kept directly in the path of the sun's rays. Those animals that were 1 m or more from the window, or close to the window, but outside of the path of the sun's rays developed rickets.

All the evidence available at present indicates that for the treatment of invalids a solarium glazed with special window glass is necessary in order to obtain beneficial results in preventing rickets and presumably for general therapeutic purposes.

During the year, and during the day, the sun's rays vary greatly in their angle of incidence upon the solarium. In this connection it is of interest to determine the loss of light by reflection from the surface and the loss by absorption in traveling through the glass, both of which increase with the angle of incidence.

The results of this inquiry show that for normal incidence of the solar rays, the loss by reflection amounts to a little less than 10 per cent, increasing to about 12 per cent for an angle of incidence of $i=45°$, about 15 per cent for $i=55°$, and about 20 per cent for $i=60°$. Similarly the optical path of a glass 2.0 mm in thickness and having a refractive index of $n=1.56$ is about 2.2 mm for an angle of 45° and about 2.40 mm for $i=60°$. Since, for glasses which transmit 30 to 50 per cent of the vitalizing rays, an increase in thickness of 0.1 mm increases the absorption by about 1.2 per cent, the maximum increase in absorption of the glass would amount to about 5 per cent. Hence, the additional loss by reflection and absorption at the maximum angle of incidence as compared with that at normal incidence, would be about 25 per cent (certainly less than 30 per cent) which is of minor importance in comparison with the question of keeping the glasses clean, and other factors, such as dust and smoke, which greatly absorb the vitalizing rays.

In connection with the foregoing discussion, it is relevant to include data on the use of heavy, wired glass, which is of importance for safety in the case of breakage, when used on a sloping roof. From

calculation on samples of glass which, for a thickness of 2.3 mm, transmit only 20 to 30 per cent, and from direct observations it is found that thick (6 mm, one-fourth inch wired) samples of this type of glass transmit only 3 to 5 per cent at 302 mμ. In a previous communication (25) it was shown that this transmission is too low for biological use. Hence, if thick samples must be used, for safety, then it is necessary to use material that has little or no absorption at 302 mμ. Otherwise, it will be necessary to use single thickness (2.3 mm = 0.09 inch) glass backed with a 1 cm wire mesh which shuts out about 10 per cent of the total light.

Another item usually overlooked in connection with the usefulness of these glasses is the importance of keeping the surfaces clean and free from dust. It requires but little contamination of the surface of the glass to decrease the transmission by 10 per cent or even more. For example, the unwashed parts of samples obtained from an animal house in a zoological park transmitted only 30 to 40 per cent as much as the adjacent parts that were cleaned before examination. When one considers that after solarization some of these glasses transmit only 20 or 30 per cent, it is evident that the windows must be kept clean in order to obtain beneficial results, especially in northern latitudes and in smoke-laden cities where the ultra-violet solar rays are almost entirely absorbed, especially in the wintertime when most needed.

This conclusion is based upon a study of a report issued by the Council of Physical Therapy (26) of the American Medical Association, which shows that only those glasses and glass substitutes which had a transmission of 30 per cent, or higher, at 302 mμ gave an appreciable protection against rickets, but this protection was not 100 per cent.

Recently we have tested an ultra-violet transmitting glass which was used in front of a carbon arc lamp to shut out the rays of wave lengths less than 280 mμ. After 300 hours' use, it was observed that the patients, who were being irradiated by this lamp, no longer responded properly to the light treatment. Our tests showed that the glasses, which were 2.6 to 2.7 mm in thickness, transmitted only 15 to 20 per cent at 302 mμ (Table 7), in comparison with about 45 per cent when new. The conclusion seems inevitable that this loss in therapeutic efficiency was owing to the decrease in transmission of the special window glass by the action of the ultra-violet rays.

Further evidence on this question is contained in a communication by Wyman (27) in which he shows that only glasses having a high transmission (for example, Corex-A and fused quartz) admitted sufficient ultra-violet solar radiation for the rapid improvement of rickets in children in Boston during the wintertime.

As mentioned elsewhere in this paper, in most of these new glasses the improvement in transparency over common window glass is obtained by shifting the long wave length side of the absorption band at 290 to 310 mμ toward the shorter wave lengths. Moreover, for glasses 2.3 mm in thickness and transmitting 30 to 50 per cent, a change in thickness of only 0.1 mm changes the transmission by about 1.2 per cent. Many of these glasses exhibit considerable absorption in the region of 302 mμ, especially after solarization. Hence, as mentioned in the preceding report (28), biological experiments are needed to determine the lowest transmission permissible at 290 to 302 mμ in order to obtain a rapid therapeutic action. In this connection the recent tests of Caldwell and Dennet (50) in New York City may be cited. They find that, as a preventative measure, exposures must be made in the direct path of the sun's rays.

The minimum transmission permissible for effective results manifestly will depend upon the altitude and the latitude of the station. Evidently the most transparent glass available will be required in our northern latitudes where the activating rays are of low intensity, while in localities where sunshine is abundant a glass having a lower transmission may prove satisfactory. The first requirement is therefore a source (or locality in the case of sunlight) having sufficient ultra-violet to prevent rickets; the second requirement is a satisfactory glass to transmit these rays; and the third requirement is proper care of the glass, to keep it clean.

In view of the misconceptions regarding the properties of window glasses it is relevant to add that these new window glasses possess no mysterious healing powers, and that no window glass, or substitute for window glass, can add short wave length ultra-violet rays to compensate for those that are lacking in sunlight. On the other hand, as shown in the foregoing pages, a glass window may greatly reduce the intensity of the short wave length ultra-violet rays that are present in sunlight. Hence, whenever it is possible, it is better to utilize direct sunlight instead of that which is transmitted through a window.

VI. SUMMARY

This paper deals with three fundamental questions, (*a*) the amount of ultra-violet in solar radiation of wave lengths less than about 310 mμ, found to be of especial use in preventing rickets, but shut out by common window glass, (*b*) the decrease in transmission that occurs in the newly developed window glasses for transmitting ultra-violet of wave length less than about 310 mμ, when exposed to ultra-violet radiation, and (*c*) the proper use of windows in order to obtain the most effective therapeutic results.

(*a*) By four methods of attack, data were obtained showing that the upper limit of the total amount of ultra-violet solar radiation, of wave

lengths less than about 310 mμ, is less than 0.004 g cal./cm²/min. at sea-level stations.

(*b*) It is shown that nearly all these newly developed window glasses decrease in transmission, especially in the ultra-violet of wave lengths less than 310 mμ, when exposed to the sun and to artificial sources containing ultra-violet radiation. In some makes of glass there is practically no decrease in transmission as the result of photochemical aging; other glasses lose almost one-half their transparency at 302 mμ in the process of photochemical stabilization.

(*c*) Concerning the use of windows, data are given showing that, with variation of the angle of incidence of the solar rays from normal upon the solarium, during the year and during the day, the amount transmitted through the glass decreases by about 20 per cent. The necessity of keeping the glasses clean is indicated by the observations that dust and dirt reduce the transmission at 302 mμ by 30 to 40 per cent.

Double thickness (one-fourth inch, 6 mm) wired glass, even when made of these newly developed materials (except, perhaps, Corex-D and pure quartz glass) after complete photochemical stabilization, transmits only 3 to 5 per cent at 302 mμ, which is probably too low for therapeutic use. Hence, a glass of single thickness ($t = 2.5$ mm), with a wire mesh under it for safety from breakage, is recommended for solarium roofs.

VII. REFERENCES

1. Coblentz, B. S. Letter Circular No. 235 (September 1, 1927); 2d rev., September 29, 1927; 3d rev., January 14, 1928. The present communication supersedes this letter circular.
2. Coblentz, Spectral Characteristics of Light Sources and Window Materials Used in Therapy, I. E. S., convention, Chicago; September, 1927; Trans. Illum. Eng. Soc., **23,** p. 247; 1928. Coblentz, Summary Data on the Transmissibility of Ultra-Violet Radiation through Glasses and Glass Substitutes used for Therapeutic Purposes, Trans. of the Twenty-fourth Annual Meeting of the Nat. Tuberculosis Assn.; 1928. Coblentz and Stair, The Effect of Solarization Upon the Ultra-Violet Transmission of Window Materials, I. E. S. convention, Toronto, September, 1928; Trans. Illum. Eng. Soc., **23,** p. 1121, 1928.
3. Heilbron, Kamm, and Morton, J. Chem. Soc., London, **263,** p. 2000; 1927. Wyman, Am. J. Diseases of Children, **34,** p. 733; 1927. Bills, Honeywell, and Cox, J. Biol. Chem., **80,** p. 557; 1928.
4. Coblentz and Kahler, B. S. Sci. Paper No. 378, **16,** p. 233; 1920.
5. Coblentz, B. S. Sci. Paper No. 413, **17,** p. 187; 1921.
6. Coblentz, B. S. Bull. No. 282, **13,** p. 423; 1916.
7. Hess and Weinstock, J. Am. Med. Assn., **80,** p. 687; 1923; Proc. Soc. Exptl. Biol. and Med., **24,** p. 759; 1927; Hess and Anderson, J. Am. Med. Assn., **89,** p. 1222; 1927.
8. Sonne and Reckling, Hospitalstidend, **70,** p. 399; 1927. See also Maughan Am. J. Physiol., **87,** p. 381; 1928.
9. Coblentz, Trans. Illum. Eng. Soc., **23,** p. 287; 1928.

10. See illustration in Figure 13, of a previous publication by Coblentz, Trans Illum. Eng. Soc., **23,** p. 287; 1928.
11. Coblentz and Kahler, B. S. Sci. Papers No. 378, **16,** p. 235; 1920.
12. Coblentz, B. S. Sci. Papers No. 438, **17,** p. 725; 1922.
13. Coblentz, Dorcas, and Hughes, B. S. Sci. Paper No. 539, **21,** p. 535; 1926.
14. The selection of these glasses is described in the preceding paper: Coblentz, Trans. Illum. Eng. Soc., **23,** p. 278; 1928.
15. In the preliminary announcements (Coblentz, Dorcas, and Hughes, B. S. Sci. Paper No. 539, **21,** p. 535; 1926) a value of 2 per cent was given, but this referred to wave lengths less than 1,400 mμ. Correcting for the water cell (tr.=78.5 per cent) the value is 1.6 per cent of all wave lengths.
16. Transmission given in B. S. Sci. Paper No. 438, **17,** p. 734; 1922.
17. Kimball and Hand, Mo. Weather Rev., **50,** p. 615; 1922.
18. Pettit, Publ. Astronom. Soc., Pacific, **38,** p. 21; 1926.
19. Dorno, Strahlentherapie, **18,** p. 72; 1924. Jüngling (cited by Mayer, Clin. Applications of Sunlight) observed the shortest wave length at 307 mμ in January and 295 mμ in July.
20. Bundesen, Lemon, Falk, and Coade, J. Am. Med. Assn., **89,** p. 187; 1927.
21. Tisdall and Brown, Am. J. Diseases of Children, **34,** p. 742; 1927.
22. Tisdall and Brown, Am. J. Diseases of Children, **34,** p. 721; 1927.
23. Janet H. Clark, Science, **68,** p. 165; August 17, 1928.
24. Eddy, Science, **68,** p. 13; October 19, 1928.
25. Coblentz, Trans. Illum. Eng. Soc., **23,** p. 247; 1928.
26. Reported in the J. Am. Med. Assn., **88,** p. 1562; 1927.
27. Wyman, Boston, Med. J., September 5, 1927.
28. Coblentz, Trans. Illum. Eng. Soc., **23,** p. 290; 1928.
29. See similar data in J. Am. Med. Assn., **88,** p. 1562; 1927.
30. J. Am. Med. Assn., **88,** p. 1567; 1927.
31. Coblentz and Stair, B. S. Jour. Research, **1** (RP6), p. 106; 1928.
32. Coblentz and Kahler, B. S. Sci. Paper No. 342, **15,** p. 215; 1919.
33. Pfund, J. Am. Med. Assn., **91,** p. 18; 1928.
34. The Transmission of Pollopas is described in B. S. Tech. Paper No. 369, **22,** p. 573; 1928.
35. Crist, Ind. Eng. Chem., **20,** p. 1367; 1928.
36. From the Luco Products Corporation, Brooklyn, N. Y.
37. Revised table taken from B. S. Letter Circular No. 235, 3d rev., issued January 14, 1928.
38. Goodman and Anderson, Boston Med. and Surg. J., **197,** p. 1316; 1928. Similar data published by Starkie and Turner (Trans. Soc. Glass Tech., **12,** p. 308; 1928) confirm our measurements. They say (p. 315) "Quartzlite had the smallest transmission of the glasses examined, being very little better than ordinary window glass."
39. See the recent paper by Starkie and Turner (Trans. Soc. Glass Tech., **12,** p. 324; 1928) on the influence of ferric oxide on the ultra-violet light transmission of soda-lime-silica glass.
40. This question is being investigated over an extended range of temperatures by A. Q. Tool and R. Stair, Glass Ind., **9,** p. 51; 1928.
41. In B. S. Letter Circular No. 235, 3d rev., January 14, 1928, it was reported that two samples each of Helioglass and Vitaglass exposed simultaneously to the sun were found to have decreased in transmission at about the same rate, but this does not seem to be the general rule for prolonged exposure.
42. Coblentz, B. S. Sci. Paper No. 438, **17,** p. 735; 1922.
43. Coblentz and Stair, B. S. Tech. Paper No. 369, **22,** p. 573; 1928.

44. Further data on quartz glass are given in B. S. Tech. Paper No. 369, **22,** p. 577; 1928.
45. Coblentz, Trans. Illum. Eng. Soc., **23,** pp. 287 and 290; 1928.
46. By removing the iron oxide from the sand used in making the glass the transparency of ordinary (soda lime) window glass is greatly increased at 302 mμ.
47. Pettit, Trans. Nat. Tuberculosis Association; 1928.
48. Clark, Am. J. Hygiene, **9,** p. 646, May; 1929.
49. Bethke and Kennard, Poultry Science, **6,** p. 290; 1927.
50. Caldwell and Dennet, J. Am. Med. Assn., **92,** p. 2088; 1929.
51. Fleming, The Military Surgeon, p. 592; May, 1928.
52. Russell and Massengale, Poultry Sci., **7,** p. 85; 1928.
53. Fabry and Buisson, Compt. Rend., **175,** p. 156; 1922.
54. Fabry and Buisson, Astrophys. J., **54,** p. 297; 1921.

Washington, March 21, 1929

PROGRESS REPORT ON INVESTIGATION OF FIRE-CLAY BRICKS AND THE CLAYS USED IN THEIR PREPARATION[1]

By R. A. Heindl and W. L. Pendergast

ABSTRACT

This is a progress report of an extensive study of fire clays and fire-clay bricks. It includes the results of a preliminary study of clays representative of those used in the manufacture of refractories throughout the United States. Chemical analyses and a summary of physical tests are given of both fire clays and the bricks manufactured from them. The thermal expansion behavior of the fire clays fired at 1,400° C. and those of the fire bricks "as received" from the manufacturer and also after firing at 1,400°, 1,500°, and 1,600° C. were studied and the materials classified into groups having characteristic thermal expansions. The moduli of elasticity and rupture were determined at 20°, 550°, and 1,000° C. The resistance of the brick to spalling in a water-quenching test is expressed in an empircal relation correlating the elasticity, strength, coefficient of expansion, and percentage of grog used in compounding the brick batches. Data are presented on individual bricks made by the same manufacturer showing probable reasons for great differences in the number of quenchings required to cause spalling in the water-dip test.

CONTENTS

	Page
I. Introduction	692
II. General information on materials	693
III. Methods of testing	694
1. Thermal expansion	694
2. Modulus of elasticity, transverse strength, maximum elongation, and plastic flow	694
3. Thermal-spalling test	695
4. Softening-point test (pyrometric cone equivalent)	695
5. Chemical analyses	696
6. Supplementary studies	696
IV. Results	696
1. Petrographic examinations	696
2. Chemical analyses	697
3. Absorption	699
4. Pyrometric cone equivalents	700
5. Thermal-spalling test	700
6. Sizes of grog	701

[1] A preliminary report of this investigation has appeared as Technologic Paper No. 4 of the American Refractories Institute.

IV. Results—Continued. Page
7. Thermal expansion ---- 702
(*a*) Fire clays ---- 702
(*b*) Fire-clay bricks ---- 704
(*c*) Effect of temperature of firing on thermal expansion behavior ---- 705
(*d*) Fire-clay bricks and fire clays entering into their manufacture ---- 708
8. Modulus of elasticity, transverse strength, and maximum elongation ---- 712
9. Bricks tested at several temperatures ---- 714
10. Some reasons for variation in resistance to thermal shock of the same brand of bricks ---- 717
11. Relation between resistance to thermal spalling and modulus of elasticity ---- 719
12. Relation between resistance to spalling and thermal expansion ---- 720
13. Relation of modulus of elasticity, expansion, transverse strength, and percentage of grog to resistance to spalling ---- 720
14. Plastic flow ---- 722
V. Fire-clay bricks prepared in the laboratory from batch materials furnished by manufacturers ---- 723
1. General ---- 723
2. Tempering water ---- 724
3. Thermal spalling test ---- 725
4. Moduli of elasticity and rupture ---- 725
5. Linear burned shrinkage ---- 725
6. Linear thermal expansion ---- 727
7. Linear thermal expansion and resistance to spalling ---- 728
VI. Summary ---- 728

I. INTRODUCTION

An extensive study was undertaken in the summer of 1926 of the representative clays and grogs used in the manufacture of clay refractories in the principal producing districts of the United States. The program outlined for this investigation includes the following studies of the fire clays and fire-clay refractories:

1. Their chemical and petrographic analyses.

2. Determination of their elastic deformation under load at room temperature, 550° and 1,000° C.

3. Observation of linear thermal dilatation.

4. Investigation of the effect of temperature on certain physical properties.

5. The effect on the finished refractory of grog fired at different temperatures, the amount and grading, and what the effect may be, whether it is crushed or ground.

6. Reactions at high temperatures of the clay refractories with typical slags.

It is also planned to make a comparison of the properties of the commercially prepared fire bricks and fire bricks made in the labora-

tory, using commercial batches. A study of the properties of blended clays, similar to that itemized above, is also contemplated.

The laboratory testing of fire-clay refractories to determine those properties which are believed to be directly related to the life of a refractory in service, as emphasized in recent publications by Geller [2] and Phelps,[3] has led to the conclusion that more data on properties other than those already generally investigated were essential. Producers of refractories are aware that the method of manufacture employed greatly affects the physical properties of the finished product. They do not know, except in a general way, either the qualities of the individual clays, raw or fired, or their relation to the properties of the final product in which they may be used. There can be little doubt that the physical properties of a refractory are affected, not only by the texture and composition of the clays and grog entering into its manufacture but also by the relation of the qualities of the blended clays, and the grogs and clays, to each other. Unless the properties of the individual clays entering into a blend are known, no conception is possible as to whether the finished product is in a highly strained state or whether during heating and cooling internal stresses are set up which may cause rupture between individual particles having different properties and eventually cause failure of the refractory.

The purpose of this work is therefore to obtain data which will lead to a better understanding of the interdependence of raw materials and manufacturing methods. It would seem evident that a knowledge of the important characteristics of the fire clays, how they are altered when subjected to different temperatures, the effect of one clay on another when blended, and how these characteristics are affected by the physical structure of the manufactured product should prove of great value in assisting the producer of fire-clay refractories to choose those clays most desirable for a particular product or a product used for a particular purpose.

II. GENERAL INFORMATION ON MATERIALS

The materials for this study have been furnished by 12 manufacturers of refractories. They include 17 different brands of fire bricks, several hundred pounds each of 26 clays used in the manufacture of these bricks, prepared grog, and green batch. With one exception, detailed information as to the composition of the batch, method of manufacture, and temperature of firing was also furnished. The clays are: 7 flint, 4 semiflint, 12 plastic, and 3 miscellaneous. The last are so classified because they can not be properly placed with clays of the

[2] B. S. Tech. Paper No. 279, Testing of Fire-Clay Brick With Special Reference to Their Use in Coal-Fired Boiler Settings.

[3] Properties of Refractories and Their Relation to Conditions in Service, A. S. M. E. Trans., Jan.–April, 1928.

three types mentioned. In addition, three samples of quartz and sand are included.

Each brand of fire-clay brick when received was assigned a key letter so that the 17 brands included in this study are identified with letters A to R, inclusive, but with the letter O omitted. The clays and other materials from which the bricks are manufactured are identified as far as possible with the same key letter as the bricks in which they are used. Since most bricks are made from two or more clays the materials are further identified by a number following the letter; for example, clays A–1 and A–2 are used in the manufacture of fire-clay brick brand A.

Since the nature of the clays and the method of manufacture of fire-clay bricks have a decided influence on the properties and, consequently, the life of the refractory under various conditions of service, it was considered advisable to obtain as much general information as possible on the materials included in this study. In succeeding tables will be found listed the various types of clays or other materials entering into the manufacture of the 17 brands of fire brick, the location from which they are obtained, and the methods employed in the manufacture of the various brands of bricks.

III. METHODS OF TESTING

1. THERMAL EXPANSION

The linear thermal expansions of the fire clays were determined by means of the interferometer.[4] This method was used because a sufficiently representative specimen of fire clay of the small size required could readily be prepared for test purposes. The thermal expansions of the fire bricks were determined by an indirect method[5] with the apparatus shown in Figure 1, on specimens approximately 1 by 1 by 6 inches cut from the brick. Because most fire-clay bricks are composed of one or more fire clays and various precentages of coarse and fine grogs, it is essential to make observations on a large specimen so that the data obtained may be representative of the whole brick. Thermal expansion determinations from 20°[6] to 1,000° C. were made on specimens cut from the bricks, "as received," after reheating for five hours at 1,400° C., 1,500° C., and again after heating three hours at 1,600° C.

2. MODULUS OF ELASTICITY, TRANSVERSE STRENGTH, MAXIMUM ELONGATION, AND PLASTIC FLOW

The apparatus used in observing deflections of the specimens under various loads and determining transverse strength (modulus of rup-

[4] Described in B. S. Sci. Paper No. 485.

[5] For a description of the apparatus and method used see J. Am. Ceram. Soc., 9 (9), pp. 555–574; 1926.

[6] Room temperature was approximately 20° C. during these experiments.

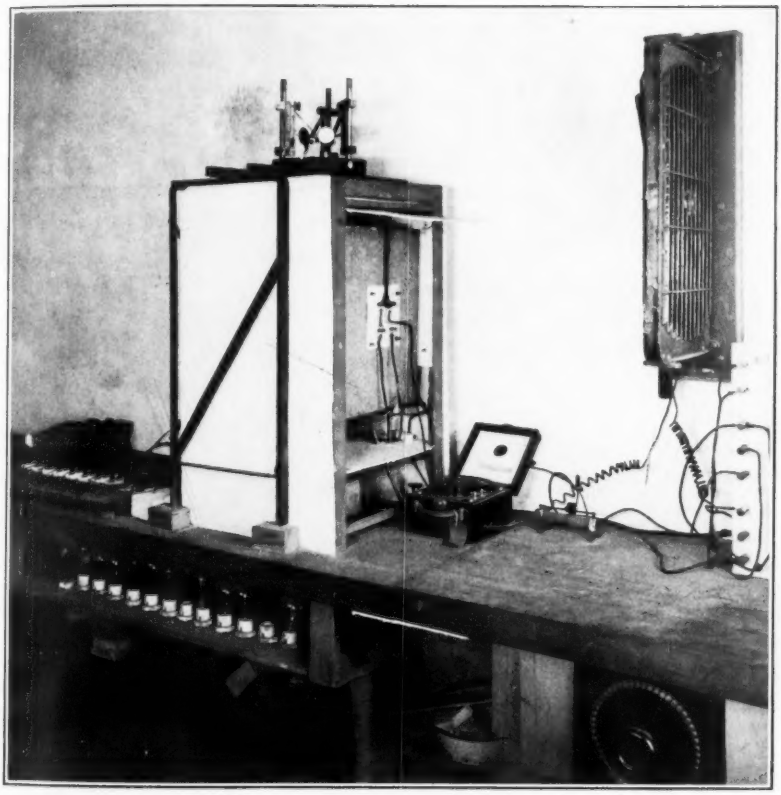

FIGURE 1.—*Furnace and apparatus used in the determination of linear thermal expansions*

UNIV. OF MICH.

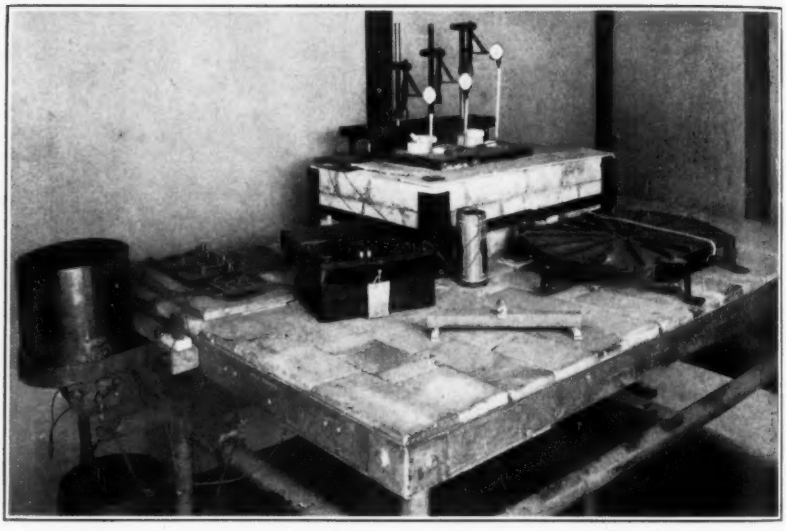

FIGURE 2.—*Apparatus used in determining elastic and plastic flow properties of fire-clay bricks*

ture) is shown in Figure 2, and a detailed description of it and the method for determining the load-deflection curves are given in the Third Progress Report of the Sagger Investigation.[7] The modulus of elasticity and modulus of rupture were determined at several temperatures, the former from the load-deflection curve and the latter using the load which broke the specimen. The values of the maximum elongation were computed by dividing the modulus of rupture by the modulus of elasticity.

The plastic flow at 1,000° C. of the various brands of fire bricks was determined with the same apparatus as was used to determine the elasticity and breaking strength. The plastic flow of the material under any particular stress increment was considered as the "set" or difference between the deflection caused by the load and the recovery of the material on removal of this load. A detailed description of the method for determining this property is given in the Fourth Progress Report of the Sagger Investigation.[8]

3. THERMAL-SPALLING TEST

The spalling test was made on five bricks which had been reheated at 1,400° C. for five hours. The general procedure followed is described in United States Government Master Specification for Fire-Clay Brick.[9] The test requires one end of the brick to be heated in the door of a suitable furnace maintained at 850° C. At hourly intervals the hot end of the brick is immersed in running water to a depth of 4 inches for three minutes. After removing and allowing the specimen to steam in the air for five minutes, the cycle is repeated until the entire end of the brick has completely spalled.

A somewhat modified form of the foregoing spalling test was introduced to permit of some comparison of results obtained on bricks tested under different conditions. Samples of the several brands of brick "as received" were placed in the door of a laboratory kiln so that one end of each brick received the prescribed reheating for five hours at 1,400° C., the other end being exposed to room temperature. The test was otherwise conducted in the same manner as that described above, except that the reheated end of the brick was immersed in water to a depth of 2 instead of 4 inches.

4. SOFTENING POINT TEST (PYROMETRIC CONE EQUIVALENT)

The softening-point (P. C. E.) test was carried out according to the method approved by the bureau, and known as the A. S. T. M. standard method, serial designation C24–20.

---

[7] J. Am. Ceram. Soc., **10** (7), pp. 524–534; 1927.
[8] J. Am. Ceram. Soc., **10** (12), pp. 995–1004; 1927.
[9] B. S. Circular No. 299.

5. CHEMICAL ANALYSES

In making the chemical analyses of the fire clays and fire-clay bricks, the procedure followed was, in general, the method of analysis for refractories described by Lundell and Hoffman.[10]

6. SUPPLEMENTARY STUDIES

The absorption of the bricks was determined "as received" from the manufacturer and also after refiring at 1,400° C. for five hours. The samples after being dried and weighed were boiled for four hours and permitted to remain in the water approximately 18 hours, after which the saturated weight was determined. The absorption, expressed in per cent, was computed by dividing the weight of water absorbed by the weight of the dry-test piece.

The various sizes of the grog in the green batch materials furnished by the several manufacturers were determined on a 500 g sample previously dried for approximately 24 hours at 110° C. After drying, sieve analysis of the sample was made by the wet method.

Petrographic examinations were made on three flint and three semiflint unfired clays.

IV. RESULTS

1. PETOGRAPHIC EXAMINATIONS[11]

Petrographic examination of the several flint and semiflint clays included in the investigation gave the following information:

Sample D–1. Missouri semiflint. "North Missouri."

(*a*) A clay mineral (kaolinite or leverrierite) is abundant, but in exceedingly fine plates.

(*b*) Isotropic (amorphous, colloidal aggregates?) material is present, but it is difficult to estimate quantity, probably less than in C–1.

(*c*) Quartz is probably somewhat coarser grained than in C–1 and is very abundant, probably more than 40 per cent.

(*d*) Minor constituents are present in small quantities. No rutile (TiO_2), siderite ($FeCO_3$) or rhodochrosite ($MnCO_3$) was observed.

Sample Q–1. Missouri flint clay.

(*a*) Consists largely of a clay mineral in fine grains and amorphous, isotropic material.

(*b*) No carbonates, such as siderite or rhodochrosite, are present.

(*c*) Quartz is present only in small amounts, probably less than 5 per cent.

(*d*) A few grains of a mineral of very high index were observed, possibly a titanium compound.

Sample B–1. Pennsylvania semiflint.

(*a*) A clay mineral (kaolinite or leverrierite) in minute plates is abundant.

(*b*) Isotropic (amorphous, colloidal aggregates?) material is somewhat less abundant than (*a*).

---

[10] Analysis of Bauxite and of Refractories of High Alumina Content, B. S. Jour. Research, 1, (RP5); July, 1928.

[11] Petrographic examinations made by H. Insley.

(*c*) Siderite or rhodochrosite is present in small amount, probably less than 5 per cent.

(*d*) Fairly coarse-grained quartz is present in small amounts, less than 10 per cent.

(*e*) There are other minor constituents, such as Fe_2O_3, TiO_2, etc.

Sample C–1. Pennsylvania flint.

(*a*) A clay mineral (kaolinite or leverrierite) in minute plates is slightly less abundant than in B–1.

(*b*) Isotropic (amorphous, colloidal aggregates?) material, index about 1.57, often containing particles of (*a*), is slightly more abundant than in B–1.

(*c*) Siderite or rhodochrosite is more abundant than in B–1, but there is probably less than 10 per cent present.

(*d*) Quartz is fairly fine grained, and in somewhat larger amounts than in B–1.

(*e*) A small amount (less than 2 per cent) of what appears to be rutile is present.

Sample I–1. Kentucky semiflint.

(*a*) A clay mineral is abundant, but occurs in small plates.

(*b*) Isotropic material is apparently not as abundant as in previous samples.

(*c*) No siderite or rhodochrosite was observed. One or two grains of calcite are present, probably less than 2 per cent.

(*d*) Nearly as much quartz is present as in D–1. It is decidedly coarser grained, but still of microscopic dimensions (maximum size about 0.15 mm; average size estimated at 0.05 mm).

(*e*) Apparently less of the minor constituents are present than in the other samples.

Sample K–1. Kentucky flint.

(*a*) Clay minerals occur as extremely minute plates. Probably a smaller amount present than in any other of the samples examined.

(*b*) Isotropic (amorphous, colloidal aggregates?) material with index about 1.57 is probably more abundant than in other samples.

(*c*) A small amount of siderite or rhodochrosite, probably less than 2 per cent, is present.

(*d*) There is very little quartz present, probably less than 5 per cent.

(*e*) Minor constituents are present in small amounts.

2. CHEMICAL ANALYSES [12]

The chemical analyses of the fire clays are given in Table 1 and that of the fire-clay brick in Table 2.

A study of the data shows a wide variation in the composition of these materials. As shown by the analyses of samples H–3, H–4, and P–1 (Table 1), these materials are composed largely of silica.

The mineralogical constitution of the several brands of fire bricks, as computed from their chemical analyses,[13] are shown in Table 2. Only two of the brands (C and Q) show an excess of alumina, although a number of brands show only a slight excess of uncombined quartz. The flux content, which appears to be rather high in a number of cases, may be partially attributed to the percentage of titanium oxide present, which was overlooked in some earlier analyses of fire-clay refractories.[13]

[12] Chemical analyses made by J. F. Klekotka.

[13] B. S. Tech. Paper No. 279 describes in detail the method used.

TABLE 1.—*Chemical analyses of fire clays*

Laboratory key letter	Ignition loss	SiO_2	Al_2O_3	Fe_2O_3	TiO_2	CaO	MgO	Total
	Per cent	*Per cent*	*Per cent*	*Per cent*	*Per cent*	*Per cent*	*Per cent*	*Per cent*
A-1	14.30	43.32	35.72	3.26	2.02	0.18	0.40	99.20
A-2	14.08	44.64	35.84	2.39	1.77	.26	.52	99.50
B-1	13.26	43.38	37.97	1.39	2.12	----	.31	98.43
B-2	14.58	43.06	37.84	2.14	1.84	.12	.04	99.62
B-3	8.16	58.68	24.95	2.39	1.70	.19	.70	96.77
C-1	13.78	42.74	39.18	1.01	2.33	----	.29	99.33
C-2	10.86	50.38	30.87	2.56	2.27	.32	.30	97.56
D-1	12.34	51.82	32.09	1.24	1.63	----	.58	99.70
E-1	14.06	45.98	37.12	.88	1.90	.12	.29	100.35
G-1	14.32	47.09	36.25	.75	1.89	.44	.06	100.80
H-1	7.42	70.29	19.46	.88	2.02	.22	.03	100.32
H-2	14.36	46.36	35.43	1.87	1.57	.44	.46	100.50
H-3	1.62	91.52	4.65	.28	.67	.26	.31	99.31
H-4	2.86	87.68	7.33	1.06	1.25	.38	.14	100.70
H-5	12.82	52.26	32.30	.84	1.72	.26	.02	100.02
H-6	8.14	68.20	21.37	.78	1.63	.34	.12	100.58
I-1	11.62	51.42	32.80	.93	2.33	----	.52	99.62
I-2	13.66	44.66	37.58	1.33	1.53	.66	.15	99.67
I-3	10.62	53.50	29.82	1.95	1.73	.23	.16	98.01
K-1	14.86	42.50	39.68	.76	2.34	----	.12	100.26
K-2	12.28	47.00	33.41	2.59	2.00	.48	.32	98.08
M-1	13.68	44.56	38.19	1.12	2.21	.14	.10	100.00
M-2	11.46	45.76	35.67	1.95	1.72	.30	.64	97.50
P-1	.28	97.48	.72	.14	.46	.16	.32	99.56
Q-1	13.32	42.32	39.63	.84	1.81	.68	.50	99.10
R-1	12.06	52.78	29.90	2.37	1.07	.04	1.20	99.42
R-2	14.66	44.46	37.31	1.13	2.76	.20	.12	100.64
R-3	7.22	72.78	18.94	.65	.61	.23	.14	100.57
T-1	10.92	60.26	25.28	1.62	1.28	.38	.16	99.90

TABLE 2.—*Analyses of fire brick*

Key letter of brand	Chemical analysis							Rational analysis		
	Al_2O_3	SiO_2	Fe_2O_3	TiO_2	CaO	MgO	Ignition loss	Clay	Uncombined quartz	Flux
	Per cent	*Per cent*	*Per cent*	*Per cent*	*Per cent*	*Per cent*	*Per cent*	*Per cent*	*Per cent*	*Per cent*
A	40.90	51.48	2.79	2.45	----	0.58	0.24	90.40	2.94	6.66
B	39.08	51.50	3.15	2.53	----	.46	.44	86.80	4.90	8.28
C	43.06	50.00	1.02	2.80	0.54	.41	.26	[1] 93.50	.00	5.96
D	35.31	58.96	1.99	2.02	.50	.30	.16	79.40	15.52	5.10
E	32.11	61.54	1.70	1.89	.50	.29	.40	72.85	21.35	5.70
F	34.54	59.64	1.71	1.97	.52	.63	.26	77.80	16.95	5.16
G	31.91	63.48	1.26	1.97	----	----	.26	71.80	23.10	4.12
H	17.18	80.12	1.02	1.76	.42	.32	.22	40.95	56.52	2.55
I	38.18	54.66	1.89	2.25	.40	.05	.36	85.05	8.62	6.32
J	33.40	57.86	2.26	2.20	.58	1.18	.50	75.60	16.65	7.82
K	36.56	54.98	2.84	2.52	.48	.59	.24	81.81	10.62	7.47
L	39.82	54.00	2.01	2.51	.36	.61	.20	88.22	6.32	5.42
M	38.99	51.56	2.45	2.98	.52	.26	.20	86.65	5.03	8.31
N	34.50	58.44	2.40	2.06	.14	.40	.12	77.78	15.95	6.30
P	27.08	69.12	1.64	1.40	.50	.25	.16	62.42	34.04	3.47
Q	46.76	47.12	1.43	2.45	1.24	.49	.18	[2] 89.40	.00	4.77
R	37.62	56.48	1.96	2.50	.72	.56	.24	83.99	10.82	5.21

[1] 0.52 per cent uncombined Al_2O_3.
[2] 5.86 per cent uncombined Al_2O_3.

3. ABSORPTION

The data on absorption of the bricks "as received" from the manufacturer and also of the bricks after reheating for five hours at 1,400° C. are given in Table 4. The absorption of the specimens "as received" ranges from 5.2 to 17.6 per cent, and for the reheated specimens from 3.0 to 17.1 per cent. Although it is appreciated that firing in a laboratory kiln and firing in an industrial kiln may affect the physical properties of a refractory somewhat differently, the absorption values before and after reheating, as given in the table, give a fair indication of the heat treatment the various fire-clay bricks have received in the manufacturing process.

Data on absorption of fire clays have been determined only after firing the material at 1,160° C. for three hours (cone 4). The data are included in Table 3 simply to make possible a comparison of the clays with one another.

TABLE 3.—*Type of clays—Origin, absorption, and P. C. E.*

Laboratory letter	Type of clay	Origin	P. C. E.	Absorption in per cent of dry weight after firing at 1,160° C. for 3 hours
A-1	Flint	Kentucky	32	11.6
A-2	Plastic	do	32	10.6
B-1	Semiflint	Pennsylvania	33	12.3
B-2	Flint	do	[1] 33	16.7
B-3	Plastic	do	29–30	7.8
C-1	Flint	do	33	16.0
C-2	Plastic	do	30	6.0
D-1	Semiflint	Missouri	31–32	7.7
E-1	do	do	30	13.8
G-1	Plastic		32	26.3
H-1	do	New Jersey	30	20.7
H-2	do	do	32	9.6
H-3	Silica sand	do	32	
H-4	do	do	32	
H-5		do	33	21.0
H-6	Plastic	do	30	20.0
I-1	Semiflint	Kentucky	31	13.0
I-2	Flint	do	33	14.6
I-3	Plastic	Ohio	30	11.5
K-1	Flint	Kentucky	32	17.6
K-2	Plastic	do	32	7.9
M-1	Flint	Pennsylvania	32–33	9.7
M-2	Plastic	do	32–33	22.3
P-1	Crushed quartz	California	33	
Q-1	Flint	Missouri	33	10.7
R-1	Plastic	California	30–31	10.4
R-2	Kaolin	do	32–33	9.2
R-3	Siliceous	do	33	26.1
T-1	Plastic	Illinois	30	8.0

[1] Higher than cone 33.

TABLE 4.—*Showing manufacturing methods and certain physical properties of fire bricks*

Laboratory key letter of brand	Method of manufacture [1]	P. C. E.	Absorption in per cent of weight of dry brick		Number of quenchings required to cause failure; fire brick heated to 1,400° C. for 5 hours				Average number of quenchings in the 4-inch dip tests
			As received	After burning 5 hours at 1,400° C.	2-inch dip [2]	4-inch dip	4-inch dip	4-inch dip	
A	HM	33+	14.1	10.7	45	49	43		46
B	HM	33+	10.9	9.5	38	16	6	9	10
C	DP	33+	9.6	8.1	45	29	32		31
D	DP	31-32	6.7	5.3	8	34	7	10	17
E	DP	31-32	5.2	6.6	5	18	16	11	15
F	SM	31	7.0	3.0	9	11	2	2	6
G	HM, repress	32	17.6	16.1	11	8	5		7
H	HM	32	16.3	17.1	12	6	3	6	5
I	HM	33	10.7	8.9	26	24	15	11	17
J	SM	28-29	8.3	3.8	6	8	6		7
K	SM	32	8.2	6.8	15	10	12		11
L	HM	33	8.2	6.8	32	17	18		18
M	HM	33	11.7	11.4	19	14	11		13
N	SM	32	5.5	4.8	4	6	5		6
P	SM, repress	30	13.8	12.4	4	8	4		6
Q	DP	34	7.2	6.9	>50	49	>41		>45
R	HM, repress	33	13.6	12.6	3	8	8	4	7

[1] HM, SM, DP refer to handmade, stiff-mud, dry-press processes, respectively.
[2] Only one end heated at 1,400° C. for 5 hours.

4. PYROMETRIC CONE EQUIVALENTS (P. C. E.)

Table 3 gives the P. C. E. values for all the materials entering into the various brands of brick. All materials, with the exception of samples B–3 and C–2 (Pennsylvania plastic fire clays), have a P. C. E. of 30 or above.

Table 4 gives the P. C. E. values as determined on the 17 brands of fire-clay brick. The data show that with the exception of samples designated J and P, all the brands of fire-clay bricks have a P. C. E. of 31 or above.

5. THERMAL-SPALLING TEST

The results of the various spalling tests are given in Table 4. Five samples of each brand of bricks were tested for resistance to spalling in the test requiring an immersion in water of 4 inches. The test was made a second time on all brands of bricks and those brands showing great differences in results between these two tests were tested a third time. The average of the several tests gives a range, in number of cycles to cause failure of from 5 for those showing the least resistance to over 46 for those having the greatest resistance.

The number of cycles required to cause spalling in the modified spalling test, in which only one end of the brick was heated in the reheat test and a 2-inch immersion used, ranged from a minimum of 3 to a maximum of over 50.

Comparison of the results obtained in the 2-inch against 4-inch immersion tests shows a decided lack of correlation between the two tests. In several instances very little difference is noted in the number of cycles required to cause failure; in some cases the number of cycles required to cause spalling is much greater with the 2-inch immersion, and in still others the reverse is true.

6. SIZES OF GROG

Grog is burned clay, either as such or in the form of broken bricks, discarded saggers, or other cast-off refractory shapes. It is usually ground or crushed and may or may not be screened to specific sizes for use. In those plants where grog is an essential constituent of the product, it is obtained as a rule by grinding or crushing broken or discarded fire brick. The analyses made of the raw batch materials furnished by manufacturers of fire bricks showed that not all of them use grog in their product. However, those manufacturers who use considerable quantities of flint clay in their batch composition grind the flint clay to a desired size. Since the particles of flint clay do not readily slake, they probably serve a purpose similar to that of grog. A macroscopic examination of all the grog or grog substitutes remaining after washing the samples of batch material on a 200-mesh sieve resulted in classifying the various compositions as follows:

1. Largely flint clay or flint and semiflint clays with varying percentages of grog.
2. Entirely flint clay or flint and semiflint clays.
3. Large percentage of quartz with varying proportions of grog.

The appearance of 14 samples of grogs or grog substitute particles indicates that 13 were crushed and only 1 was ground.

If it is arbitrarily assumed that the material which passes a 200-mesh sieve is clay substance, then the material which did not pass the sieve, and which may be considered as grog or grog substitutes in this study, ranges from a total of 40 to 80 per cent of the raw brick batch. Table 5 tabulates the respective percentages of grog materials retained on various mesh sieves, together with the percentages of grog and clay comprising the raw brick batches.

TABLE 5.—*Sieve analysis of grog or grog substitutes used in 14 raw fire-clay brick batches*

Sample key letter	Per cent passing and retained on sieves—							
	No. 4 mesh	4 to 10	10 to 20	20 to 40	40 to 100	100 to 200	Through 200	Total grog[1]
A	2.30	17.20	21.40	11.50	11.00	4.05	32.55	67.45
B		22.00	21.20	9.40	9.80	3.40	34.20	65.80
C		9.75	33.25	16.25	15.75	5.37	19.60	80.40
D and N		1.25	18.75	22.75	20.75	6.00	30.50	69.50
E and F		.25	18.50	20.65	20.50	7.00	30.60	69.40
G	.25	11.00	11.62	7.12	13.12	5.75	51.10	48.90
H	1.12	2.64	9.50	8.25	12.75	8.74	57.00	43.00
I		9.75	28.30	12.87	11.50	3.87	33.75	66.25
J		1.50	17.75	11.28	8.62	2.25	58.60	41.40
K and L		8.75	24.25	11.00	11.00	4.87	40.10	59.90
M	.50	18.85	18.75	8.75	10.00	7.50	39.40	60.60
P		6.20	7.90	4.40	18.00	6.20	57.30	42.70
Q		1.50	19.90	39.40	14.50	13.70	11.00	89.00
R		7.50	15.38	8.50	13.25	4.63	50.70	49.30

[1] Material that did not pass a No. 200-mesh sieve was considered as grog.

7. THERMAL EXPANSION

(a) FIRE CLAYS

The thermal expansions of the 24 fire clays as well as the 5 samples of sand and quartz were determined from room temperature to 900° C. Specimens made from these materials, with the exception of 3 of the silica sands, were fired at 1,400° C. for 5 hours. The materials may be classified according to the thermal expansion behavior into five groups as follows:

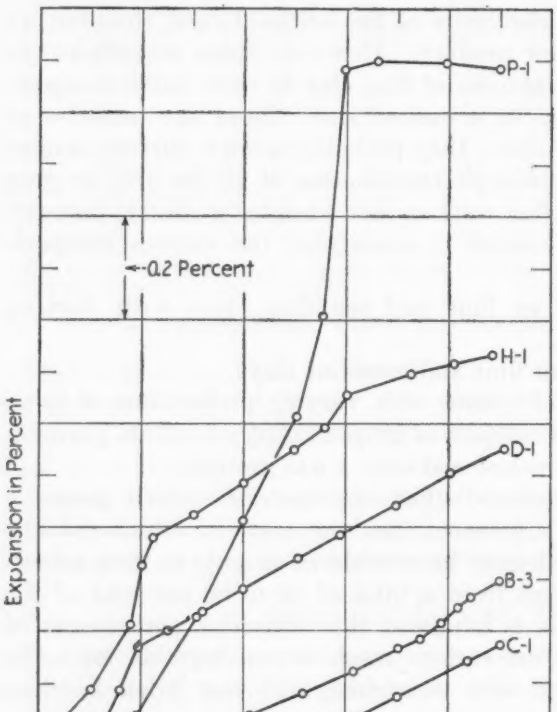

FIGURE 3.—*Curves showing linear thermal expansions characteristic of different types of fire clays*

To avoid overlapping, the curves have not all been drawn from a common origin.

1. Eleven have a high rate of expansion below 200° C. and a somewhat less and more uniform one between approximately 200° and 900° C. The curves indicate that any free silica present is either in the form of tridymite or cristobalite. Clays Nos. A-1, B-2, D-1, E-1, G-1, H-2, I-1, I-2, K-1, R-2, and T-1 belong in this group.

2. Four have a high rate of expansion below 200° C. and also between approximately 540° and 600° C. These curves show that quartz, cristobalite, and tridymite are all present in the clays. However, the expansion curves indicate the presence of only a small amount of quartz. Samples Nos. R-3, H-1, H-5, and H-6 belong in this group.

3. Three have a comparatively uniform rate of expansion throughout the range observed except for an increased expansion at approximately 575° to 600° C. These curves indicate that all silica is present in the form of free quartz. Samples Nos. H-3, H-4, and P-1 are classed in this group.

4. Three clays have a uniform expansion from room temperature to approximately 750° C. At this temperature the expansion per degree increases up to approximately 850° C., after which it gradually decreases. The clays in this group are all of the so-called plastic type, and it is quite possible that after firing for five hours at 1,400° C. sufficient glass is present to cause this change in the rate of expansion more or less typical of some glasses.[14] Samples Nos. B–2, C–2, and I–3 belong to this group.

5. Eight clays have a uniform expansion throughout the entire range of 20° to 900° C.

The materials tested, therefore, include all those having the several types of expansion due to a substantially quartz-free condition or to the presence of quartz either as such or in one of its allotropic modifications. Curves, showing the thermal expansion behavior from 20° to 900° C. of materials representative of each of the foregoing groups are given in Figure 3. The total linear expansion values per unit length from 100° to 900° C. at 100° C. intervals and also the value obtained at 550° C. are given in Table 6. The initial measurement of the specimen was made at approximately 20° C.

TABLE 6.—*Total linear thermal expansion per unit length at temperatures indicated of fire clays fired at 1,400° C. for five hours*

Laboratory key letter	Temperature° (C.)										Classed according to type of expansion in group
	100	200	300	400	500	550	600	700	800	900	
A-1	0.000484	0.001773	0.002254	0.002804	0.003352	0.003607	0.003899	0.004429	0.004979	0.005548	1
A-2	.000310	.000807	.001223	.001697	.002105	.002430	.002736	.003274	.003847	.004413	5
B-1	.000216	.000597	.001025	.001454	.001930	.002172	.002412	.002847	.003407	.003905	5
B-2	.000500	.001094	.001488	.001927	.002385	.002559	.002835	.003992	.003741	.004227	1
B-3	.000194	.000562	.000900	.001285	.001697	.001878	.002184	.002502	.003164	.003884	4
C-1	.000219	.000559	.000890	.001325	.001762	.001976	.002234	.002659	.003201	.003717	5
C-2	.000240	.000560	.000926	.001351	.001815	.002024	.002450	.002687	.003175	.003719	4
D-1	.000654	.002730	.003230	.003791	.004358	.004637	.004915	.005461	.006019	.006484	1
E-1	.000612	.002256	.002772	.003305	.003835	.004102	.004370	.004899	.005462	.005972	1
G-1	.000581	.002340	.002879	.003456	.004038	.004318	.004662	.005189	.005688	.006093	1
H-1	.000826	.003122	.004219	.004879	.005650	.005790	.005860	.006496	.007152	.007373	2
H-2	.000437	.001329	.001778	.002265	.002763	.003011	.003283	.003797	.004375	.004880	1
H-3[1]	.000820	.002321	.003810	.006258	.008915	.011020	.015300	.015450	.015400	.015214	3
H-4[1]	.000913	.002555	.004253	.006578	.009577	.010586	.015000	.015100	.015050	.014980	3
H-5	.000673	.002701	.003346	.003911	.004496	.004824	.005270	.005925	.006318	.006623	2
H-6	.000723	.004693	.006128	.006798	.007494	.007783	.008224	.008766	.009064	.009290	2
I-1	.000555	.002263	.002806	.003329	.003872	.004131	.004426	.004960	.005363	.005766	1
I-2	.000447	.001244	.001710	.002189	.002657	.002926	.003198	.003737	.004322	.004911	1
I-3	.000266	.000787	.001118	.001568	.001966	.002150	.002388	.002883	.003352	.003731	4
K-1	.000707	.002182	.002646	.003198	.003743	.004181	.004321	.004837	.005375	.005875	1
K-2	.000226	.000628	.001015	.001440	.001900	.002129	.002371	.002866	.003546	.004118	5
M-1	.000241	.000690	.001092	.001500	.001968	.002219	.002475	.002976	.003577	.004298	5
M-2	.000252	.000651	.001053	.001519	.001993	.002242	.002494	.002879	.003613	.004392	5
P-1[1]	.000896	.002347	.003886	.006121	.008570	.010610	.014840	.014900	.014860	.014850	3
Q-1	.000235	.000673	.001062	.001552	.002022	.002271	.002540	.003089	.003917	.004530	1
R-1	.000235	.000666	.001042	.001462	.001897	.002125	.002356	.002798	.003324	.003871	5
R-2	.000735	.002048	.002587	.003125	.003700	.003970	.004348	.004808	.005365	.005308	1
R-3	.000748	.003549	.006194	.007017	.007810	.008247	.009000	.009441	.009671	.009794	2
T-1	.000676	.003571	.004273	.004872	.005490	.005794	.006122	.006717	.007166	.007569	1

[1] Observations made on the raw material which is composed largely of silica and did not sinter at 1,400° C.

[14] B. S. Sci. Paper No. 393.

(b) FIRE-CLAY BRICKS

The linear thermal expansions of the fire-clay bricks were observed from approximately 20° to 1,000° C. on a specimen cut from each of the 17 brands of bricks. Observations were made on these specimens representing bricks (*a*) as received from the manufacturer, (*b*) after refiring for five hours at 1,400° C., (*c*) after the same specimen had been fired again at 1,500° C. for five hours, and (*d*) an additional firing for three hours at 1,600° C.

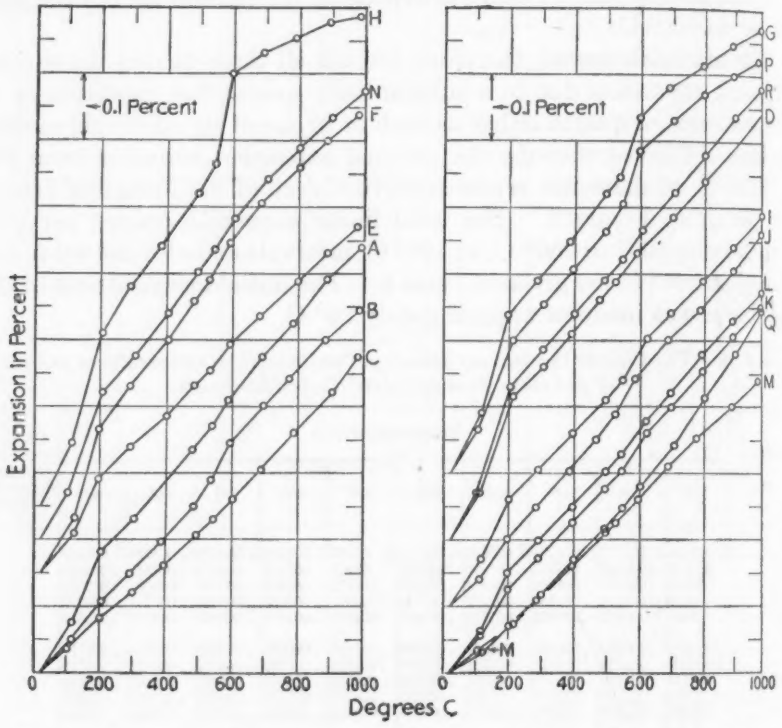

FIGURE 4.—*Curves showing linear thermal expansions of 17 brands of fire-clay brick as "received" from the manufacturer*

To avoid overlapping, the curves have not all been drawn from a common origin.

The bricks may be classified into four groups according to the type of expansion observed on the specimen as received from the manufacturer.

1. Three brands, C, M, and Q, were found to have a comparatively uniform rate of expansion.

2. Three brands, D, N, and R, had a high rate of expansion below 200° C. and a uniform rate from approximately 200° to 1,000° C.

3. One brand only, J, showed a high expansion between 550 and 600° C., indicating an inversion of alpha-to-beta quartz.

4. The other 10 brands show an increased expansion both below 200° C. and also between approximately 550° and 600° C., although the

alpha-to-beta quartz inversion is comparatively slight in the case of seven brands in this group.

Thermal expansion curves, plotted from observations on the 17 brands of fire-clay bricks as received from the manufacturer, are shown in Figure 4.

Check determinations were made on 6 specimens of fire clay and 11 of fire-clay bricks. The greatest variation in the data obtained on the same body was less than 2½ per cent.

(c) EFFECT OF TEMPERATURE OF FIRING ON THERMAL EXPANSION

The changes in the physical composition of the bricks brought about by reheating them at 1,400°, 1,500°, and 1,600° C. are well illustrated by the data obtained on the linear thermal expansion.[15]

In Table 7 are given data on the expansion behavior of the bricks "as received" and after reheating in the laboratory kiln at 1,400°, 1,500°, and 1,600° C. The total linear expansions per unit length between 100° and 200° C., 500° and 600° C., and 20° to 1,000° C., together with the coefficient of expansion between the latter temperatures are tabulated. The data shown for these temperature ranges illustrate the effect on the thermal expansion of the refractory produced by progressively increased firing temperatures. With few exceptions the expansion decreases as the temperature of firing is increased. These data also show that it would be very misleading to consider an average coefficient of expansion for a single range as large as from 20° to 1,000° C. as representative of the expansion behavior of the material, since it does not indicate whether the rate throughout this range is uniform or highly irregular. A typical example of this is illustrated by the data for brand H. The variation in total expansion from 20° to 1,000° C. is comparatively small with change of firing temperatures, although the change in this property is quite large between 100° and 200° C. and especially so between 500° and 600° C. In addition, the expansion increased between 100° and 200° C. and decreased between 500° and 600° C.

TABLE 7.—*Expansion in per cent and coefficient of expansion of fire brick*

Brand	Temperature of firing	Range of temperature (° C.)			Coefficient [1] expansion of 20 to 1,000° C.
		100 to 200	500 to 600	20 to 1,000	
A	(2)	0.116	0.069	0.635	6.5
	(3)	.053	.053	.473	4.8
	(4)	.048	.050	.485	5.0
	(5)	.046	.046	.440	4.5
B	(2)	.064	.089	.541	5.5
	(3)	.038	.047	.421	4.3
	(4)	.043	.046	.419	4.3
	(5)	.047	.059	.483	4.9

Footnotes at end of table.

[15] Thermal expansion data similar to those obtained in this investigation were found by Miehr, Kratzert, and Immke, described in their paper, Influence of Firing on the Chemical and Physical Properties of Refractory Clays, Tonindustrie Zeitung, **52** (16); 1928.

TABLE 7.—*Expansion in per cent and coefficient of expansion of fire brick*—Con.

Brand	Temperature of firing	Range of temperature (° C.)			Coefficient of expansion [1] 20 to 1,000° C.
		100 to 200	500 to 600	20 to 1,000	
C	[2]	0.059	0.058	0.462	4.7
	[3]	.035	.046	.410	4.2
	[4]	.035	.046	.412	4.2
	[5]	.038	.045	.402	4.1
D	[2]	.141	.051	.603	6.4
	[3]	.091	.045	.497	5.1
	[4]	.033	.038	.390	4.0
	[5]	.028	.041	.358	3.7
E	[2]	.096	.061	.530	5.4
	[3]	.079	.046	.486	5.0
	[4]	.035	.040	.365	3.7
	[5]	.042	.052	.398	4.1
F	[2]	.150	.078	.698	7.1
	[3]	.093	.043	.509	5.2
	[4]	.025	.044	.355	3.6
	[5]	.028	.039	.347	3.5
G	[2]	.153	.121	.680	6.9
	[3]	.153	.111	.642	6.5
	[4]	.166	.055	.716	7.3
	[5]	.045	.044	.424	4.3
H	[2]	.177	.218	.770	7.8
	[3]	.190	.175	.739	7.5
	[4]	.205	.068	.730	7.5
	[5]	.225	.047	.740	7.6
I	[2]	.098	.077	.590	6.1
	[3]	.047	.055	.492	5.0
	[4]	.044	.051	.442	4.5
	[5]	.047	.050	.421	4.3
J	[2]	.062	.085	.569	5.7
	[3]	.036	.041	.439	4.4
	[4]	.035	.042	.399	4.5
	[5]	.031	.051	.466	4.7
K	[2]	.079	.067	.546	5.6
	[3]	.055	.050	.412	4.2
	[4]	.038	.051	.432	4.5
	[5]	.038	.058	.446	4.5
L	[2]	.096	.065	.571	5.9
	[3]	.036	.045	[6] .341	[6] 4.0
	[4]	.038	.042	.421	4.3
	[5]	.038	.050	.441	4.5
M	[2]	.038	.052	.472	4.8
	[3]	.037	.051	.433	4.4
	[4]	.039	.045	.437	4.5
	[5]	.039	.047	.438	4.3
N	[2]	.155	.074	.673	6.9
	[3]	.110	.054	.574	5.9
	[4]	.037	.046	[6] .384	[6] 4.4
	[5]	.037	.043	.450	4.6
P	[2]	.127	.117	.632	6.5
	[3]	.098	.101	.546	5.6
	[4]	.066	.058	.542	5.5
	[5]	.054	.042	.487	5.0
Q	[2]	.043	.061	.544	5.5
	[3]	.033	.055	.500	5.1
	[4]	.037	.054	.493	5.0
	[5]	.035	.056	.520	5.3
R	[2]	.151	.068	.678	6.9
	[3]	.105	.062	.612	6.3
	[4]	.040	.050	.405	4.1
	[5]	.035	.045	.447	4.6

[1] To be multiplied by 10^{-6}.
[2] Data obtained on bricks as received from the manufacturer.
[3] Data obtained after firing 5 hours in laboratory kiln at 1,400° C.
[4] Data obtained after firing 5 hours in laboratory kiln at 1,500° C.
[5] Data obtained after firing 3 hours in laboratory kiln at 1,600° C.
[6] Data obtained at 900° C.

The change in total expansion because of progressive heat treatment ranges from a low of approximately 5 per cent to a high of 50 per cent.

Those brands of bricks showing an excess of alumina in their rational composition [16] or only a small percentage of free silica as computed from the chemical analyses, showed the least change in expansion after the heating treatment. Very little change was apparent in the expansion data of these brands after the firings at either 1,400°, 1,500°, or 1,600° C. The greatest change in this property appears to have been in those brands having uncombined silica exceeding 10 per cent. Typical curves showing the change in thermal expansion due to progressive heat treatment of the various types of bricks are shown in Figures 5 and 6. The curves shown in these

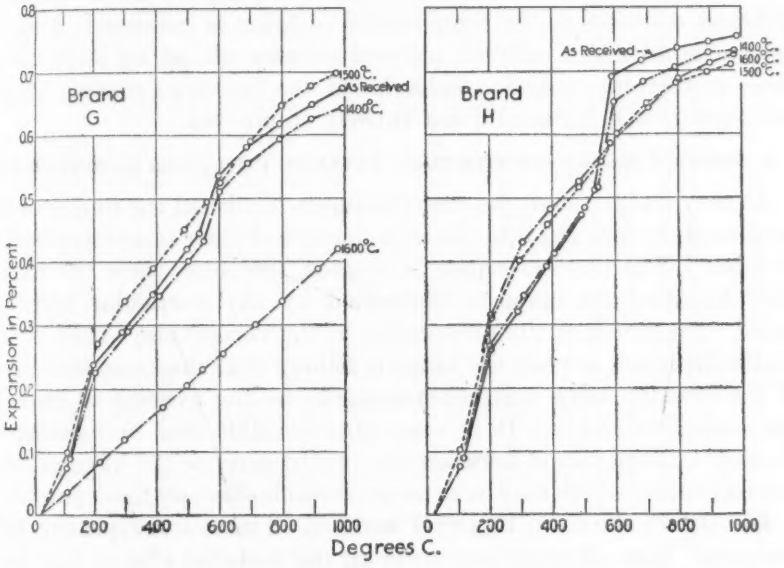

FIGURE 5.—*Effect on the thermal expansions of highly siliceous fire brick caused by progressively increasing firing temperatures*

figures illustrate the rates of expansion as well as the total linear thermal expansion from approximately 20° to 1,000° C. that are typical of the various brands of fire-clay bricks manufactured in this country. The data, from which the points on these curves were computed, were determined on bricks of widely different expansion behavior, such as those of brand H, having a high as well as irregular rate of expansion below 600° C.; to those of type Q, having a moderate but uniform rate throughout the range observed. These data indicate that, in those bricks showing high rates of expansion due to inversions both of cristobalite and quartz, there is first, solution of the latter form of

[16] B. S. Tech. Paper No. 279, p. 126.

silica and then of the former. The linear thermal expansion curves of 14 of the 17 brands of fire-clay bricks when tested "as received" were irregular. With but one exception (brand H) after heating these bricks at either 1,400°, 1,500°, or 1,600° C. the expansion became uniform and lower. In other words, it appears that if heated sufficiently, all fire-clay bricks of the quality included in this study will have practically the same type and rate of thermal expansion regardless of the nature of the materials used originally in their manufacture. Brand H, which is an exception, is a highly siliceous brick. A petrographic examination of fire-clay bricks of brands G and H, after the final reheating at 1,600° C., showed the materials to consist of only well-developed crystals of mullite embedded in glass.

Since these data show that the thermal expansions of the majority of bricks decrease as the temperature of firing is increased, it might be concluded that finally all internal stresses caused by large differences in thermal-expansion behavior of the fire clays making up the brick are greatly reduced if not entirely eliminated.

(d) FIRE-CLAY BRICKS AND FIRE CLAYS ENTERING INTO THEIR MANUFACTURE

As previously stated, the manufacturers furnished the names of the various clays entering into the manufacture of their respective brands of brick. The thermal-expansion curves, therefore, show the results from blending the clays as illustrated by any particular brand of brick. Inasmuch as the proportions of the various clays used in any particular batch are not the same, it follows that the expansion curve of the fire-clay brick will not necessarily be the average of those of the individual clays. It is also quite possible that a reaction or physical change occurs between the constituents of the various clays during heating which may have an appreciable effect on the expansion.[17]

The curves shown in Figures 7 and 8 in all instances represent data computed from observations made on the material after it had been fired at 1,400° C. for five hours. The thermal expansions of each of the three materials (broken lines) entering into the composition of fire-clay brick brand R as well as that of the brick (full line) are shown in Figure 7. These curves illustrate the large differences which may occur in expansion behavior of the individual materials entering into one composition and the resultant effect on the final product. In this instance the expansion of the brick is approximately the computed average of those of the materials entering into its composition based on the percentage of each material present. It would be logical to assume that such large differences in the thermal expansions between materials constituting a refractory would cause interstructural stresses greatly affecting the life of the product.

[17] Willi M. Cohn discusses the behavior of minerals and ceramic bodies on heating in his paper entitled "Some Factors Influencing the Thermal Properties of Minerals and Products of the Ceramic Industry," J. Am. Ceram. Soc., **11** (5); 1928.

FIGURE 6.—*Effect on the thermal expansions of fire-clay brick, not of the highly siliceous type, caused by progressively increasing firing temperatures*

In contrast to the expansion curves for materials entering into fire-clay brick R (fig. 7) are shown, to the left in Figure 8, expansion curves obtained on the different clays entering into the manufactur

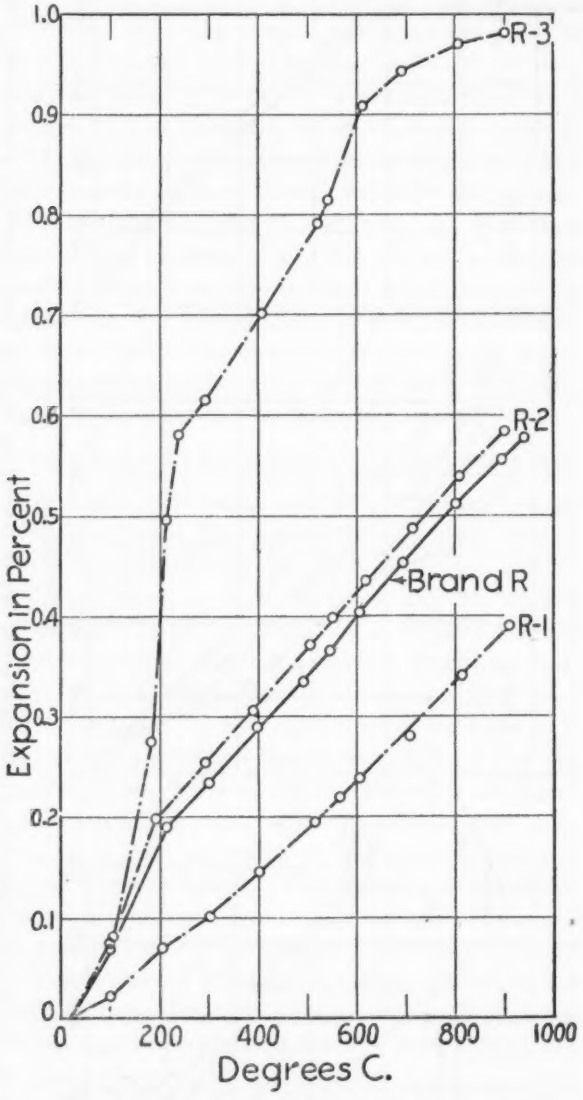

FIGURE 7.—*Thermal expansion curves of materials entering into the manufacture of fire-clay brick R and that of the finished product*

of brick C as well as e expansion curve of the finished product. The thermal expansions of the two clays used in this brand of brick are very nearly alike; the expansions are uniform throughout

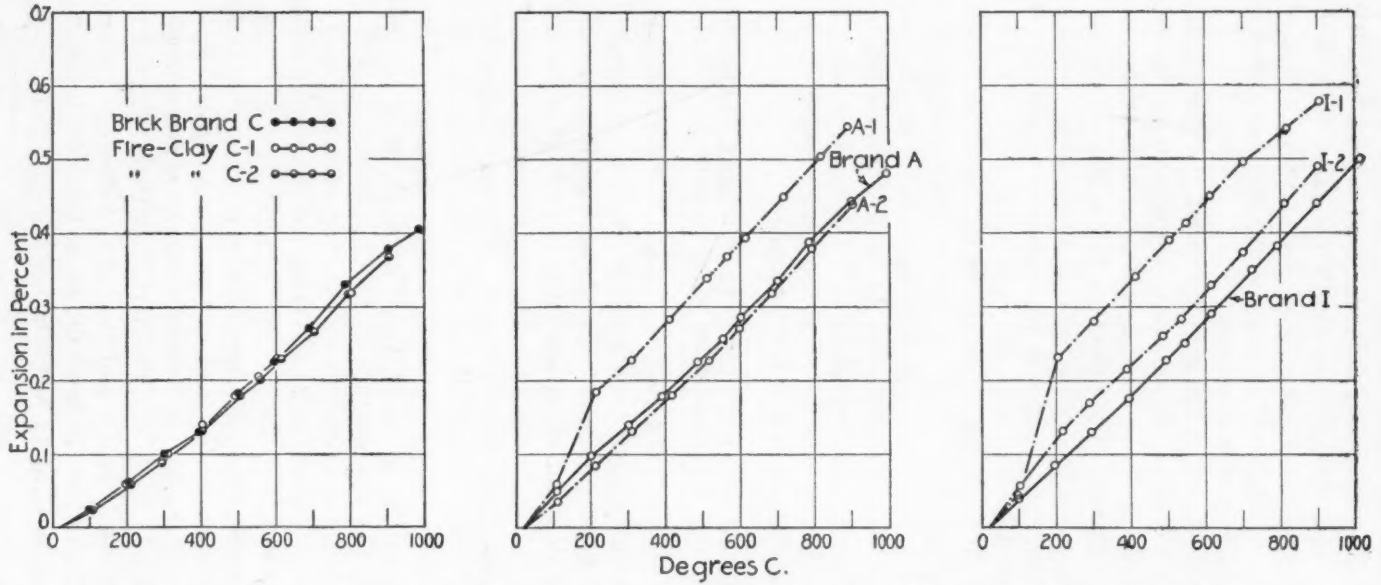

FIGURE 8.—*Showing the expansion curves of three brands of brick and the clays used in their manufacture*

the range observed, and the total expansions are low for fire-clay materials. The expansion data observed on the brick (shown as a full line in the graph) are practically the same as those for the two clays. The expansion behavior of the clays as well as that of the brick might be considered as approaching the ideal, since the internal stresses should be at a minimum.

The curves shown in the center section of Figure 8 illustrate the expansion behavior of the two clays (broken lines) entering into the manufacture of fire-clay brick brand A as well as that observed on the brick (full line). The inflection, below 200° C., in the expansion curve for clay A–1 has completely disappeared in the finished product, the expansion behavior of which closely approaches that of the bonding clay A–2.

On the right in Figure 8 are shown the linear expansion curves of the two clays (broken lines) blended in the manufacture of fire-clay brick brand I, together with that determined on the final product. The expansion curve for the fire brick in this case not only fails to show any sign of an inflection at 200° C., which is quite pronounced in the curve for fire clay I–1, but also is appreciably lower than that of either clay from which it is prepared.

8. MODULUS OF ELASTICITY, TRANSVERSE STRENGTH, AND MAXIMUM ELONGATION

Figure 9 shows the deflections, typical of fire-clay bricks, corresponding to the various loads applied to bricks of brand C and plotted to a convenient scale. The stress (load) strain (deformation) curves were determined on specimens 1 inch in cross section and 9 inches long, cut from the fire bricks. They were placed across an 8-inch span and loaded at the center. The curves shown in Figure 9 were obtained on bricks, all tested at approximately 20° C., (*a*) as received from the manufacturer, (*b*) after reheating at 1,400° C., and (*c*) after reheating at 1,500° C. The decrease in flexibility of the material, as the temperature of firing is raised, is well illustrated. The data obtained at 20° C. on the modulus of elasticity of the 17 brands of bricks tested after receiving the three heat treatments are given in Table 8.

The transverse strengths (moduli of rupture) of the various brands of bricks were computed from the loads required to break the specimens on which the load-deflection curves were determined. The values are shown in Table 8. The data show that the modulus of elasticity had increased greatly and that the modulus of rupture had also increased, but not to the same degree as the modulus of elasticity, as the temperature of firing was raised.

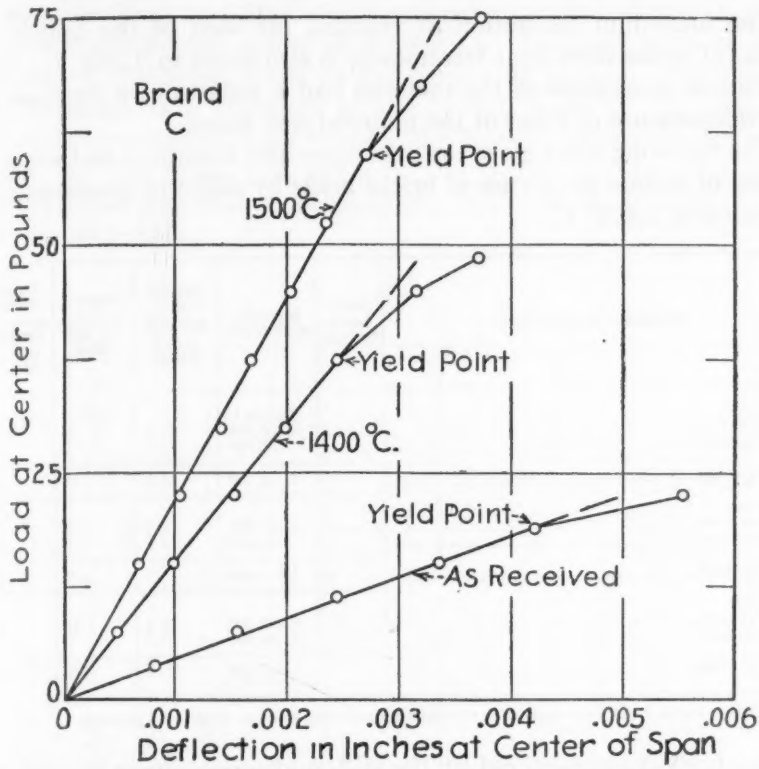

FIGURE 9.—*Curve showing the typical stress (load), strain (deformation), relationship of fire-clay bricks as the temperature of firing is increased*

TABLE 8.—*Properties of commercial fire-clay brick tested at 20° C.*

Laboratory key letter of brand	As received from manufacturer			After reheating at 1,400° C. for 5 hours			After reheating at 1,500° C. for 5 hours		
	Modulus of—		Maximum elongation (R/E)[2]	Modulus of—		Maximum elongation (R/E)[2]	Modulus of—		Maximum elongation (R/E)[2]
	Elasticity[1]	Rupture		Elasticity[1]	Rupture		Elasticity[1]	Rupture	
	Lbs./in.[2]	*Lbs./in.*[2]	*Per cent*	*Lbs./in.*[2]	*Lbs./in.*[2]	*Per cent*	*Lbs./in.*[2]	*Lbs./in.*[2]	*Per cent*
A	631	270	0.04	920	525	0.06	2,430	875	0.04
B	1,434	640	.04	1,350	380	.03	2,670	560	.02
C	510	265	.05	1,890	520	.03	2,450	805	.03
D	974	620	.06	1,520	830	.06	4,040	1,485	.04
E	640	1,030	.16	2,670	1,415	.05	8,380	2,000	.02
F	2,800	1,560	.06	3,170	1,775	.06	9,490	1,575	.02
G	920	760	.08	1,070	625	.06	2,605	980	.04
H	250	235	.09	353	335	.09			
I	990	590	.06	2,300	885	.04	3,665	1,345	.04
J	2,580	1,355	.05	6,400	1,470	.02	[3]	[3]	[3]
K	2,170	1,195	.05	2,700	925	.03	4,995	1,230	.02
L	2,145	580	.03	3,145	910	.03	4,440	1,485	.03
M	2,110	720	.03	4,500	1,210	.03	6,920	1,295	.02
N	3,345	1,430	.04	3,950	1,415	.04	3,635	1,420	.04
P	1,665	950	.06	1,950	955	.05	2,930	1,230	.04
Q	2,025	915	.04	2,700	1,190	.04	5,340	1,520	.03
R	3,350	1,225	.04	3,720	1,285	.03	4,630	1,495	.03

[1] To be multiplied by 10.[3]

[2] Maximum elongation of extreme fiber at point of rupture of specimens $= \frac{\text{Modulus of rupture}}{\text{Modulus of elasticity}} = R/E$.

[3] Bloated.

The maximum elongation at rupture, for each of the brands of bricks after the three heat treatments, is also given in Table 8. The maximum elongation of the material had a tendency to decrease as the temperature of firing of the material was raised.

The following table gives the maximum and minimum and average values of certain properties of bricks made by different processes and reheated at 1,400° C.:

Method of manufacture	Number of brands	Modulus of elasticity	Absorption in per cent of dry weight	Failed in quenching test after	Linear thermal expansion between 100° to 200° C.
		Lbs./in.[2]		*Cycles*	*Per cent*
Handmade:					
Maximum		4,500,000	17.1	46	0.190
Minimum		353,000	6.8	5	.036
Average	8	2,139,000	11.6	15	.082
Dry press:					
Maximum		3,140,000	8.1	45	.079
Minimum		1,520,000	5.3	15	.033
Average	4	2,305,000	6.7	>27	.059
Stiff mud:					
Maximum		6,400,000	12.4	11	.110
Minimum		2,050,000	3.0	5	.055
Average	5	3,654,000	[1] 6.1	7	.078

[1] Omitting brand P (12.4 per cent) from this group causes this value to drop to 4.6 per cent.

The bricks manufactured by the stiff-mud process have the highest average modulus of elasticity and the lowest average absorption. These qualities, together with the high rate of thermal expansion between 100° and 200° C. and the possibility of laminated structure, may be the causes of the low resistance to spalling of this type of bricks.

The low rate of thermal expansion between 100° to 200° C. indicated by the dry-press brick is probably the explanation for the high resistance to spalling shown.

9. BRICKS TESTED AT SEVERAL TEMPERATURES

The modulus of elasticity, transverse strength, and maximum elongation of each of the 17 brands of bricks after reheating at 1,400° C. for five hours, were determined at 20°, 550°, and 1,000° C. The results of these tests (given in Table 9), with but two exceptions, show that both the modulus of elasticity and transverse strength were greater at 550° C. than at 20° C. The percentage increase in modulus of elasticity attending an increase in temperature from 20° to 550° C. is greater than the corresponding increase in transverse strength. The effect of higher temperatures on the modulus of elasticity is illustrated in Figure 10. The average modulus of elasti-

city determined at 550° C. as compared with that at 20° C. of the bricks made by the stiff-mud process had increased twice as much as that of the bricks made by the handmade process. The increase in the modulus of elasticity of the bricks, made by the dry-press method, was intermediate between the increases shown by the bricks made by the other two methods. At 1,000° C. the modulus of rupture had increased moderately and the modulus of elasticity had decreased greatly.

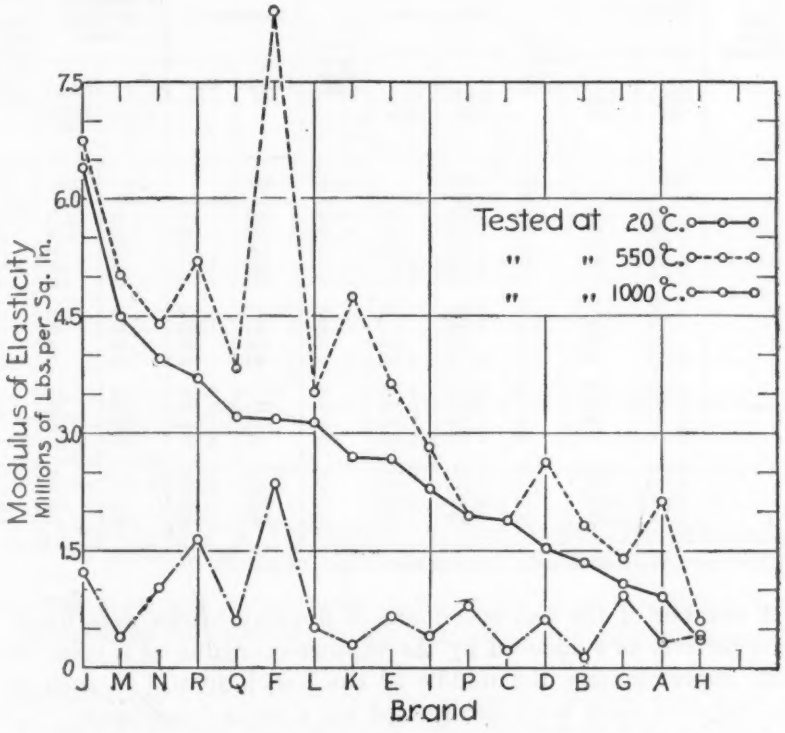

FIGURE 10.—*Effect of temperature on the modulus of elasticity of 17 brands of fire-clay brick*

At 550° C. the maximum elongation of the extreme fiber had decreased when compared with that obtained at 20° C. The formula for computing the outer fiber deformation is based on a linear relationship of the load-deflection curve. At 1,000° C. this relationship was found to be not linear; therefore, the secant modulus of elasticity was computed and this value substituted in the formula for determining maximum strain values at 1,000° C.[18] Table 9 shows the maximum elongation values as computed, using either the tangent or secant

[18] Maximum strain values at 1,000° C. of clay bodies are discussed in detail in the Fourth Progress Report of the Sagger Investigation, J. Am. Ceram. Soc., **10** (12), pp. 995–1004; 1927.

modulus. It is believed that the values obtained using the secant modulus represent more nearly the true deformation of the clays at 1,000° C.

TABLE 9.—*Properties of commercial brands of fire brick reheated at 1,400° C. for five hours*

Key letter of brand	Tested at 20° C.			Tested at 550° C.			Tested at 1,000° C.				
	Modulus of—		Maximum elongation	Modulus of—		Maximum elongation	Modulus of—		Maximum elongation using		Plastic flow (inches) after 1 hour stress
	Elasticity	Rupture		Elasticity	Rupture		Elasticity	Rupture	Tangent modulus	Secant modulus	
	1,000 lbs./in.²	*Lbs./in.²*	*Per cent*	*1,000 lbs./in.²*	*Lbs./in.²*	*Per cent*	*1,000 lbs./in.²*	*Lbs./in.²*	*Per cent*	*Per cent*	*60 lbs./in.²*
A	920	525	0.06	2,220	710	0.03	333	730	0.22	0.51	0.0008
B	1,350	380	.03	1,820	770	.04	147	640	.43	1.50	.0015
C	1,890	520	.03	1,890	550	.03	227	560	.25	.44	.0008
D	1,520	830	.06	2,660	1,275	.05	626	1,015	.16	.45	[1].0099
E	2,670	1,415	.05	3,640	1,610	.04	674	2,010	.30	.40	.0012
F	3,170	1,775	.06	8,400	2,520	.03	2,372	3,320	.14	1.65	.0002
G	1,070	625	.06	1,400	850	.06	894	1,275	.14	.20	.0003
H	353	335	.09	610	450	.07	426	695	.16	.29	.0005
I	2,300	885	.04	2,840	1,140	.04	424	810	.19	.32	[1].0008
J	6,400	1,470	.02	6,750	2,100	.03	1,217	2,620	.22	.69	.0047
K	2,700	925	.03	4,760	1,355	.03	331	2,750	.83	.90	.0042
L	3,145	995	.03	3,520	1,390	.04	531	1,390	.26	.47	.0007
M	4,500	1,210	.03	5,025	1,550	.04	410	2,320	.57	-------	.0006
N	3,950	1,415	.04	4,400	1,650	.04	1,032	1,525	.12	.16	.0001
P	1,950	955	.05	1,950	980	.05	808	1,375	.17	.27	.0004
Q	3,210	1,195	.04	3,830	1,200	.03	614	1,135	.18	.60	.0002
R	3,720	1,285	.03	5,200	1,620	.03	1,649	1,550	.09	.17	.0016

[1] These values were obtained using a stress of approximately 120 lbs./in.².

A number of the test specimens of fire-clay bricks were found to be defective, as evidenced by the rupture occurring at a point other than approximately the middle of the 8-inch span. In such cases the required data were determined on a second specimen. Check determinations of moduli of elasticity and rupture were made on 10 specimens and the results procured on the same body varied in the majority of cases less than 10 per cent. The two values obtained for each material are given in Table 10.

TABLE 10.—*Determinations and checks of moduli of elasticity and rupture obtained on commercial and laboratory prepared fire-clay brick after firing five hours at 1,400° C.*

Specimen	Modulus of elasticity	Modulus of rupture	Results obtained at—
	Lbs./in.[2]	*Lbs./in.*[2]	
H[1]	365,000	310	Room temperature.
	340,000	360	Do.
L[1]	2,900,000	950	Do.
	3,390,000	1,040	Do.
P[1]	1,849,000	920	Do.
	2,050,000	990	Do.
Q[1]	3,140,000	1,125	Do.
	3,280,000	1,260	Do.
Q—(SM)	3,400,000	950	Do.
	3,480,000	1,000	Do.
C—(DP)	2,250,000	865	550° C.
	1,900,000	790	Do.
E—(SM)	7,230,000	2,530	Do.
	8,120,000	(2)	Do.
I—(HM)	4,175,000	1,445	Do.
	4,010,000	1,400	Do.
L—(DP)	2,530,000	995	Do.
	2,890,000	825	Do.
Q—(SM)	2,680,000	830	Do.
	2,720,000	855	Do.

[1] Commercially prepared firebricks.
[2] No data.

NOTE.—(SM), (DP), and (HM) refer to stiff-mud, dry-press, and handmade methods of preparation of bricks made in the laboratory.

10. SOME REASONS FOR VARIATION IN RESISTANCE TO THERMAL SHOCK OF THE SAME BRAND OF BRICKS

The individual bricks in each set on which the thermal spalling test was made varied considerably in the number of quenchings required to produce failure. Two bricks which had been subjected to this test and which showed a great difference in spalling resistance were, therefore, selected from one set of each of two different brands of bricks. In addition, two bricks showing approximately the same resistance were selected from one set of a third brand. The modulus of elasticity, transverse strength, and thermal expansion of specimens cut from each of these bricks were determined. Curves showing the thermal expansion behavior are given in Figure 11. The curves plotted in the center section and in the section to the left of the center were obtained on bricks showing a large difference in spalling resistance. The lower curve in each case represents the expansion behavior of the bricks from one set showing the greater resistance to spalling. The expansion behavior of bricks showing approximately the same resistance to spalling is illustrated by the curve in the section to the

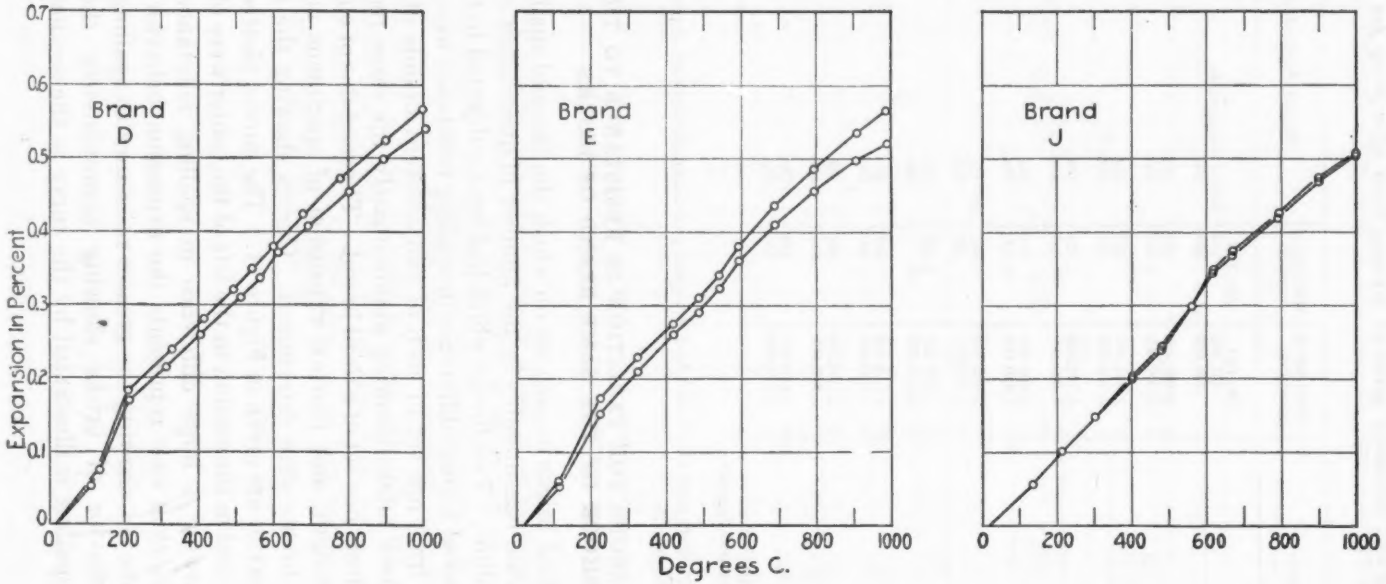

FIGURE 11.—*Curves showing expansion behavior of two bricks each of brands D, E, and J*

Individual bricks in one test of brands D and E showed great differences in resistance to spalling whereas the two of brand J showed practically the same resistance.

right of the center. The rate of expansion of the two bricks is practically identical. Results of the other tests made on these specimens are as follows:

Brand letter	Number of quenchings to cause spalling	Modulus of elasticity	Modulus of rupture	Total thermal expansion at 1,000° C.
		Lbs./in.²	*Lbs./in.²*	*Per cent*
D	3	3,360,000	420	0.567
D	45	2,318,000	300	.540
E	5	1,530,000	1,310	.568
E	15	836,000	775	.517
J	8	904,000	420	.508
J	9	976,000	710	.504

These data show that the large variations in spalling behavior of bricks of the same brand are not altogether due to the method of testing for resistance to spalling, but may be caused by large differences in the properties of the individual bricks. It will be noted that very little difference is shown in the modulus of elasticity and thermal expansion of the two bricks of brand J, showing practically the same resistance to spalling, whereas bricks of brands D and E show large differences in these properties and also show great differences in resistance to spalling. The bricks of both brands D and E having low resistance to thermal shock have the higher moduli of elasticity and higher thermal expansion.

The results obtained in these tests are not comparable with those tabulated in Table 8, since the tests were made on specimens using a 6-inch instead of an 8-inch span. The results show that the modulus of rupture decreases greatly after a brick has been subjected to the thermal shock test, as may be seen from a comparison of the results in the foregoing tabulation with those in Table 8. Such a relation has also been found by Parmelee and Westman.[19]

11. RELATION BETWEEN RESISTANCE TO THERMAL SPALLING AND MODULUS OF ELASTICITY

If the various brands of bricks are grouped into two classes, according to whether they withstood a greater or lesser number of quenchings than 15 in the spalling test and the averages of these groups are compared with the average moduli of elasticity of the same groups, the following results are obtained:

Number of brands[a]	Average number of quenchings to cause spalling	Average modulus of elasticity
		Lbs./in.²
6	27	2,190,000
9	9	3,505,000

[a] Brands G and H are omitted from these averages because of their highly siliceous nature, and their early failure in the water spalling test is in all probability due primarily to high thermal dilatation.

[19] The Effect of Thermal Shock on the Transverse Strength of Fire-Clay Brick, J. Am. Ceram. Soc., 11 (12); 1928.

These averages indicate that the resistance of bricks to spalling increases as the modulus of elasticity decreases.

12. RELATION BETWEEN RESISTANCE TO SPALLING AND THERMAL EXPANSION

The brands of bricks were grouped into two classes, according to whether the total expansion, per unit length, between 100° and 200° C. after firing at 1,400° C., as given in Table 4, was greater or less than 0.06 per cent. The averages of these groups are compared with the average number of quenchings the groups withstood before failure in the spalling test. The results are as follows:

Number of brands	Average thermal expansion	Average number of quenchings to cause spalling
	Per cent	
9	0.039	22
8	.102	8

These averages indicate that high thermal expansion is conducive to early failure in the thermal spalling test.

13. RELATION OF MODULUS OF ELASTICITY, EXPANSION, TRANSVERSE STRENGTH, PERCENTAGE OF GROG TO RESISTANCE TO SPALLING

Some data have been presented by Norton [20] and Booze [21] indicating a possible relation between resistance of fire brick to spalling and the three factors (1) modulus of elasticity, (2) thermal expansion, and (3) rate of temperature change or diffusivity. An empirical relation, combining the three factors, (1) modulus of elasticity, (2) expansion, and (3) transverse strength, expressing the relative resistance R of saggers to failure due to thermal shock is given in the Third Progress Report of the Investigation of Sagger Clays.[22] It has been shown in the present report that a relation apparently exists between resistance of brick to spalling and elasticity and thermal expansion. A study of the data also indicates that bricks having an absorption below 5 and above 12 per cent show less resistance to spalling than do those having absorptions within these limits. The formula with which the resistance factor R may be computed has been changed to include a value for total grog present in the green brick batch. It is

[20] J. Am. Ceram. Soc., 8 (1); 1925.
[21] J. Am. Ceram. Soc., 8 (6); 1925.
[22] J. Am. Ceram. Soc., 10 (7), pp. 524–534; 1927.

believed that this value gives some indication of the relative thermal conductivity of the materials. The formula at present reads as follows:

$$R = \frac{M.\ G}{E.\ e}$$

where

R = factor indicating relative resistance of brick to spalling.
M = modulus of rupture.
G = grog expressed in parts of green batch materials (in per cent divided by 100).
E = modulus of elasticity.
e = coefficient of expansion for the temperature range 20° to 250° C.

The computed resistance values R are given in Table 11, together with the number of quenchings required to cause failure. Figure 12

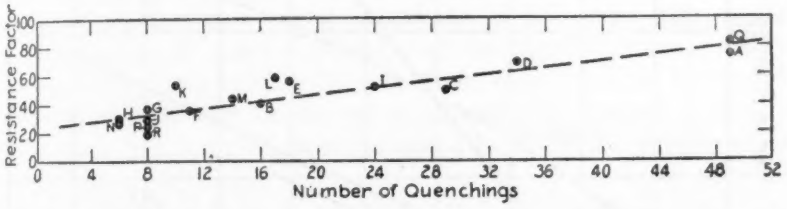

FIGURE 12.—*The computed resistance (R) of bricks to spalling plotted against the number of quenchings required to cause failure*

shows that the factor R is roughly proportional to the number of quenchings showing that the quantity $\frac{M.\ G}{E.\ e}$ is a fairly good indication of the resistance of a brick to spalling.

TABLE 11.—*Showing computed resistance factor and number of quenchings required to cause failure of fire bricks*

Laboratory key letter of brand	Resistance factor R	Number of quenchings to cause failure	Laboratory key letter of brand	Resistance factor R	Number of quenchings to cause failure
A	74	49	J	29	8
B	41	16	K	54	10
C	50	29	L	59	17
D	70	34	M	44	14
E	57	18	N	27	6
F	36	11	P	25	8
G	38	8	Q	83	49
H	31	6	R	19	8
I	52	24			

14. PLASTIC FLOW

If the form of a body is found to be permanently altered when the stress exceeds a certain value, the body is said to be plastic for stresses in excess of this value.[23] Typical load-deflection curves as obtained at 1,000° C. on a specimen cut from fire-clay brick brand K reheated at 1,400° C. are shown in Figure 13. The upper curve shows the plastic flow of the material under various loads, the lower curve the total deformation under these same loads, and the middle curve the elastic properties. The elastic recovery of the material was considered as the difference between the total deflection caused by the

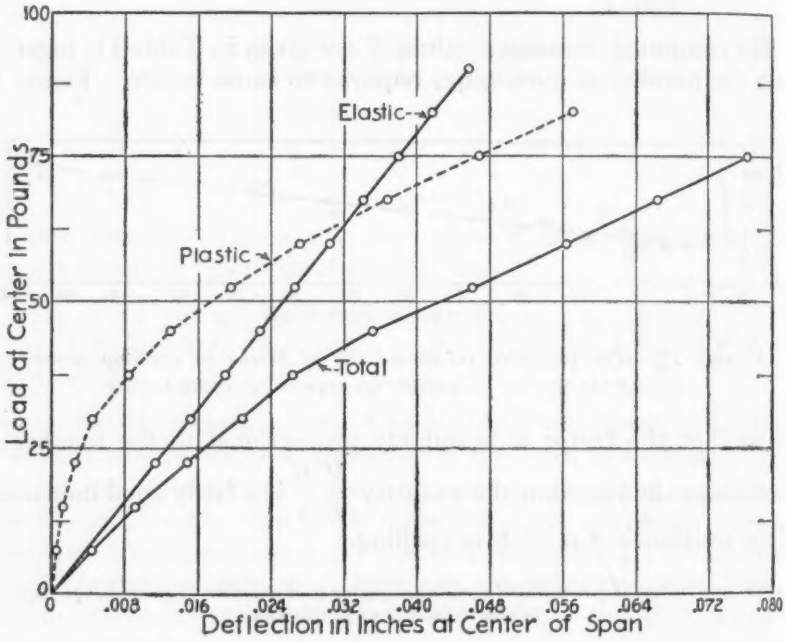

FIGURE 13.—*Load-deflection curves of fire-clay brick, brand K, at 1,000° C.*

The total deflection, plastic flow or set, and the elastic properties obtained with various stresses are shown.

load and the "set" of the material on removal of this load. The plastic flow of the various brands of bricks is given in Table 9. The values given represent the flow of the material at a temperature of 1,000° C. at the end of one hour using a load of approximately 60 lbs./in.^{2}, a specimen with a cross section of approximately 1 inch, and an 8-inch span. The smallest deflection, 0.0001 inch, is shown by brand N and the largest deflection, 0.0047 inch, by brand J. It is possible that certain of these values not only include the deflection

[23] B. S. Sci. Paper No. 278.

associated with softening of the matrix, but also may represent a partial breaking down of the physical structure. However, no breaking down in structure was evident in tests made with equivalent loads at room temperature.

V. FIRE-CLAY BRICKS PREPARED IN THE LABORATORY FROM BATCH MATERIALS FURNISHED BY MANUFACTURERS

1. GENERAL

Bricks have been made in the laboratory by each of the three methods most commonly employed in the manufacture of fire-clay bricks; namely, dry-press, stiff-mud-extruded (end cut), and handmade from prepared batch materials furnished by 14 manufacturers of fire-clay refractories.[24] These bricks were fired at 1,400° C. for five hours. In preparing these bricks it was realized that (*a*) it would be impossible to duplicate firing conditions of industrial kilns in the laboratory kiln; (*b*) exact duplication of the physical structure of the laboratory-prepared brick with that of the manufactured brick could not be expected, due to use of small-scale laboratory apparatus; (*c*) the same batch materials as furnished by the manufacturer would rarely, if ever, be used in the manufacture of fire bricks by the three methods, though it is quite common practice to use the same batch composition for bricks prepared by the dry-press and stiff-mud processes. However, it was believed that information of value would be obtained from this study not only to compare with test data of manufactured brick, but also to learn what effect a variation in the structure would have on certain physical properties. A photomicrograph of a specimen cut from burned bricks (batch P) made by each of the three methods of manufacture is shown in Figure 14. This particular batch material [25] is used commercially for making a stiff-mud brick. However, it is believed that the texture incident to each of the three processes of manufacture is well illustrated. The laminations in the brick prepared by the stiff-mud process are very pronounced, and the structure of the handmade brick appears to be considerably more dense than either of the bricks manufactured by the other processes. The brick made by the dry-press method shows probably the greatest uniformity.

The study of these bricks included the determination of: (*a*) Resistance to spalling, (*b*) absorption, (*c*) modulus of elasticity and transverse strength at 20° C. and at 550° C., (*d*) total linear burned shrinkage, and (*e*) linear thermal expansion from 20° to 1,000° C.

[24] A description of the various methods of manufacture of fire-clay brick may be found in B. S. Circular No. 282, Fire-Clay Brick. Their Manufacture, Properties, Uses, and Specifications.

[25] There is very little difference in composition between this manufacturer's batch materials used for brick prepared by the stiff-mud and handmade processes.

2. TEMPERING WATER

The "tempering" or "conditioning water"—that is, the percentage of water considered as desirable for securing proper molding of the laboratory-prepared fire bricks—is given in Table 12. The loss in weight on heating a finished brick at 110° C. for approximately 18 hours was considered as the water necessary for molding. It was found that the water required for molding bricks from the various batch materials by the (*a*) dry-press method ranged from a low of 6.3 per cent to a high of 13.7 per cent, (*b*) stiff-mud-extruded process ranged from 10.9 to 24.1 per cent, and (*c*) handmade method ranged from 13 to 29.2 per cent.

TABLE 12.—*Data determined on fire-clay brick made in the laboratory from prepared batch materials furnished by the manufacturer*

Laboratory key letter	Method of preparation [1]	Tempering water	Linear burned shrinkage in per cent of wet length	Absorption in per cent of dry weight	Average number of quenchings to cause failure	Total expansion at 1,000° C. [2]	Modulus of elasticity [3] at—		Modulus of rupture at—	
							20° C.	550° C.	20° C.	550° C.
		Per cent				*Inches/inch*	*Lbs./in.²*	*Lbs./in.²*	*Lbs./in.²*	*Lbs./in.²*
A	DP	10.2	5.8	7.2	18	568	2,230	2,440	840	1,340
	HM	15.4	10.0	8.2	12	560	2,860	3,600	1,085	1,020
	SM	16.4	10.1	7.7	9	566	2,880	3,960	1,020	1,110
B	DP	9.1	5.5	6.7	17	442	1,640	1,780	740	715
	HM	12.4	8.4	9.0	19	448	3,050	4,280	1,275	1,550
	SM	16.5	10.4	7.7	17	432	2,230	3,240	820	920
C	DP	6.4	3.5	9.3	18	442	2,310	2,075	985	830
	HM	14.2	8.2	11.5	18	449	2,740	2,700	1,015	1,000
	SM	13.0	8.4	9.4	9	470	1,860	1,800	680	620
D and N	DP	7.9	6.8	6.3	5	622	2,000	3,450	965	1,370
	HM	14.8	12.1	5.3	1	656	1,810	7,040	2,400	1,920
	SM	17.1	13.2	4.4	2	627	4,990	6,030	2,050	2,400
E and F	DP	7.1	6.4	5.3	6	508	1,990	3,860	1,140	1,710
	HM	16.1	13.6	4.9	3	607	5,090		1,290	
	SM	19.7	14.2	2.9	2	570	4,920	7,230	2,600	2,530
G	DP	11.2	3.1	14.1	7	654	830	1,260	450	690
	HM	18.1	6.9	16.1	9	640	1,500	1,380	875	940
	SM	22.0	8.2	15.3	8	643	1,390	1,680	755	1,045
H	DP	11.8	2.0	14.4	6	746	240	340	365	360
	HM	16.3	5.5	17.3	9	736	440		360	
	SM	23.9	9.6	16.1	11	717	170	320	150	335
I	DP	7.6	5.1	6.7	20	529	1,010	1,660	620	780
	HM	13.3	9.3	7.1	15	531	3,110	4,090	1,265	1,420
	SM	15.4	10.0	7.1	28	526	1,625	2,200	810	975
J	DP	7.6	4.6	5.1	3	412	6,430	6,530	1,590	1,945
	HM	16.1	10.0	4.9	3	412	5,330	8,100	1,625	1,590
	SM	20.1	10.4	3.9	3	416	5,300	6,700	1,670	1,740
K and L	DP	8.0	5.7	7.1	16	475	2,810	2,710	1,000	910
	HM	12.3	8.4	7.6	13	484	5,180	6,270	1,526	1,635
	SM	16.3	11.2	6.7	16	499	2,550	2,830	1,028	1,135
M	DP	6.3	3.3	8.0	6	419	3,410	5,050	1,030	1,500
	HM	10.9	5.5	8.6	7	435	4,910	3,920	890	1,075
	SM	14.5	7.6	7.7	5	447	4,530	4,830	1,335	1,195
P	DP	13.1	3.9	14.6	2	622	550	740	390	545
	HM	24.1	8.9	13.6	3	586	1,420	1,670	865	955
	SM	29.2	12.4	13.9	3	610	1,100	1,320	485	620
Q	DP	10.7	10.4	4.8	24	445	2,700	3,390	955	1,065
	HM	24.5	10.4	6.1	28	453	4,880	5,470	1,270	1,460
	SM	24.2	11.5	5.8	33	435	3,440	2,700	975	845
R	DP	13.7	5.3	10.9	7	595	1,660	2,280	840	930
	HM	22.2	6.7	11.8	4	617	3,030	3,970	870	1,325
	SM	25.4	11.2	11.9	8	579	1,960	2,390	725	900

[1] DP, HM, SM, refer to dry press, handmade, stiff mud, respectively.
[2] Values to be multiplied by 10^{-4}.
[3] Values to be multiplied by 10^{3}.

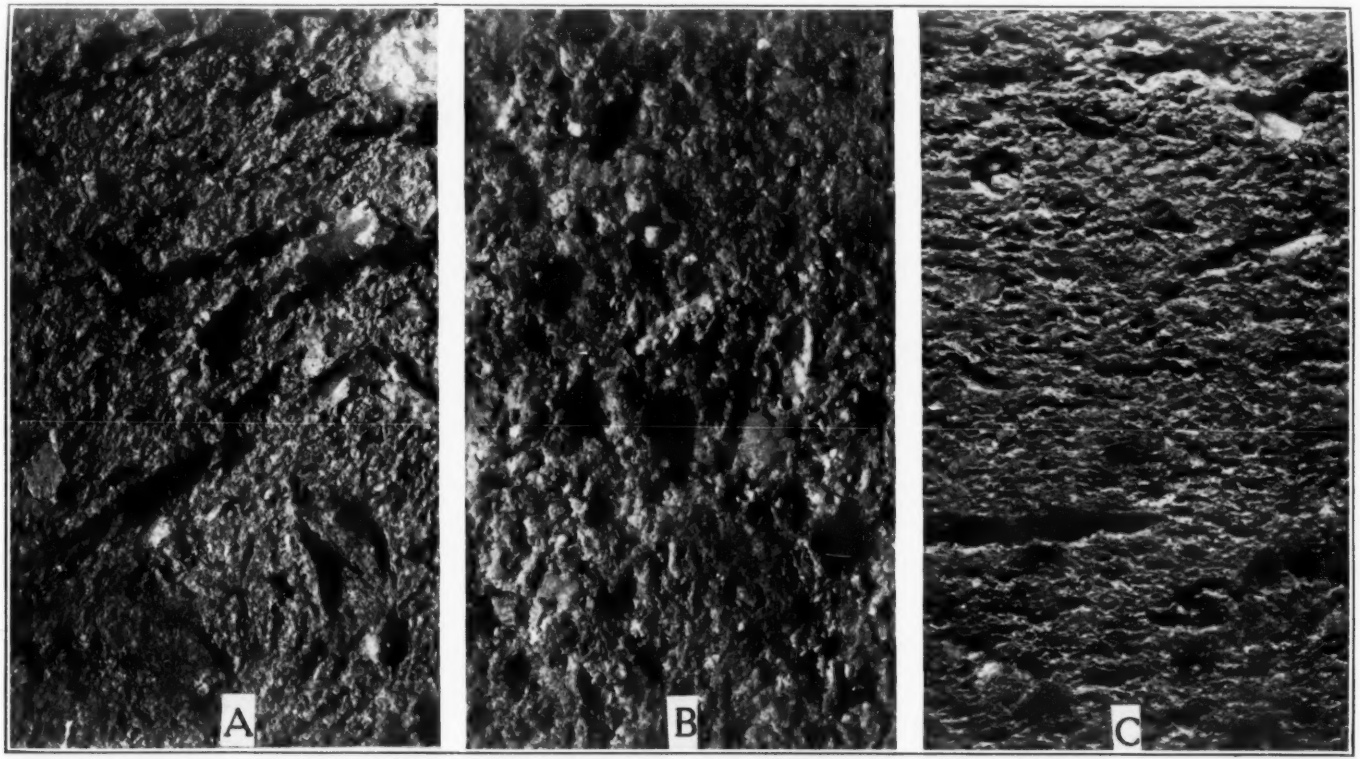

FIGURE 14.—*Photomicrograph, (4.5 diameters), showing structure of bricks made in the laboratory from a manufacturer's green batch material*

(A) is a section cut from a brick made by the stiff-mud method; (B), dry-press; and (C), handmade.

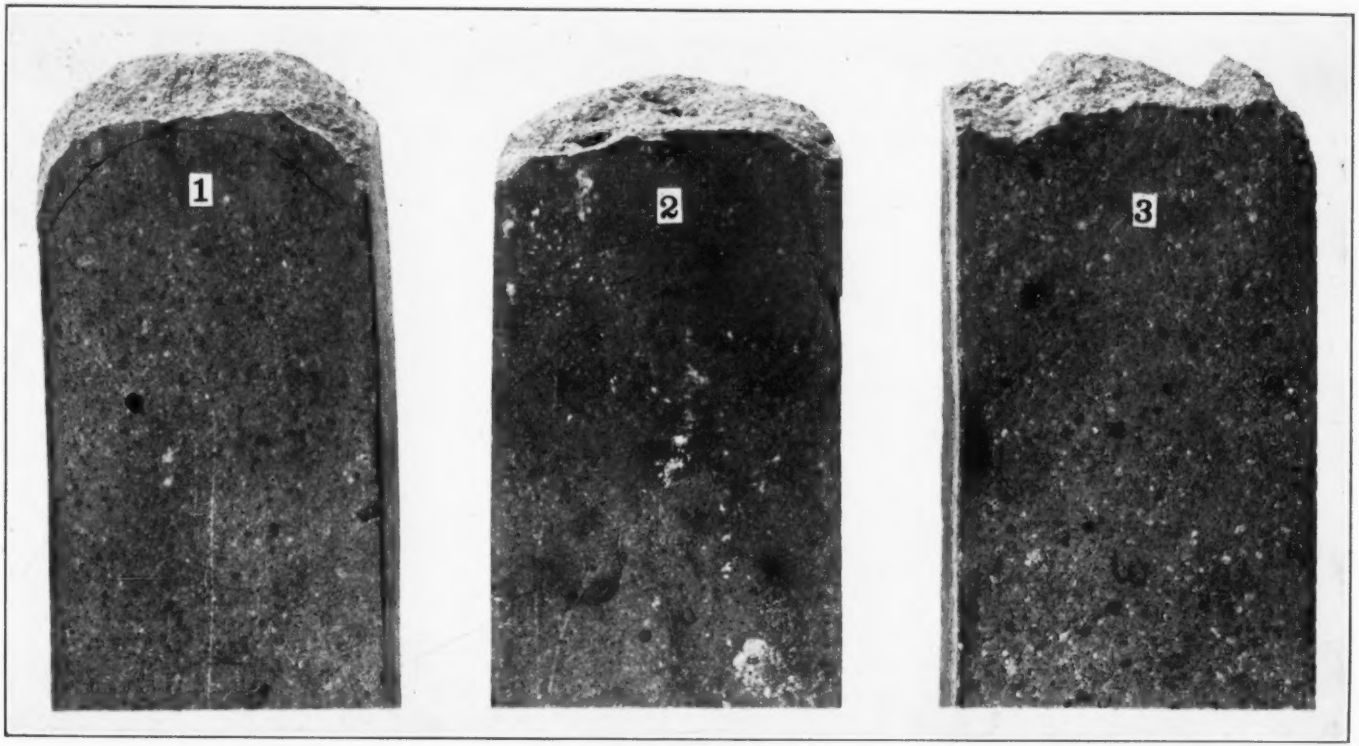

FIGURE 15.—*Types of failures of bricks when subjected to the water-quenching test*

The bricks were made by the following methods: (1), Stiff mud extruded; (2), handmade; (3), dry-press.

3. THERMAL SPALLING TEST

The results of the quenching test as conducted on a total of 42 different sets of 5 bricks each are given in Table 12. These results show (1) the average number of quenchings required to cause failure to range from 1 to 33; (2) those bricks (with one exception) with alumina content over 38 per cent have considerably greater resistance to spalling than those containing less than 38; and (3) although some sets show little difference in spalling resistance between bricks prepared by the different methods, others show almost 100 per cent difference.

A photograph of bricks prepared by the three methods from the same raw batch material and subjected to the thermal shock test is given in Figure 15. This illustrates well the types of spalling considered representative of fire-clay brick manufactured by the stiff-mud, handmade, and dry-press processes.

4. MODULI OF ELASTICITY AND RUPTURE

The modulus of elasticity and transverse strength of specimens cut from the 42 different bricks were determined at 20° and 550° C., and are given in Table 12, with the exception of the results for the handmade specimens E and H, at 550° C. There is a wide range in the values both at 20° and at 550° C., for elasticity and strength. The lowest value for modulus of elasticity obtained on specimen H (stiff-mud process) was 176,000 lbs./in.^{2}, and the lowest modulus of rupture, also obtained on this specimen was 150 lbs./in.^{2}, both values determined at approximately 20° C. The highest modulus of elasticity, found on specimen J (handmade process) at 550° C., was 8,100,000 lbs./in.^{2} and the highest modulus of rupture, found on specimen E (stiff-mud process) at 20° C., was 2,600 lbs./in.^{2} With few exceptions, it was found that the material gave higher values for both modulus of elasticity and transverse strength at 550° C. than at 20° C.

5. LINEAR BURNED SHRINKAGE

The linear burned shrinkage in per cent of length when wet is included in Table 12 with the other data determined on these bricks. The range in shrinkage, for all the groups, is from 2.0 to 14.2 per cent. The greatest range in shrinkage for any individual group representing specimens prepared from one batch composition by three different methods is from 6.4 to 14.2 per cent.

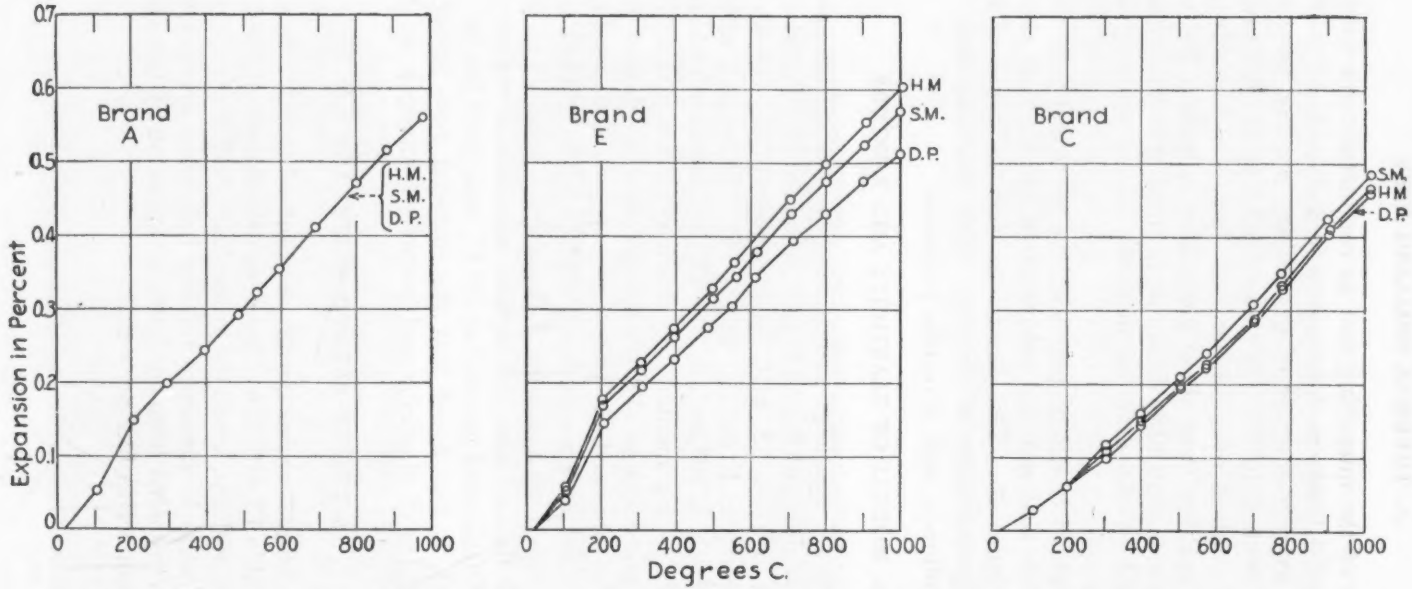

FIGURE 16.—*Curves showing linear thermal expansions of bricks made in the laboratory by three methods, namely, stiff-mud-extrudea (S. M.); handmade (H. M.); and dry-press (D. P.) from manufacturers' prepared "green batch"*

6. LINEAR THERMAL EXPANSION

No detailed data are presented on thermal expansion observations of laboratory-made bricks since the curves obtained for these materials closely parallel those observed on the fire bricks furnished by the manufacturers of the corresponding raw batch materials. However, a number of curves are given in Figure 16 to show either what effect the structure of the bricks may have on this property or that the material from which the bricks were made was nonhomogeneous, causing a variation in expansions as observed.

The graph on the left in Figure 16 shows the curves obtained on laboratory-made brick corresponding to brand A. This is the only instance in which observations on bricks made from the same batch material by the three different processes were identical throughout the entire range of temperature from 20° to 1,000° C. This is especially noteworthy, since the bricks spalled in the quenching test after 9, 12, and 18 dips for the handmade, stiff-mud, and dry-press processed bricks, respectively. In addition, the difference in absorption was only 1 per cent, and the inflexion shown in the curve between 100° and 200° C. indicates that an appreciable quantity of quartz may have been converted to cristobalite.

The center graph of Figure 16 shows the expansion curves obtained on laboratory-made bricks corresponding to brand E. These curves show the greatest difference in thermal expansion determinations on bricks made from the same batch material by the three different processes. The total expansion at 1,000° C. of the brick made by the handmade process is approximately 20 per cent greater than the total expansion of the brick made by the dry-press method. An examination of the thermal expansion curves for these bricks shows that a good portion of this difference in expansion is caused by the greater inflexion of the curve at approximately 200° C. for the handmade bricks, possibly due to more of the quartz originally present having been converted to cristobalite. The brick made by the dry-press method still shows quite an appreciable inflexion between 550° and 600° C. Table 12 gives the absorption of the brick made by the handmade process as 2.9 per cent, and the brick made by the dry-press process as 5.3 per cent. This would possibly indicate that the conversion of quartz to cristobalite may be accelerated in the brick of the lower absorption, due to the probability of the fluxes being in more intimate contact with the quartz.

The graph on the right in Figure 16 shows the curves obtained on laboratory-made brick corresponding to brand C. These curves are given to illustrate the difference in total expansion that may occur in bricks having little or no free quartz and are molded by the three different methods. The difference in expansions may be due to either errors in sampling or to the structure of the material.

7. LINEAR THERMAL EXPANSION AND RESISTANCE TO SPALLING

The total observed linear thermal expansion at 1,000° C. for the 42 specimens of laboratory-made brick are given in Table 12. The greatest variation in the data for any one series of bricks made by the three different methods occurs in those bricks prepared from batch materials having a relatively large percentage of free or converted quartz present in a very finely divided condition. This may be expected, since the method of preparation of the bricks in these cases would have slightly more influence on the speed of reactions taking place during heating than in those bricks having only a small percentage of free quartz or if the quartz is present in comparatively coarse grains. Although in a number of cases there appears to be little or no relation between the total expansion and the resistance to spalling for any series of bricks made by the three methods, there are a large number of instances where a definite relation is apparent between these two properties. Typical examples that show this relation are the bricks identified by letters G and H. In a number of cases only two of the three sets in any one series show this relation. Groups E and M may be cited as examples.

VI. SUMMARY

The materials furnished by manufacturers of refractories for this study include 17 different brands of fire-clay bricks, 14 green batches, 26 fire clays, and 3 samples of quartz and silica sand.

The chemical analyses of the fire bricks and fire clays are reported, and the results of such determinations as absorption, pyrometric cone equivalent values, thermal spalling, and sieve analysis of grog used in green batch materials are recorded in a series of tables. The thermal expansions of the fire clays fired at 1,400° C. and those of the fire bricks "as received" from the manufacturer and after reheating in the laboratory kilns at 1,400°, 1,500°, and 1,600° C. are given, and the materials are classified into groups according to the type of expansion. In addition, the modulus of elasticity and transverse breaking strength of the bricks have been determined not only at several temperatures, but also after the brick had received several different heat treatments.

These data show that the thermal expansions of the majority of bricks decrease as the temperature of firing is increased. This would lead to the conclusion that interstructural stresses, which may be caused by differences in the thermal expansions initially present between materials entering into the manufacture of a brick, are gradually reduced.

Data are presented which indicate that the thermal expansion of the finished brick may not necessarily be the average of the expansions of the clays entering into its composition.

The moduli of elasticity of the bricks were generally much greater when tested at 550° C. than when tested at 20° C. At 1,000° C. the modulus of elasticity was less than results obtained at either 20° or 550° C.; that is, the bricks became less rigid and more subject to plastic deformation. The modulus of elasticity and transverse strength increase as the temperature of firing of the bricks is increased. The increasing percentage of glass formed would cause this behavior.

Resistance of fire bricks to spalling on an average decreased with increase of modulus of elasticity and increase of thermal expansion.

Data are given to show that sufficient differences exist in the physical properties of bricks of the same brand to cause large variations in the number of quenchings required to cause spalling.

Bricks were made in the laboratory by the dry-press, stiff-mud-extruded, and handmade methods from manufacturer's green batch materials. Test results indicated no apparent relation between method of preparation of bricks and their thermal expansion, but there is direct relation between expansion and resistance to spalling.

An empirical relation is given which expresses the resistance of fire-clay brick to spalling as varying directly as the modulus of rupture and grog content and inversely as the modulus of elasticity and coefficient of expansion.

WASHINGTON, February 4, 1929.

73113°—29——8

THE FIRST SPECTRUM OF XENON

By William F. Meggers, T. L. deBruin, and C. J. Humphreys

ABSTRACT

Although 30 years have passed since the discovery of xenon, comparatively little has been known about its spectra, and all attempts to analyze the structure of the Xe_I spectrum have been foiled by the incompleteness and inaccuracy of the available data. This situation has been improved, as follows:

Discharge tubes were filled with pure Xe gas and operated so as to emit only the spectrum of neutral xenon atoms. This spectrum was photographed with quartz-prism and with diffraction grating spectrographs from the ultra-violet to the infra-red. Wave lengths ranging from 3,442.77 to 10,107.2 A have been determined for 318 lines and are supplemented by estimates of relative intensity. Analysis of these new data has resulted in the identification of spectral terms, combinations of which account for practically all of the observed lines.

The normal state of the neutral Xe atom (s^2p^6) is represented by a single level, and successive excited states arise from the addition of *s*-, *p*-, *d*-, *f*- electrons to the xenon ion (s^2p^5). In the notation first introduced to describe the Ne_I spectrum, and subsequently used for A_{II}, Kr_{II}, and now also for Xe_{II}, the single level is called "p_0", and the term groups produced by addition of *s*-, *p*-, *d*-, *f*- electrons are designated "*s*," "*p*," "*d* and *s*," "*x* and *y*," respectively. These groups in the order named theoretically consist of 4, 10, 12, and 12 levels. Each group divides into two subgroups converging in the limit to the two levels of a ^2P term characterizing the normal state of the xenon ion. This subdivision is striking in Kr_{II}, but especially so in Xe_I on account of the large separation (9,621) of the Xe_{II} doublet.

From the limits of the most regular series in the Xe_I spectrum, and from certain combinations, the absolute value of the $1s_5$ term is established as 30,766.98, and all other term values are based on this one. The resonance lines in the extreme ultra-violet (1,469.61 and 1,295.56 A) then fix the value of the largest term $p_0 = 97{,}835$ from which the ionization potential of 12.078 volts is deduced for neutral xenon atoms.

CONTENTS

		Page
I.	Introduction	732
II.	Wave-length measurements	734
III.	Analysis of the Xe_I spectrum	736
	1. Theoretical terms	736
	2. Absolute term values; ionization potential of Xe	738
	3. The principal series ($1s_i = mp_k$)	741
	4. The "fundamental" series (*X*, *Y*, *Z*, *U*, *V*, and *W*)	716
	5. The subordinate series	720
	6. The Xe_I spectrum in the extreme ultra-violet	723
	7. Identification of the experimental terms	725
	8. List of Xe_I lines	727

I. INTRODUCTION

Xenon, the heaviest and rarest of the atmospheric gases, was discovered in 1898 by Ramsay and Travers [1] who announced that:

> This gas possesses a spectrum analogous in character to that of argon, but differing entirely in the position of the lines. With the ordinary discharge the gas shows three lines in the red and about five very brilliant lines in the blue; while with the jar and spark gap these lines disappear and are replaced by four brilliant lines in the green, intermediate in position between the two groups of argon lines, the glow in the tube changing from blue to green.

This first reference to the spectrum of xenon points out that there are two entirely different spectra depending on the conditions of excitation, and it has since been the custom to refer to that excited without capacity and external spark gap as the first spectrum, while that produced by a disruptive discharge is called the second spectrum. A prismatic spectrogram showing 15 lines of the second spectrum of xenon was reproduced in color by Ramsay and Travers [2] in 1901. Approximate wave lengths of 250 lines (3,454 to 6,596 A) were published in 1901 by Liveing and Dewar,[3] but this list includes lines of both spectra. The most extensive and accurate descriptions of xenon spectra were published in 1903 by Baly,[4] who measured 92 lines (2,536.58 to 6,198.70 A) in the first spectrum and 1,247 lines (2,414.88 to 6,097.80 A) in the second, a small number of lines being common to both. Eleven of Baly's lines for the first spectrum are identifiable with mercury, so that 81 lines remain in his list (3,469.95 to 6,198.70 A). No extension to Baly's list was made until 1919, when Merrill [5] reported the wave lengths of 54 new lines in the red and infra-red (5,931.2 to 9,162.76 A). Ten strong lines of the first spectrum (4,500.978 to 4,923.246 A) and two of the second (4,603.028 and 4,844.333 A) were measured relative to the primary standard (6,438.4696 A of Cd) by Meggers,[6] and three of the former (4,624.275, 4,671.225, and 4,734.154 A) were also investigated and confirmed by Perard.[7]

Forty-two xenon lines (4,078 to 6,768 A) were examined with Lummer-Gehrcke interferometer plates by Gehrcke and Janicki;[8] they reported fine structure for only two lines, namely, 4,501.13 and 4,734.30 A.

The resonance lines of xenon (1,469.61 and 1,295.56 A) were discovered in 1926 by Hertz and Abbink,[9] and a more extensive investigation of Xe spectra in the extreme ultra-violet was subsequently

[1] Ramsay and Travers, Rep. British Assoc., p. 828; 1898.
[2] Ramsay and Travers, Phil. Trans, **A 197,** p. 47; 1901.
[3] Liveing and Dewar, Proc. Roy. Soc., **68,** p. 389; 1901.
[4] Baly, Phil. Trans., **A 202,** p. 183; 1903.
[5] Merrill, B. S. Sci. Paper, **15,** p. 251 (No. 345); 1919.
[6] Meggers, B. S. Sci. Paper, **17,** p. 193 (No. 414); 1921.
[7] Perard, Comptes rendus, **184,** p. 681; 1927.
[8] Gehrcke and Janicki, Ann. d. Phys., **81,** p. 314; 1926.
[9] Hertz and Abbink, Natuurwiss., **14,** p. 648; 1926.

made by Abbink and Dorgelo,[10] who published the wave lengths for 15 lines (1,469.61 to 1,027.04 A) assigned to the first spectrum of Xe.

The electrodeless discharge for xenon was investigated by L. Bloch, E. Bloch, and Déjardin [11] for the purpose of separating successive stages of ionization. Among 1,000 lines, 91 (3,550 to 7,120 A) were assigned to the arc spectrum or first spectrum of xenon (from neutral atoms), and the remaining lines were ascribed to singly, doubly, or trebly ionized atoms. This method of excitation appears to favor the production of spark lines, but it is, in general, a very inefficient source of arc lines. The Zeeman effect of Xe lines has not been investigated at all.

Many attempts have been made to find regularities in the first spectrum of xenon, but on account of inadequate data most of these have failed to yield results of any value. In 1914 Paulson [12] published four triplets, two of which are now known to involve true terms. Sommer [13] arranged 142 lines (including mercury impurity lines) in pairs and groups with 25 wave number differences ranging from 58 to $5{,}840 \pm 3$. It appears that a large majority of these "constant" differences are fortuitous and have no physical significance. Hicks [14] and Williams [15] have also discussed the structure of the first spectrum of xenon, but their results, too, are mostly spurious. Finally, McLennan and Ruedy [16] made absorption experiments with excited xenon gas and found two infra-red lines (8,232 and 8,819 A) to show absorption. Assuming that these lines involved the metastable level s_5, they succeeded in establishing a number of *sp* combinations, but the data available did not permit the assignment of any line to a definite transition.

The above-mentioned attempts to analyze the structure of the Xe_I spectrum emphasize the importance of having a satisfactory description of the spectrum, and our efforts have been directed toward this end in connection with similar work on the Kr_I spectrum.[17]

The purest krypton obtainable contained a trace of xenon, and it was therefore considered advisable to study the xenon spectra also. Furthermore, the practical reason for our study of krypton spectra originates with a proposal to adopt a Kr line as a primary standard of wave length [18] instead of the Cd line now recognized as such. The argument that Kr lines are sharper than Cd lines applies with even greater force to Xe lines with which it is theoretically possible at low temperatures to produce interference phenomena with retarda-

[10] Abbink and Dorgelo, Zeit. f. Phys., **47**, p. 221; 1928.
[11] L. Bloch, E. Bloch, Déjardin, Ann. de. Phys. (10), **2**, p. 461; 1924.
[12] Paulson, Astrophys. J., **40**, p. 307; 1914.
[13] Sommer, Zeit. f. Phys., **13**, p. 85; 1923.
[14] Hicks, Phil. Trans., **A 220**, p. 335; 1919.
[15] Williams, Ciencias Fisicas y Matematicas (No. 82), p. 255; 1928.
[16] McLennan and Ruedy, Trans. Roy. Soc. Can. (3), **22**, p. 15; 1928.
[17] Meggers, deBruin and Humphreys, B. S. Jour. Research, **3** (No. 89), p. 129; 1929.
[18] 7 Conf. Gen. Poids et Mesures, p. 52; 1927.

tions of a meter. The possibilities in this direction appear to be worth investigating, and the present paper may be regarded as a contribution to such a program. It is obviously desirable in the first place to describe the first spectrum of xenon with sufficient completeness and accuracy to permit analysis of its structure and classification of its lines. Certain properties of spectral lines are now known to be related to spectral terms (atomic energy levels), so that a classification of the lines enables one to draw upon theoretical considerations in a discussion of their suitability as standards of wave length. The present paper, therefore, deals with a preliminary description and with the interpretation of the Xe_I spectrum. It presents new values for the wave lengths and estimated intensities of 318 lines characterizing neutral xenon atoms and identifies spectral terms which, by their combinations, account for practically all of the observed lines. From the limits of term sequences and from combinations the absolute values of all terms are established. The largest term is ^1S_o (p_o) representing the normal state of the neutral xenon atom; its value is 97,835, corresponding to an ionization potential of 12.078 volts. The structure of this spectrum is compared with that of the analogous spectrum of the preceding rare gases, Ne, A, Kr, and a certain grouping of the terms is seen to be associated with the coordination of terms to limits representing the ground levels of the ions. This analysis of the Xe_I spectrum has uncovered additional evidence that *f*-type electrons (in addition to *s*-, *p*-, and *d*- electrons) may play a part in the production of rare gas spectral terms.

It will be desirable to supplement this description and analysis with investigations to record fainter lines and far infra-red lines, to compare the wave lengths of the stronger lines with the primary standard or with the meter itself, to study the hyperfine structure of complex lines, and to observe the Zeeman effects.

II. WAVE-LENGTH MEASUREMENTS

The sources of radiation, spectrographs, and procedure employed in this study of the Xe_I spectrum were almost identical with those described in our report on the Kr_I spectrum, so that it will suffice to give a brief summary of them here. Glass discharge tubes with aluminum disk electrodes like those described by Nutting [19] were filled with remarkably pure Xenon gas purchased from the Linde Gesellschaft für Eismaschinen in Höllriegelskreuth b. München. These tubes were operated on a. c. transformers rated to give 10,000 volts in one case and 40,000 volts in the other. The current in the tube in either case was about 20 milliamperes. The pressure of gas in the tubes and condition of operation was such that an almost

[19] Nutting, B. S. Sci. Papers, 4, p. 511; 1907.

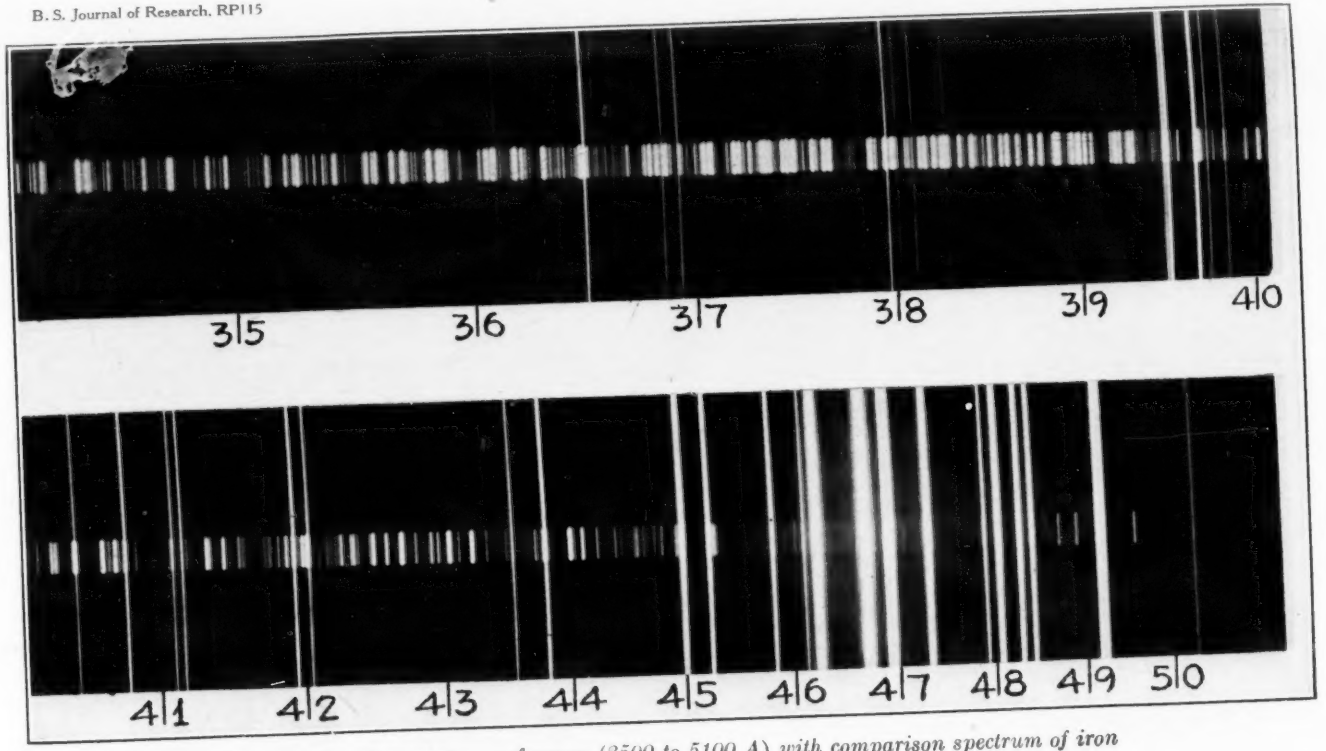

FIGURE 1.—*Arc spectrum of xenon (3500 to 5100 A) with comparison spectrum of iron*

Quartz prism spectrograph

UNIV. OF MICH.

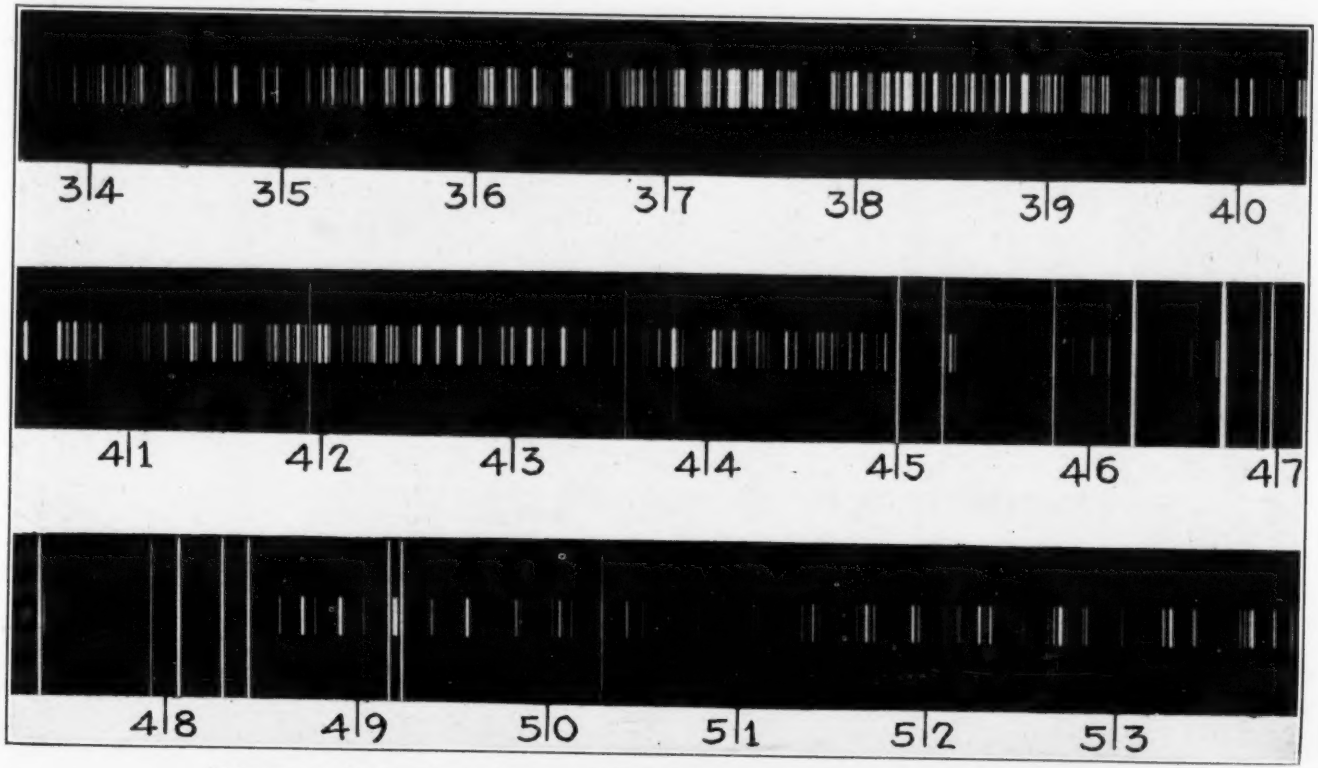

FIGURE 2.—*Arc spectrum of xenon (3400 to 5400 A) with comparison spectrum of iron*

Grating spectrograph

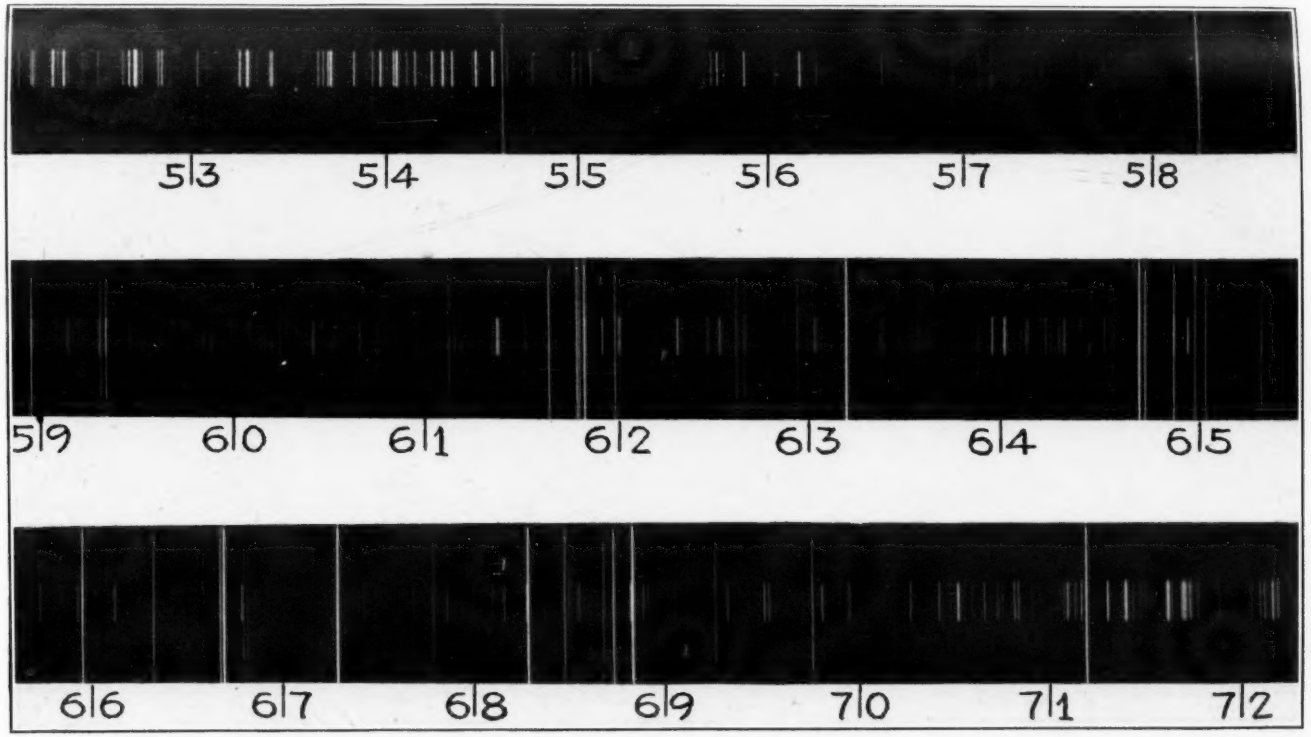

FIGURE 3.—*Arc spectrum of xenon (5300 to 7200 A) with comparison spectrum of iron*

Grating spectrograph

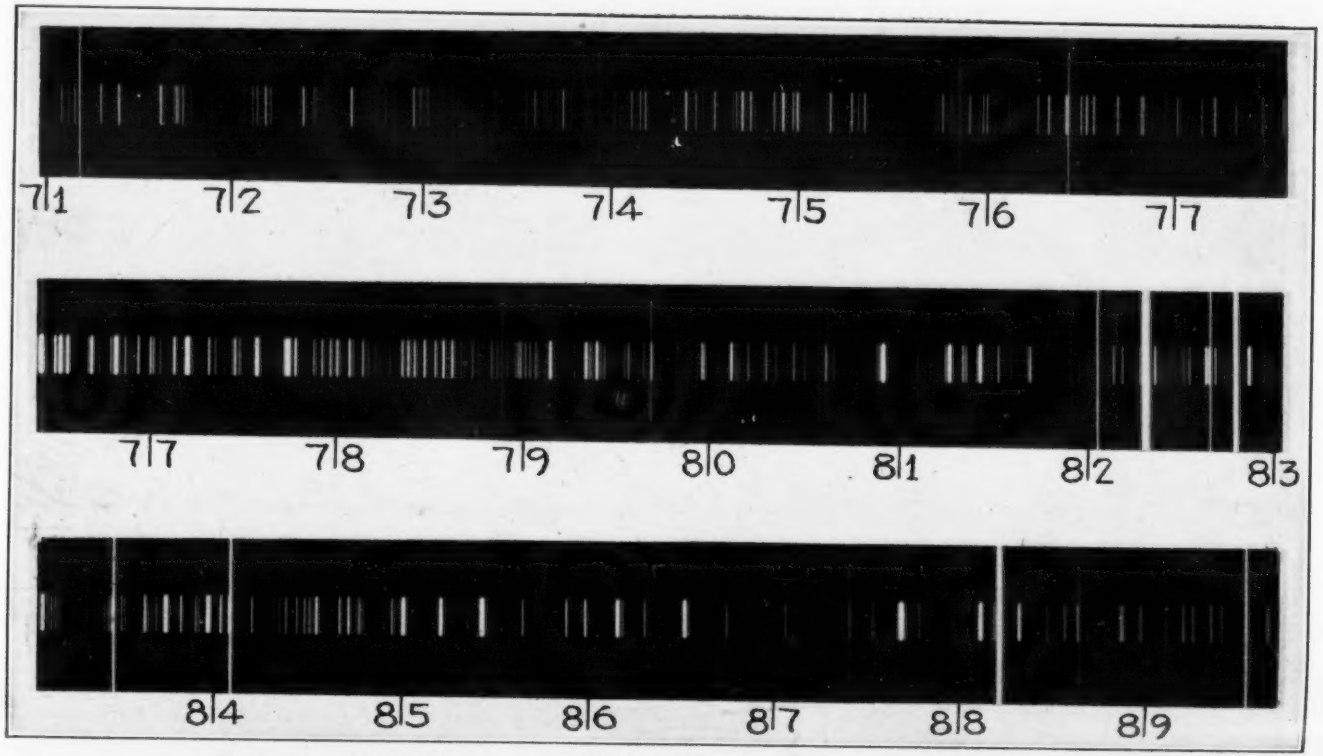

FIGURE 4.—*Arc spectrum of xenon (7100 to 8950 A) with comparison spectrum of iron*

Grating spectrograph

FIGURE 4.—*Arc spectrum of xenon (7100 to 8950 A) with comparison spectrum of iron*

Grating spectrograph

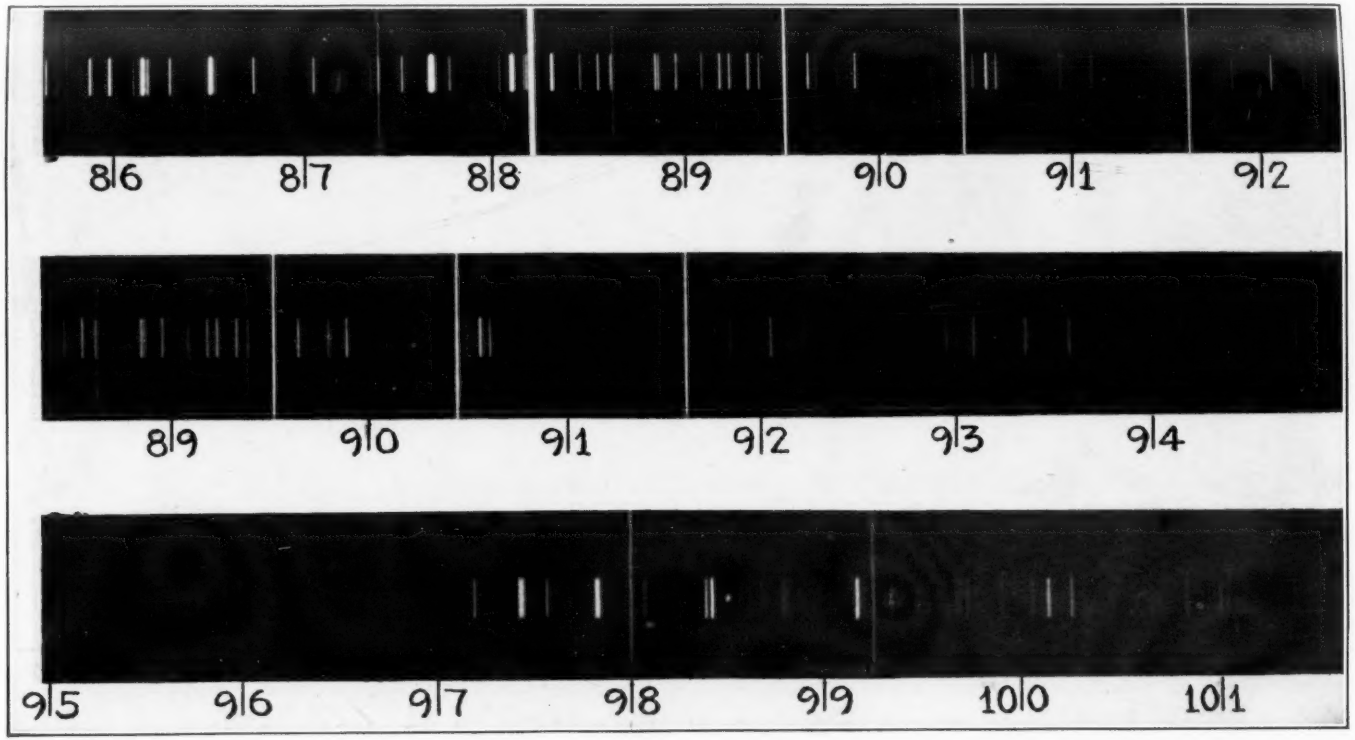

FIGURE 5.—*Arc spectrum of xenon (8600 to 10100 A) with comparison spectrum of iron*

Grating spectrograph

perfectly pure arc spectrum (Xe_I) was emitted, only traces of three or four most intense spark lines (Xe_{II}) showing on the longest exposures. Electrode evaporation occurs when the discharge is passing so that the bulbs are opaque after 10 to 20 hours, but the tubes are good sources of Xe spectra for several hundred hours operation. Most of the spectrograms were made in the first and second order of a 6-inch grating of 21 feet radius of curvature, mounted stigmatically as described before.[20] These were supplemented by several made with a Hilger E_1 autocollimating quartz spectrograph to record faint lines in the ultra-violet end of the spectrum. Eastman's No. 33 photographic plates were used regularly except for the longer wave regions, where No. 36 plates bathed in photosensitizing solutions of dyes were employed. The exposure times ranged from 10 to 48 hours, the latter exposure being sufficient to record a line in the infra-red at 10107.2 A.

Comparison spectra of iron were impressed upon the plates before and after each of the long exposures to xenon and wave-length measurements [21] were made relative to the secondary standards in the spectrum of the iron arc. Most of the lines were measured on four or five spectrograms, and the average probable error of the mean in such cases is not more than one or two hundredths of an Ångstrom unit. Some faint lines were observed only once; that is, on the strongest exposure. The wave lengths of such lines are not given beyond one decimal place. The observed wave lengths, estimated intensities, and term combinations of the Xe_I spectrum are presented in Table 14 at the end of this paper.

Since no complete photographic map of the xenon arc spectrum has ever been published, we are reproducing portions of our spectrograms in Figures 1, 2, 3, 4, and 5. These show the first spectrum of xenon from its limit in the ultra-violet near 3400 A to the infra-red near 10000 A. Xe resembles the preceding rare gases, Ne, A, and Kr, in that its first spectrum consists of groups of very intense lines, one in the blue (4501 to 4923 A) and another beginning at 8206 A in the infra-red and probably extending far beyond the photographic limit. The intervening region is well filled with lines of medium and lower intensity, the strongest visible lines being 5824, 6182, and 6470 A. When the tables of wave length were first compiled, it was rather surprising to find that about 50 per cent more lines were observed for the Xe_I spectrum than for the Kr_I spectrum which was produced and studied in essentially the same manner. The explanation of this superior abundance of Xe_I lines is found in the analysis of the Xe_I spectrum. (See the fundamental series.)

[20] Meggers and Burns, B. S. Sci. Papers, **18**, p. 191; 1922.

[21] We are indebted to Bourdon F. Scribner for many of the wave-length computations.

III. ANALYSIS OF THE Xe_I SPECTRUM

1. THEORETICAL TERMS

Neutral xenon ($Z=54$) has in the unexcited state, the atomic configuration of a closed shell with two $5s$- and six $5p$- electrons, symbolized by $5s^2\ 5p^6$. The spectral term which characterizes the normal state is a single level, $^1S_0$ according to Hund's theory.[22] The xenon ion, Xe^+, is characterized by the electron group $s^2\ p^5$, giving rise to an inverted doublet term $^2P_{2,1}$[23] in the Xe_{II} spectrum, and the terms representing the excited states of the neutral atom arise from the interaction of the series electron with the s^2p^5 group. The theoretical terms which may be expected to account for the first spectrum of xenon are thus obtained by adding in turn the electrons ns, np, nd, and nf to the term ^2P, as shown in Table 1.

TABLE 1.—*Electron configurations and theoretical terms of the Xe_I spectrum*

Electron configuration	Theoretical terms based on $^2P_{2,1}$ of Xe_{II}				Number of levels
$s^2\ p^6$	$^1S_0$				1
$(s^2\ p^5)\ s$	$^1P_1$		$^3P_{2,1,0}$		4
$(s^2\ p^5)\ p$	$^1S_0\ ^1P_1\ ^1D_2$	$^3S_1$	$^3P_{2,1,0}$	$^3D_{3,2,1}$	10
$(s^2\ p^5)\ d$	$^1P_1\ ^1D_2\ ^1F_3$	$^3P_{2,1,0}$	$^3D_{3,2,1}$	$^3F_{4,3,2}$	12
$(s^2\ p^5)\ f$	$^1D_2\ ^1F_3\ ^1G_4$	$^3D_{3,2,1}$	$^3F_{4,3,2}$	$^3G_{5,4,3}$	12

Paschen,[24] in his analysis of the Ne_I spectrum, introduced a special notation for these levels. The set of four levels resulting from the addition of an s-electron were called "s-terms," s_2, s_3, s_4, s_5 in the order of increasing magnitude. The set of 10 levels was referred to as "p-terms," $p_{1,2,3,\ldots\ldots 10}$, and the 12 levels from the d-electron were represented in part as "d-terms" and the remainder as "s-terms." Two terms of the following group (originating with an f-electron) were recognized and designated as "X- and Y- terms." The same notation was used by Meissner [25] in his analysis of the A_I spectrum and by the authors [26] in their description of the Kr_I spectrum. On account of certain difficulties and uncertainties in the translation of this Paschen notation into the modern quantum symbols, we shall retain the older notation also for the discussion of the Xe_I spectrum. This facilitates intercomparison of these four spectra but it is important to remember that homologous terms in the different spectra may have different inner quantum numbers. In all cases Ne_I, A_I, Kr_I, and Xe_I, the 4 s-terms are strictly comparable, but if the 10 p-terms

[22] Hund, Linienspektren und periodisches System der Elemente, p. 144, Julius Springer, Berlin; 1927.

[23] For convenience in printing and reading the inner quantum numbers of levels belonging to even multiplicities are increased by one-half.

[24] Paschen, Ann. d. Phys., **60**, p. 405; 1919; **63**, p. 201; 1920.

[25] Meissner, Zeit. f. Phys., **27**, p. 238; 1926; **39**, p. 172; 1926; **40**, p. 839; 1927.

[26] Meggers, de Bruin and Humphreys, B. S. Jour. Research, **3** (No. 89), p. 129; 1929.

are numbered (with subscripts) in order of magnitude they must be rearranged to compare levels with the same inner quantum numbers as shown in Table 2.

TABLE 2.—*Corresponding terms in Ne_I, A_I, Kr_I, and Xe_I spectra*

j	0	1	0	2	1	2	1	2	3	1	1	0	1	2
NeI	p_1	p_2	p_3	p_4	p_5	p_6	p_7	p_8	p_9	p_{10}	s_2	s_3	s_4	s_5
AI	p_1	p_2	p_3	p_3	p_4	p_6	p_7	p_8	p_9	p_{10}	s_2	s_3	s_4	s_5
KrI	p_1	p_3	p_5	p_2	p_4	p_6	p_7	p_8	p_9	p_{10}	s_2	s_3	s_4	s_5
XeI	p_1	p_3	p_5	p_3	p_4	p_6	p_7	p_9	p_8	p_{10}	s_2	s_3	s_4	s_5

In each case it has been found that the group of terms may be divided into subgroups converging to two limits separated by a "displacement constant," A. The limits are the two ground levels, $^2P_2$ and $^2P_1$ of the ion. The displacement constant, A, found from the limits of the Ritzian and non-Ritzian series, is related to the coordination of the arc spectrum levels to the two levels $^2P_{2,1}$ of the ion and is approximately the same magnitude as the separation of these levels. The data for the four rare gas spectra are given in Table 3.

TABLE 3.—*Displacement constants and level separations in rare gas spectra*

	Neon	Argon	Krypton	Xenon
A	780.0	1,423.20	5,330±	Vide infra.
$^2P_{2,1}$	782	1,431	5,371	9,621
$1s_5$-$1s_3$	776.90	1,409.92	5,219.90	9,129.24
$^2P_2$-$^2P_0$				
Centers of gravity of $3p$-term groups	788	1,451	5,353	Vide infra.

On account of the very large separation of $^2P_{2,1}$ for xenon, it is impossible to find any but the first members of the non-Ritzian sequence $np_{1,2,3,4}$, since the second members would give negative term values. It is therefore not possible to determine the displacement constant A of xenon from the series limits. However, an upper limit can be found from the distance between centers of gravity of the $^2p_{5,6\ \ldots\ 10}$ and the $^2p_{1,2,3,4}$ groups. This upper limit has the value 10,540. The lower limit for this A is the $1s_5$-$1s_3$ separation, which amounts to 9,129.24. The $^2P_{2,1}$ separation in Xe_{II} has been found [27] to be 9,621, which is in satisfactory agreement with the two limits 9,129 and 10,540 just discussed. For calculating the effective quantum numbers of the non-Ritzian Xe_I terms we have assumed A=9,621.

[27] Humphreys and deBruin, Sci., **68**, p. 573; 1928.

2. ABSOLUTE TERM VALUES; IONIZATION POTENTIAL OF Xe

Among the various series identified in Ne_I, A_I, and Kr_I spectra, one, namely, $2p_9$-md_4', was unique in the regularity of its effective quantum numbers. The analogous series in Xe_I is $2p_8$-md_4', and again it is the most regular as well as the longest. As in the preceding cases, this series has been employed for the determination of absolute term values, since it is probable that the best values must result from extrapolation of the longest series following most closely a Ritz formula. The $2p_8$-md_4' series fixes the level $2p_8 = 19{,}431.49$, and addition of the wave number $1s_5$-$2p_8 = 11{,}335.49$, places the $1s_5$ level at 30,766.98. The same level can be arrived at independently from several different series. The results are summarized as follows:

1. Series $2p_8$-md_4' and $1s_5$-$2p_8$	$1s_5 = 30{,}766.98$
2. Series $2p_9$-md_4 and $1s_5$-$2p_9$	$1s_5 = 30{,}768.26$
3. Series $2p_6$-md_1' and $1s_5$-$2p_6$	$1s_5 = 30{,}767.61$
4. Series $1s_3$-mX and $1s_5$-$1s_3$	$1s_5 = 30{,}766.12$
5. Series $1s_5$-mp_6	$1s_5 = 30{,}767.24$
6. Series $1s_5$-mp_8	$1s_5 = 30{,}765.28$

The mean of the six values is 30,766.91, practically identical with the first one, which is chosen as the basic value. All remaining term values are relative to $1s_5 = 30{,}766.98$, and any error in this level is therefore the same for all the other terms. The details of the above-mentioned calculations of $1s_5$ are presented in Table 4.

TABLE 4.—*Determination of absolute term values*

Series $2p_8$-md_4'

$$\nu = A - \frac{R}{[m+\mu+\alpha(A-\nu)]^2}$$

$R_{Xe} = 109{,}736.66$
$A = 19431.489$
$\alpha = -0.000001377271113$
$\mu = +0.5197276575 \pm 10^{-10}$

m	Int.	$\lambda_{obs.}$	$\nu_{obs.}$	$\nu_{calc.}$	ν obs.$-$ ν calc.
2				[a]1, 809. 645	
3	3	9, 513. 33	10, 508. 71	10, 511. 369	−2. 66
4	30	7, 119. 58	14, 041. 91	14, 041. 910	0. 00
5	30	6, 318. 08	15, 823. 22	15, 823. 220	0. 00
6	8	5, 934. 14	16, 846. 98	16, 847. 045	−0. 06
7	3	5, 716. 14	17, 489. 48	17, 489. 456	+0. 02
8	1	5, 579. 16	17, 918. 88	17, 918. 929	−0. 05
9	1−	5, 486. 90	18, 220. 18	18, 220. 180	0. 00

$2p_8 = 19{,}431.489$
$1s_5 - 2p_8 = 11{,}335.49$

$1s_5 = 30{,}766.98$

Series $2p_9$-md_4

$A = 19{,}716.015$
$\alpha = +0.000006775882325$
$\mu = +0.5392837788 \pm 10^{-10}$

m	Int.	$\lambda_{obs.}$	$\nu_{obs.}$	$\nu_{calc.}$	ν obs.$-$ ν calc.
2				4, 036. 67	
3	5	9, 167. 47	10, 905. 14	11, 233. 42	−328. 28
4	60	6, 882. 15	14, 526. 35	14, 472. 71	+53. 64
5	20	6, 182. 41	16, 170. 45	16, 170. 45	0. 00
6	4	5, 824. 76	17, 163. 33	17, 163. 33	0. 00
7	2	5, 618. 80	17, 792. 47	17, 792. 08	+0. 39
8	1−	5, 488. 56	18, 214. 69	18, 214. 69	0. 00
9	1−	5, 400. 4	18, 512. 01	18, 512. 15	−0. 14

$2p_9 = 19{,}716.015$
$1s_5 - 2p_9 = 11{,}052.25$

$1s_5 = 30{,}768.26$

[a] Exact calculation given on p. 748.

TABLE 4.—*Determination of absolute term values*—Continued

Series $2p_6$-md_1'

$A=18{,}622.663$
$\alpha=+0.000002752635528$
$\mu=+0.6180082686\pm10^{-10}$

m	Int.	$\lambda_{obs.}$	$\nu_{obs.}$	$\nu_{calc.}$	ν obs.− ν calc.
2				3, 121. 40	
3	2	9, 685. 29	10, 322. 11	10, 344. 02	−21. 91
4	6	7, 393. 77	13, 521. 19	13, 508. 22	+12. 97
5	20	6, 595. 54	15, 157. 85	15, 157. 85	0. 00
6	4	6, 200. 86	16, 122. 35	16, 122. 35	0. 00
7	2	5, 974. 08	16, 734. 35	16, 734. 34	+0. 01
8	1	5, 830. 47	17, 146. 52	17, 146. 52	0. 00
9	1−	5, 733. 4	17, 436. 83	17, 437. 20	−0. 37

$2p_6=18{,}622.663$
$1s_5-2p_6=12{,}144.95$
$1s_5=30{,}767.61$

Series $1s_3$-mX

$A=21{,}636.880$
$\alpha=+0.000002293149515$
$\mu=+0.9439590749\pm10^{-10}$

m	Int.	$\lambda_{obs.}$	$\nu_{obs.}$	$\nu_{calc.}$	ν obs.− ν calc.
3	40	6, 827. 30	14, 643. 04	14, 639. 10	+3. 94
4	15	5, 823. 89	17, 165. 90	17, 165. 90	0. 00
5	4	4, 392. 74	18, 538. 30	18, 538. 30	0. 00
6	2	5, 162. 66	19, 364. 48	19, 364. 48	0. 00
7	1−	5, 023. 80	19, 899. 71	19, 899. 71	0. 00

$1s_3=21{,}636.880$
$1s_5-1s_3=9{,}129.24$
$1s_5=30{,}766.12$

Series $1s_5-mp_6$

$A=30{,}767.237$
$\alpha=-0.000003114322468$
$\mu=+0.4985618368\pm10^{-10}$

m	Int.	$\lambda_{obs.}$	$\nu_{obs.}$	$\nu_{calc.}$	ν obs.− ν calc.
2	300	8, 231. 62	12, 144. 95	12, 353. 55	−208. 60
3	150	4, 624. 29	21, 618. 90	21, 654. 54	−35. 64
4	15	3, 950. 92	25, 303. 42	25, 303. 42	0. 00
5	3	3, 685. 91	27, 122. 65	27, 122. 65	0. 00
6	1	3, 549. 84	28, 162. 27	28, 162. 27	0. 00
7	1−	3, 469. 96	28, 810. 56	28, 812. 44	−1. 88

$1s_5=30{,}767.24$

TABLE 4.—*Determination of absolute term values*—Continued

Series $1s_5 - mp_8$

$A = 30{,}765.284$
$\alpha = -0.000004234844672$
$\mu = +0.4630334435 \pm 10^{-10}$

m	Int.	$\lambda_{obs.}$	$\nu_{obs.}$	$\nu_{calc.}$	ν obs.− ν calc.
2	200	8, 819. 43	11, 335. 49	11, 409. 57	−74. 08
3	300	4, 671. 22	21, 401. 71	21, 401. 71	0. 00
4	20	3, 967. 55	25, 197. 37	25, 197. 37	0. 00
5	3	3, 963. 51	27, 066. 84	27, 067. 19	−0. 35
6	1	3, 554. 03	28, 129. 07	28, 129. 07	0. 00
7	1−	3, 472. 49	28, 790. 06	28, 790. 61	−0. 55

$1s_5 = 30{,}765.28$

The resonance lines of xenon lie in the extreme ultra-violet at 1469.61 and 1295.56 A. They form the connecting link between the ground term p_0 ($^1S_0$) and the excited states $1s_2$ and $1s_4$ ($^1P_1$ and $^3P_1$), and permit the evaluation of this largest term, and calculation of the ionization potential. Thus, from the terms $1s_4 = 29{,}789.34$ and $1s_2 = 20{,}649.44$, we obtain:

$$p_0 - 1s_4 = 1469.61 \text{ A}; \quad \nu = 68{,}045.3; \quad p_0 = 97{,}834.6$$
$$p_0 - 1s_2 = 1295.56 \text{ A}; \quad \nu = 77{,}186.7; \quad p_0 = 97{,}836.1$$

The final value of the normal state of neutral xenon atoms is therefore

$$p_0\ (^1S_0) = 97{,}835.3$$

corresponding to an ionization potential of 12.078 volts. This is in good agreement with the estimation of Abbink and Dorgelo [28] on the absorption of spark lines (ca. 12.0 volts) but somewhat higher than the value obtained by Hertz and Kloppers [29] from critical potential measurements (ca. 11.5 volts).

3. THE PRINCIPAL SERIES $1s_1$-mp_k

The data for the 10 principal series $1s_1$-mp_k are presented in Table 5, where the observational data are represented by estimated intensity of the spectral line (in parenthesis) followed by the measured wave length λ. The corresponding wave number in vacuum, ν, was computed with the aid of Kayser's "Tabelle der Schwingungszahlen," except for lines in the unexplored infra-red region which are represented by term differences. Values of mp have been calculated from each combination, and finally the mean value of each term and the effective quantum number $\sqrt{\frac{R}{mp}}$, associated with it are given.

[28] Abbink and Dorgelo, Zeit. f. Phys., **47**, p. 232; 1928.
[29] Hertz and Kloppers, Zeit. f. Phys., **31**, p. 403; 1925.

TABLE 5.—*Xe principal series, $1s_1$-m_k*

Series, mp_1

Limits: $1s_2 = 20{,}649.44$
$1s_4 = 29{,}789.34$

Comb.	m	ν
s_2p_1	λ	(8)7, 887. 38
	ν	12, 675. 00
	mp_1	7, 974. 44
s_4p_1	λ	(30)4, 582. 74
	ν	21, 814. 92
	mp_1	7, 974. 42
Mean	mp_1	7, 974. 43
	$\sqrt{\frac{R}{mp_1+A}}$	2. 4973

$A = 9{,}621$

Series, mp_2

Limits: $1s_2 = 20{,}649.44$
$1s_3 = 21{,}637.74$
$1s_4 = 29{,}789.34$
$1s_5 = 30{,}766.98$

Comb.	m	ν
s_2p_2	λ	(20)8, 266. 53
	ν	12, 093. 65
	mp_2	8, 555. 79
s_3p_2	λ	(15)7, 642. 02
	ν	13, 081. 95
	mp_2	8, 555. 79
s_4p_2	λ	(2)4, 708. 19
	ν	21, 233. 66
	mp_2	8, 555. 68
s_5p_2	λ	(100)4,500.99
	ν	22, 211. 12
	mp_2	8, 555. 86
Mean	mp_2	8, 555. 78
	$\sqrt{\frac{R}{mp_2+A}}$	2. 4571

$A = 9{,}621$

TABLE 5.—*Xe principal series, $1s_1$-m_k*—Continued

Series, mp_3

Limits: $1s_2 = 20{,}649.44$
$1s_4 = 29{,}789.34$
$1s_5 = 30{,}766.98$

Comb.	m	ν
s_2p_3	λ	(50)8, 346. 86
	ν	11, 977. 26
	mp_3	8, 672. 18
s_4p_3	λ	(100)4, 734. 15
	ν	21, 117. 23
	mp_3	8, 672. 21
s_5p_3	λ	(50)4, 524. 68
	ν	22, 094. 83
	mp_3	8, 672. 15
Mean	mp_3	8, 672. 18
	$\sqrt{\frac{R}{mp_3+A}}$	2. 4492

$A = 9{,}621$

Series, mp_4

Limits: $1s_2 = 20{,}649.44$
$1s_3 = 21{,}637.74$
$1s_4 = 29{,}789.34$
$1s_5 = 30{,}766.98$

Comb.	m	ν
s_2p_4	λ	(5)8, 930. 81
	ν	11, 194. 03
	mp_4	9, 455. 41
s_3p_4	λ	(25)8, 206. 34
	ν	12, 182. 36
	mp_4	9, 455. 38
s_4p_4	λ	(50)4, 916. 50
	ν	20, 334. 01
	mp_4	9, 455. 33
s_5p_4	λ	(25)4, 690. 97
	ν	21, 311. 61
	mp_4	9, 455. 37
Mean	mp_4	9, 455. 37
	$\sqrt{\frac{R}{mp_4+A}}$	2. 3984

$A = 9{,}621$

NOTE.—The use of 6-point type for the remaining series does not reflect on their importance.

TABLE 5.—*Xe principal series, $1s_1$-m_k*—Continued

Series, mp_5
Limits: $1s_2$=20,649.44
$1s_4$=29,789.34

Comb.	m	2	3	4	5	6
s_2p_5	λ		(5)8, 576. 03	(15d)6, 504. 16		
	ν	2, 933. 85	11, 657. 21	15, 370. 54		
	mp_5	17, 715. 59	8, 992. 23	5, 278. 90		
s_4p_5	λ	(150)8, 280. 16	(100)4, 807. 01	(20)4, 078. 81	(4)3, 809. 90	(2)3, 669. 94
	ν	12, 073. 75	20, 797. 16	24, 510. 06	26, 239. 99	27, 240. 67
	mp_5	17, 715. 59	8, 992. 18	5, 279. 28	3, 549. 35	2, 548. 67
Mean	mp_5	17, 715. 59	8, 992. 20	5, 279. 09	3, 549. 35	2, 548. 67
	$\sqrt{\frac{R}{mp_5}}$	2. 4888	3. 4933	4. 5593	5. 5604	6. 5618

Series, mp_6
Limits: $1s_2$=20,649.44
$1s_4$=29,789.34
$1s_5$=30,766.98

Comb.	m	2	3	4	5	6	7
s_2p_6	λ		(3)8, 692. 08	(3)6, 583. 15			
	ν	2, 027. 40	11, 501. 57	15, 186. 11			
	mp_6	18, 622. 04	9, 147. 87	5, 463. 33			
s_4p_6	λ	(50)8, 952. 25	(60)4, 843. 29	(10)4, 109. 71	(2)3, 823. 76	(4)3, 677. 62	
	ν	11, 167. 31	20, 641. 37	24, 325. 78	26, 144. 88	27, 183. 79	
	mp_6	18, 622. 03	9, 147. 97	5, 463. 56	3, 644. 46	2, 605. 55	
s_5p_6	λ	(300)8, 231. 64	(200)4, 624. 29	(20)3, 950. 92	(4)3, 685. 91	(2)3, 549. 84	(1)3, 469. 96
	ν	12, 144. 92	21, 618. 90	25, 303. 43	27, 122. 65	28, 162. 27	28, 810. 55
	mp_6	18, 622. 06	9, 148. 06	5, 463. 55	3, 644. 33	2, 604. 71	1, 956. 43
Mean	mp_6	18, 622. 04	9, 147. 97	5, 463. 48	3, 644. 40	2, 604. 93	1, 956. 43
	$\sqrt{\frac{R}{mp_6}}$	2. 4275	3. 4635	4. 4817	5. 4874	6. 4905	7. 4893

Series, mp_7
Limits: $1s_2$=20,649.44
$1s_3$=21,637.74
$1s_4$=29,789.34
$1s_5$=30,766.98

Comb.	m	2	3	4	5	6
s_2p_7	λ		(6)8, 648. 51			
	ν	1, 770. 94	11, 559. 51			
	mp_7	18, 878. 50	9, 089. 93			
s_3p_7	λ		(10)7, 967. 33			
	ν	2, 759. 24	12, 547. 81			
	mp_7	18, 878. 50	9, 089. 93			
s_4p_7	λ	(40)9, 162. 66	(70)4, 829. 71	(15)4, 116. 11	(3)3, 826. 86	(1)3, 679. 31
	ν	10, 910. 87	20, 699. 41	24, 287. 95	26, 123. 70	27, 171. 30
	mp_7	18, 878. 47	9, 089. 93	5, 501. 39	3, 665. 64	2, 618. 04
s_5p_7	λ	(60)8, 409. 21	(8)4, 611. 88	(1)3, 956. 88		
	ν	11, 888. 46	21, 677. 08	25, 265. 31		
	mp_7	18, 878. 52	9, 089. 90	5, 501. 67		
Mean	mp_7	18, 878. 50	9, 089. 92	5, 501. 53	3, 665. 64	2, 618. 04
	$\sqrt{\frac{R}{mp_7}}$	2. 4110	3. 4743	4. 4661	5. 4714	6. 4742

TABLE 5.—*Xe principal series, $1s_1$-m_k*—Continued

Series, mp_8
Limit: $1s_5$=30,766.98

Comb.	m	2	3	4	5	6	7
s_2p_8	λ	(200)8, 819. 44	(300)4, 671. 22	(30)3, 967. 55	(5)3, 693. 50	(2)3, 554. 03	(1)3, 472. 43
	ν	11, 335. 47	21, 401. 71	25, 197. 37	27, 066. 92	28, 129. 07	28, 790. 06
	mp_8	19, 431. 51	9, 365. 27	5, 569. 61	3, 700. 06	2, 637. 91	1, 976. 92
Mean	mp_8	19, 431. 51	9, 365. 27	5, 569. 61	3, 700. 06	2, 637. 91	1, 976. 92
	$\sqrt{\frac{R}{mp_8}}$	2. 3764	3. 4231	4. 4388	5. 4459	6. 4498	7. 4504

Series, mp_9
Limits: $1s_3$=20,649.44
$1s_4$=29,789.34
$1s_5$=30,766.98

Comb.	m	2	3	4	5
s_1p_9	λ		(50)8, 952. 25		
	ν	934. 72	11, 167. 31		
	mp_9	19, 714. 72	9, 482. 13		
s_4p_9	λ	(10)9, 923. 10	(60)4, 923. 15	(4)4, 135. 12	
	ν	10, 074. 74	20, 306. 55	24, 176. 30	
	mp_9	19, 714. 60	9, 482. 79	5, 613. 04	
s_5p_9	λ	(50)9, 045. 46	(70)4, 697. 02	(5)3, 974. 42	(1)3, 696. 82
	ν	11, 052. 24	21, 284. 16	25, 153. 81	27, 042. 61
	mp_9	19, 714. 74	9, 482. 82	5, 613. 17	3, 724. 37
Mean	mp_9	19, 714. 72	9, 482. 80	5, 613. 1	3, 724. 37
	$\sqrt{\frac{R}{mp_9}}$	2. 3593	3. 4018	4. 4216	5. 4281

Series, mp_{10}
Limits: $1s_3$=20,649.44
$1s_4$=21,637.74
$1s_4$=29,789.34
$1s_5$=30,766.98

Comb.	m	2	3	4	5
s_1p_{10}	λ		(1)9, 306. 56	(4)6, 678. 94	(1)5, 921. 79
	ν	84. 11	10, 724. 17	14, 968. 31	16, 882. 12
	mp_{10}	20, 565. 33	9, 907. 27	5, 681. 13	3, 767. 32
s_2p_{10}	λ		(2)8, 522. 49	(4)6, 265. 28	(1)5, 594 21
	ν	1, 072. 41	11, 730. 44	15, 956. 57	17, 870. 68
	mp_{10}	20, 565. 33	9, 907. 30	5, 681. 17	3, 767. 06
s_4p_{10}	λ		(15)5, 028. 26		
	ν	9, 224. 01	19, 882. 07		
	mp_{10}	20, 565. 33	9, 907. 27		
s_5p_{10}	λ	(20)9, 799. 65	(20)4, 792. 61	(5)3, 985. 22	(1)3, 702. 72
	ν	10, 201. 65	20, 859. 64	25, 085. 65	26, 999. 52
	mp_{10}	20, 565. 33	9, 907. 34	5, 681. 33	3, 767. 46
Mean	mp_{10}	20, 565. 33	9, 907. 29	5, 681. 21	3, 767. 26
	$\sqrt{\frac{R}{mp_{10}}}$	2. 3100	3. 3281	4. 3950	5. 3972

From Table 5 it can readily be seen that the 10 principal series, $1s_1$-mp_k, are separated into two groups, $p_{1,2,3,4}$ going to the higher level $^2P_1$ of the ion, and $p_{5,6,7,8,9,10}$ to the lower level $^2P_2$. In the Kr I analysis we were able to establish two members of the non-

Ritzian series, but in Xe_I only the first members can be obtained, since, on account of the very large displacement constant A, the second members will have negative term values.

No lines of the principal series can be expected shorter than 3249 A, and between this limit and the resonance line at 1469 A, no Xe_I lines can be produced. The longest wave length of the principal series in the Xe_I spectrum is given by the combination $1s_2 - 2p_{10} = 84.11$, corresponding to a wave length of 1,188,919 A = 118.8919 μ = 1/8 mm (approximately).

4. THE "FUNDAMENTAL" SERIES (X, Y, Z, U, V, AND W)

Paschen found two unidentified terms, x and y, in the Ne_I spectrum and when Messiner found three similar terms in the A_I spectrum, he called them X, Y, and Z. Meissner [30] pointed out that these series begin with order number $m = 4$, are hydrogen-like, and might, therefore, be regarded as f-terms. Since, however, these terms combined with s- and d-terms but not with p-terms, the simple selection rule $\Delta l = \pm 1$ was violated and it was necessary to hold in reserve the final interpretation of these f-type terms.

The authors also found two series, X and Y, in the Kr_I spectrum, and interpreted them as terms arising from the configuration $(s^2 p^5) f$. We now feel certain that this is the correct explanation, because we have found this term group much more fully developed in the Xe_I spectrum. In fact, 6 series and 34 terms belonging to the $(s^2 p^5) f$ configuration have been detected in Xe_I; the X and Y series combinations with s-terms are presented in Table 6.

TABLE 6.—*Xe_I fundamental series, $1s_1$-mf_k*

SERIES, mX

Limits: $1s_2 = 20{,}649.44$
$1s_3 = 21{,}637.74$
$1s_4 = 29{,}789.34$
$1s_5 = 30{,}766.98$

Comb.	m	4	5	6	7	8	9
s_2X	λ	(5)7,321.46	(7)6,179.66	(3)5,696.44	(1)5,440.2	(1)5,286.1	(1−)5,185.33
	ν	13,654.73	16,177.65	17,549.96	18,376.58	18,912.29	19,279.82
	mX	6,994.71	4,471.79	3,099.48	2,272.86	1,737.15	1,369.62
s_3X	λ	(40)6,827.30	(20)5,823.89	(4)5,392.74	(2)5,162.66	(1)5,023.84	
	ν	14,643.04	17,165.91	18,538.31	19,364.48	19,899.56	
	mX	6,994.70	4,471.83	3,099.43	2,273.26	1,738.18	
s_4X	λ	(10)4,385.75	(1)3,948.70				
	ν	22,794.73	25,317.65				
	mX	6,994.61	4,471.69				
s_5X	λ	(3)4,205.37					
	ν	23,772.45					
	mX	6,994.53					
Mean	mX	6,994.68	4,471.82	3,099.40	2,273.04	1,737.83	1,369.62
	$\sqrt{\frac{R}{mX}}$	3.9609	4.9538	5.9503	6.9482	7.9464	8.9510

[30] Meissner, Zeit. f. Phys., **39**, p. 178; 1926.

TABLE 6.—*Xe_I fundamental series, $1s_1$-mf_k*—Continued

SERIES mY

Limits: $1s_2$=20,649.44
$1s_4$=29,789.34
$1s_5$=30,766.98

Comb.	m	4	5	6	7	8	9
s_2Y	λ	(5)7,316.28	(9)6,178.30	(5)5,695.74	(1)5,440.2	(1)5,286.1	(1−)5,185.33
	ν	13,664.39	16,181.21	17,552.12	18,377.60	18,912.29	19,279.82
	mY	6,985.05	4,468.23	3,097.32	2,271.84	1,737.15	1,369.62
s_4Y	λ	(15)4,383.90	(5)3,948.19	(2)3,745.44	(2)3,633.15		
	ν	22,804.35	25,320.92	26,691.57	27,516.51		
	mY	6,984.99	4,468.42	3,097.77	2,272.83		
s_5Y	λ	(10)4,203.69	(3)3,801.43	(2)3,613.07			
	ν	23,781.95	26,298.45	27,669.43			
	mY	6,985.03	4,468.53	3,097.55			
Mean	mY	6,985.03	4,468.35	3,097.50	2,272.14	1,737.15	1,369.62
	$\sqrt{\frac{R}{mY}}$	3.9636	4.9557	5.9521	6.9496	7.9480	8.9510

These X and Y series are hydrogenlike in every case and may, therefore, be called "fundamental" to distinguish them from "principal" and "subordinate" series. The terms of the f-series have nearly the same value in different rare-gas spectra, tending to increase slightly with heavier atoms. The first members of the X and Y series (and effective quantum numbers) in different spectra are compared in Table 7, to which is added a comparison of the values for the $3d_4'$ term. It is seen that the 12 d-terms arising from the $(s^2p^5)\,3d$ configuration assume a relatively deeper position in the energy diagram as we pass from lighter to heavier atoms. This is exemplified by the increase of $3d_4'$ from 12,339 in Ne_I to 17,636 in Xe_I. The md-mf combinations in Ne_I, A_I, and Kr_I fall in the infra-red outside of the range of photographic investigation, but in Xe_I, on account of the larger interval between the d- and f-terms, it was possible to observe the $3d$-mf combinations. This explains why we observed about 50 per cent more lines in Xe_I than in Kr_I although essentially the same procedure was used in both. These combinations may be expected to be even more prominent in the spectrum of Radon.

TABLE 7.—*Comparison of d- and f-terms in rare-gas spectra*

	Ne_I	A_I	Kr_I	Xe_I	Rn_I
$4X$ (f_6)	6,876.73	6,922.91	6,950.21	6,994.68	(7,000±)
n_{eff}	3.9940	3.9813	3.9726	3.9609	?
$4Y$ (f_5)	6,860.23	6,881.55	6,893.68	6,985.03	(7,000±)
n_{eff}	3.9988	3.9933	3.9896	3.9636	?
$3d_4'$	12,339.15	14,362.0	(15,400±)	17,636.85	(20,000±)
n_{eff}	2.9816	2.7642	(2.6694)	2.4944	?

It is quite probable that some of the unidentified A_I and Kr_I lines in the infra-red are combinations of this type. The $(s^2\ p^5)\ f$ terms combine with the terms arising from $(s^2\ p^5)\ 1s$ and from $(s^2\ p^5)\ 3d$ as shown in Table 8. These combinations, as well as the analogous ones in the Ne_I, A_I and Kr_I spectra, are in perfect accord with the revised rules governing transitions when two or more electrons are involved.[31] Transitions occur for which the l of one electron changes ± 1 while the l of another changes 0 or ± 2. In other words, transitions occur only when the sum of all changes in l is odd. Thus, the sf combinations may be interpreted as double electron jumps in which the s electron makes a transit to a p orbit ($\Delta l = 1$) while the p electron is passing to an f orbit ($\Delta l = 2$).

The series $3d_4'$-mZ and $3d_1''$-mZ can be used for the calculation of the term values $3d_4'$ and $3d_1''$, not obtainable in any other way. The values thus derived are $3d_4' = 17{,}637.11$ and $3d_1'' = 16{,}863.45$. This permits the exact calculation of an important line in the far infra-red, namely, $2p_8$-$3d_4'$ (see Table 9). The wave number of this line is $\nu = 18{,}431.77 - 17{,}637.11 = 1{,}794.66$, and the wave length 5.562 μ. An approximate value for this line can be obtained by extrapolating the $2p_8$-md_4' series to its first member. This procedure gives $\nu = 2p_8 - 3d_4' = 1{,}809.64$; which compares favorably with the exact calculation above, remembering that the approximation could be expected to yield too large a value since the calculated second member $\nu_{calc.} = 10{,}511.37$ is somewhat larger than the observed $\nu_{obs.} = 10{,}508.71$.

Furthermore, it is now possible to calculate the leading member of the $2p_9$-$3d_4$ series in the infra-red; $2p_9 - 3d_4 = 19{,}714.98 - 17{,}512.15 = 2{,}202.84$; $\lambda = 4.5396$ μ.

[31] Hund, Linienspektren und periodisches System der Elemente, p. 132, Julius Springer, Berlin; 1927.

TABLE 8.—*Xe; fundamental series, $2p_x$-md_4', and $3d_4$-mf*

TABLE 8.—*Xe I fundamental series, $1s_1$–mf_k and $5d_1$–mf_k*

m	d_1'' 1	d_4 3	d_4' 4	d_5 1	d_6 0	s_3 1	s_3 0	s_4 1	s_5 2	
	16, 863. 49	17, 511. 89	17, 636. 65	17, 847. 94	18, 063. 13	20, 649. 44	21, 637. 74	29, 789. 34	30, 766. 98	
4				(1) 10, 853. 26	(2) 11, 068. 50	(5) 13, 654. 73	(40) 14, 643. 04	(10) 22, 794. 73	(3) 23, 772. 45	6, 994. 68 / 4, 471. 82 — *mX* *j*=1
5				(2) 13, 375. 97	(2) 13, 591. 45	(7) 16, 177. 65	(20) 17, 165. 91	(1) 25, 317. 65		3, 099. 40
6				(3) 14, 748. 27	(3) 14, 963. 65	(3) 17, 549. 96	(4) 18, 538. 31			2, 273. 04
7				(3) 15, 574. 62	(2) 15, 790. 01	(1) 18, 376. 58	(2) 19, 364. 48			1, 737. 83
8					(1) 16, 325. 65	(1) 18, 912. 29	(1) 19, 899. 56			1, 369. 62
9						(1−) 19, 279. 82				
4		(2) 10, 526. 79		(2) 10, 862. 89		(5) 13, 664. 39		(15) 22, 804. 35	(10) 23, 781. 95	6, 985. 03 / 4, 468. 35 — *mY* *j*=2
5		(2d) 13, 043. 58		(3) 13, 379. 72		(9) 16, 181. 21		(5) 25, 320. 92	(3) 26, 298. 45	3, 097. 50
6		(2) 14, 414. 42		(4) 14, 750. 56		(5) 17, 552. 12		(2) 26, 691. 57	(2) 27, 669. 43	2, 272. 14
7		(2) 15, 239. 75		(2) 15, 575. 74		(1) 18, 377. 60		(2) 27, 516. 51		1, 737. 15
8		(1) 15, 774. 74				(1) 18, 912. 29				1, 369. 62
9						(1−) 19, 279. 82				
4	(1) 9, 861. 22		(5) 10, 664. 12				(1−)			6, 972. 73 / 4, 455. 97 — *mZ* *j*=3
5	(8) 12, 407. 78		(8) 13, 180. 88							3, 089. 26
6	(3) 13, 774. 22		(2) 14, 547. 59							2, 266. 31
7	(3) 14, 597. 23		(1d) 15, 370. 64							1, 732. 92
8	(2) 15, 130. 42		(3) 15, 903. 93							1, 367. 71
9	(1) 15, 495. 76		(1) 16, 269. 14							1, 106. 75
10	(1−) 15, 756. 61		(1) 16, 530. 10							
4		(3) 10, 584. 59							(30) 23, 839. 63	6, 927. 30 / 4, 433. 20 — *mU* *j*=3
5		(4) 13, 078. 78							(10) 26, 333. 78	3, 076. 37
6		(5) 14, 435. 37							(3) 27, 640. 51	2, 258. 67
7		(5) 15, 253. 26							(1) 28, 506. 31	1, 728. 89
8		(2) 15, 783. 76							(1−) 29, 038. 09	1, 364. 65
9		(1) 16, 147. 24								
4		(11) 10, 587. 96		(1) 10, 923. 54		(4) 13, 725. 04		(3) 22, 865. 11	(1) 13, 842. 62	6, 924. 40 / 4, 430. 38 — *mV* *j*=2
5		(15) 13, 081. 95		(1) 13, 417. 29		(15d) 16, 219. 33				3, 074. 46
6				(2) 14, 773. 40		(2) 17, 574. 98				2, 257. 28
7				(1) 15, 590. 73		(1) 18, 392. 13				
4			(1) 10, 747. 64							6, 889. 21 / 4, 412. 59 — *mW* *j*=3
5	(3) 12, 450. 42		(2) 13, 224. 26							3, 063. 94
6	(1) 13, 799. 21		(3) 14, 572. 91							2, 290. 14
7	(1) 14, 613. 08		(1) 15, 386. 71							1, 721. 99
8	(1) 15, 140. 92		(1) 15, 914. 86							

TABLE 9.—*Determination of $3d_4'$ and $3d_2''$*

Series, $3d_4'$-mZ

$$\nu = A - \frac{R}{[m+\mu+a(A-\nu)]^2}$$

$R_{Xe} = 109{,}736.66$
$A = 17{,}637.112$
$a = +0.000001918490443$
$\mu = +0.9538523722 \pm 10^{-10}$

M	Int.	$\lambda_{obs.}$	$\nu_{obs.}$	$\nu_{calc.}$	$\nu_{obs.}-\nu_{calc.}$
3	5	9, 374. 67	10, 664. 12	10, 664. 80	−0. 68
4	8	7, 584. 66	13, 180. 88	13, 180. 88	0. 00
5	20	6, 872. 10	14, 547. 59	14, 547. 59	0. 00
6	15*d*	6, 504. 16	15, 370. 54	15, 370. 60	−0. 06
7	3	6, 286. 02	15, 903. 93	15, 903. 97	−0. 04
8	1	6, 144. 91	16, 269. 14	16, 269. 14	0. 00
9	1−	6, 047. 9	16, 530. 10	16, 529. 93	+0. 17

$3d_4' = 17{,}637.11$

Series, $3d_2''$-mZ

$A = 16{,}863.453$
$a = +0.000001943114582$
$\mu = +0.954056552 \pm 10^{-10}$

M	Int.	$\lambda_{obs.}$	$\nu_{obs.}$	$\nu_{calc.}$	$\nu_{obs.}-\nu_{calc.}$
3	1	10, 107. 2	9, 891. 22	9, 892. 45	−1. 23
4	8	8, 057. 25	12, 407. 78	12, 407. 78	0. 00
5	3	7, 257. 94	13, 774. 22	13, 774. 22	0. 00
6	3	6, 848. 73	14, 597. 23	14, 597. 11	+0. 12
7	2	6, 607. 38	15, 130. 42	15, 130. 42	0. 00
8	1	6, 451. 6	15, 495. 76	15, 495. 55	+0. 21
9	1−	6, 344. 79	15, 756. 61	15, 756. 41	+0. 20

$3d_2'' = 16{,}863.45$

5. THE SUBORDINATE SERIES

All the observed combinations of ms_1 and md_1 levels with the mp_k-terms are collected in Table 10. It is seen from this table that some of the combinations which can be expected on the basis of assigned inner quantum numbers have not been observed, some on account of faintness, and others because they lie in the unexplored infra-red. Especially the combinations with the non-Ritzian group $2p_{1,2,3,4}$ lie far outside the range of photographic investigations. Radiometric investigations of the infra-red spectra of both krypton and xenon are desirable and important.

TABLE 10.—*Xe I subordinate series*

TABLE 10.—Xe_I *subordinate series*

m	p_5 0 17,715.59	p_6 2 18,622.04	p_7 1 18,878.50	p_8 3 19,431.51	p_9 2 19,714.72	p_{10} 1 20,565.33		
3		(2)11,719.93			(3)12,812.65		6,902.07	
4		(1)14,209.65	(3)14,466.12		(10)15,302.33	(1)16,153.08	4,412.35	ms_4
5			(1)15,831.24		(3)16,667.42	(4)17,518.11	3,047.28	$j=1$
6			(1−)16,635.96		(1)17,471.27		2,242.54	
3		(2)11,592.12	(1)11,848.46	(7)12,401.49	(2)12,684.78	(5)13,535.44	7,029.96	
4		(2)14,185.84		(15)14,995.23	(5)15,278.55	(8)16,129.13	4,436.21	ms_5
5		(2)15,547.69		(5)16,357.22	(2)16,640.43	(2)17,490.80	3,074.36	$j=2$
6		(1)16,366.06		(1)17,175.84	(1)17,459.37		2,255.67	
4		(2)10,322.11		(2)11,131.64	(3)11,414.83		8,299.90	
5		(6)15,521.18		(10)14,330.57	(1)14,613.08		5,101.14	
6		(20)15,157.58		(5)15,967.02	(2)16,250.31		3,464.47	md_1'
7		(4)16,122.34		(2)16,931.78	(1)17,215.24		2,199.72	$j=3$
8		(2)16,734.33		(1)17,543.93			1,887.64	
9		(1)17,146.50					1,475.54	
10		(1−)17,436.83					1,184.64	
5		(3)13,509.10	(1)13,765.57	(3)14,318.52	(10)14,601.83	(40)15,452.38	5,112.94	
6		(1)15,127.17	(15)15,383.43	(1)15,936.56	(15*d*)16,219.82	(2)17,070.53	3,494.90	md_1''
7			(5)16,357.22		(3)17,193.66	(1−)18,044.89	2,521.17	$j=2$
8			(1)16,975.80		(1)17,812.44		1,902.54	
9			(1)17,392.24		(1−)18,229.15		1,485.91	
4			(1)10,287.07		(3)11,123.50	(2)11,974.24	8,591.24	
5		(?)	(2)13,758.00		(3)14,594.37	(20)15,544.96	5,120.42	
6		(10)15,073.27	(5)15,329.67			(15)17,016.51	3,548.81	md_5
7		(3)16,062.12	(2)16,318.51			(4)18,005.47	2,559.92	$j=1$
8		(1)16,692.36				(2)18,635.72	1,929.64	
9		(1)17,116.80				(1)19,059.76	1,505.40	
10		(1)17,416.72					1,205.32	

TABLE 10.—Xe_1 *subordinate series*—Continued

m	p_8 0 17, 715. 59	p_8 2 18, 622. 04	p_7 1 18, 878. 50	p_8 3 19, 431. 51	p_9 2 19, 714. 72	p_{10} 1 20, 565. 33		
4				(2) 10, 621. 98	(5) 10, 905. 13		8, 809. 56	md_4 $j=3$
5		(1) 13, 433. 84		(3) 14, 243. 20	(60) 14, 526. 32		5, 188. 33	
6				(5) 15, 887. 25	(20) 16, 170. 46		3, 544. 26	
7				(2) 16, 880. 07	(6) 17, 163. 23		2, 551. 44	
8				(1) 17, 509. 52	(3) 17, 792. 47		1, 922. 12	
9					(2) 18, 214. 77		1, 499. 95	
10					(1) 18, 512. 01		1, 202. 71	
4				(3) 10, 508. 71			8, 922. 80	md_4' $j=4$
5				(30) 14, 041. 91			5, 389. 60	
6				(30) 15, 823. 22			3, 608. 29	
7				(8) 16, 846. 98			2, 584. 53	
8				(3) 17, 489. 48			1, 942. 03	
9				(1) 17, 918. 88			1, 512. 63	
10				(1−) 18, 220. 18			1, 211. 33	
4						(8) 11, 280. 66	9, 284. 67	md_2 $j=1$
5		(2) 13, 466. 12	(5) 13, 722. 51		(7) 14, 558. 79	(20) 15, 409. 41	5, 155. 94	
6		(3) 15, 015. 61	(2) 15, 272. 16		(2) 16, 108. 45	(15) 16, 958. 87	3, 606. 38	
7		(1) 16, 016. 14			(1) 17, 108. 59	(4) 17, 959. 31	2, 606. 01	
8						(2) 18, 644. 14	1, 921. 19	
9						(1) 19, 045. 96	1, 519. 37	
5						(40) 14, 990. 78	5, 574. 55	md_6 $j=0$
6			(1) 15, 168. 58			(8) 16, 855. 25	3, 710. 08	
7						(3) 17, 910. 73	2, 654. 60	
8						(2) 18, 531. 64	2, 033. 69	
9						(1) 19, 059. 76	1, 505. 57	

The following additional combinations (Table 11), give a plausible explanation for an outstanding group of lines in the longer wave-length region, but one or more permitted combinations are absent in each row or column.

TABLE 11.—*Additional s'p combinations*

j		s_1''	s_1''''	s_1'''	s_1'
		2	3	2 (1)	1
	Term	6, 387. 01	6, 087. 89	5, 706. 16	5, 574. 55
1	p_{10}			(50) 14, 859. 15	(40) 14,990. 78
2	p_9	(2) 13, 327. 71	(4) 13, 626. 85		
3	p_8	(2d) 13, 043. 58	(2) 13, 343. 60		
1	p_7				
2	p_6	(3) 12, 235. 01		(2) 12, 915. 88	
0	p_5			(2) 12, 009. 29	

6. THE Xe_I SPECTRUM IN THE EXTREME ULTRA-VIOLET

The following lines in the extreme ultra-violet (Table 12) have been reported by Abbink and Dorgelo [32] as characteristic of the first spectrum of xenon.

TABLE 12.—*First spectrum of Xe in the extreme ultra-violet*

Line No.	Intensity	Wave length λ	Wave No. ν	Combination	Calculated term
1	20	1, 469. 61	68, 045. 3	p_0-$1s_4$	29, 798. 0
2	10	1, 295. 56	77, 186. 7	p_0-$1s_2$	20, 648. 6
3	6	[a] 1, 277. 50	78, 277. 9		19, 557. 4
4	5	1, 250. 24	79, 984. 6	p_0-$3d_5$	17, 850. 7
5	5	1, 192. 02	83, 891. 2	p_0-$2s_4$	13, 944. 1
6	15	[a] 1, 100. 46	90, 871. 1		6, 964. 2
7	10	1, 088 94	91, 832. 4		6, 002. 9
8	4	1, 083. 89	92, 260. 3	p_0-$3s_1'$	5, 575. 0
9	15	1, 074. 50	93, 066. 5	p_0-$2s_2$	4, 768. 8
10	5	1, 067. 10	93, 711. 9		4, 123. 4
11	10	1, 048. 18	95, 403. 5		2, 431. 8
12	12	1, 041. 30	96, 033. 8		1, 800. 5
13	8	1, 037. 71	96, 366. 0		1, 469. 3
14	8	1, 032. 51	96, 857. 4		783. 9
15	10	1, 027. 04	97, 367. 2		468. 1

[a] Adherence to Xe doubtful.

[32] Abbink and Dorgelo, Zeit. f. Phys., **47**, p. 221; 1928.

Since all true Xe_I lines in the extreme ultra-violet must be combinations involving the normal level $p_o = 97{,}835.3$, it is possible to calculate the combining levels, all of which must have the inner quantum number $j = 1$. The first two levels give the resonance lines; they have been used for determining the normal state. The calculated level 17,850.7 is, without doubt, our level 17,847.94, identified as $3d_5$. The level 5,575.0 may be identified with $3s_1' = 5{,}574.55$. The levels 13,944.1 and 4,768.8 may be identified with $2s_4$ and $2s_2$, respectively, because they have a separation of 9,175.3; the separation $1s_4$-$1s_2$ is 9,139.90, and this term difference is expected to increase with higher terms approaching the $^2P_{2,1}$ interval, 9,621, in the limit.

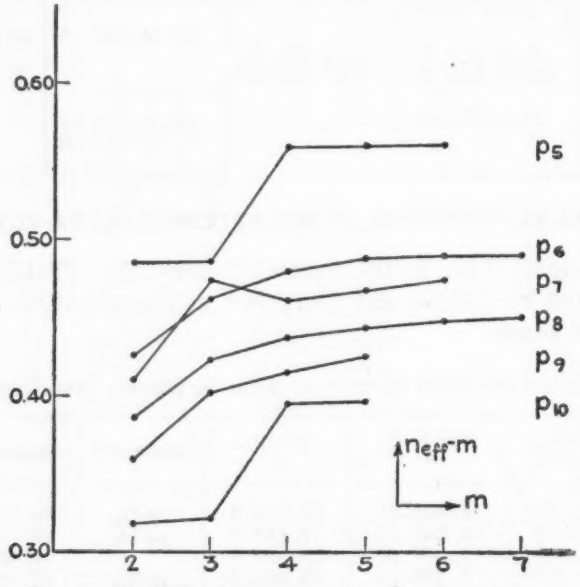

FIGURE 6.—*Effective quantum numbers for p-terms*

At this point we may also refer to the $2s_3$ level; it must be a little larger than $2s_2$, and the combination with $2p_{10}$ should have a wave number of about 15,700 cm^{-1}. Now, the only unclassified line in this region is $\nu = 15{,}729.52$. which is accordingly interpreted as $2p_{10}$-$2s_3$. The only other possible *sp* combination is $2p_7$-$2s_3$ ($\nu_{calc.} = 14{,}042.74$), which unfortunately is masked by the strong line $2p_8$-$5d'_4$ ($\nu_{obs.} = 14{,}041.91$).

In the case of Kr_I, it was possible to account for all the extreme ultra-violet lines, but it is seen from Table 12 that a considerable number of strong lines attributed to the Xe_I spectrum by Abbink and Dorgelo remains unclassified. It appears that another interpretation will have to be sought for the remaining lines.

7. IDENTIFICATION OF THE EXPERIMENTAL TERMS

A complete list of the identified Xe_I terms is presented in Table 13. The first column contains the type of electron which, when added to s^2p^5, gives rise to groups of terms shown in the second column (Paschen notation), followed by the inner quantum numbers assigned

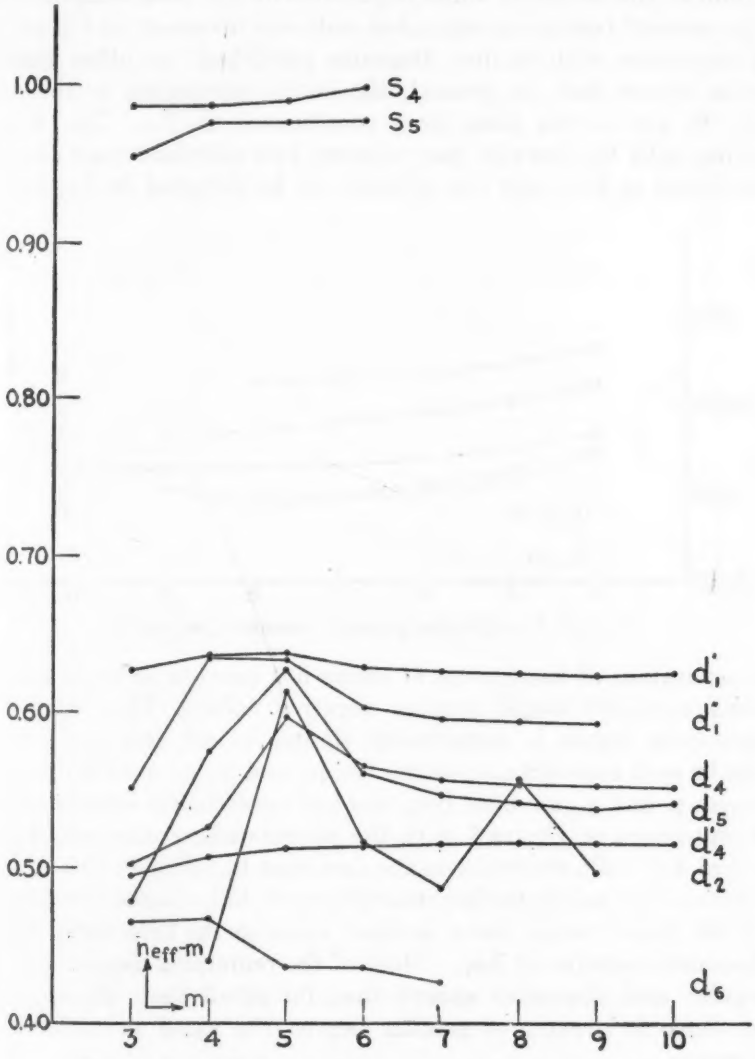

FIGURE 7.—*Effective quantum numbers for d- and s-terms*

to the terms. The absolute value of the ground level or highest term appears in column 4, and the remaining columns contain alternately the term values and the corresponding effective quantum numbers. The latter are an excellent criterion for arranging terms in series, and when they are plotted as a function of order number they reveal

certain relations and regularities not otherwise obvious. Such plots are shown in Figures 6, 7, and 8, p-terms in Figure 6, d- and s'-terms in Figure 7, and f-terms in Figure 8. The order numbers (m) of the terms in the series are taken for abscissæ and the fractional part of the corresponding effective quantum numbers (n_{eff}-m) as ordinates. On account of the relatively small departures of n_{eff} from integral values in the cases of f-terms an expanded scale was necessary in Figure 8.

Comparison with similar diagrams published for other rare gas spectra shows that, in general, the series converging to the upper limit $^2P_1$ are shorter than those coordinated to $^2P_2$. This is most striking with the heavier gas; whereas two members each of $p_{1,2,3,4}$ were found in Kr_I, only one of each can be detected in Xe_I because

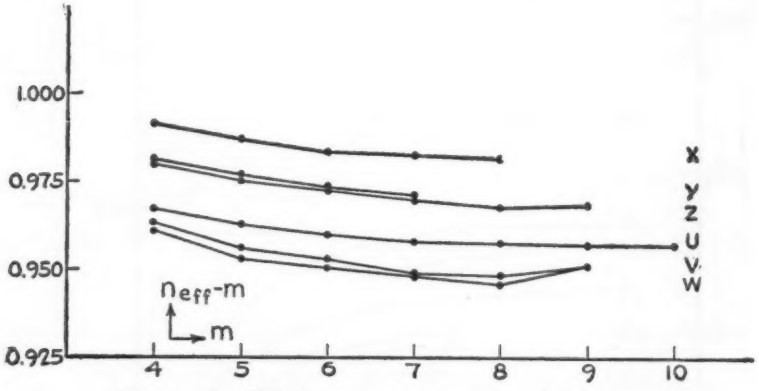

FIGURE 8.—*Effective quantum numbers for f-terms*

the separation of the groups of terms has become so large that the second members would acquire negative values. The behavior of homologous terms is remarkably similar in all rare gas spectra Thus, in each case certain p-terms (p_6, p_7, and p_8, p_9) are fairly regular, whereas p_5 and p_{10} are most irregular but nevertheless remain parallel.

Comparison of Figure 7 with the corresponding diagrams for Ne_I A_I, and Kr_I calls attention to the fact that in all cases the d'_4 series gives the most nearly perfect smooth curves, but whereas the constant α of the Ritz formula has a positive value in the first three spectra it becomes negative in Xe_I. Most of the remaining d-series are very irregular and dissimilar except that for $m=5$ they all appear to experience in greater or smaller degree the same perturbation or resonance.

The curves for the f-terms (fig. 8) show no large discontinuities; they behave more like the hydrogen series, as would be expected if they really involve the larger f-orbits.

TABLE 13.—*Terms and effective quantum numbers of*

Electron	j	Paschen notation		m= 1		2		3		4		5		
p	0	p_0	97, 835. 3											
s	2	s_5		30, 766. 98	1. 8886			7, 029. 96	3. 9510	4, 436. 21	4. 9736	3, 074. 36	5. 9745	2, 2
	1	s_4		29, 789. 34	1. 9193	13, 944. 1	2. 8054	6, 902. 07	3. 9874	4, 412. 35	4. 9851	3, 047. 28	6. 0010	2, 2
	0	s_3		21, 637. 74	1. 8736	4, 835. 76	2. 7552							
	1	s_2		20, 649. 44	1. 9040	4, 768. 8	2. 7617							
p	1	p_{10}				20, 565. 33	2. 3100	9, 907. 29	3. 3281	5, 681. 21	4. 3950	3, 767. 26	5. 3972	
	2	p_9				19, 714. 72	2. 3593	9, 482. 80	3. 4018	5, 613. 10	4. 4216	3, 724. 37	5. 4281	
	3	p_8				19, 431. 51	2. 3764	9, 365. 27	3. 4231	5, 569. 61	4. 4388	3, 700. 06	5. 4459	2, 6
	1	p_7				18, 878. 50	2. 4110	9, 089. 92	3. 4743	5, 501. 53	4. 4661	3, 665. 64	5. 4714	2, 6
	2	p_6				18, 622. 04	2. 4275	9, 147. 97	3. 4635	5, 463. 48	4. 4817	3, 644. 40	5. 4874	2, 6
	0	p_5				17, 715. 59	2. 4888	8, 992. 20	3. 4933	5, 279. 09	4. 5593	3, 549. 35	5. 5604	2, 5
	1	p_4				9, 455. 37	2. 3984							
	2	p_3				8, 672. 18	2. 4492							
	1	p_2				8, 555. 78	2. 4571							
	0	p_1				7, 974. 43	2. 4973							
d	0	d_0						18, 063. 13	2. 4648	9, 125. 98	3. 4677	5, 574. 55	4. 4368	3, 7
	4	d_4'						17, 636. 85	2. 4944	8, 922. 80	3. 5070	5, 389. 60	4. 5122	3, 6
	3	d_4						17, 511. 89	2. 5033	8, 809. 56	3. 5295	5, 188. 33	4. 5990	3, 5
	1	d_2								9, 284. 67	3. 4379	5, 155. 94	4. 6134	3, 6
	1	d_5						17, 847. 94	2. 4796	8, 591. 24	3. 5740	5, 120. 42	4. 6294	3, 5
	2	d_1''						16, 863. 49	2. 5510	8, 289. 42	3. 6365	5, 112. 94	4. 6328	3, 4
	3	d_1'						15, 907. 90	2. 6264	8, 299. 90	3. 6362	5, 101. 14	4. 6381	3, 4
	2	s_1''						6, 387. 01	2. 6182					
	3	s_1''''						6, 087. 89	2. 6430					
	2	s_1'''						5, 706. 16	2. 6757					
	1	s_1'						5, 574. 55	2. 6823					
f	1	$X(f_6)$								6, 994. 68	3. 9609	4, 471. 82	4. 9538	3, 0
	2	$Y(f_5)$								6, 985. 03	3. 9636	4, 468. 35	4. 9557	3, 0
	3	$Z(f_4)$								6, 972. 73	3. 9671	4, 455. 97	4. 9626	3, 0
	3	$U(f_3)$								6, 927. 30	3. 9801	4, 433. 20	4. 9753	3, 0
	2	$V(f_2)$								6, 924. 40	3. 9810	4, 430. 38	4. 9769	3, 0
	3	$W(f_1)$								6, 889. 21	3. 9911	4, 412. 59	4. 9869	3, 0

6		7		8		9		10	
2, 255. 67	6. 9749								
2, 242. 54	6. 9953								
2, 637. 91	6. 4498	1, 976. 92	7. 4504						
2, 618. 04	6. 4742								
2, 604. 93	6. 4905	1, 956. 43	7. 4893						
2, 548. 67	6. 5618								
3, 710. 08	5. 4386	2, 654. 60	6. 4295	2, 033. 69	7. 3457	1, 505. 57	8. 5374		
3, 608. 29	5. 5147	2, 584. 53	6. 5160	1, 942. 03	7. 5171	1, 512. 63	8. 5174	1, 211. 83	9. 5160
3, 544. 26	5. 5643	2, 551. 44	6. 5582	1, 922. 12	7. 5559	1, 499. 95	8. 5534	1, 202. 71	9. 5520
3, 606. 38	5. 5162	2, 606. 01	6. 4891	1, 921. 19	7. 5577	1, 519. 37	8. 4985		
3, 548. 81	5. 5608	2, 559. 92	6. 5473	1, 929. 64	7. 5412	1, 505. 40	8. 5378	1, 205. 32	9. 5417
3, 494. 90	5. 6035	2, 521. 17	6. 5974	1, 902. 54	7. 5947	1, 485. 91	8. 5936		
3, 464. 47	5. 6280	2, 499. 72	6. 6257	1, 887. 64	7. 6246	1, 475. 54	8. 6238	1, 184. 64	9. 6246
3, 099. 40	5. 9503	2, 273. 04	6. 9482	1, 737. 83	7. 9464	1, 369. 62	8. 9510		
3, 097. 50	5. 9521	2, 272. 14	6. 9496	1, 737. 15	7. 9480	1, 369. 62	8. 9510		
3, 089. 26	5. 9601	2, 266. 31	6. 9586	1, 732. 92	7. 9577	1, 367. 71	8. 9573	1, 106. 75	9. 9575
3, 076. 37	5. 9725	2, 258. 67	6. 9703	1, 728. 89	7. 9670	1, 364. 65	8. 9674		
3, 074. 46	5. 9744	2, 257. 26	6. 9724						
3, 063. 94	5. 9847	2, 250. 14	6. 9835	1, 721. 99	7. 9829				

8. LIST OF Xe_I LINES

A complete list of the observed lines characteristic of the first spectrum of xenon is presented in Table 14, in which the estimated intensities appear in the first column, the wave lengths (international scale) in the second, wave numbers (vacuum) in the third, and term combinations in the last. Practically all of the 318 observed lines are accounted for as combinations of established terms presented in the preceding table. Only a few lines, most of which are very faint, remain unclassified; it will perhaps be possible to place them when related, but still fainter lines have been recorded.

TABLE 14.—*List of Xe_I lines*

Intensity	Wave length	Wave number	Combination
1	10, 107. 2	9, 891. 22	$3d_1''$-$4Z$
10	9, 923. 10	10, 074. 74	$1s_4$-$2p_9$
20	9, 799. 65	10, 201. 65	$1s_5$-$2p_{10}$
1	9, 718. 27	10, 287. 07	$2p_6$-$4d_5$
2	9, 685. 29	10, 322. 11	$2p_6$-$4d_1'$
6	9, 513. 34	10, 508. 67	$2p_8$-$4d_4'$
2	9, 496. 97	10, 526. 79	$3d_4$-$4Y$
3	9, 445. 34	10, 584. 37	$3d_4$-$4U$
1—	9, 442. 1	10, 587. 96	$3d_4$-$4V$
2	9, 411. 86	10, 621. 98	$2p_8$-$4d_4$
5	9, 374. 67	10, 664. 12	$3d_4'$-$4Z$
1	9, 306. 56	10, 742. 17	$1s_2$-$3p_{10}$
1	9, 301. 82	10, 747. 64	$3d_4'$-$4W$
1	9, 211. 3	10, 853. 26	$3d_5$-$4X$
2	9, 203. 13	10, 862. 89	$3d_5$-$4Y$
5	9, 167. 48	10, 905. 13	$2p_9$-$4d_4$
40	9, 162. 66	10, 910. 87	$1s_4$-$2p_7$
1	9, 152. 03	10, 923. 54	$3d_5$-$4V$
1	9, 095. 57	10, 990. 87	
50	9, 045. 46	11, 052. 24	$1s_5$-$2p_9$
2	9, 032. 17	11, 068. 50	$3d_6$-$4X$
1	9, 025. 74	11, 076. 38	
3	8, 987. 51	11, 123. 50	$2p_9$-$4d_5$
2	8, 980. 94	11, 131. 64	$2p_8$-$4d_1'$
50	8, 952. 25	11, 167. 31	$1s_2$-$3p_9$ / $1s_4$-$2p_6$
5	8, 930. 81	11, 194. 03	$1s_3$-$2p_4$
1	8, 913. 33	11, 216. 08	
4	8, 908. 70	11, 221. 91	
8	8, 862. 30	11, 280. 66	$2p_{10}$-$4d_2$
200	8, 819. 44	11, 335. 47	$1s_5$-$2p_8$
3	8, 758. 13	11, 414. 83	$2p_9$-$4d_1'$
10	8, 739. 36	11, 439. 35	$2p_{10}$-$4d_3$
1	8, 725. 4	11, 457. 65	
1	8, 709. 6	11, 478. 43	$3d_1'$-$5V$?
3	8, 696. 80	11, 495. 33	$3d_1'$-$5W$
3	8, 692. 08	11, 501. 57	$1s_3$-$3p_6$
6	8, 648. 51	11, 559. 51	$1s_2$-$3p_7$
2	8, 624. 18	11, 592. 12	$2p_6$-$3s_5$
5	8, 576. 03	11, 657. 21	$1s_2$-$3p_5$
2	8, 530. 13	11, 719. 93	$2p_6$-$3s_4$

TABLE 14.—*List of Xe_1 lines*—Continued

Intensity	Wave length	Wave number	Combination
2	8, 522. 49	11, 730. 44	$1s_3$-$3p_{10}$
1	8, 437. 6	11, 848. 46	$2p_7$-$3s_5$
60	8, 409. 21	11, 888. 46	$1s_5$-$2p_7$
1	8, 392. 4	11, 912. 27	
1	8, 368. 4	11, 946. 44	
2	8, 348. 97	11, 974. 24	$2p_7$-$3s_4$ $2p_{10}$-$4d_5$
50	8, 346. 86	11, 977. 26	$1s_2$-$2p_3$
2	8, 324. 6	12, 009. 26	$2p_5$-s_1'''
2	8, 319. 46	12, 016. 71	
150	8, 280. 16	12, 073. 75	$1s_4$-$2p_5$
20	8, 266. 53	12, 093. 65	$1s_2$-$2p_2$
1	8, 258. 0	12, 106. 15	
300	8, 231. 64	12, 144. 92	$1s_5$-$2p_6$
1?	8, 228. 7	12, 149. 25	
25	8, 206. 34	12, 182. 36	$1s_3$-$2p_4$
1	8, 191. 7	12, 204. 13	
3	8, 171. 02	12, 235. 01	$3d_5$-$4p_9$
2	8, 143. 8	12, 275. 91	
2	8, 101. 95	12, 339. 32	
7	8, 061. 33	12, 401. 49	$2p_8$-$3s_5$
8	8, 057. 25	12, 407. 78	$3d_1''$-$5Z$
3	8, 029. 65	12, 450. 42	$3d_1''$-$5W$
10	7, 967. 33	12, 547. 81	$1s_3$-$3p_7$
1	7, 937. 47	12, 595. 02	$2p_5$-$5d_5$
8	7, 887. 38	12, 675. 00	$1s_2$-$2p_1$
2	7, 881. 30	12, 684. 78	$2p_9$-$3s_5$
3	7, 802. 64	12, 812. 65	$2p_9$-$3s_4$
2	7, 783. 63	12, 843. 94	$3d_1'$-$6W$
2	7, 740. 28	12, 915. 88	$2p_6$-s_1'''
2*d*	7, 664. 5	13, 043. 58	$3d_4$-$5Y$ $2p_8$-s_1''
4	7, 643. 87	13, 078. 78	$3d_4$-$5U$
15	7, 642. 02	13, 081. 95	$1s_3$-$2p_2$ $3d_4$-$5V$
1—	7, 587. 6	13, 175. 78	
8	7, 584. 66	13, 180. 88	$3d_4'$-$5Z$
2	7, 559. 78	13, 224. 26	$3d_4'$-$5W$
2	7, 501. 10	13, 227. 71	$2p_9$-s_1''
2	7, 492. 17	13, 343. 60	$2p_8$-s_1''''
2	7, 474. 04	13, 375. 97	$3d_5$-$5X$
3	7, 471. 94	13, 379. 72	$3d_5$-$5Y$
1	7, 451. 02	13, 417. 29	$3d_5$-$5V$
1	7, 441. 84	13, 433. 84	$2p_6$-$5d_4$
2	7, 424. 0	13, 466. 12	$2p_6$-$5d_3$
3	7, 400. 38	13, 509. 10	$2p_6$-$5d_1''$
6	7, 393. 77	13, 521. 18	$2p_6$-$5d_1''$
5	7, 385. 98	13, 535. 44	$2p_{10}$-$3s_5$
2	7, 355. 54	13, 591. 45	$3d_6$-$5X$
4	7, 336. 44	13, 626. 85	$2p_9$-s_1''
5	7, 321. 46	13, 654. 73	$1s_2$-$4X$
5	7, 316. 28	13, 664. 39	$1s_2$-$4Y$

TABLE 14.—*List of Xe_I lines*—Continued

Intensity	Wave length	Wave number	Combination
5	7, 285. 29	13, 722. 51	$2p_7$-$4d_2$
4	7, 283. 95	13, 725. 04	$1s_2$-$4V$
2	7, 266. 50	13, 758. 00	$2p_7$-$5d_5$
1	7, 262. 5	13, 765. 57	$2p_7$-$5d_1''$
3	7, 257. 94	13, 774. 22	$3d_1''$-$6Z$
1	7, 244. 8	13, 799. 21	$3d_1''$-$6W$
30	7, 119. 58	14, 041. 91	$2p_7$-$2s_3$ $2p_8$-$5d_4'$
2	7, 047. 34	14, 185. 84	$2p_6$-$4s_5$
1	7, 035. 53	14, 209. 65	$2p_6$-$4s_4$
3	7, 018. 96	14, 243. 20	$2p_8$-$5d_4$
3	6, 982. 04	14, 318. 52	$2p_8$-$5d_1''$
10	6, 976. 17	14, 330. 57	$2p_8$-$5d_1'$
2	6, 935. 59	14, 414. 42	$3d_4$-$6Y$
5	6, 925. 52	14, 435. 37	$3d_4$-$6U$
3	6, 910. 80	14, 466. 12	$2p_7$-$4s_4$
60	6, 882. 16	14, 526. 32	$2p_9$-$5d_4$
20	6, 872. 10	14, 547. 59	$3d_4'$-$6Z$
7	6, 866. 81	14, 558. 79	$2p_9$-$5d_2$
1	6, 863. 21	14, 566. 43	
3	6, 860. 16	14, 572. 91	$3d_4'$-6W
3	6, 850. 07	14, 594. 37	$2p_9$-$5d_5$
3	6, 848. 73	14, 597. 23	$3d_1''$-$7Z$
10	6, 846. 57	14, 601. 83	$2p_9$-$5d_1''$
1	6, 841. 30	14, 613. 08	$3d_1''$-$7W$ $2p_9$-$5d_1'$
40	6, 827. 30	14, 643. 04	$1s_3$-$4X$
1	6, 818. 30	14, 662. 37	
3	6, 778. 59	14, 748. 27	$3d_5$-$6X$
4	6, 777. 53	14, 750. 56	$3d_5$-$6Y$
2	6, 767. 06	14, 773. 40	$3d_5$-$6V$
50	6, 728. 00	14, 859. 16	
3	6, 681. 02	14, 963. 65	$3d_6$-$6Z$
4	6, 678. 94	14, 968. 31	$1s_2$-$4p_{10}$
40	6, 668. 93	14, 990. 78	$2p_{10}$-$5d_6$
15	6, 666. 95	14, 995. 23	$2p_8$-$4s_5$
3	6, 657. 90	15, 015. 61	$2p_8$-$6d_2$
10	6, 632. 43	15, 073. 27	$2p_6$-$6d_5$
1	6, 608. 8	15, 127. 17	$2p_6$-$6d_1''$
2	6, 607. 38	15, 130. 42	$3d_1''$-$8Z$
1	6, 602. 8	15, 140. 92	$3d_1''$-$8W$
20	6, 595. 54	15, 157. 58	$2p_6$-$6d_1'$
1	6, 590. 76	15, 168. 56	$2p_7$-$6d_6$
3	6, 583. 15	15, 186. 11	$1s_2$-$4p_8$
2	6, 559. 98	15, 239. 75	$3d_4$-$7Y$
5	6, 554. 17	15, 253. 26	$3d_4$-$7U$
2	6, 546. 06	15, 272. 16	$2p_7$-$6d_2$
5	6, 543. 32	15, 278. 55	$2p_9$-$4s_5$
10	6, 533. 15	15, 302. 33	$2p_9$-$4s_4$
5	6, 521. 50	15, 329. 67	$2p_7$-$6d_5$
15*d*	6, 504. 16	15, 370. 54	$3d_4$-$7Z$ $1s_2$-$4p_5$
1—	6, 500. 23	15, 379. 83	

TABLE 14.—*List of Xe_1 lines*—Continued

Intensity	Wave length	Wave number	Combination
15	6, 498. 71	15, 383. 43	$2p_7$-$6d_1''$
1	6, 497. 3	15, 386. 76	$3d_4'$-$7W$
20	6, 487. 75	15, 409. 41	$2p_{10}$-$5d_2$
20	6, 472. 82	15, 444. 96	$2p_{10}$-$5d_5$
40	6, 469. 71	15, 452. 38	$2p_{10}$-$5d_1''$
1	6, 451. 6	15, 495. 76	$3d_1''$-$9Z$
1—	6, 450. 10	15, 499. 36	
2	6, 430. 05	15, 547. 69	$2p_6$-$5s_5$
3	6, 418. 93	15, 574. 62	$3d_5$-$7X$
2	6, 418. 47	15, 575. 74	$3d_5$-$7Y$ $2p_6$-$5s_4$
1	6, 412. 3	15, 590. 73	$3d_5$-$7V$
2	6, 355. 72	15, 729. 52	$2p_{10}$-$2s_3$
1—	6, 344. 79	15, 756. 61	$3d_1''$-$10Z$
1	6, 337. 5	15, 774. 74	$3d_4$-$8Y$
2	6, 333. 88	15, 783. 76	$3d_4$-$8U$
2	6, 331. 37	15, 790. 01	$3d_6$-$7Z$
30	6, 318. 08	15, 823. 23	$2p_8$-$6d_4'$
1	6, 314. 88	15, 831. 24	$2p_7$-$5s_4$
1	6, 294. 36	15, 882. 85	
5	6, 292. 62	15, 887. 25	$2p_9$-$6d_4$
3	6, 286. 02	15, 903. 93	$3d_4'$-$8Z$
1	6, 281. 7	15, 914. 86	$3d_4'$-$8W$
1	6, 277. 2	15, 926. 27	
1	6, 273. 15	15, 936. 56	$2p_8$-$6d_1''$
4	6, 265. 28	15, 956. 57	$1s_3$-$4p_{10}$
5	6, 261. 18	15, 967. 02	$2p_8$-$6d_1'$
1	6, 241. 98	16, 016. 14	$2p_6$-$7d_2$
3	6, 224. 11	16, 062. 12	$2p_6$-$7d_5$
2	6, 206. 21	16, 108. 45	$3d_5$-$8X$ $2p_9$-$6d_2$
4	6, 200. 86	16, 122. 34	$2p_6$-$7d_1'$
8	6, 198. 25	16, 129. 13	$2p_{10}$-$4s_5$
1?	6, 191. 3	16, 147. 24	$3d_4$-$9U$
1	6, 189. 06	16, 153. 08	$2p_{10}$-$4s_4$
20	6, 182. 41	16, 170. 46	$2p_9$-$6d_4$
7	6, 179. 66	16, 177. 66	$1s_2$-$5X$
9	6, 178. 30	16, 181. 21	$1s_2$-$5Y$
15*d*	6, 163. 78	16, 219. 33	$1s_2$-$5V$ $2p_9$-$6d_1''$
2	6, 152. 03	16, 250. 31	$2p_9$-$6d_1'$
1	6, 144. 91	16, 269. 14	$3d'_4$-$9Z$
1	6, 126. 32	16, 318. 51	$2p_7$-$7d_5$
1—	6, 123. 64	16, 325. 65	$3d_6$-$8X$
1	6, 114. 7	16, 349. 52	
5	6, 111. 82	16, 357. 22	$2p_8$-$5s_5$ $2p_7$-$7d_1''$
1—	6, 108. 52	16, 366. 06	$2p_6$-$6s_5$
1	6, 047. 9	16, 530. 10	$3d_4$-$10Z$
1	6, 043. 2	16, 542. 95	
1—	6, 009. 41	16, 635. 96	$2p_7$-$6s_4$
2	6, 007. 80	16, 640. 43	$2p_9$-$5s_5$
3	5, 998. 07	16, 667. 42	$2p_9$-$5s_4$
1	5, 989. 11	16, 692. 36	$2p_6$-$8d_5$

TABLE 14.—*List of Xe_I lines*—Continued

Intensity	Wave length	Wave number	Combination
2	5, 974. 09	16, 734. 33	$2d_5$-10XY / $2p_8$-$8d_1'$
10	5, 934. 15	16, 846. 96	$2p_8$-$7d_4'$
8	5, 931. 23	16, 855. 25	$2p_{10}$-$6d_6$
1—	5, 925. 33	16, 872. 03	
2	5, 922. 51	16, 880. 07	$2p_9$-$7d_4$
1	5, 921. 79	16, 882. 12	$1s_2$-$5p_{10}$
2	5, 904. 42	16, 931. 78	$2d_5$-11XY / $2p_8$-$7d_1'$
15	5, 894. 99	16, 958. 87	$2p_{10}$-$6d_2$
1	5, 889. 11	16, 975. 80	$2p_7$-$8d_1''$
15	5, 875. 02	17, 016. 51	$2p_{10}$-$6d_5$
2	5, 856. 43	17, 070. 53	$2p_{10}$-$6d_1''$
1—	5, 849. 47	17, 090. 83	
1	5, 843. 4	17, 108. 59	$2p_9$-$7d_2$
1	5, 840. 6	17, 116. 80	$2p_6$-$9d_5$
1	5, 830. 48	17, 146. 50	$2p_6$-$9d_1'$
6	5, 824. 78	17, 163. 28	$2p_9$-$7d_4$
20	5, 823. 89	17, 165. 91	$1s_3$-5X
1	5, 820. 52	17, 175. 84	$2p_8$-$6s_5$
3	5, 814. 49	17, 193. 66	$2p_9$-$7d_1''$
1	5, 807. 2	17, 215. 24	$2p_9$-$7d_1'$
1	5, 748. 1	17, 392. 24	$2p_7$-$9d_1''$
1	5, 740. 2	17, 416. 72	$2p_6$-$10d_5$
1—	5, 733. 4	17, 436. 83	$2p_6$-$10d_1'$
1	5, 726. 0	17, 459. 37	$2p_9$-$6s_5$
1	5, 722. 1	17, 471. 27	$2p_6$-$10d_5$ / $2p_9$-$6s_4$
4	5, 716. 14	17, 489. 48	$2p_8$-$8d_4'$
2	5, 715. 71	17, 490. 80	$2p_{10}$-$5s_5$
1	5, 709. 6	17, 509. 52	$2p_9$-$8d_4$
1—	5, 706. 8	17, 518. 11	$2p_{10}$-$5s_4$
1—	5, 698. 4	17, 543. 93	$2p_8$-$8d_1'$
3	5, 696. 44	17, 549. 96	$1s_2$-6X
5	5, 695. 74	17, 552. 12	$1s_2$-6Y
2	5, 688. 31	17, 575. 05	$1s_2$-6V
3	5, 618. 80	17, 792. 47	$2p_9$-$8d_4$
1	5, 612. 5	17, 812. 44	$2p_9$-$8d_1''$
1	5, 594. 21	17, 870. 68	$1s_3$-$5p_{10}$
3	5, 581. 70	17, 910. 73	$2p_{10}$-$7d_6$
2	5, 579. 19	17, 918. 78	$2p_6$-$9d_4'$
4	5, 566. 60	17, 959. 31	$2p_{10}$-$7d_2$
4	5, 552. 33	18, 005. 47	$2p_7$-$7d_5$
1—	5, 540. 2	18, 044. 89	$1s_2$-$6p_8$ / $2p_{10}$-$7d_1''$
2	5, 488. 53	18, 214. 77	$2p_9$-$9d_4$
1	5, 487. 05	18, 219. 68	$2p_8$-$10d_4'$
1—	5, 484. 2	18, 229. 15	$2p_9$-$9d_1''$
1	5, 440. 2	18, 376. 58	$1s_2$-7X
1	5, 439. 9	18, 377. 60	$1s_2$-7Y
1	5, 435. 6	18, 392. 13	$1s_2$-7V
1	5, 418. 0	18, 451. 88	
1	5, 400. 4	18, 512. 01	$2p_9$-$10d_4$
2	5, 394. 68	18, 531. 64	$2p_{10}$-$8d_6$

TABLE 14.—*List of Xe_1 lines*—Continued

Intensity	Wave length	Wave number	Combination
4	5, 392. 74	18, 538. 31	$1s_5$-$6X$
1—	5, 368. 99	18, 620. 31	
1	5, 367. 0	18, 627. 22	
2	5, 364. 55	18, 635. 72	$2p_{10}$-$8d_5$
2	5, 362. 13	18, 644. 14	$2p_{10}$-$8d_2$
1—	5, 328. 5	18, 761. 80	
1—	5, 306. 23	18, 840. 55	
1	5, 286. 1	18, 912. 29	$1s_2$-$8Y$
1	5, 249. 0	19, 045. 96	$2p_{10}$-$9d_2$
1	5, 245. 2	19, 059. 76	$2p_{10}$-$9d_5$
1—	5, 185. 33	19, 279. 82	$1s_2$-$9Y$
2	5, 162. 66	19, 364. 48	$1s_3$-$7X$
15	5, 028. 26	19, 882. 07	$1s_4$-$3p_{10}$
1	5, 023. 84	19, 899. 56	$1s_3$-$8XY$
60	4, 923. 15	20, 306. 55	$1s_4$-$3p_9$
50	4, 916. 50	20, 334. 01	$1s_4$-$2p_4$
60	4, 843. 29	20, 641. 37	$1s_4$-$3p_6$
70	4, 829. 71	20, 669. 41	$1s_4$-$3p_7$
100	4, 807. 01	20, 797. 16	$1s_4$-$3p_5$
20	4, 792. 61	20, 859. 64	$1s_5$-$3p_{10}$
1—	4, 755. 69	21, 017. 17	
1*h*?	4, 746. 40	21, 062. 73	
100	4, 734. 15	21, 117. 23	$1s_4$-$2p_3$
2	4, 721. 01	21, 176. 00	
2	4, 708. 19	21, 233. 66	$1s_4$-$2p_2$
70	4, 697. 02	21, 284. 16	$1s_5$-$3p_9$
25	4, 690. 97	21, 311. 61	$1s_5$-$2p_4$
300	4, 671. 22	21, 401. 71	$1s_5$-$3p_8$
1	4, 636. 55	21, 561. 74	$1s_5$-$3p_6$
200	4, 624. 29	21, 618. 90	
1	4, 621. 36	21, 632. 61	
8	4, 611. 88	21, 677. 08	$1s_5$-$3p_7$
30	4, 582. 74	21, 814. 92	$1s_4$-$2p_1$
1	4, 574. 86	21, 852. 49	
50	4, 524. 68	22, 094. 83	$1s_5$-$2p_3$
100	4, 500. 99	22, 211. 12	$1s_5$-$2p_2$
10	4, 385. 75	22, 794. 73	$1s_4$-$4X$
15	4, 383. 90	22, 804. 35	$1s_4$-$4Y$
3	4, 372. 25	22, 865. 11	$1s_4$-$4V$
1	4, 215. 5	23, 715. 32	
3	4, 205. 37	23, 772. 45	$1s_5$-$4X$
10	4, 203. 69	23, 781. 95	$1s_5$-$4Y$
30	4, 193. 51	23, 839. 68	$1s_5$-$4U$
1	4, 192. 99	23, 842. 62	$1s_5$-$4V$
4	4, 135. 12	24, 176. 30	$1s_4$-$4p_9$
15	4, 116. 11	24, 287. 95	$1s_4$-$4p_7$
10	4, 109. 71	24, 325. 78	$1s_4$-$4p_6$
20	4, 078. 81	24, 510. 06	$1s_4$-$4p_5$
1	4, 057. 80	24, 636. 96	
5	3, 985. 22	25, 085. 65	$1s_5$-$4p_{10}$

TABLE 14.—*List of Xe_I lines*—Continued

Intensity	Wave length	Wave number	Combination
5	3, 974. 42	25, 153. 81	$1s_5$-$4p_9$
30	3, 967. 55	25, 197. 37	$1s_5$-$4p_8$
1	3, 956. 88	25, 265. 31	$1s_5$-$4p_7$
20	3, 950. 92	25, 303. 43	$1s_5$-$4p_6$
1	3, 948. 70	25, 317. 65	$1s_4$-$6X$
5	3, 948. 19	25, 320. 92	$1s_4$-$5Y$
1	3, 842. 4	26, 018. 05	
3	3, 826. 86	26, 123. 70	$1s_4$-$5p_7$
2	3, 823. 76	26, 144. 88	$1s_4$-$5p_6$
4	3, 809. 90	26, 239. 99	$1s_4$-$5p_5$
3	3, 801. 43	26, 298. 45	$1s_5$-$5Y$
10	3, 796. 33	26, 333. 78	$1s_5$-$5U$
2	3, 745. 44	26, 691. 57	$1s_4$-$6Y$
1	3, 702. 72	26, 999. 52	$1s_5$-$5p_{10}$
1	3, 696. 82	27, 042. 61	$1s_5$-$5p_9$
5	3, 693. 50	27, 066. 92	$1s_5$-$5p_8$
4	3, 685. 91	27, 122. 65	$1s_5$-$5p_6$
1	3, 679. 31	27, 171. 30	$1s_4$-$6p_7$
1—	3, 677. 62	27, 183. 79	$1s_4$-$6p_6$
2	3, 669. 94	27, 240. 67	$1s_4$-$6p_5$
2	3, 633. 15	27, 516. 51	$1s_4$-$7Y$
2	3, 613. 07	27, 669. 43	$1s_5$-$6Y$
3	3, 610. 32	27, 690. 51	$1s_5$-$6U$
2	3, 554. 03	28, 129. 07	$1s_5$-$6p_8$
2	3, 549. 84	28, 162. 27	$1s_5$-$6p_6$
1	3, 506. 75	28, 508. 31	$1s_5$-$7U$
1	3, 472. 43	28, 790. 06	$1s_5$-$7p_8$
1	3, 469. 96	28, 810. 55	$1s_5$-$7p_6$
1—	3, 442. 77	29, 038. 09	$1s_5$-$8U$

The general features of this classification of Xe_I lines parallel those of the preceding rare gases, Ne_I, A_I, Kr_I, and are also in accord with the structure expected on theoretical grounds. Many resemblances among these four spectra have been alluded to in this paper, but we shall reserve further discussion and interpretation of them so as to include comparisons with the fifth spectrum, that of radon, which is now under investigation.

The cooperation of the authors has been made possible in this investigation through the grant of a research fellowship to one of them (T. L. deB.) by the International Education Board.

WASHINGTON, May 10, 1929.

RP 116

THE ARC SPECTRUM OF ARSENIC

By William F. Meggers and T. L. deBruin

ABSTRACT

Metallic arsenic was vaporized in graphite or copper arcs, and the line emission spectrum was investigated throughout the entire range accessible to photography with concave grating and with quartz prism spectrographs. The measured wave lengths range from 1889.85 to 10023.98 A. The spectrum is relatively simple but difficult to analyze because many important lines lie either in the far ultra-violet or in the infra-red. The new data (vacuum wave numbers, estimated relative intensities, and self-reversal of certain lines) have made possible a fairly complete analysis of the As_I spectrum.

Forty-two levels have been identified; they include practically all of the spectral terms arising from the addition of a $4p$, $5s$, and $4d$ electron to the s^2p^2 configuration of the As^+ ion. The normal state is represented by a $^4S_2$ term for which the absolute value is estimated to be 80692.72, corresponding to an ionization potential of about 10 volts. Combinations of the identified terms account for 100 observed As_I lines, ranging in wave length from 1574.7 to 10614.0 A, our observations being supplemented by two infra-red lines detected radiometrically by Randall and 19 lines in the Schumann region obtained with a fluorite spectrograph in vacuo by L. and E. Bloch.

CONTENTS

	Page
I. Introduction	765
II. Wave-length measurements	766
III. Analysis of the arc spectrum of arsenic	769
1. Theoretical terms	770
2. The multiplets	771
3. The term table	776
4. List of classified As_I lines	778

I. INTRODUCTION

The first observations of the arc spectrum of arsenic were made by Kayser and Runge [1] in 1893. They excited the spectrum by placing metallic arsenic in a carbon arc and photographed it from 6000 A to shorter waves but found no lines in the visible spectrum. In the ultra-violet between 3119.69 and 2009.31 A they recorded 33 As lines but assigned no intensities to the last seven lying below 2113 A, probably because the strong absorption of ordinary gelatin emulsions for light in this region makes the photographic images appear very weak and thin. The only other attempt to derive wave lengths from a photographic study of the arc spectrum of arsenic

[1] Kayser and Runge, Abhandl. Berlin Akad.; 1893; Wiedemann's Ann., **52**, p. 93; 1894.

was made by Exner and Haschek[2] in 1904. The observations were made with an alloy of 40 per cent As with nickel; wave lengths ranging from 3119.70 to 2271.46 A were measured for 18 lines.

A portion of the infra-red emission spectrum of arsenic was investigated radiometrically by Randall[3] in 1911; 10 lines were observed between 8823.3 and 10614.6 A.

The above-mentioned three papers contain all that was known of the arc spectrum of arsenic up to the present time. The wave lengths are relative to Rowland's scale of standards, since the measurements were made before the new international standards were adopted. The spectra of arsenic excited in high-potential condensed sparks have been studied more or less extensively by Hartley and Adeney,[4] by Exner and Haschek,[5] and by Herpertz.[6] The latter also investigated the spectra emitted by Geissler tubes containing arsenic. These high-potential sources develop spectra of greater complexity. About 500 lines have been recorded in the visible and ultra-violet. These include most of the lines ascribed to the arc spectrum, but the reverse is not true; that is, the arc spectrum can be produced without exciting any spark lines. The spark spectrum of arsenic has been observed by L. and E. Bloch[7] in the Schumann region, but it is impossible to distinguish arc from spark lines in this region without an arc comparison.

After summarizing these data in the section on arsenic in their Handbuch, Kayser and Konen[8] remark that "Das Spektrum ist eben noch sehr unvollkommen bekannt." We are aware of no additional published observations in recent years but have now completed a new description of the As_I spectrum covering the entire range accessible photographically to ordinary spectrographs. The new observations for As_I lines which have been classified are presented in this paper.

II. WAVE-LENGTH MEASUREMENTS

When the new infra-red photosensitizing dye, neocyanine, became available in 1926, it was immediately tested and found useful for the extension of spectrographic information already obtained by means of dicyanine. It was also employed for the study of certain spectra which had been previously neglected; arsenic became one of these at the suggestion of Dr. Otto Laporte. The arc spectrum of arsenic was found to contain a group of powerful lines in the infra-red, and it was

[2] Exner and Haschek, Tabelle der Bogenspektra, Wien; 1904.
[3] Randall, Astrophys. J., **34**, p. 1; 1911.
[4] Hartley and Adeney, Phil. Trans., **175**, I, p. 63; 1884.
[5] Exner and Haschek, Tabelle der Funkenspektra, Wien; 1902.
[6] Herpertz, Zeitschr. f. wiss. Phot., **4**, p. 175; 1906.
[7] L. and E. Bloch, C. R., **158**, p. 416; 1914; **171**, p. 709; 1920.
[8] Kayser and Konen, Handbuch der Spectrotroscopie, **7**, p. 63; 1924, Hirzel, Leipzig.

immediately recognized that these were structurally related to the ultra-violet lines described by Kayser and Runge 33 years earlier. Then the observations were extended to cover the visible spectrum and the ultra-violet down to 3119 A. This interval was supposed to contain no lines of the As_I spectrum, but a considerable number of fairly strong lines were detected in the blue and green. No structural connection, however, has been found between the stronger visible lines and the invisible ones.

At this point it was apparent that a satisfactory analysis of the As_I spectrum could not be continued without reobserving the ultra-violet portion so as to establish the wave lengths of these lines relative to the modern international standards and to obtain more homogeneous data as to relative intensities. The results will show that this procedure was justified; some new lines have been discovered in the ultra-violet, and certain details of spectral structure have thus been revealed which otherwise would have remained obscure.

In this investigation the source was usually a graphite arc in which metallic arsenic was vaporized, although some exposures were made with a copper arc to which arsenic was added. The arcs were operated with 8 to 10 amperes on a 220-volt direct current circuit. The lower electrode was bored out and filled with lumps of arsenic metal. The metal vaporized and sublimed so rapidly that frequent fillings were necessary during an exposure. More than 400 gms of metal were thus consumed in about 10 hours of exposing time. Mallinckrodt's "pure" arsenic metal was used, and all the lines not duplicated in the graphite or copper comparison spectra were measured. The final list of wave lengths was compared with Kayser's [9] Hauptlinien for the identification of impurities. Evidence for a considerable number of impurities was found, especially in the ultra-violet where the raies ultimes of most elements occur. The main impurities were found to be Sb, Bi, Si, Sn, Pb, Cu, Fe, Ni, and traces of Mg, Al, Ag, and Te.

The infra-red spectrum was photographed with an Anderson grating (21-foot radius, 6-inch grating, with 7,500 lines per inch) in a Wadsworth mounting described in other papers [10] and successfully used in describing the long wave portions of various spectra. The first-order spectrum of this grating has a scale of approximately 10.4 A per mm.

"Eastman 36" plates, stained in the laboratory with neocyanine, were used in the infra-red. The greatest wave length recorded photographically in the arsenic spectrum was 10024 A, a good image of this line being impressed by an exposure of one hour.

[9] Kayser, Tabelle der Hauptlinien der Linienspektren aller Elemente, Julius Springer, Berlin; 1927.
[10] Meggers and Burns, B. S. Sci. Papers 18 (No. 441), p. 191; 1922.

The same grating was used in exploring the spectrum through the visible and near ultra-violet where a number of lines not previously noted in the arc spectrum of arsenic and not identifiable with impurities were found. These observations were recently repeated and confirmed with another grating ruled by Prof. R. W. Wood. This grating resembles the Anderson grating in giving an exceptionally bright first-order spectrum, but it has twice as many lines (15,000 per inch) and consequently twice the dispersion and theoretically twice the resolving power in corresponding orders. The scale in the ultra-violet of the first-order spectrum is about 5.3 A per mm. Observations with the Wood grating were extended to 2288 A. "Eastman 33" plates were used in this range; they were sensitized to the green, yellow, and red by bathing in solutions of pinaverdol and pinacyanol.

The shorter ultra-violet was investigated with a Hilger E_1 quartz autocollimating spectrograph. Although it is not usually used below 2100 A, by remounting the prism and lens 10 cm nearer the plate holder it was possible to extend the range of this instrument to 1860 A. The shortest arsenic wave length which was recorded with an exposure of one hour was 1889 A. Four settings of the E_1 spectrograph were chosen to cover the interval from 1860 to 3600 A with overlaps. "Eastman process" plates were used from 3600 to 2160 A and "Hilger Schumann" plates from 2300 to 1860 A. In the ultra-violet this type of spectrograph compares favorably in dispersion and resolving power with the largest diffraction gratings, and it has a considerably greater light efficiency. The scale is 0.96 A per mm at 1900 A, 1.19 A per mm at 2000 A, 2.73 A per mm at 2500 A, 4.93 A per mm at 3000 A.

Wave-length measurements were made relative to the international secondary standards in the spectrum of the iron arc.[11] Since no standards have been adopted shorter than 3370 A, from this point to 2370 A the iron arc wave lengths published by Burns [12] were used, and for the still shorter wave-length region to 1900 A Shenstone's value for Cu_I,[13] Cu_{II},[14] and Ag_{II}[15] lines were employed. The comparison spectrum in the latter region was a condensed spark between a copper and a silver electrode.

All of the spectrograms were measured in two directions, those made with the gratings were reduced assuming a linear scale and applying corrections derived from the standards, while the prism spectrograms were reduced according to the standard method involving the Hartman-Cornu formula.[16] Most of the lines were observed on three or

[11] Trans. Internat. Astronom. Union, **3**, p. 77; 1928.
[12] Burns, Zeitschr. f. wiss. Phot., **12**, p. 207; 1913; **13**, p. 235; 1914.
[13] Shenstone, Phys. Rev., **28**, p. 449; 1926.
[14] Shenstone, Phys. Rev., **29**, p. 380; 1927.
[15] Shenstone, Phys. Rev., **31**, p. 317; 1928.
[16] Meggers, Glazebrook's Dictionary of Applied Physics, **4**, p. 890; 1923

FIGURE 1.—*Arc spectrum of arsenic from 1930 to 2120 A*

Quartz prism spectrograph.
1 and 4, copper spark spectrum; 2, 5, and 8, arsenic in graphite; 3 and 6, copper + silver spark spectrum; 7, graphite arc spectrum; and 9, copper arc spectrum.

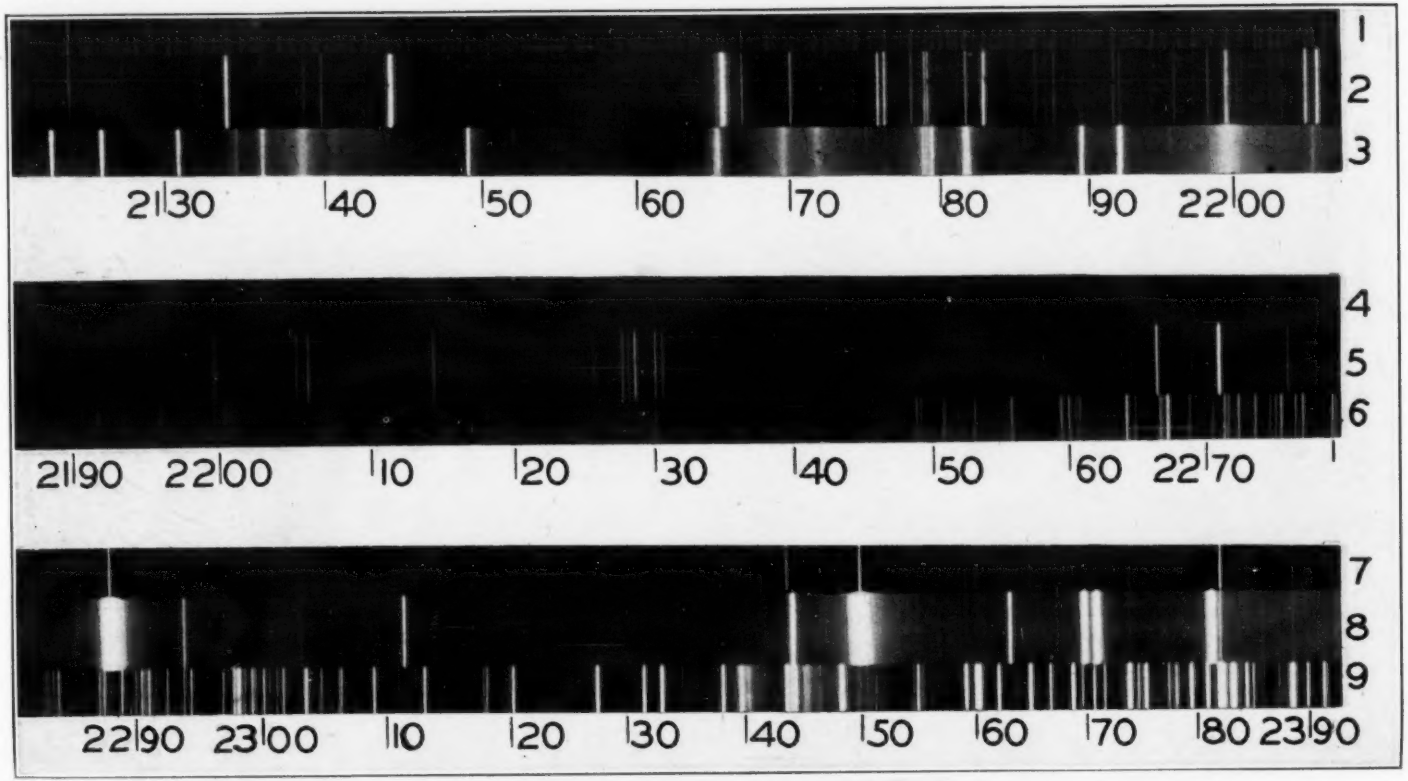

FIGURE 2.—*Arc spectrum of arsenic from 2120 to 2390 A*

Quartz prism spectrograph.
1, 4 and 7, graphite arc spectrum; 2, 5, and 8, arsenic in graphite; 3, copper arc spectrum; and 6 and 9, iron arc spectrum.

Quartz prism spectrograph.
1, 4 and 7, graphite arc spectrum; 2, 5, and 8, arsenic in graphite; 3, copper arc spectrum; and 6 and 9, iron arc spectrum.

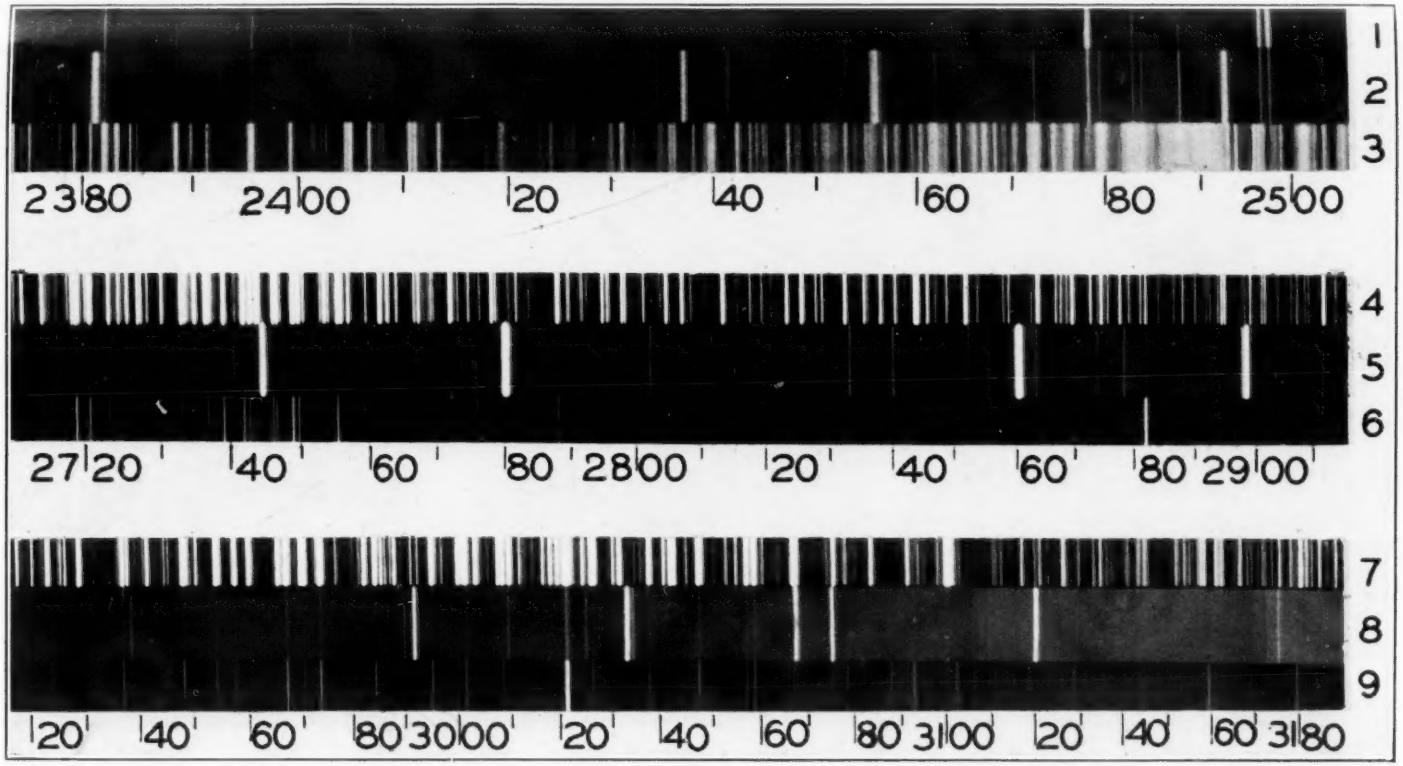

FIGURE 3.—*Arc spectrum of arsenic from 2380 to 3180 A*

Quartz prism spectrograph.
1, 6, and 9, graphite arc spectrum; 2, 5, and 8, arsenic in graphite; and 3, 4, and 7, iron arc spectrum.

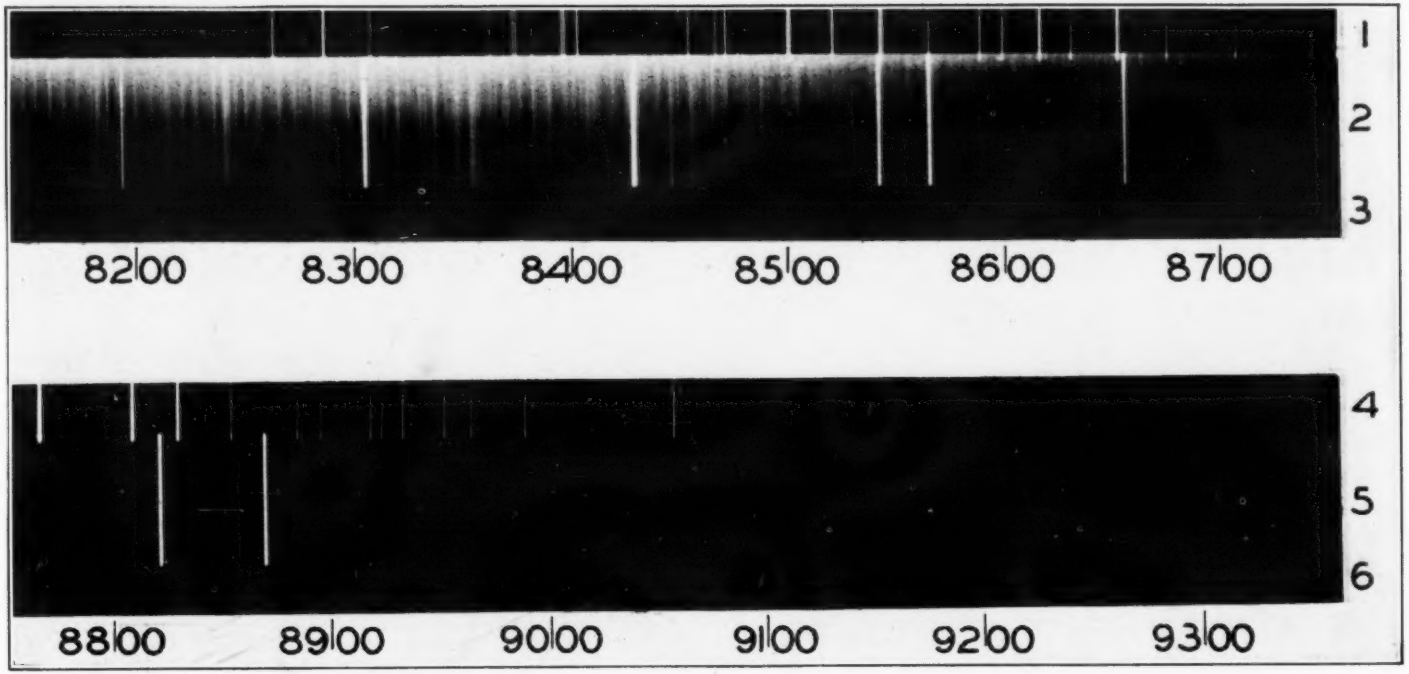

FIGURE 4.—*Arc spectrum of arsenic from 8200 to 9300 A*

Grating spectrograph.
1 and 4, iron arc spectrum; 2 and 5, arsenic in graphite; and 3 and 6, graphite arc spectrum.

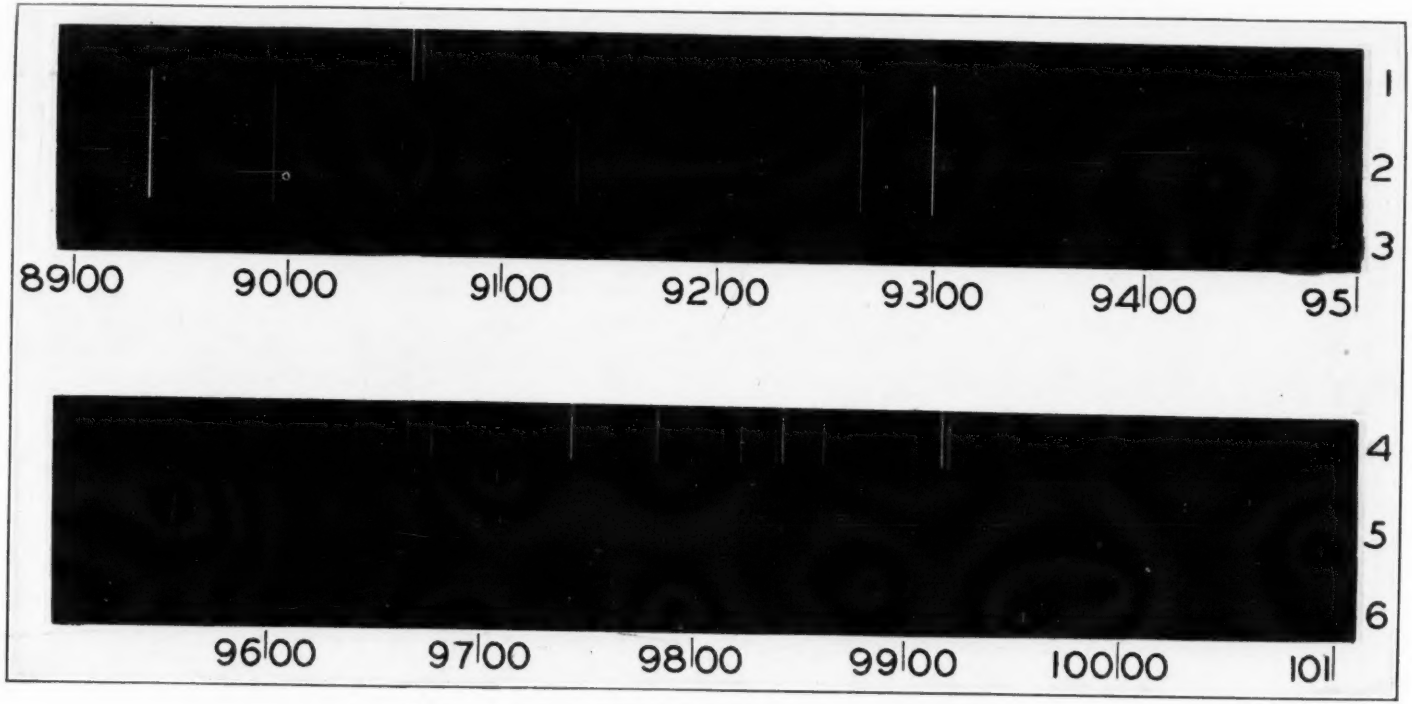

FIGURE 5.—*Arc spectrum of arsenic from 8900 to 10100 A*

Grating spectrograph.
1 and 4, iron arc spectrum; 2 and 5, arsenic in graphite; and 3 and 6, graphite arc spectrum.

UNIV. OF MICH.

more spectrograms, and the final mean wave length is probably not in error by more than one or two hundredths of an Ångstrom unit on the average.

No supplementary data, such as Zeeman effect, temperature classification, absorption phenomena, etc., are available for arsenic. Neither the Zeeman effect nor temperature classification has ever been investigated, and the absorption experiments have all given negative results for atomic arsenic. Thus, McLennan, Young, and Ireton [17] reported that no line reversals were obtained in any part of the spectrum down to 1850 A, and similar failure is recorded by Dobbie and Fox [18] and by Ruark, Mohler, Foote, and Chenault.[19]

Fortunately, certain lines of arsenic have been observed to be partially self-reversed in the arc. These reversals appear to be of two types distinguished in our tables by *R* and *r*, the former being considerably wider and more conspicuous than the latter. These observations, in addition to a satisfactory list of wave lengths and estimated intensities have enabled us to identify spectral terms which account for nearly all of the lines detected in the infra-red and ultra-violet. The strongest lines in these two regions are reproduced in Figures 1, 2, 3, 4, and 5. Attention is called to the widely reversed lines at 1937 and 1972 A, which appear to have superposed on their sides some finer absorption lines probably belonging to some compound of arsenic.

III. ANALYSIS OF THE ARC SPECTRUM OF ARSENIC

The arc spectrum of arsenic is relatively simple, and still it is difficult to analyze because so many important lines lie in the incompletely explored ultra-violet and infra-red regions. Kayser and Runge [20] first sought for regularities among the 33 lines observed by them in the ultra-violet, and they found 20 of the lines to be connected by wave-number differences of 461 and 8058. These differences are now interpreted as the intervals between three important low levels $^2P_1$, $^2P_2$, and $^2D_2$ of the As I spectrum.

Two additional low levels were found by Ruark, Mohler, Foote, and Chenault,[21] but they interpreted the low energy levels as a set of middle terms and assigned the wrong quantum numbers in several cases. McLennan and McLay [22] gave the correct interpretation for the low energy levels but added nothing to the observational data or to the regularities. Without new and extended material, it was

[17] McLennan, Young, and Ireton, Trans. Roy. Soc. Can., **13**, 3, p. 7; 1919.
[18] Dobbie and Fox, Proc. Roy. Soc., **A98**, p. 147; 1920.
[19] Ruark, Mohler, Foote, and Chenault, B. S. Sci. Papers, **19** (No. 490), p. 463; 1924.
[20] Kayser and Runge, Wiedem. Ann., **52**, p. 93; 1894.
[21] Ruark, Mohler, Foote, and Chenault, B. S. Sci. Papers, **19** (No. 490), p. 463; 1924.
[22] McLennan and McLay, Trans. Roy. Soc. Can., **21**, 3, p. 63; 1927.

obvious that no real progress could be made in the analysis of the arsenic spectrum.

1. THEORETICAL TERMS

The neutral arsenic atom has 33 electrons ($Z=33$), but only 5 of these are of interest spectroscopically. According to the theory of spectral terms and electron configurations elaborated by Hund,[23] the terms which represent the excited states of the arsenic atom will result from the interaction of the series electron with the electron group s^2p^2 which characterizes the unexcited state of the ion, As^+. The terms arising from s^2p^2 are ^3P, ^1D, ^1S, the lowest levels of the As_{II} spectrum. We may, therefore, obtain the terms representing the excited states of the neutral atom by adding in turn the electron, *ns*, *np*, *nd*, etc., to the basic terms ^3P, ^1D, ^1S. The normal state of the As atom is formed by the configuration s^2p^3 giving rise to the five low levels [24] $^4S_2$, $^2D_{2,3}$, $^2P_{1,2}$. The complete set of theoretical terms which may be expected to account for the As_I spectrum is presented in Table 1.

TABLE 1.—*Predicted terms in the As_I spectrum*

Electron configuration As_{II}	$^3P_{1,2,3}$	$^1D_2$	$^1S_1$
$s^2p^3.4p$	$^4S_2$ $^2D_{2,3}$ $^2P_{1,2}$		
$s^2p^3.5s$	$^4P_{1,2,3}$ $^2P_{1,2}$	$^2D_{2,3}$	$^2S_1$
$s^2p^3.5p$	$^4D_{1,2,3,4}$ $^4P_{1,2,3}$ $^4S_2$ $^2D_{2,3}$ $^2P_{1,2}$ $^2S_1$	$^2F_{3,4}$ $^2D_{2,3}$ $^2P_{1,2}$	$^2P_{1,2}$
$s^2p^3.4d$	$^4F_{2,3,4,5}$ $^4D_{1,2,3,4}$ $^4P_{1,2,3}$ $^2F_{3,4}$ $^2D_{2,3}$ $^2P_{1,2}$	$^2G_{4,5}$ $^2F_{3,4}$ $^2D_{2,3}$	$^2D_{2,3}$

The normal electron configuration of the outer shell of As is s^2p^3, and the foregoing excited states arise from the displacement of one of the *p*-electrons. It is also possible that terms involving the displacement of an *s*-electron are present. Thus, from the configuration sp^4 we may expect the terms,

$$^4P_{1,2,3}\ ^2P_{1,2}\ ^2D_{2,3}\ ^2S.$$

Terms of this character have indeed been found by Bowen[25] in the analogous N_I spectrum and by Ingram[26] in the analogous S_{II} spectrum.

[23] Hund, Linienspektren und periodisches System der Elemente, Julius Springer, Berlin; 1927.

[24] For greater convenience of writing, printing, and reading the inner quantum numbers of levels belonging to even multiplicities are increased by one-half in this paper.

[25] Bowen Phys. Rev., **29**, p. 231; 1927.

[26] Ingram, Phys. Rev., **32**, p. 172; 1928.

2. THE MULTIPLETS

The combinations accompanying the electron transition $5s \rightarrow 4p$ are presented as a supermultiplet in Table 2. This supermultiplet contains 35 ultra-violet lines, including most of those observed as reversed in the arc. Fourteen of these lines are contained in the wave-number scheme of Kayser and Runge. Six lines fall in the vacuum region; they are represented by wave numbers calculated from relative term values. It is possible that five of these calculated lines are identifiable with lines observed by L. and E. Bloch[27] in the arsenic spark spectrum as follows:

Intensity	λ	Observed	Calculated	Combinations
1	1, 831. 1	54, 612	54, 606	$^4S_2$–$^2P_2$
3	1, 844. 3	54, 221	54, 219	$^2D_2$–$^3S_1$
1	1, 881. 08	53, 143	53, 135	$^4S_2$–$^2P_1$
1	1, 644. 0	60, 827	60, 834	$^4S_2$–$^3D_2$
			60, 814	$^4S_2$–$^3D_3$

The sixth line (64,810 $^4S_2$–$^2S_1$) falls just beyond the limit of the observations.

It is to be noted, further, that while the terms originating with ^3P are regular, (level values increase with decreasing inner quantum number), the $^2D_{3,\,2}$ arising from ^1D is inverted. Attention is called also to the fact that the level separations $5s\ ^4P_{1,\,3}$ and $5s\ ^2P_{1,\,2}$ have exactly the ratio 3:2 which might be anticipated from considerations of convergence to limits in the As_{II} spectrum. This ratio has been found in several 7-electron systems[28] to be 4:3, but in these cases the convergence to limits is uncertain because of inverted terms.

The $5p \rightarrow 5s$ multiplets, involving 23 infra-red lines of arsenic are given as a supermultiplet in Table 3. The following remarks are pertinent to the terms and combinations shown here. It is not possible at present to assign all the quantum numbers of the $5p$-terms with positiveness, but in most cases a plausible interpretation can be suggested. Thus, although no satellites have been observed to support the $5p\ ^4P$–$5s\ ^4P$ multiplet, the line intensities, term differences, and interval ratio are of the order that can be expected. Furthermore, it is possible by interpolation to predict the spectral region in which this multiplet should occur. This is illustrated in Table 4 where the first column contains the atomic number, the second the chemical symbol, the third the $p \rightarrow s$ "electron jump" symbolized by spectral term differences. The actual values, so far as known,

[27] L. and E. Bloch, J. de. Phys., **4**, p. 622; 1914, Comptes rendus, **171**, p. 709; 1920.
[28] deBruin, Zeitschr. f. Phys., **53**, p. 661; 1929.

are given in wave numbers in column 4. A fairly regular progression of wave number with increasing atomic number appears to exist, and it sustains the construction placed upon 9973.35 of As_I. It may be added that if this identification is correct $5p\ ^4P$ has a lower position in the energy diagram of As_I than $5p\ ^4D$.

TABLE 2.—*As_I supermultiplet $5s \rightarrow 4p$*

$5s$ \ $4p$	$^4S_2$ 80,692.72	$^2D_2$ 70,101.26	$^2D_3$ 69,779.03	$^2P_1$ 62,507.46	$^2P_2$ 62,046.13
$^4P_1$	1, 000 *R*	50		20	50
	1, 972. 03	2, 492. 91		3, 075. 32	3, 119. 60
	50, 692. 72	40, 101. 60		32, 507. 53	32, 046. 13
30, 000. 00	50, 692. 72	40, 101. 26		32, 507. 46	32, 046. 13
$^4P_2$	1, 000 *R*	50	200 *r*	20	40
	1, 937. 02	2, 437. 23	2, 456. 53	2, 990. 99	3, 032. 68
	51, 608. 91	41, 017. 74	40, 695. 45	33, 424. 02	32, 962. 68
29, 083. 52	51, 609. 20	41, 017. 72	40, 695. 51	33, 423. 94	32, 962. 61
$^4P_3$	1, 000 *R*	10	150 *r*		2
	1, 889. 85	2, 363. 05	2, 381. 20		2, 918. 82
	52, 896. 62	42, 305. 24	41, 983. 17		34, 250. 40
27, 795. 83	52, 896. 89	42, 305. 43	41, 983. 20		34, 250. 30
$^2P_1$	1	500 *R*		100 *r*	50 *r*
	1, 881. 08	2, 349. 84		2, 860. 44	2, 898. 71
	53, 143	42, 543. 05		34, 949. 42	34, 488. 06
27, 558. 28	53, 134. 44	42, 542. 98		34, 949. 28	34, 487. 85
$^2P_2$	1	50	500 *R*	50 *r*	200 *r*
	1, 831. 1	2, 271. 36	2, 288. 12	2, 745. 00	2, 780. 22
	54, 612	44, 012. 85	43, 690. 49	36, 419. 07	35, 957. 76
26, 088. 49	54, 604. 23	44, 012. 77	43, 690. 54	36, 418. 97	35, 957. 64
$^2D_3$	1	50 *r*	300 *R*		100 *r*
	1, 644. 0	1, 990. 49	2, 003. 34		2, 370. 78
	60, 827	50, 222. 74	49, 900. 41		42, 167. 32
19, 878. 59	60, 814. 13	50, 222. 67	49, 900. 44		42, 167. 54
$^2D_2$	1	200 *R*	20 *r*	50	80 *r*
	1, 644. 0	1, 989. 71	2, 002. 54	2, 344. 03	2, 369. 67
	60, 827	50, 242. 42	49, 920. 34	42, 648. 49	42, 187. 07
19, 858. 89	60, 833. 83	50, 242. 37	49, 920. 14	42, 648. 49	42, 187. 24
$^2S_1$		3		100 *r*	100 *r*
		1, 844. 3		2, 144. 10	2, 165. 52
		54, 221		46, 624. 87	46, 163. 74
15, 882. 49	64, 810. 23	54, 218. 77		46, 624. 97	46, 163. 64

TABLE 3.—*As I supermultiplet* $5p \rightarrow 5s$

$5p$ \ $5s$	$^4P_1$ 30,000.00	$^4P_2$ 29,083.52	$^4P_3$ 27,795.83	$^2P_1$ 27,558.28	$^2P_2$ 26,088.49
$^4P_1$	80 9, 833. 76 10, 166. 27				
19, 833. 73	10, 166. 27	9, 249. 79			
$^4P_2$		100 10, 023. 98 9, 973. 35			
19, 110. 17	10, 889. 83	9, 973. 35	8, 685. 66		
$^4P_3$			150 9, 923. 03 10, 074. 81		
17, 721. 02		11, 362. 50	10, 074. 81		
$^4D_1$	150 8, 821. 76 11, 332. 50	10 9, 597. 94 10, 416. 05			
18, 667. 48	11, 332. 52	10, 416. 04			
$^4D_2$	50 8, 541. 65 11, 704. 13	25 9, 267. 29 10, 787. 68			
18, 295. 86	11, 704. 14	10, 787. 66	9, 499. 97		
$^4D_3$		100 8, 564. 71 11, 672. 62	8 9, 626. 69 10, 384. 94		
17, 410. 89		11, 672. 63	10, 384. 94		
$^4D_4$			150 8, 654. 16 11, 551. 96		
16, 243. 87			11, 551. 96		
$^4S_2$		50 8, 305. 62 12, 036. 73	50 9, 300. 62 10, 749. 03		
17, 046. 80	12, 953. 20	12, 036. 72	10, 749. 03		
$^2D_2$	100 8, 428. 94 11, 860. 63	15 9, 134. 81 10, 944. 13		25 10, 614 9, 418. 9	
18, 139. 38	11, 860. 62	10, 944. 14	9, 656. 45	9, 418. 90	7, 949. 11
$^2D_3$		25 7, 960. 26 12, 558. 95	100 8, 869. 69 11, 271. 26		60 10, 453 9, 564. 0
16, 524. 57		12, 558. 95	11, 271. 26		9, 563. 92
$^2P_1$				20 8, 993. 08 11, 116. 62	
16, 441. 66				11, 116. 62	9, 646. 83
$^2P_2$		4 7, 863. 45 12, 713. 57		50 8, 935. 58 11, 188. 15	
16, 370. 04		12, 713. 48		11, 188. 24	9, 718. 45
$^2S_1$		8 7, 410. 16 13, 491. 27		10 8, 355. 00 11, 965. 60	
15, 592. 46		13, 491. 06		11, 965. 82	10, 445. 93

TABLE 4.—*Homologous electron jumps in several spectra*

Z	Element	$p \longrightarrow s$	ν	Remarks
31	Ga	$^2S_1$–$^2P_2$	(8, 265)	Calculated from terms.[1]
32	Ge	$^3P_2$–$^3S_1$		
33	As.	$^4P_2$–$^4P_2$	9, 973. 35	
34	Se	$^5S_2$–$^5P_2$	(11, 029)	Extrapolated from series.[2]
35	Br	$^4P_3$–$^4P_4$	12, 084. 98	Observed.[3]
36	Kr	$^3P_2$–$^3D_3$	12, 322. 60	Do.[4]
37	Rb	$^2S_1$–$^2P_2$	12, 816. 72	Do.[5]

[1] Paschen-Götze, Seriengesetze der Linienspektren, p. 129, Julius Springer, Berlin; 1922.
[2] Paschen-Götze, Seriengesetze der Linienspektren, p. 140.
[3] Kiess and deBruin, B. S. Jour. Research (in press).
[4] Meggers, de Bruin, and Humphreys, B. S. Jour. Research, **3**, (No. 89), p. 129; 1929.
[5] Paschen-Götze, Seriengesetze der Linienspektren, p. 61.

The $5s\ ^4P_1$–$5p\ ^4S_2$ combination should be a fairly strong line, but it was not observed; it may be possible that $^2D_2$ and $^4S_2$ should be interchanged, but in this case the ^2D interval becomes smaller and ^4S deeper than would be expected.

Finally, it is admitted that the identification of $5p\ ^2P_{2,1}$ is somewhat doubtful because the level separation is abnormally small. However, in the infra-red only a few faint unclassified lines remain and there seems to be no choice for another arrangement.

Now, we can discuss a group of levels (still higher than the $5p$-terms) which combines with the deep ^2P and ^2D as shown in Table 5. Combinations with the normal state ^4S nearly all fall in the unobserved ultra-violet. In developing this group of terms, we succeeded first in evaluating 8 levels (possibly 9) with inner quantum numbers, $j=1$ or 2 and then 5 levels with $j=3$. This is precisely the number of levels of each class which can be produced by the configuration $s^2p^2.4d$, and this group is accordingly interpreted as having this origin. In addition to the 13 levels with $j=1, 2, 3$ we expect 3 levels with $j=4$ and 1 with $j=5$. Unfortunately, the levels with $j=4$ can give only one combination with deep terms, but their selection is not entirely arbitrary, because so few lines remain unclassified that there is scarcely any choice. The level $j=5$ is not expected to combine with any of the deep terms. We have hazarded an interpretation of these 16 high levels (Tables 5 and 6), but we wish to emphasize at the same time the desirability of regarding the identifications and groupings as tentative rather than final.

Table 5 contains 13 ultra-violet lines observed only by L. and E. Bloch. These are distinguished from our observations by 5-place wave numbers instead of 7.

TABLE 5.—*As*$_1$ *supermultiplet* $4d \rightarrow 4p$

$4d$ \ $4p$	$^4S_2$ 80,692.72	$^2D_2$ 70,101.26	$^2D_3$ 69,779.03	$^2P_1$ 62,507.46	$^2P_2$ 62,046.13
$^4F_4$			20*r*		
			1, 958. 29		
			51, 048. 28		
18, 730. 75			51, 048. 28		
$^4F_3$	1	5	4		25
	1, 593. 4	1, 916. 61	1, 928. 58		2, 266. 70
	62, 759	52, 158. 31	51, 834. 69		44, 103. 32
17, 942. 81	62, 749. 91	52, 158. 45	51, 836. 22		44, 103. 32
$^4F_2$	2			15	20
	1, 574. 7			2, 205. 97	2, 228. 66
	63, 504			45, 317. 35	44, 856. 03
17, 190. 10	63, 502. 62	52, 911. 16	52, 588. 93	45, 317. 36	44, 856. 03
$^4D_1$		1		20	10
		1, 872. 33		2, 182. 94	2, 205. 16
		53, 391		45, 795. 40	45, 334. 00
16, 712. 10	63, 980. 62	53, 389. 16		45, 795. 36	45, 334. 03
$^4D_2$				15	5
				2, 176. 26	2, 198. 34
				45, 935. 95	45, 474. 63
16, 571. 50	64, 121. 22	53, 529. 76	53, 207. 53	45, 935. 96	45, 474. 63
$^4D_3$		1	1		5
		1, 859. 90	1, 871. 07		2, 187. 75
		53, 748	53, 427		45, 694. 72
16, 351. 41	64, 341. 31	53, 749. 85	53, 427. 62		45, 694. 72
$^4D_4$			2		
			1, 854. 4		
			53, 926		
15, 853			53, 926		
$^4P_1$?				100	30
				2, 113. 01	2, 133. 81
				47, 310. 81	46, 849. 69
15, 196. 55	65, 496. 17	54, 904. 71		47, 310. 91	46, 849. 58
$^4P_1$		2		30	10
		1, 789. 2		2, 069. 83	2, 089. 79
		55, 891		48, 297. 66	47, 836. 41
14, 209. 76	66, 482. 96	55, 891. 50		48, 297. 70	47, 836. 37
$^4P_2$				40	25
				2, 065. 41	2, 085. 29
				48, 401. 00	47, 939. 63
14, 106. 48	66, 586. 24	55, 994. 78	55, 672. 55	48, 400. 98	47, 939. 65
$^4P_3$		1			25
		1, 772. 5			2, 067. 16
		56, 417			48, 360. 03
13, 686. 10	67, 006. 62	56, 415. 16	56, 092. 93		48, 360. 03
$^2F_4$			5		
			1, 805. 6		
			55, 383		
14, 396			55, 383		

TABLE 5.—*As*$_I$ *supermultiplet* $4d \rightarrow 4p$—Continued

$4d$ \ $4p$	$^4S_2$ 80,692.72	$^2D_2$ 70,101.26	$^2D_3$ 69,779.03	$^2P_1$ 62,507.46	$^2P_2$ 62,046.13
$^2F_3$		3 1, 758. 2 56, 876			50 2, 047. 59 48, 822. 17
13, 223. 96	67, 468. 76	56, 877. 30	56, 555. 07		48, 822. 17
$^2P_1$				20 2, 010. 04 49, 734. 10	4 2, 028. 87 49, 272. 58
12, 773. 46	67, 919. 26	57, 327. 80		49, 734. 00	49, 272. 67
$^2D_2$		1 1, 732. 8 57, 710		100r 1, 994. 79 50, 114. 51	50r 2, 013. 32 49, 653. 10
12, 392. 99	68, 299. 73	57, 708. 27	57, 386. 04	50, 114. 47	49, 653. 14
$^2P_2$				25 1, 994. 25 50, 128. 08	20 2, 012. 77 49, 666. 66
12, 379. 43	68, 313. 29	57, 721. 83	57, 399. 60	50, 128. 03	49, 666. 70
$^2D_3$		1 1, 729. 8 57, 810	2 1, 739. 4 57, 491		100r 2, 009. 18 49, 755. 38
12, 290. 75	68, 401. 97	57, 810. 51	57, 488. 28		49, 755. 38

Two new lines in the visible spectrum, 5,361.12 (10) and 5,497.10 A (4) deserve special mention because they can be interpreted as the "forbidden" combinations $4p\ ^4S_2$–$4p\ ^2P_{1,2}$. The $^4S_2$ level calculated from the line at 1,972.03 A ($4p\ ^4S_2$–$5s\ ^4P_1$) is 80,692.72, while the above-mentioned pair yields 80,693.80. If this interpretation is correct, these visible lines are of the same character as the nebular lines.[29]

We may mention, also, at this point the possibility of interpreting two extreme ultra-violet lines as "forbidden"; they are as follows:

Intensity	λ	$\nu_{obs.}$	$\nu_{calc.}$	Combination
2	1, 612. 3	62, 023	62, 025. 24	$4p\ ^4S_2$–$5p\ ^4D_1$
1	1, 558. 4	64, 168	64, 168. 15	$4p\ ^4S_2$–$5p\ ^2D_2$

3. THE TERM TABLE

All of the terms thus far established in the As$_I$ spectrum are given in Table 6. Comparison with Table 1 shows that practically all the terms resulting from the (s^2p^2) $4p$, $5s$, $5p$, $4d$ configurations have been found. Unfortunately, it is not possible at this stage to determine final absolute term values from term series, first, because the

[29] Bowen, Astrophys. J., 67 ,p. 1; 1928.

$4p$, $5p$ series will give values which are too high, and, second, because the higher terms of the spectrum are not completely described. It is, however, possible to make an estimation of the absolute term values of the As_I spectrum by comparison with the analogous terms in the spectra of neighboring elements as shown in Table 7.

We have taken 30,000 as a reasonable value for $5s\ ^4P_1$ and have based all the other terms on this value. This fixes the ground term $^4S_2$ tentatively at 80,692.72, which corresponds to an ionization potential of about 10 volts, 1.5 volts lower than the value measured by Ruark, Mohler, Foote, and Chenault.[30]

TABLE 6.—*Relative terms in the As_I spectrum*

Electron configuration	Term symbol	Term value	Level separations
	$^4S_2$	80, 692. 72	
	$^2D_2$	70, 101. 26	322. 23
$s^2p^2.4p$	$^2D_3$	69, 779. 03	
	$^2P_1$	62, 507. 46	461. 33
	$^2P_2$	62, 046. 13	
	$^4P_1$	30, 000. 00	916. 48
	$^4P_2$	29, 083. 52	1, 287. 69
$s^2p^2.5s(^3P)$	$^4P_3$	27, 795. 83	
	$^2P_1$	27, 558. 28	1, 469. 79
	$^2P_2$	26, 088. 49	
$s^2p^2.5s(^1D)$	$^2D_3$	19, 878. 59	−19. 70
	$^2D_2$	19, 858. 89	
$s^2p^2.5s(^1S)$	$^2S_1$	15, 882. 49	
	$^4P_1$	19, 833. 73	723. 56
	$^4P_2$	19, 110. 17	1, 389. 15
	$^4P_3$	17, 721. 02	
	$^4D_1$	18, 667. 48	371. 62
	$^4D_2$	18, 295. 86	884. 97
	$^4D_3$	17, 410. 89	1, 167. 02
$s^2p^2.5p$	$^4D_4$	16, 243. 87	
	$^4S_2$	17, 046. 80	
	$^2D_2$	18, 139. 38	1, 614. 81
	$^2D_3$	16, 524. 57	
	$^2P_1$	16, 441. 66	71. 62
	$^2P_2$	16, 370. 04	
	$^2S_1$	15, 592. 46	

[30] Ruark, Mohler, Foote, and Chenault, B. S. Sci. Paper 19 (No. 490), p. 463; 1924.

TABLE 6.—*Relative terms in the As_I spectrum*—Continued

Electron configuration	Term symbol	Term value	Level separations
	$X(^1D)$	7, 448. 76	
	$^4F_5$		
	$^4F_4$	18, 730. 75	−787. 94
	$^4F_3$	17, 942. 81	−752. 71
	$^4F_2$	17, 190. 10	
	$^4D_1$	16, 712. 10	140. 60
	$^4D_2$	16, 571. 50	220. 09
	$^4D_3$	16, 351. 41	498
	$^4D_4$	15, 853	
	$^4P_1$?	15, 196. 55	
$s^2p^2.4d$	$^4P_1$	14, 209. 76	103. 28
	$^4P_2$	14, 106. 48	420. 38
	$^4P_3$	13, 686. 10	
	$^2F_4$	14, 396	−1, 172
	$^2F_3$	13, 223. 96	
	$^2P_1$	12, 773. 46	394. 03
	$^2P_2$	12, 379. 43	
	$^2D_2$	12, 392. 99	102. 22
	$^2D_3$	12, 290. 75	

TABLE 7.—*Center of gravity of 5s-terms in several spectra*

Z	Element	Center of gravity of 5s-terms	Remarks
31	Ga	23, 591	[1]
32	Ge	26, 568	[2]
33	As	(28, 500)	
34	Se	29, 462	Extrapolated from series.[3]
35	Br	30, 246	[4]
36	Kr	31, 238	[5]

[1] Paschen-Götze, Seriengesetze der Linienspektren, p. 129.
[2] Rao, Proc. Roy. Soc., **A 124,** p. 465; 1929.
[3] Paschen-Götze, Seriengesetze der Linienspektren, p. 140.
[4] Kiess and deBruin, B. S. Jour. Research (in press).
[5] Meggers, deBruin, and Humphreys, B. S. Jour. Research **3** (No. 89), p. 129; 1929.

4. LIST OF CLASSIFIED As_I LINES

The classified lines of the arc spectrum of arsenic are collected in Table 8. Relative intensities estimated from photographic plates appear in the first column and galvanometer deflections for 10 infrared lines observed radiometrically by Randall are in the second. In the extreme ultra-violet Bloch's intensities occupy column 2. Column 3 contains the wave length measurements, the first two lines being observed only by Randall and the last 17 only by L. and E.

Bloch. The corresponding vacuum wave numbers are given in column 5 and the term combinations in the last. This list contains most of the observed As_I lines and from this point of view may be regarded as a fairly complete description of the As_I spectrum. We plan, however, to extend the observations into the Schumann region, so that certain ambiguities referred to above may be removed, and also to identify higher series terms which will fix the absolute term values.

We wish to thank the International Education Board for facilitating the cooperation of the authors in the investigation described in this paper by the grant of a fellowship to one of us (T. L. deB.).

Acknowledgment is made to Bourdon F. Scribner for assistance with the wave-length calculations.

TABLE 8.—*List of classified As_I lines*

Intensity		λ	ν (vac)	Combination
M	R			
	25	10, 614	9, 418. 9	$5s\ ^2P_1$–$5p\ ^2D_2$
	60	10, 453	9, 564. 0	$5s\ ^2P_2$–$5p\ ^2D_3$
4	100	10, 023. 98	9, 973. 35	$5s\ ^4P_2$–$5p\ ^4P_2$
5	150	9, 923. 03	10, 074. 81	$5s\ ^4P_3$–$5p\ ^4P_3$
5	80	9, 833. 76	10, 166. 27	$5s\ ^4P_1$–$5p\ ^4P_1$
8	140	9, 826. 69	10, 384. 94	$5s\ ^4P_3$–$5p\ ^4D_3$
10	100	9, 597. 94	10, 416. 05	$5s\ ^4P_2$–$5p\ ^4D_1$
50		9, 300. 62	10, 749. 03	$5s\ ^4P_3$–$5p\ ^4S_2$
25		9, 267. 29	10, 787. 68	$5s\ ^4P_2$–$5p\ ^4D_2$
15		9, 134. 81	10, 944. 13	$5s\ ^4P_2$–$5p\ ^2D_2$
20		8, 993. 08	11, 116. 62	$5s\ ^2P_1$–$5p\ ^2P_1$
50	15	8, 935. 58	11, 188. 15	$5s\ ^2P_1$–$5p\ ^2P_2$
100	15	8, 869. 69	11, 271. 26	$5s\ ^4P_2$–$5p\ ^2D_3$
150	10	8, 821. 76	11, 332. 50	$5s\ ^4P_1$–$5p\ ^4D_1$
100		8, 654. 16	11, 551. 96	$5s\ ^4P_3$–$5p\ ^4D_4$
100		8, 564. 71	11, 672. 62	$5s\ ^4P_2$–$5p\ ^4D_3$
50		8, 541. 65	11, 704. 13	$5s\ ^4P_1$–$5p\ ^4D_2$
100		8, 428. 94	11, 860. 63	$5s\ ^4P_1$–$5p\ ^2D_2$
10		8, 355. 00	11, 965. 60	$5s\ ^2P_1$–$5p\ ^2S_1$
50		8, 305. 62	12, 036. 73	$5s\ ^4P_1$–$5p\ ^4S_2$
5		8, 055. 72	12, 410. 13	$5s\ ^2D_2$–X
10		8, 042. 95	12, 429. 83	$5s\ ^2D_3$–X
25		7, 960. 26	12, 558. 95	$5s\ ^4P_2$–$5p\ ^2D_3$
4		7, 863. 45	12, 713. 57	$5s\ ^4P_2$–$5p\ ^2P_2$
8		7, 410. 07	13, 491. 43	$5s\ ^4P_2$–$5p\ ^2S_1$
50		3, 119. 60	32, 046. 13	$5s\ ^4P_1$–$4p\ ^2P_2$
20		3, 075. 32	32, 507. 53	$5s\ ^4P_1$–$4p\ ^2P_1$
40		3, 032. 85	32, 962. 68	$5s\ ^4P_2$–$4p\ ^2P_2$
20		2, 990. 99	33, 424. 02	$5s\ ^4P_2$–$4p\ ^2P_1$
50r		2, 898. 71	34, 488. 06	$5s\ ^2P_1$–$4p\ ^2P_2$

TABLE 8.—*List of classified As I lines*—Continued

Intensity		λ	ν (vac)	Combination
M	B			
100*r*		2, 860. 44	34, 949. 42	$5s\ ^2P_1$–$4p\ ^2P_1$
200*r*		2, 780. 22	35, 957. 76	$5s\ ^2P_2$–$4p\ ^2P_2$
50*r*		2, 745. 00	36, 419. 07	$5s\ ^2P_2$–$4p\ ^2P_1$
50		2, 492. 91	40, 101. 60	$5s\ ^4P_1$–$4p\ ^2D_2$
200*r*		2, 456. 53	40, 695. 45	$5s\ ^4P_2$–$4p\ ^2D_3$
50		2, 437. 23	41, 017. 74	$5s\ ^4P_2$–$4p\ ^2D_2$
150*r*		2, 381. 18	41, 983. 17	$5s\ ^4P_3$–$4p\ ^2D_3$
100*r*		2, 370. 77	42, 167. 50	$5s\ ^2D_3$–$4p\ ^2P_2$
80*r*		2, 369. 67	42, 187. 07	$5s\ ^2D_2$–$4p\ ^2P_2$
10		2, 363. 05	42, 305. 24	$5s\ ^4P_3$–$4p\ ^2D_2$
500*R*		2, 349. 84	42, 543. 05	$5s\ ^2P_1$–$4p\ ^2D_2$
50		2, 344. 03	42, 648. 49	$5s\ ^2D_2$–$4p\ ^2P_1$
500*R*		2, 288. 12	43, 690. 49	$5s\ ^2P_2$–$4p\ ^2D_3$
50		2, 271. 36	44, 012. 85	$5s\ ^2P_2$–$4p\ ^2D_2$
25		2, 266. 70	44, 103. 32	$4p\ ^2P_2$–$4d\ ^4F_3$
20		2, 228. 66	44, 856. 03	$4p\ ^2P_2$–$4d\ ^4F_2$
15		2, 205. 97	45, 317. 35	$4p\ ^2P_1$–$4d\ ^4F_2$
10		2, 205. 16	45, 334. 00	$4p\ ^2P_2$–$4d\ ^4D_1$
5		2, 198. 34	45, 474. 63	$4p\ ^2P_2$–$4d\ ^4D_2$
5		2, 187. 75	45, 694. 72	$4p\ ^2P_2$–$4d\ ^4D_3$
20		2, 182. 94	45, 795. 40	$4p\ ^2P_1$–$4d\ ^4D_1$
15		2, 176. 26	45, 935. 95	$4p\ ^2P_1$–$4d\ ^4D_2$
100*r*		2, 165. 52	46, 163. 74	$4p\ ^2P_2$–$5s\ ^2S_1$
100*r*		2, 144. 10	46, 624. 87	$4p\ ^2P_1$–$5s\ ^2S_1$
30		2, 133. 81	46, 849. 69	$4p\ ^2P_2$–$4d\ ^4P_1$
100		2, 113. 01	47, 310. 81	$4p\ ^2P_1$–$4d\ ^4P_1$
10		2, 089. 79	47, 836. 41	$4p\ ^2P_2$–$4d\ ^4P_1$
25		2, 085. 29	47, 939. 63	$4p\ ^2P_2$–$4d\ ^4P_2$
30		2, 069. 83	48, 297. 66	$4p\ ^2P_1$–$4d\ ^4P_1$
25		2, 067. 16	48, 360. 03	$4p\ ^2P_2$–$4d\ ^4P_3$
40		2, 065. 41	48, 401. 00	$4p\ ^2P_1$–$4d\ ^4P_2$
50		2, 047. 59	48, 822. 17	$4p\ ^2P_2$–$4d\ ^2F_3$
4		2, 028. 87	49, 272. 58	$4p\ ^2P_2$–$4d\ ^2P_1$
50*r*		2, 013. 32	49, 653. 10	$4p\ ^2P_2$–$4d\ ^2D_2$
20		2, 012. 77	49, 666. 66	$4p\ ^2P_2$–$4d\ ^2P_2$
20		2, 010. 04	49, 734. 10	$4p\ ^2P_1$–$4d\ ^2P_1$
100*r*		2, 009. 18	49, 755. 38	$4p\ ^2P_2$–$4d\ ^2D_3$
300*R*		2, 003. 34	49, 900. 41	$4p\ ^2D_2$–$5s\ ^2D_3$
20*r*		2, 002. 54	49, 920. 34	$4p\ ^2D_3$–$5s\ ^2D_2$
100*r*		1, 994. 79	50, 114. 51	$4p\ ^2P_1$–$4d\ ^2D_2$
25		1, 994. 25	50, 128. 08	$4p\ ^2P_1$–$4d\ ^2P_2$
50*r*		1, 990. 49	50, 222. 74	$4p\ ^2D_2$–$5s\ ^2D_3$
200*R*		1, 989. 71	50, 242. 42	$4p\ ^2D_2$–$5s\ ^2D_2$
1000*R*		1, 972. 03	50, 692. 72	$4p\ ^4S_2$–$5s\ ^4P_1$
20*r*		1, 958. 29	51, 048. 28	$4p\ ^2D_3$–$4d\ ^4F_4$
1000*R*		1, 937. 02	51, 608. 91	$4p\ ^4S_2$–$5s\ ^4P_2$
4		1, 928. 58	51, 834. 69	$4p\ ^2D_3$–$4d\ ^4F_3$
5		1, 916. 61	52, 158. 31	$4p\ ^2D_2$–$4d\ ^4F_3$
1000*R*		1, 889. 85	52, 896. 62	$4p\ ^4S_2$–$5s\ ^4P_3$
	1	1, 881. 08	53, 143	$4p\ ^4S_2$–$5s\ ^2P_1$

TABLE 8.—*List of classified As I lines*—Continued

Intensity		λ	ν (vac)	Combination
M	B			
	1	1, 872. 33	53, 391	$4p\ ^2D_2$–$4d\ ^4D_1$
	1	1, 871. 07	53, 427	$4p\ ^2D_3$–$4d\ ^4D_3$
	1	1, 859. 90	53, 748	$4p\ ^2D_2$–$4d\ ^4D_3$
	2	1, 854. 4	53, 926	$4p\ ^2D_3$–$4d\ ^4D_4$
	3	1, 844. 3	54, 221	$4p\ ^2D_2$–$5s\ ^2S_1$
	1	1, 831. 1	54, 612	$4p\ ^4S_2$–$5s\ ^2P_2$
	5	1, 805. 6	55, 383	$4p\ ^2D_3$–$4d\ ^2F_4$
	2	1, 789. 2	55, 891	$4p\ ^2D_2$–$4d\ ^4P_1$
	1	1, 772. 5	56, 417	$4p\ ^2D_2$–$4d\ ^4P_3$
	3	1, 758. 2	56, 876	$4p\ ^2D_2$–$4d\ ^2F_3$
	2	1, 739. 4	57, 491	$4p\ ^2D_3$–$4d\ ^2D_3$
	1	1, 732. 8	57, 710	$4p\ ^2D_2$–$4d\ ^2D_2$
	1	1, 729. 8	57, 810	$4p\ ^2D_2$–$4d\ ^2D_2$
	1	1, 644. 0	60, 814	$4p\ ^4S_2$–$5s\ ^2D_3$
	1	1, 593. 4	62, 759	$4p\ ^4S_2$–$4d\ ^4F_3$
	2	1, 574. 7	63, 504	$4p\ ^4S_2$–$4d\ ^4F_2$

WASHINGTON, June 29, 1929.

METALLOGRAPHIC POLISHING. I. AUTOMATIC METALLOGRAPHIC POLISHING MACHINE

By S. Epstein and John P. Buckley

ABSTRACT

An automatic metallographic polishing machine, designed particularly for studying polishing methods, but which should be useful in any metallographic laboratory, is described. The metal specimen is mounted in a metal ring and held in an arm which moves it back and forth along a radius of the turning polishing disk. At the same time the specimen is rotated. There are three arms to a disk, so that three times as many specimens as there are disks in the machine can be polished at a time. A high quality polish, free from pitting and scratches, is obtained. An outline of the proposed study of polishing methods is given.

CONTENTS

	Page
I. Introduction	783
II. General requirements	784
III. Description of machine	786
IV. Mounting of specimens	789
V. Method of polishing used and results obtained	790
VI. Proposed outline of study of polishing methods	792
VII. Summary	794

I. INTRODUCTION

Polishing metal specimens for microscopic examination is an art not easily learned. The usual college course in metallography seldom gives the student sufficient experience to acquire the necessary skill, and even after long experience metallographers will find themselves spending a great deal of time in rectifying poor polishing results or in trying out various modifications, generally minor ones, in their polishing procedure. Such modifications seem to have consisted mainly in fluctuations about a norm, for the polishing procedure followed by a majority of metallographers to-day is not much different from that in use 10, 20, or 30 years ago. Although there has been continual concern over polishing methods, very little systematic study has been given to the subject since the early days of metallography. The bureau has recently undertaken such a study, the object of which is to make thorough trials of the important variables in the procedure, such as abrasives, the matrix for the abrasives (that is, cloths, metal laps, pitch polishers, etc.), speeds, pressures, etc. It is hoped that a recommended practice for metallographic

polishing can be developed from the results of this study. Later, an inquiry into the theoretical matters involved may, perhaps, be desirable.

It was realized that, in the study of the polishing procedure, it would be necessary to eliminate, as far as possible, all irregularities and errors due to the personal equation such as would inevitably arise with the use of hand polishing. This desired condition would be obtained by means of a properly devised automatic polishing machine. Moreover, it was apparent that the building of a sucessful automatic polishing machine would, aside from its use in this study, be a sufficient end in itself. Hand polishing not only requires skill hard to attain, especially where a high quality polish is desired, but also is exceedingly tedious and time consuming. Every effort was made, in designing the machine, to construct it along such lines as would render it a highly serviceable piece of equipment in any metallographic laboratory with manifest advantages over hand polishing. It should be stated here that several models of automatic polishing machines were available in the market when this work was begun, but for various reasons they were regarded as not being fully suitable and the development of a new model was preferred. Such a machine has been developed, and it has proved very satisfactory after several months' operation under routine laboratory conditions. It was considered advisable to publish at this time a description of this machine without waiting for the study of polishing methods to be completed.

II. GENERAL REQUIREMENTS

In optical glass polishing automatic methods are practically universal and it might seem, therefore, that both the optical methods and machines could be adapted to metallographic work. However, there are radical differences between optical and metallographic polishing. In optical polishing, and this applies also to such operations as gage lapping where mechanical polishing is very successfully used, the material polished is always very hard, no special precautions have to be taken to prevent any flow or disturbance of the polished surface, and the main consideration is the contour or the dimensions of the finished object. In metallographic polishing, on the other hand, most of the specimens are relatively soft, the contour of the surface is of secondary importance as only a rough approximation to optical planeness is required, and the essential thing is the quality of the finished surface which must be undisturbed, with all the constituents left in place and not covered or removed. It may be mentioned in passing that an optically ground and polished lens, for instance, is of considerable and permanent value, whereas ordinarily a polished metallographic specimen is of only momentary value usually being discarded once the microscopic examination is over.

Because of the above differences metallographic polishing has followed a different course from that of optical polishing. In optical polishing machines, the work itself is usually moved over a slowly turning polisher and, in general, the speeds used are much slower than in metallographic polishing, especially during grinding where high speeds, of course, might cause cracking of the glass. The pressures are considerably greater in optical polishing, since there is little concern over disturbing or flowing the surface. Toward the end of the operation, as the work makes optical contact with the polisher, the forces between them become quite large and considerable viscous flow probably occurs. Hard metallic laps and pitch polishers are generally used instead of cloth-covered disks, as in metallographic polishing, in order to get more accurate contours. Such comparatively hard backings for the abrasives would be of advantage in metallographic polishing in decreasing rounding at edges, relief polishing of hard constituents, and pitting about cracks and inclusions, which effects are mainly due to the soft and yielding nature of the polishing cloth. However, the difficulty with pitch and other such polishing disks is that with all metals except hardened steel the specimen becomes impregnated with the abrasive and a matted, instead of a polished, surface is obtained. Unless some way of lubricating the hard polishing disks is devised which will entirely obviate this, the use of cloth-covered disks with their attendant disadvantages will have to be continued.

It may be emphasized here that it seemed essential to put high quality workmanship and material into the construction of the polishing machine. In the average laboratory the importance of having a good polishing machine appears to have been neglected or not sufficiently recognized. This has undoubtedly resulted in a deplorable waste of time in metallographic work as well as in lowering the quality of such work. In reality, the polishing machine is almost as important a piece of apparatus as the microscope itself. Ordinarily, a great deal more of the metallographer's time is spent in polishing, etching and repolishing the specimens than in examining them under the microscope and photographing them.

In designing the automatic polishing machine, the underlying principles employed did not depart in any essential respects from those in every-day use in metallographic hand polishing. The purpose of securing a high quality polish at least equal, or superior if possible, to that obtained by hand methods was kept uppermost. It might be mentioned that Pulsifer[1] has described a more rapid method of preparing microsections, by alternate grinding and etching, in which method the basic idea is that the preparation of a highly polished surface is unnecessary for revealing the structure. Aside from the

[1] H. B. Pulsifer, Structural Metallography, Chemical Publishing Co., Easton, Pa.

fact that his method is not applicable to the study of inclusions and saves time only for the soft metals and not for iron or steel, it may be questioned on broad grounds whether such a rough method should be recommended for general use. The possibility of errors in judgment in microscopic work is very great, even with most painstaking preparation of specimens and after much experience, and it appears unwise, if only from the psychological standpoint, to advocate a method which for the sake of speed might seem to countenance carelessness and which might fail to instill the requisite pride in good looking and accurate work.

III. DESCRIPTION OF MACHINE

The details of the machine are given in Figures 1, 2, 3, 4, and 5. The machine consists essentially of a polishing disk mounted horizontally on a suitably designed table and a driving mechanism, actuated by an alternating current variable speed motor of 300 to 1,200 r. p. m., for rotating the disk at a speed of approximately 250 r. p. m.

The specimen to be polished is mounted in a metal ring, which will accommodate specimens up to 1¼ inches diameter and about 1½ inches high. This specimen holder, containing the specimen, is positively held in an arm, through which it is geared to an eccentric gear attached at the top of a shaft passing vertically through the axis of the polishing disk (fig. 3) and is slowly moved back and forth (about two times a minute) along a radius of the turning disk. At the same time the specimen is slowly rotated so that the direction in which it is polished changes continually. This rotating movement was deemed essential to prevent pitting and the formation of "comet tails" at inclusions. An intermittent gear for halting the oscillation of the arm for a brief interval during which the specimen holder was rotated through approximately 90° was tried out, but this arrangement proved to be superfluous. Three arms are supplied to one polishing disk, which is 9 inches in diameter, so that with one or more units (according to the number of polishing stages used) three times as many specimens as units employed can be polished at a time.

The shaft carrying the polishing disk is mounted in ball bearings to insure smooth working. Ample provision has been made to protect all bearings from abrasives and water. A belt drive, for connecting the driving mechanism to the motor, was chosen as being superior to a frictional drive, especially for this type of machine.

The abrasive may be continually supplied from a flask on a shelf placed above the polishing disk. The water containing the abrasive is agitated by an air stream, and the flow is regulated by a stopcock. A brass rod "wiper" attached to the wall of the pan, within which the polishing disk is placed, and resting upon the rim of the disk has

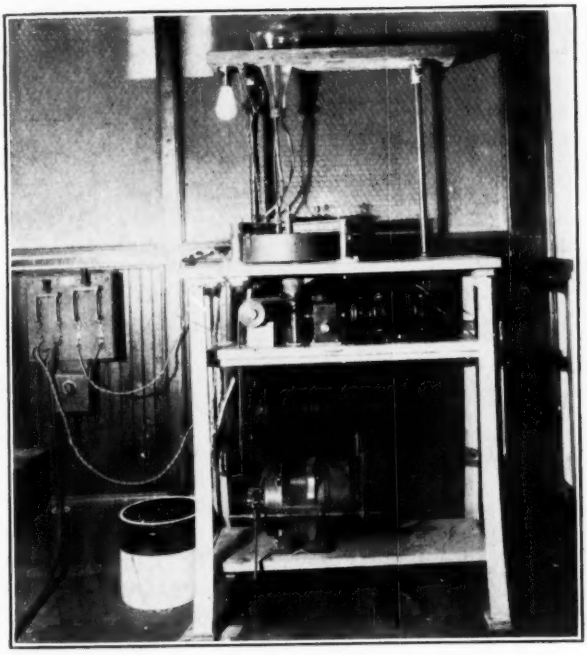

FIGURE 1.—*Side view of first model of automatic polishing machine*

UNIV. OF MICH.

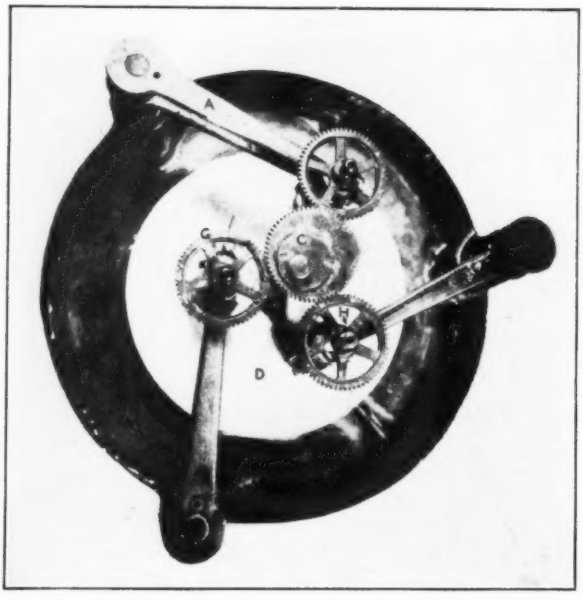

FIGURE 3.—*Plan view of the top of the machine*

A, Oscillating arm which carries the specimen and its holder; G, gear for rotating the specimen as it is moved across the polishing disk; D, C, cam gear by which the oscillation of the arms is brought about. Through the hole, H, a weighted pin may be inserted so as to rest upon the specimen.

been found useful in preventing the clogging of the disk with abrasive by distributing it more evenly over the disk.

A most important part of the machine is the means of holding the specimen flat on the polishing disk and applying the necessary light pressure. This is very conveniently accomplished by a spring arrangement attached to the end of the arm. This is shown in Figure 5. Pressure is applied to the "back side" (that is, on the side opposite to the direction of rotation of the polishing disk) of the specimen holder by means of a yoke to which the spring is attached,

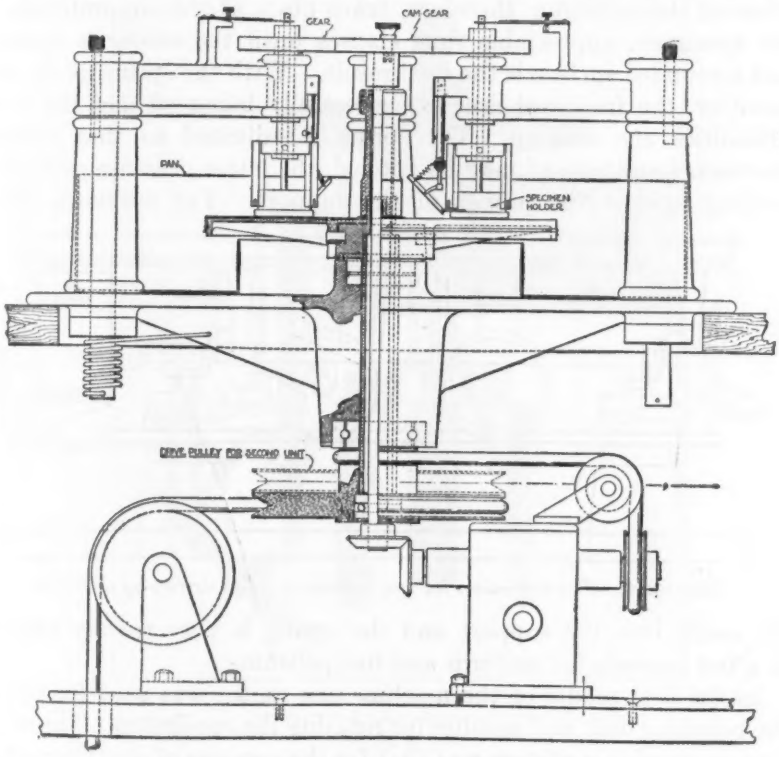

FIGURE 2.—*Assembly drawing of new model*

Some changes in dimensions were made for greater convenience in working. The spring arrangement placed at the side of the specimen holder for balancing it during polishing is shown.

resting upon a flange at the bottom of the holder. Additional pressure may be applied through a sufficiently weighted pin which bears on the center of the mounted specimen. Before the spring arrangement was installed the pressure was applied from overhead only through this pin. The polishing results then obtained were very unsatisfactory because of the rounding of the surface, deep scratching, and slow polishing. The explanation seemed to be as follows: As the turning disk moves past the specimen a good deal of drag is set up between the "front side" and the cloth of the polishing disk. It

is this frictional pressure which causes a specimen to fly out of the hand during hand polishing. In polishing by hand one instinctively compensates for the tendency to dig in at the "front" by a slight pressure on the "back"; this keeps the specimen balanced and eliminates the frictional pull. If something similar is not done in mechanical polishing, the specimen holder will jam tightly against the prongs of the support in which it is held and thereby be pressed hard against the disk so that deep scratches are formed. At the same time the holder no longer rests flatly on the disk but is tilted slightly. Most of the polishing, therefore, takes place at the circumference of the specimen, appreciable time elapses until the center is touched, and a rounded surface is the final result. With the spring at the side, however, the frictional drag is successfully balanced and the above difficulties are avoided. The spring is adjusted so that pressure downward and inward may be applied, the latter pressure preventing cocking against the prongs of the support. The specimen holder

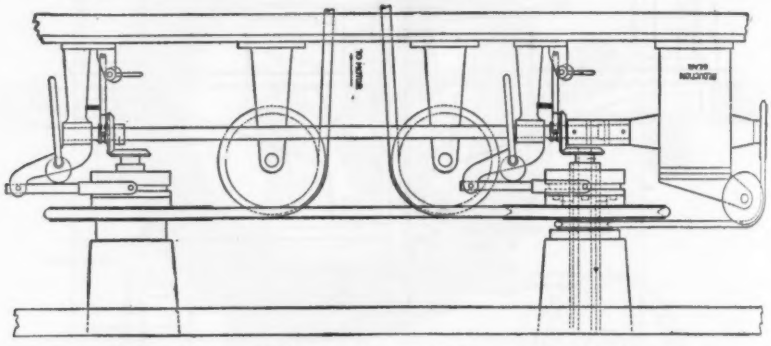

FIGURE 4.—*Transmission for two polishing units driven by one motor*

fits easily into the support and the spring is very readily adjusted in a few seconds for uniform and flat polishing.

In the first model of the machine one motor was used for driving the polishing disk and another for rotating the specimens. The reason for the use of two motors was that for the purpose of studying polishing methods it was desired to have independent control of the speed of turning of the polishing disk and the speed of rotation of the specimen. A revolution counter for the polishing disk was also attached. Figure 1 shows a side view of this machine, before the spring attachment to the specimen holder was adopted. Another machine provided with two polishing disks is now being built along essentially the same lines, but with slight changes in dimensions for greater convenience. One motor will drive the two polishing disks, the same motor also rotating the specimens. Figure 2 shows an assembly drawing of this machine for one polishing disk. Figure 4 shows the transmission for the two polishing disks. Each disk may, of course, be turned on or off independently of the other.

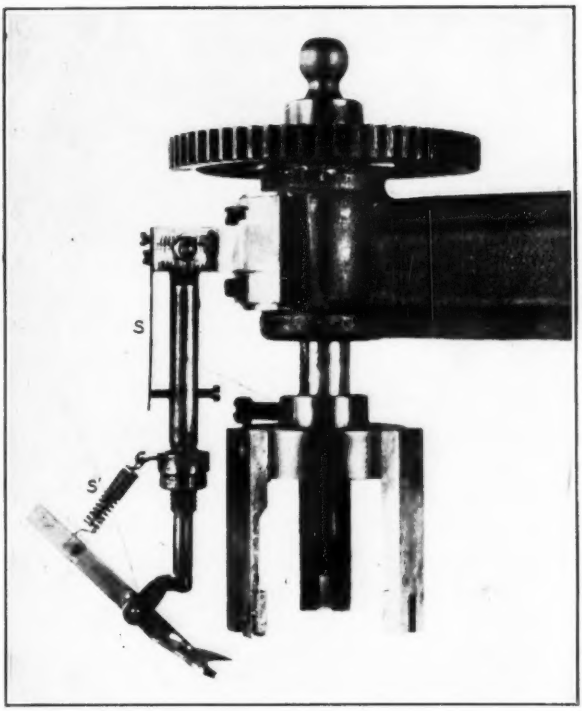

FIGURE 5.—*Specimen holder, somewhat smaller than actual size*

By means of the springs S and S′ pressure is applied to the specimen holder in two directions, perpendicular to each other. The specimen mounted in the ring is held by means of the slots in the "fingers" which form lower part of device.

IV. MOUNTING OF SPECIMENS

In hand polishing, specimens, such as filaments, sheets, or other odd shapes and small sizes, usually are mounted, but in this type of machine all specimens must be mounted. The question, therefore, of a suitable mounting medium becomes a very important one. Of course, materials usually employed for this purpose, such as the white metal alloys and litharge-glycerine cement, may be used, but these have decided disadvantages. They tend to smear and clog the polishing disk and may also scratch the specimen, but, above all, they seriously interfere with the subsequent etching of the specimen, since they are readily attacked by both acid and alkaline etching reagents.

In work recently done at the bureau on dental alloys sulphur was found to be a very convenient mounting medium. It has a sufficiently low melting point (120° C.), quickly hardens after solidifying, is clean, and is inert to acid etching solutions although it is attacked by alkaline sodium picrate and will disintegrate in the boiling solution of this reagent used for etching steel. However, the polished specimen is very readily knocked out of the surrounding sulphur without spoiling the surface and may then be etched without interference. A disadvantage of sulphur is that sometimes during the polishing, it forms tiny pits on the surface of steel which may be mistaken for inclusions; it also tarnishes copper and its alloys. It has been stated that the latter effect may be overcome by adding about 1 per cent of powdered graphite to the sulphur. A very useful precaution is to cut away the sulphur surrounding the specimen so that it does not come in contact with the polishing disk. This may be very readily done soon after the sulphur solidifies when it is comparatively soft. In mounting with sulphur the specimen and ring may first be ground flat and then laid face down on the glass side of an old photographic plate. By previously moistening the plate with glycerine the specimen and ring will stick to the plate and come out level with each other after the sulphur solidifies; this will save subsequent grinding to obtain a level surface. A slight amount of glycerine left in the ring before pouring in the molten sulphur will lift the sulphur from the glass and thus minimize the amount of cutting away required to keep the sulphur out of contact with the polishing disk. In general, sulphur makes a very convenient mounting medium if the above-mentioned precautions are taken.

Condensation products of phenol, such as bakelite, have even better properties than sulphur. Bakelite is very hard, can be molded at about 150° C., and is practically inert in both acid and alkaline reagents. The difficulty is that it must be molded under pressure so that some additional equipment is required. However, this is not prohibitive as a very small press is sufficient, the molding pressure

needed being only 2,000 lbs./in.^{2}. A small electric furnace for obtaining the necessary temperature and a steel die for holding the metal ring may readily be made. The metal ring is fitted into the steel die, the specimen is inserted, and the bakelite in powdered form is poured around it. The die may advantageously be preheated to the required temperature of about 150° C. Pressure is then applied, and the molding is completed in about 10 minutes. Bakelite shrinks somewhat on cooling so that the molded specimen may become loose in the ring. This can be avoided by turning a few shallow grooves in the inner wall of the ring or else by drilling holes through the wall. There is no difficulty in knocking the bakelite out of the ring, which is then used over again. Figure 6 shows the press, steel die, and small furnace used for the molding operation. A good many other substances have been suggested as mounting materials, such as blocking wax, ozokerite, dumold (pyroxylin base), dental cement, plastic wood, balata, and paraffin. None of these seems to offer any special advantages. Some are soluble in alcohol, which is a great disadvantage in etching and cleaning the specimen.

V. METHOD OF POLISHING USED AND RESULTS OBTAINED

The stages in the automatic polishing procedure are exactly the same as those in hand polishing followed at the bureau. The specimens are first ground by hand with emery paper which is mounted on vertical disks directly attached to the armature shaft of a 500 to 1,200 r. p. m. direct-current motor. Mechanical means for the grinding stages appear to be unnecessary, since it is so rapidly done by hand. The papers used are emery paper 1/2 (American), Hubert (French) 1 G, 0, and 00. Recently, the quality of the finer papers available has not been of the best, and fairly deep grinding scratches have to be eliminated during the subsequent wet grinding with emery powder. This is a great disadvantage as it lengthens the time of polishing considerably and reduces the quality of the polish, for most of the pitting occurs during the wet grinding and polishing. Aloxite waterproof paper No. 400 is of excellent quality, although too coarse for the final grinding. It is unfortunate that a finer paper of this type, such as No. 600, is not manufactured.

After the final grinding the specimen is mounted in sulphur, bakelite, or white metal alloy. With the latter two materials, it is difficult to level the specimen with the mounting ring unless both are ground together after mounting. With sulphur, however, according to the procedure described, the specimen may be finally ground beforehand and then mounted perfectly level with the ring, no subsequent grinding on the emery papers being necessary; the precaution should be

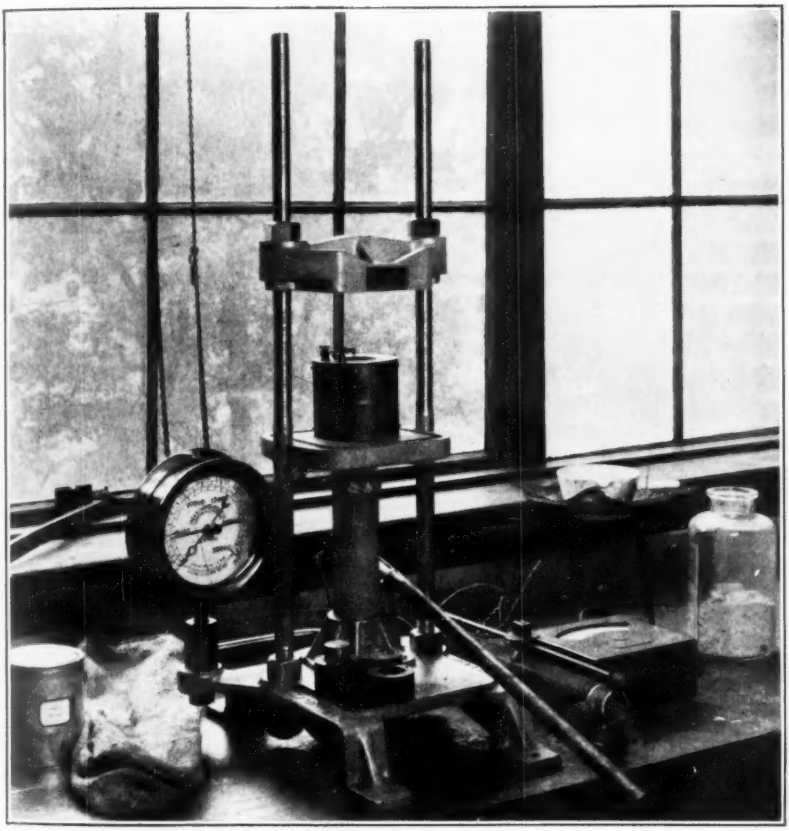

FIGURE 6.—*Press, steel die, and small electric furnace used for mounting specimens in bakelite*

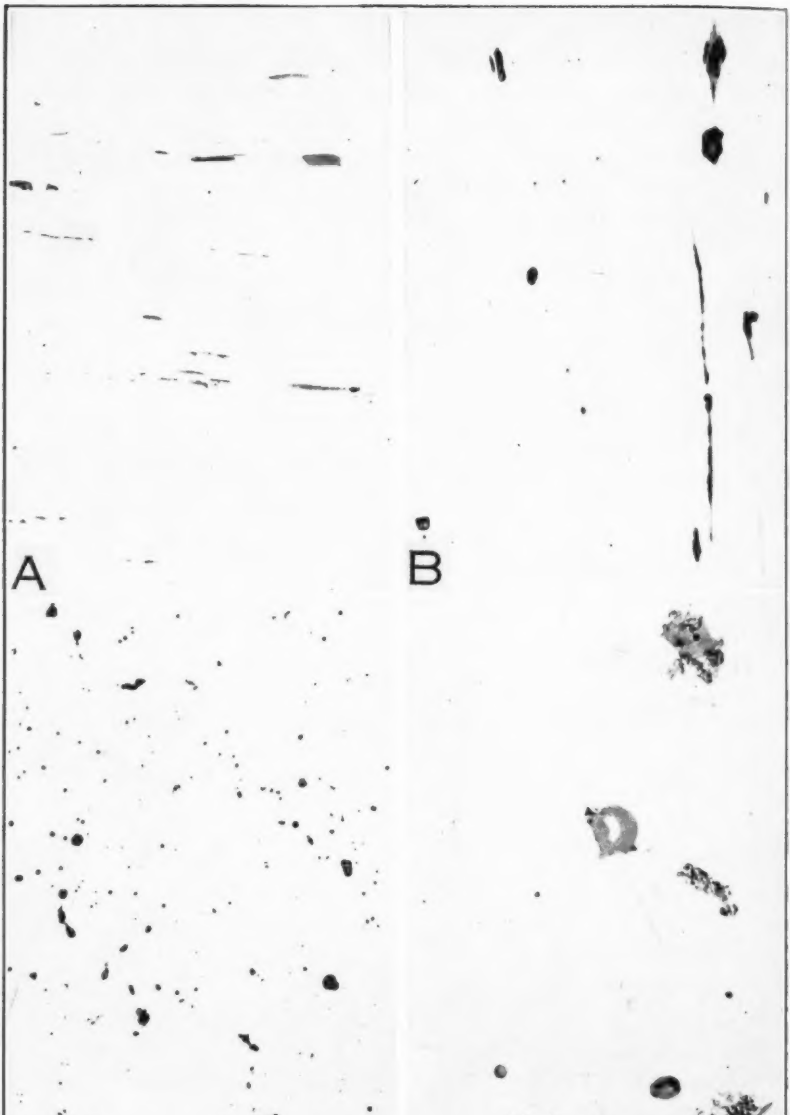

FIGURE 7.—*Representative micrographs of steel specimens polished in the machine, showing various types of inclusions. Not etched*

A, Sulphide inclusions in rail steel, × 100; B, alumina and sulphide inclusions in carburizing steel, × 500; C, large number of inclusions in experimental medium carbon steel ingot deoxidized with boron, × 100; D, same as C, but at × 500, silicate, sulphide and iron-boron-carbide inclusions are shown. These microsections appear to be practically free from "pitting."

taken, however, of testing for planeness by rubbing on the final emery paper, before proceeding further.

The mounted specimen is now polished automatically in the machine, first with 320 alundum suspended in water, then with either 500 or 600 alundum, and finally with Merck's reagent magnesia. For the alundum powders a strong cotton cloth, of about the same weave and weight as coarse linen, is used. Cotton cloth is superior to linen because of the knots and loose fibers usually present in the latter. The essential requisites of the cloth for wet grinding are a fairly coarse weave and absence of nap, otherwise pitting will occur. The emery powder and water should be used very sparingly. For the final polishing of the metal surface with magnesia the disk is covered with velvet. Care should be taken to brush the cloth-covered disks frequently with a stiff brush to clean them of débris and dirt. This applies especially to the magnesia disk, since wet magnesia hardens on exposure to air. The magnesia is not previously mixed with water, but is sprinkled dry on the moistened velvet cloth and then rubbed in with the fingers, water alone being supplied during the polishing. The support for the specimen holder may be easily wiped with a cloth or washed with water through a rubber tube. The spring is adjusted to press very lightly on the flange of the specimen holder, the amount of pressure being judged by lifting the holder. Auxiliary pressure is then applied through the pin which rests on the specimen, the pressure varying from about 3 to 6 ounces or more as desired.

For a high quality polish about 5 minutes polishing is generally given with the coarser alundum, 10 minutes with the finer alundum, and, finally, 15 minutes with the magnesia. Generally the total time of polishing in the machine is about a half hour or somewhat longer, the time consumed depending largely on the quality of polish desired. For merely revealing the structure, the pressure and speed may be increased and the polishing done more rapidly. Nevertheless, for any individual specimen automatic polishing in the machine is not any faster than polishing by hand. The saving in time only becomes considerable when a good many specimens are to be polished. With 3 specimens polishing on 1 disk, 9 specimens can be polished simultaneously on 3 polishing units, and 12 on 4, which would be available if 2 of the double disk machines described were used. Since the polishing is usually done in 3 stages 3 polishing units should be provided to obviate changing of disks and the difficulties attendant upon using more than one abrasive in a unit. Moreover, since the final polishing with magnesia takes the longest time, the best arrangement might be to have 4 disks; the final polishing could then be done on 2 of the disks, and the coarse and fine wet grinding on the other 2. As a matter of fact, the polishing machine has proved

to be a great convenience, whenever a high-grade polish is desired, even when the number of specimens to be polished is small and practically no time is saved by using the machine. In the laboratory it was found that men inexperienced at polishing, quickly learned to get good results with the machine—very much sooner than they could have learned to polish by hand, which, of course, is a most valuable advantage.

A very high quality polish, fully the equal of that possible by hand, is obtained in the machine. The criterion of a good polish is not so much the absence of scratches, although that is, of course, important, as the freedom from pitting, especially in low-carbon steels. In fact, tests of the quality of steel based on the number and type of inclusions present are worse than useless unless a good quality polish free from pitting is to be had. Figure 7 shows a number of micrographs of inclusions in steel specimens polished in the machine; the microsections appear to be quite free from pitting. Figure 8 shows micrographs of a cracked piece of rail steel and of a specimen of gray cast iron. In examining cracks it is very desirable to get as little pitting as possible; gray cast iron is seldom well polished because of the dragging out of graphite flakes. As may be seen in these micrographs, the cracks in the steel do not appear to have been widened or pitted during the polishing, and the graphite flakes in the cast iron are sharply defined and intact. The softer metals may also be polished successfully in the machine. Figure 9 shows the results obtained on tin, wrought duralumin, and cast aluminum.

VI. PROPOSED OUTLINE OF STUDY OF POLISHING METHODS

As was stated in the introduction, the primary purpose in undertaking this work was to study the effect of the variables in the polishing procedure with a view to working out a recommended practice, and also, perhaps, to go into the theoretical aspects of the subject. Aside from developing the automatic machine, little progress has been made, but a brief outline of the proposed work may be given. The most obvious matters for study are the most suitable pressures and speeds for the various stages of polishing of the different metals. Here the use of an automatic machine, by which reproducible results should be obtainable, will be of value.

The subject of the best cloths has always been an uncertain matter. After a cloth has been chosen, a constant source of supply should be made available. Various disks have been suggested as improvements over cloth, such as paraffin, pitch, white metal alloy, cast iron, aluminum, etc. Such disks have been tried and discharged by many investigators, but it is, perhaps, possible that with proper lubrication

FIGURE 8.—*Micrographs of steel and cast-iron specimens polished in automatic machine*

A, Rail steel showing small cracks, × 500, etched with 5 per cent picric acid in alcohol; B, gray cast-iron showing graphite flakes and inclusions, × 500, not etched. Practically no pitting or rounding off of edges was produced at the cracks by the mechanical polishing. The graphite flakes also remained intact.

UNIV OF MICH.

FIGURE 9.—*Micrographs of several specimens of softer metals polished in the machine*

A, Tin (0.25 Cu; 0.02 Pb; 0.02 Fe; Zn. not detected), showing dendritic structure and large twins, × 500, etched with 10 per cent aqueous solution of potassium hydroxide; B, segregated spot in wrought duralumin, × 500, not etched; C, cast aluminum, × 100, not etched; D, same as C, × 500

they may prove successful. The grinding and polishing powders have usually been suspended in water, although soap solutions and oil have been tried. Polishing powders are now marketed in which the abrasive is held in suspension in an oil or gum base liquid. Possibly such compounds may improve results and reduce the amount of abrasive consumed.

The question of grinding papers is an important one, especially the finer grades. If a satisfactory fine paper were available it would be possible to improve considerably the quality of polish and save time, and one of the steps in the wet grinding might even be eliminated. The main requirements of abrasive powders are their cutting quality and uniformity, and these might advantageously be studied with the microscope. A large number of grinding powders are available under different trade names; recently, due to the problem of polishing the hard tungsten carbide alloys, calcium boride and boron carbide have been added to the list. Titanium nitride is one of the hard materials to be tried out.

The number of polishing powders is also very great, among them being the oxides of iron, chromium, tin, zinc, manganese, aluminum, and magnesium. From the standpoint of cleanliness the last two, which are white powders, appear to be the most convenient. Tin oxide is also a white powder. Glazebrook[2] states that putty powder (SnO_2) was at one time extensively used as a polishing powder, but has been discarded for reasons of health. Magnesium oxide appears to be the most uniformly fine powder available. An objection to its use is its tendency to harden on exposure to air. The usual grade of levigated alumina contains traces of alkali, which are objectionable for polishing aluminum and its alloys, because the surface becomes tarnished. Alkali-free alumina of a fineness equal to magnesia would be preferable to the latter because of the tendency of magnesia to harden.

A microtome is available in this laboratory, and the question of the preliminary preparation of a plane surface of soft metals by means of this instrument will receive attention. An interesting proposal for preparing specimens with a cutting tool is that of turning with a diamond. This has been tried by the Bausch & Lomb Co., and may, perhaps, be considered further.

The question of the mechanism of the polishing action has long provided a topic of discussion to physicists, the principal issue being whether the action consists in removing the glass or metal from ridges or in flowing the material and filling in the grooves left by grinding. Apparently, measurements made on glass spheres during polishing[3] show an appreciable decrease in diameter indicating that material is

[2] Glazebrook. Dictionary of Applied Physics, **4**, p. 339.

[3] J. W. French, Some Notes on Glass Polishing, Trans. Opt. Soc. (London), **27**, No. 2, p. 24; November, 1916.

removed. There is also evidence that surface flow occurs, so that probably both removal and flowing take place during polishing. Rosenhain has observed that all of the usual polishing materials are oxides and he, therefore, supposes that the polishing action may be partly chemical.

VI. SUMMARY

In order to obtain reproducible results in a projected study of polishing methods an automatic metallographic polishing machine was developed. A very high quality polish can be obtained, and the machine promises to be of great value for routine metallographic polishing. A description of the machine with photographs and drawings is given, some examples of the results obtained are shown, and the method of polishing used is discussed. A brief outline of the proposed study of polishing methods is also given.

ACKNOWLEDGMENT

Acknowledgment is gratefully made to Dr. H. W. Gillett, chief of the division of metallurgy, who initiated this study and whose encouragement made possible the building of the automatic polishing machine.

WASHINGTON, May 25, 1929.

CORRECTING ENGINE TESTS FOR HUMIDITY

By Donald B. Brooks

ABSTRACT

Data obtained on a 6-cylinder automobile engine indicate a loss of engine power with increasing humidity proportional to the volumetric loss of oxygen content of the atmosphere. It is shown that power and fuel consumption may be corrected by subtracting observed water vapor pressure from atmospheric pressure and using the result in place of barometric pressure in the usual correction formula. The humidity correction may be as large as that due to changes in barometric pressure.

Simple nomograms are presented for obtaining the humidity correction, both near sea level and at higher altitudes. An appendix gives methods of computation of these nomograms.

CONTENTS

	Page
I. Introduction	795
II. Test apparatus and procedure	795
1. Test series No. 1	797
2. Test series No. 2	797
3. Test series No. 3	798
III. Discussion of results	799
IV. Humidity correction chart	801
V. Conclusions	803
VI. Appendix—Method of computation of charts	803

I. INTRODUCTION

Tests made by A. W. Gardiner [1] using a 1-cylinder engine having indicated that atmospheric humidity has a very appreciable effect on some phases of engine performance, a test program was undertaken at the Bureau of Standards further to study this effect, using a multicylinder engine.

II. TEST APPARATUS AND PROCEDURE

Tests were made on a 6-cylinder, 3-port, overhead valve engine of 3⅛-inch bore and 4½-inch stroke, coupled to a Sprague electric dynamometer and spark accelerometer. In the three series of tests three different fuels were used, being selected so as to give little or no detonation at optimum spark advance under any test condition.

Power measurements were made on the dynamometer and friction measurements by use of the spark accelerometer,[2] the latter being

[1] See J. S. A. E., p. 155; February, 1929.

[2] Method described in paper by Brooks on Operating Factors and Engine Acceleration presented at S. A. E. annual meeting, January, 1929. See J. Soc. Automotive Eng., p. 130; August, 1929.

checked against friction measurements on the dynamometer. Humidification was obtained by passing steam and cold air into a mixing chamber and thence to an air heater. Measurements of humidity were made by continuously passing a part of the carburetor air supply over calibrated dry and wet bulb thermometers graduated to 0.2° F. Measurements of humidity are expressed as pressure of water vapor in mm Hg.

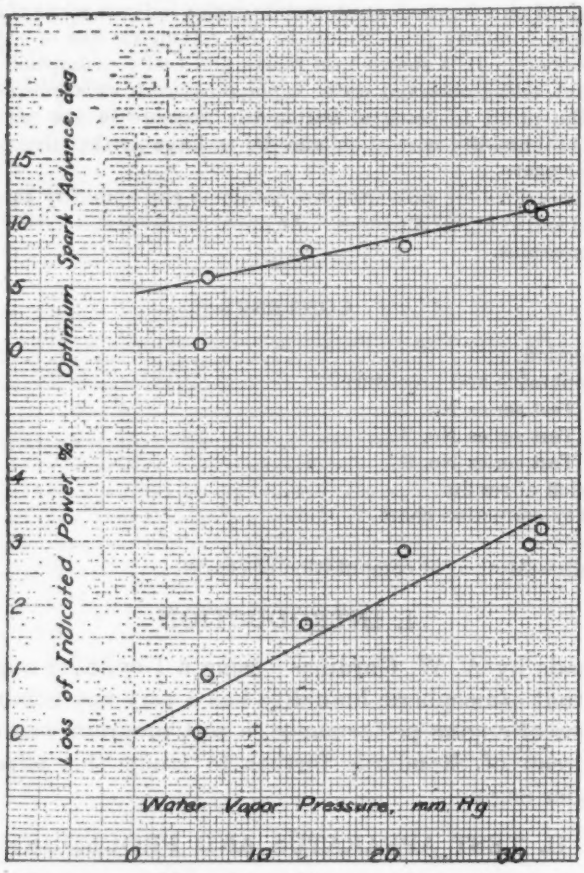

FIGURE 1.—*Effect of humidity on engine performance*

Tests were made at full throttle at an engine speed of 500 r. p. m. Cylinder and manifold jackets were maintained at the same temperature, this being from 60° to 80° C. in the different series of tests but being constant for any one series.

In the first two series of tests readings were taken at from 6 to 8 spark advances for each humidity and air-fuel ratio. From the results, plotted against spark advance, faired values of maximum power and optimum spark advance were obtained. In the third test series optimum advance was found by trial.

1. TEST SERIES NO. 1

The tests of this series were made with a mixture of 2 parts of eastern domestic aviation gasoline to 1 part of motor benzol. A fixed carburetor adjustment was used, giving an air-fuel ratio of about 13.5. Carburetor air temperature was maintained at 30° C.

Optimum power and spark advance were determined at humidities from 5.1 mm Hg to saturation (31.9 mm Hg). Figure 1 shows the results, plotted against water vapor pressure.

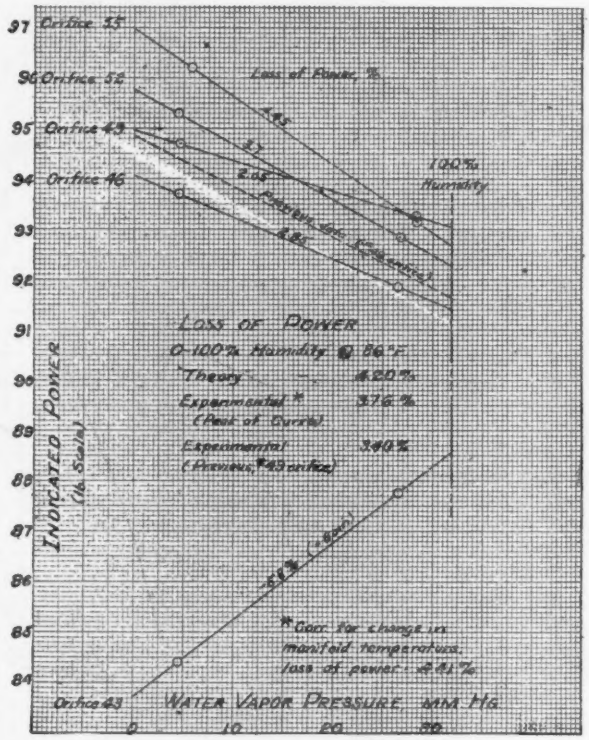

FIGURE 2.—*Effect of humidity on power*

2. TEST SERIES NO. 2

The tests of this series were made with a mixture of equal parts of eastern domestic aviation gasoline and motor benzol. A series of 5 carburetor metering jets were used, giving air-fuel ratios from about 12 to about 16. Carburetor air temperature was maintained at 30° C.

With each air-fuel ratio optimum power and spark advance were determined at two humidities, 4.5 and 27 mm Hg, respectively. Figure 2 shows the results, plotted against water-vapor pressure. It is notable that with orifice 43 an apparent increase of power with

humidity is shown. This is the leanest orifice used; the apparent increase in power seems to be due to automatic enrichment of the mixture at higher humidities.

3. TEST SERIES NO. 3

The tests of this series were made with a commercial brand of aviation gasoline approximately equal in antiknock value to a mixture of equal parts of eastern domestic aviation gasoline and motor benzol.

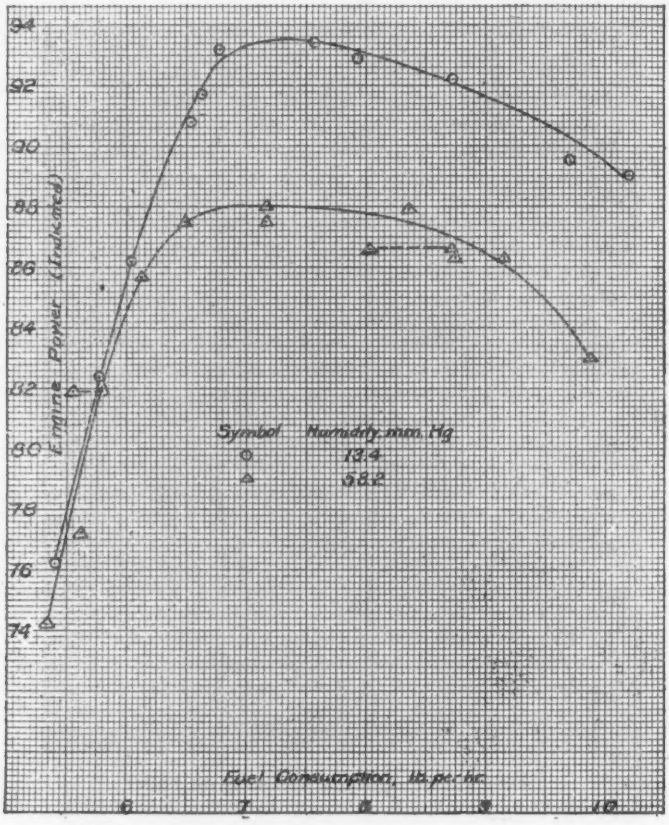

FIGURE 3.—*Effect of humidity on power*

For this series of tests the carburetor was equipped with a needle valve, and tests were made over a range corresponding roughly to air-fuel ratios of 9 to 17. Carburetor air temperature was maintained at 41° C.

At two humidities, corresponding to 13.4 and 58.2 mm Hg, fuel consumption, power, and optimum spark advance readings were taken at 12 points over the range of air-fuel ratios stated above. Results are shown in Figures 3 and 4.

III. DISCUSSION OF RESULTS

The tests shown in Figure 1 indicate a linear relation between loss of power and absolute humidity; the more extensive tests by Gardiner agree with this. Moreover, if the humidity be expressed as percentage of barometric pressure, the loss of power in percentage is roughly equal to the humidity. From this has arisen the "oxygen content" hypothesis, stating that the power is proportional to the oxygen content of unit volume of the atmosphere.

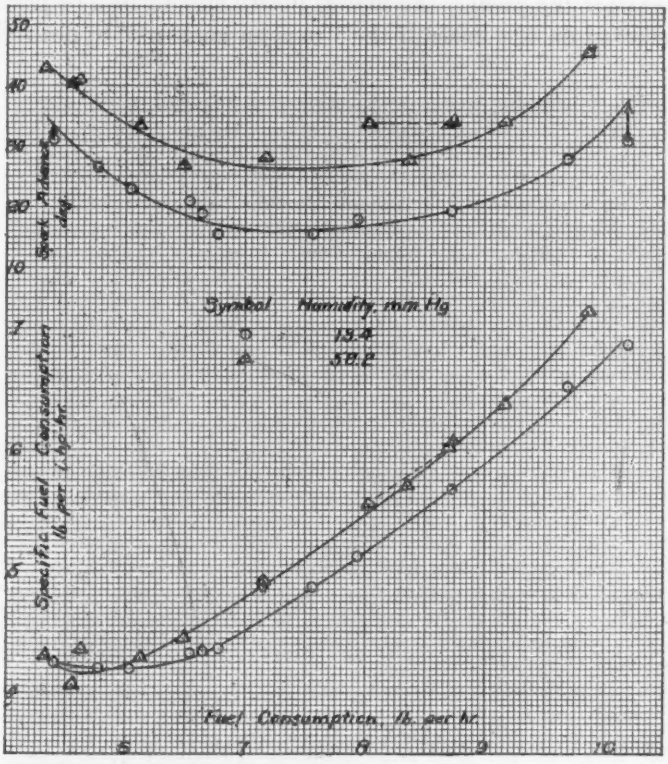

FIGURE 4.—*Effect of humidity on specific fuel consumption*

To test this hypothesis, values of loss of maximum power from the three series of tests were plotted against the loss predicted on the basis of the oxygen content hypothesis. Figure 5 shows the agreement between the measurements and the hypothesis, the weighted mean observed loss of power being 101 per cent of that predicted. However, other factors than decrease in oxygen content may affect the power.

Figure 6 summarizes the results in regard to variation of optimum spark advance with humidity. A decided increase in spark advance is seen to be required with increasing humidity. This rate of increase seems to be a constant, irrespective of the magnitude of advance.

The upper curve is the mean of observations by Gardiner on another engine, operating at different speed and compression ratio and with generally different operating conditions. For all these curves, however, the required advance is 2.1° per cm Hg of water-vapor pressure within the limits of experimental error. On the basis of curves presented in N. A. C. A. Technical Report No. 276, and if the progress of combustion is similar at all humidities, this rate of increase of spark advance should entail a loss of power equal to 13 per cent of that due to the decrease of oxygen; that is, if only oxygen content and spark advance affect the power, the loss of power should be 113 per cent of that predicted on the basis of the "oxygen content" hypothesis.

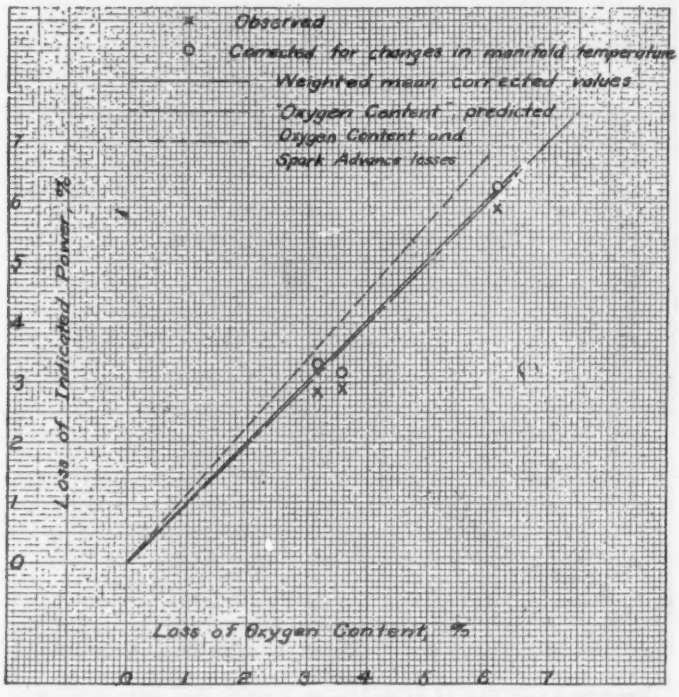

FIGURE 5.—*Summary of tests showing effect of humidity on power*

On the basis of the Bureau of Standards tests, which show but 101 per cent ± 2.6 per cent of the loss predicted from the oxygen content hypothesis, there is a 99.8 per cent probability that other factors tend to compensate for the loss occasioned by reduction of oxygen and increase of optimum spark advance. Such other factors may include lower radiation, dissociation, and less change of specific heats, due to lower maximum temperatures.

In Figure 4 it is seen that the specific fuel consumption curves at the two humidities are displaced horizontally but have practically the

same minimum. Moreover, this horizontal displacement is equal, in per cent, to the percentage difference in oxygen content. This indicates that fuel consumption as well as power should be corrected for change in humidity, since fuel consumption is used in place of air-fuel ratio. This has been done for test series No. 3, in Figure 7. The results obtained at the two humidity values are seen to lie on the same curve within experimental error.

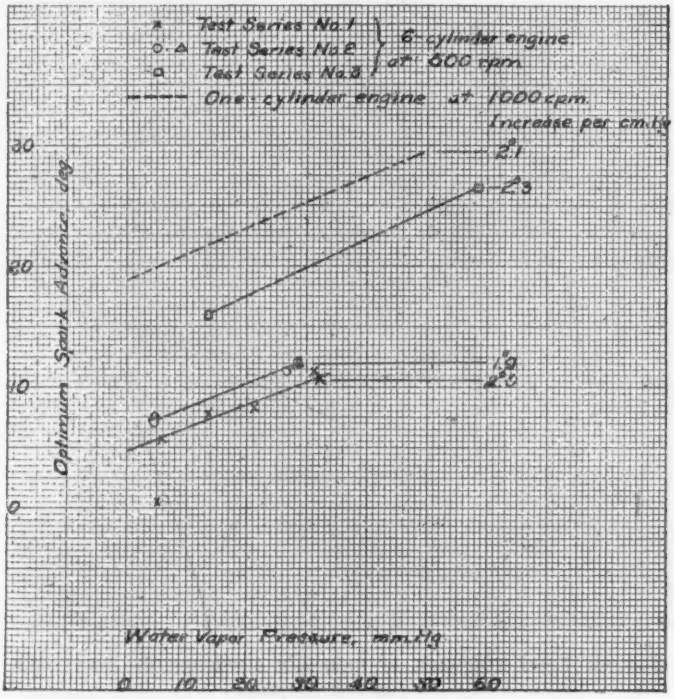

FIGURE 6.—*Effect of humidity on optimum spark advance*

IV. HUMIDITY CORRECTION CHART

Figure 8 is a nomogram for obtaining water-vapor pressure (humidity correction to barometer) from wet and dry bulb and barometer readings. Figure 8 is constructed for units of °C. and mm Hg. Figure 9 is a similar nomogram for units of °F. and inches Hg.

To use these charts, place a straightedge so that it intersects the $t-t'$ scale at the value of the difference between wet and dry bulb readings and intersects the t' scale at the value of the wet-bulb temperature. At its point of intersection of the true (corrected) barometer value read the humidity in the units shown on the scale at the extreme right.

For convenience a barometer-temperature correction nomogram is located at the lower right of the chart. To use this, align a straight-

edge through the center of the small circle at the bottom of the chart and through the barometer temperature on the vertical scale to the right. At its intersection with the observed barometer reading read barometer correction on the same scale used for humidity correction. This correction chart is for barometers with brass scales.

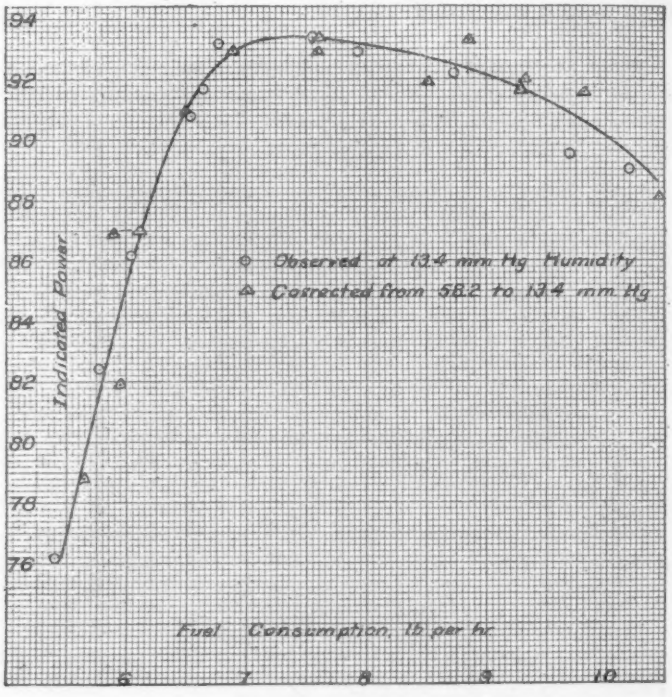

FIGURE 7.—*Verification of humidity correction to power and fuel consumption*

The humidity charts are based on Smithsonian values [3] for water-vapor pressure and on the formula deduced by Professor Ferrel [4]

$$e = e' - 0.000367B(t - t')\left(1 + \frac{t' - 32}{1{,}571}\right)$$

for English units in which

e = pressure of water vapor in inches Hg corresponding to dry and wet bulb temperatures t and t' in °F., respectively.

B = true barometric pressure in Hg.

e' = saturation water-vapor pressure at t',

and on the same formula with appropriate constants for metric units.

[3] Smithsonian Meteorological Tables.

[4] Annual Report of the Chief Signal Officer, Appendix 24, pp. 233–259; 1886.

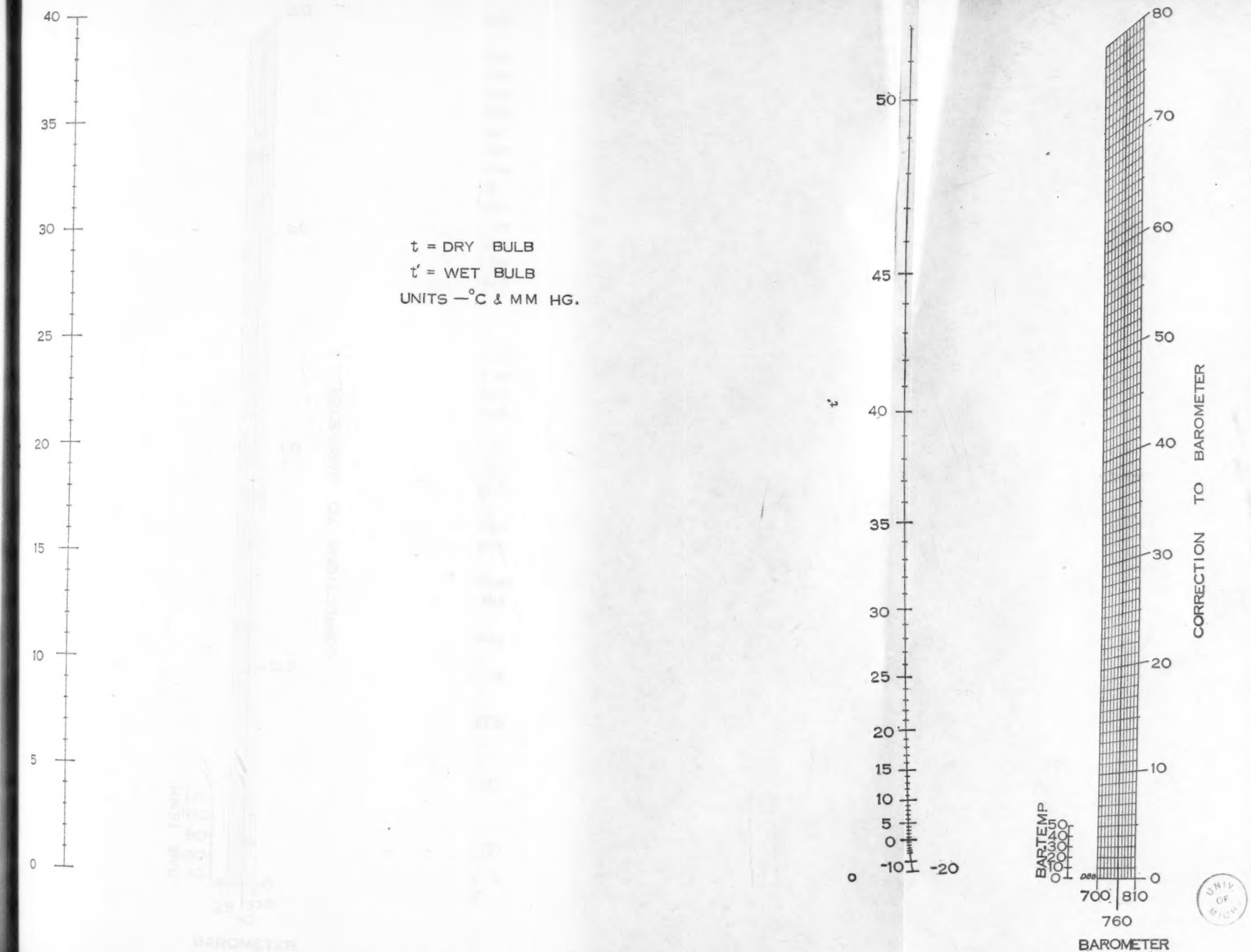

FIGURE 8.—*Nomogram for obtaining corrections for humidity and barometer temperature*

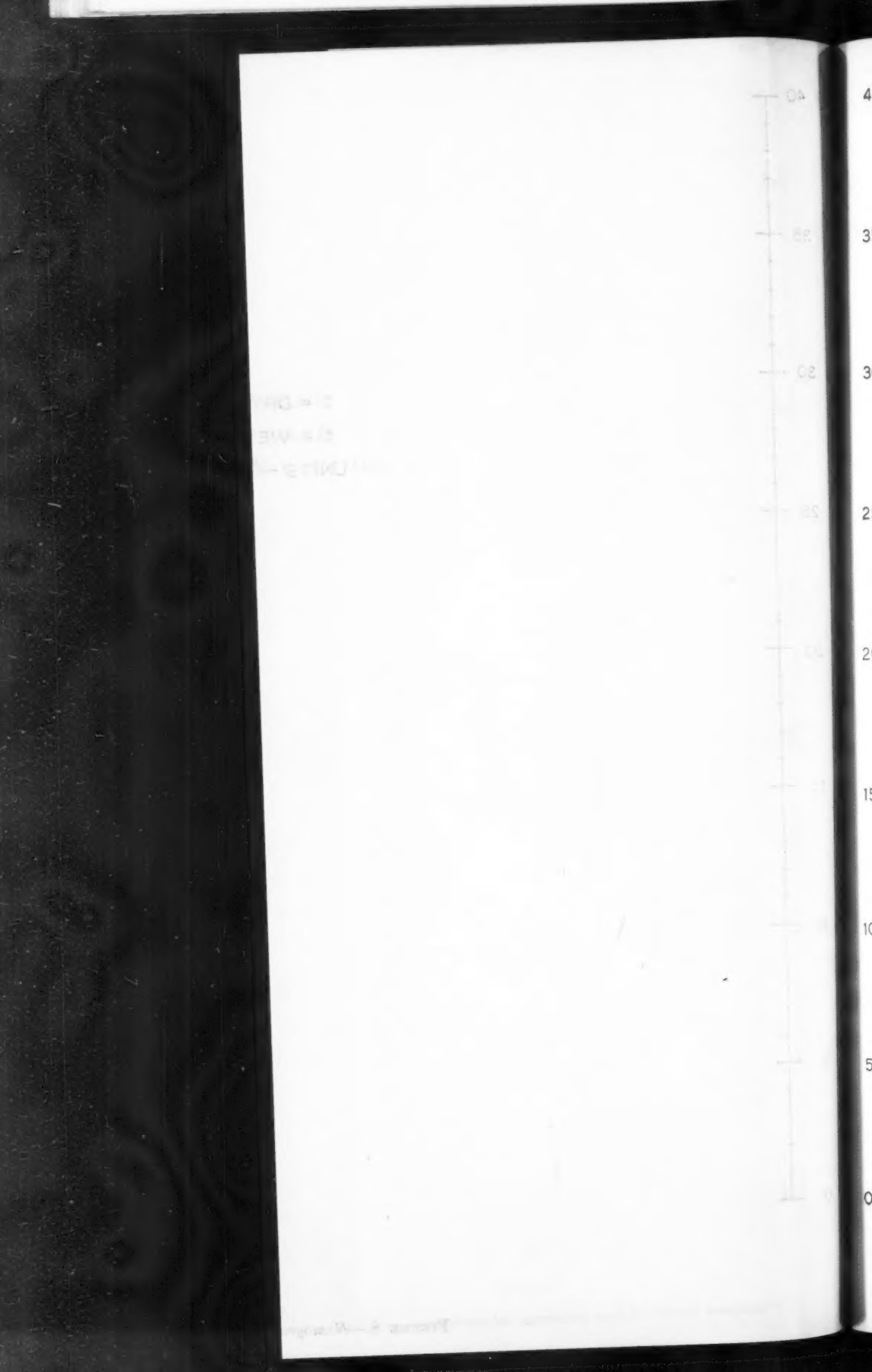

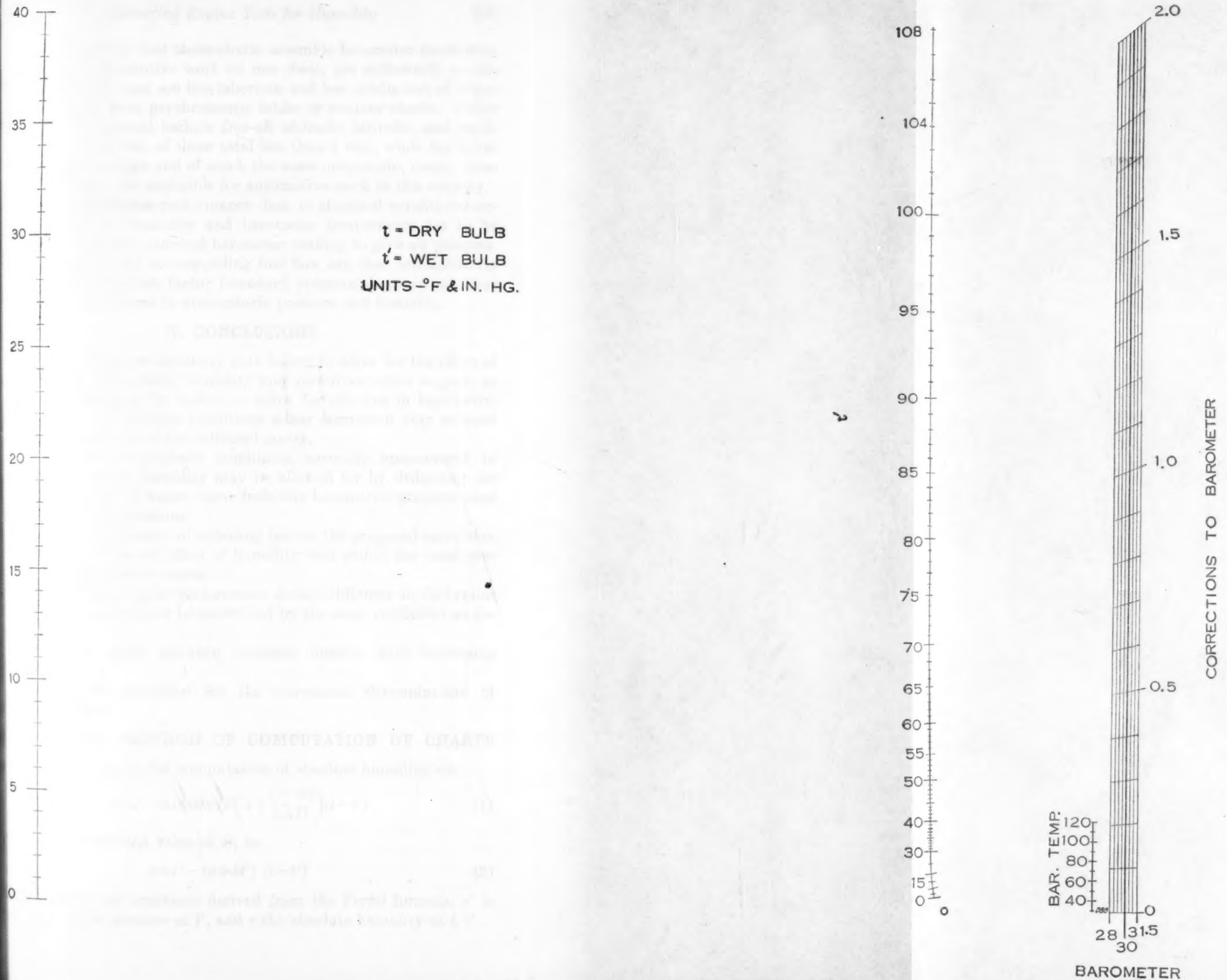

FIGURE 9.—*Nomogram for obtaining corrections for humidity and barometer temperature*

It is to be noted that these charts assemble barometer corrections significant in automotive work on one sheet, are sufficiently precise for their purpose, and are less laborious and less productive of errors of computation than psychrometric tables or contour charts. Other barometer corrections include free-air altitude, latitude, and capillarity. The first two of these total less than 1 mm, while the latter is of the opposite sign and of much the same magnitude; hence, these three corrections are negligible for automotive work in this country.

In correcting engine-performance data to standard conditions corrections for both humidity and barometer temperature are to be subtracted from the observed barometer reading to give air pressure. Observed power and corresponding fuel flow are then multiplied by the pressure correction factor (standard pressure/air pressure), thus allowing for variations in atmospheric pressure and humidity.

V. CONCLUSIONS

1. This work shows definitely that failure to allow for the effect of differences in atmospheric humidity may introduce errors as great as would be occasioned by failure to allow for changes in barometric pressure. Under extreme conditions either correction may amount to nearly 10 per cent of the indicated power.

2. Under all atmospheric conditions normally encountered in automotive testing, humidity may be allowed for by deducting the observed pressure of water vapor from the barometric pressure used in the power computations.

3. Due to cancellation of opposing factors the proposed correction represents the observed effect of humidity well within the usual precision of power measurements.

4. In correcting engine-performance data at different air-fuel ratios the fuel flow values must be multiplied by the same coefficient as the power values.

5. Optimum spark advance increases linearly with increasing humidity.

6. Charts are presented for the convenient determination of humidity values.

VI. APPENDIX—METHOD OF COMPUTATION OF CHARTS

The Ferrel formula for computation of absolute humidity viz,

$$e = e' - 0.000367B\left(1 + \frac{t' - 32}{1{,}571}\right)(t - t') \qquad (1)$$

reduces, for a selected value of B, to

$$e = e' - (a + bt')\ (t - t') \qquad (2)$$

where a and b are constants derived from the Ferrel formula, e' is the water vapor pressure at t', and e the absolute humidity at t, t'.

With this as a basis, the chart is constructed as follows: Suitable scales are selected for $(t-t')$ and for (e), as in Figure 10. Let the length corresponding to one unit of $(t-t')$ be m; the vertical length corresponding to one unit of (e) be n; and the horizontal distance between the $(t-t')$ and (e) scales be p. The t' scale is then located

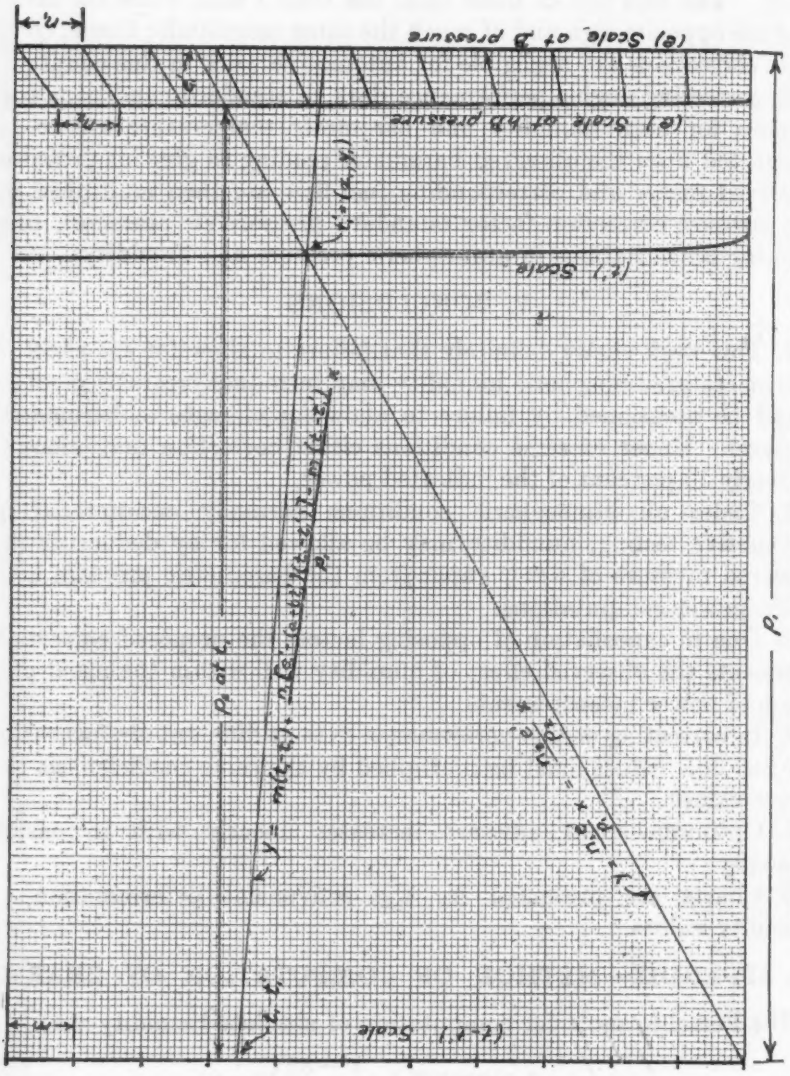

FIGURE 10.—*This figure illustrates the method of determining the t' scale*

by the following considerations: When $(t-t')$ is 0, the vapor pressure is obviously e', the saturation pressure at t'. When $(t-t')$ has any value, the vapor pressure is

$$e_1 = e_1' - (a+bt_1')\ (t_1 - t_1') \tag{2a}$$

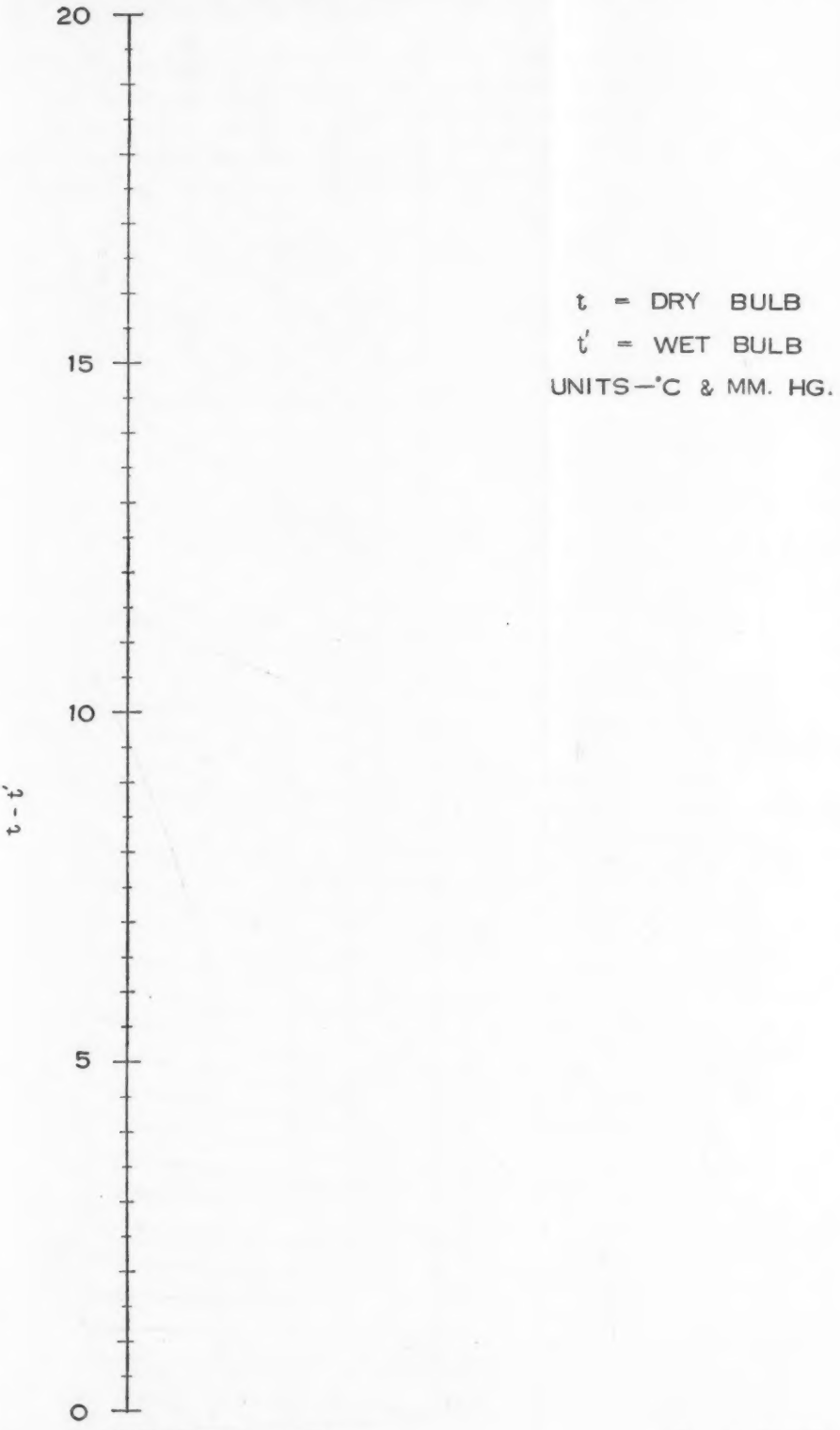

73113°—29. (Face p. 805.)

FIGURE 11.—*Nomogram for de*

FIGURE 10.—*This figure illustrates the method of determining the t' scale*

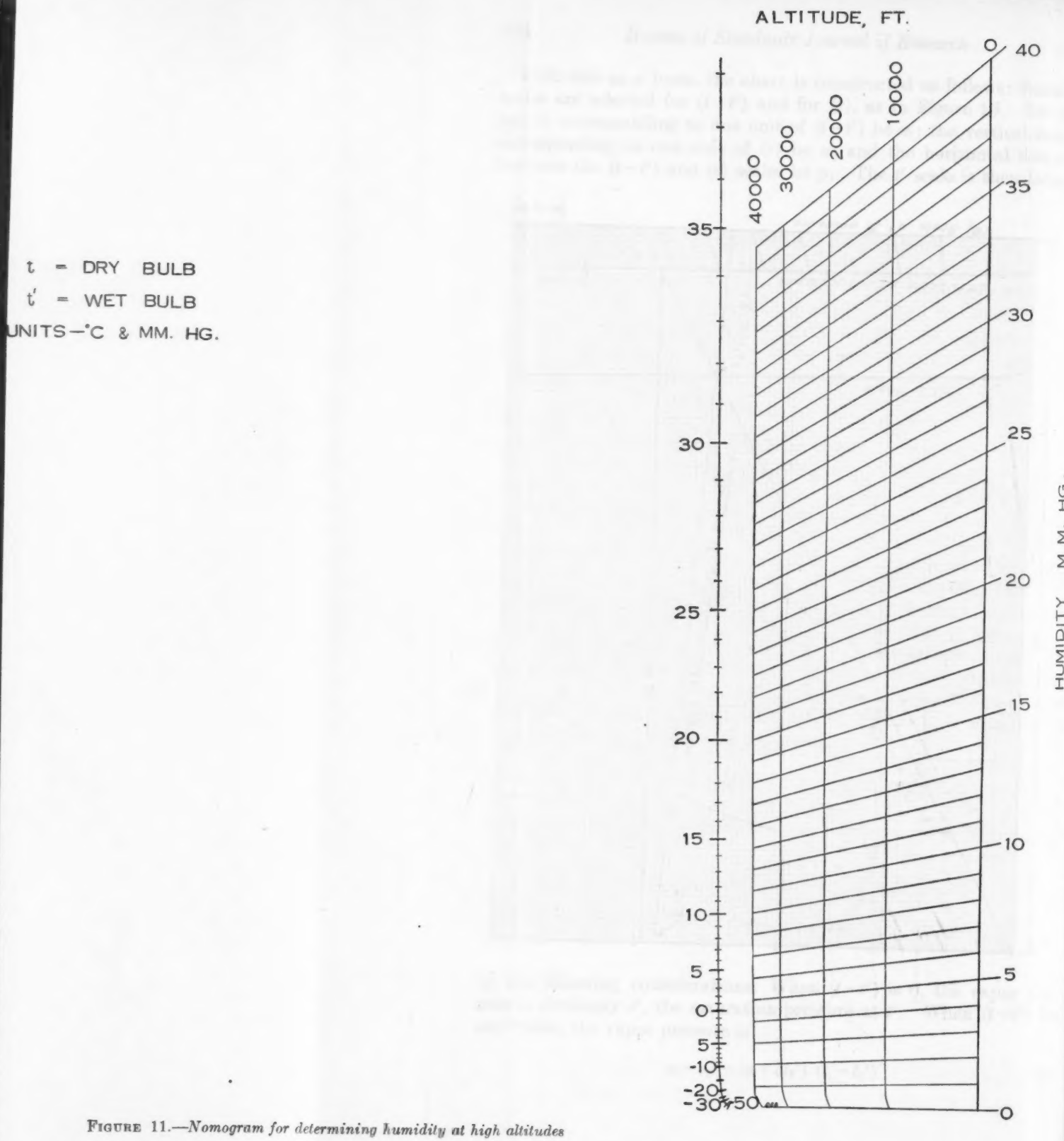

FIGURE 11.—*Nomogram for determining humidity at high altitudes*

If a line be drawn from 0 on the $(t-t')$ scale to e' on the (e) scale, and another line from any other value on the $(t-t')$ scale to the corresponding value on the (e) scale as given by (2a), the intersection of these lines fixes the corresponding value of t_1' on the (t') scale. In terms of the scale divisions, the equations of these lines are

$$y=\frac{ne_1'}{p_1x} \tag{3}$$

and

$$y=m\,(t_1-t_1')+\frac{n\,[e_1'-(a+bt_1')(t_1-t_1')\,]-m(t_1-t_1')}{p_1}x \tag{4}$$

The solution for the point of intersection gives

$$\begin{aligned} x&=\frac{pm}{m+na+nbt'} \\ y&=\frac{mne}{m+na+nbt'} \end{aligned} \tag{5}$$

where subscripts have been dropped, as the solution is general, giving the locus of the t' scale in terms of functions of t'. It is to be noted that the solution for x and y does not contain (t_1-t_1'); hence, the requirements of equation (2) are satisfied by a line. This verifies the choice of the nomogram. From specific values of x and y from (5) the t' scale is constructed.

In subsequently constructing scales for values at different barometric pressures the following considerations apply. Since x and y are now to be regarded as fixed, it is desired to alter p so that equation (1) shall be satisfied at some other barometric pressure. Calling the new barometric pressure hB, and letting

$p_1=$ value of p with B barometric pressure,

$p_2=$ value of p with hB barometric pressure,

then, from (3),

$$\frac{n_1}{p_1}=\frac{n_2}{p_2} \tag{6}$$

where

$n_1=$ value of n with B barometric pressure,

$n_2=$ value of n with hB barometric pressure.

Since x also is to be fixed, from (5)

$$\frac{p_1m}{m+n_1(a+bt')}=\frac{p_2m}{m+n_2h(a+bt')} \tag{7}$$

Hence,

$$mp_1+n_2hap_1+n_2hbt'p_1-mp_2-n_1ap_2-n_1bt'p_2=0$$

$$m\ (p_1-p_2)=n_1ap_2(1-h)+n_1bt'p_2\ (1-h)$$

$$m\ (p_1-p_2)=n_1p_2\ (a+bt')\ (1-h)$$

$$\frac{p_1-p_2}{p_2}=\frac{n_1(a+bt')(1-h)}{m}$$

$$\frac{p_1}{p_2}=\frac{n_1(a+bt')(1-h)+m}{m}$$

$$p_2=\frac{mp_1}{m+n_1(1-h)(a+bt')} \tag{8}$$

which defines p_2, and hence n_2 in terms of known quantities.

Figure 11 is a chart for determining humidity in connection with high altitude tests, constructed on the basis of (8). From this chart it is seen that p_2 is sensibly constant with t'. Figures 8 and 9 are based on the Smithsonian Tables, in which p_2 can be found from the relation

$$p_2=p_1-k\ (1-h) \tag{9}$$

in which k is a constant for values of h near unity.

WASHINGTON, April 20, 1929.

ANALYSIS OF DIAPHRAGM SYSTEM FOR THE X-RAY STANDARD IONIZATION CHAMBER

By Lauriston S. Taylor

ABSTRACT

Several observers have shown that an arbitrary choice of diaphragm system, for defining the X-ray beam in standard measurements, may introduce an uncertain error in the fundamental determination of the International *r* X-ray unit. A geometrical analysis shows that under certain experimental conditions the X-ray tube focus may be considered as a point source of radiation, while under other conditions it must be considered as an extended source. The difference between the two is considerable, and can not be neglected. Curves are given showing the experimental conditions which must be used with a given X-ray tube and a standard ionization chamber. An approximate measurement is made of the radiation coming from parts of the target face other than the focus, and it is shown how this may introduce error in the measurements. The energy distribution over the area of the beam was calculated, and measurements made photographically gave good agreement with the calculations—indicating clearly the region of the beam that must be used to insure uniformity within the prescribed limits of accuracy. An analysis of the several standard ionization chambers used in other laboratories showed with one exception that their error in defining the beam was less than 0.5 per cent.

CONTENTS

	Page
I. Introduction	807
II. Geometrical analysis of the diaphragm system	809
1. Behnken's analysis, assuming a point source of radiation	809
2. Analysis assuming an extended source of radiation	811
(*a*) General treatment	811
(*b*) Effective volume of air ionized	813
III. Experimental study of diaphram system	815
1. Type of diaphram used	815
2. Test of inverse square law	815
3. Uniformity of X-ray flux	817
4. Choice of operating conditions	818
IV. Influence of off-focus radiation	821
V. Errors due to energy distribution about the target	823
VI. Summary	826

I. INTRODUCTION

In measuring the ionization in an *unrestricted volume of atmospheric air*, according to the internationally adopted definition of the *r* unit,[1] the accuracy of the determination depends principally on, first,

[1] The *r* unit is defined as "the quantity of radiation which, when the secondary electrons are fully utilized and the wall effect of the chamber is avoided, produces in 1 cubic centimeter of atmospheric air at 0° C. and 76 cm mercury pressure such a degree of conductivity that 1 electrostatic unit of charge is measured at saturation current."

the electrical measurements of the ionization and control of the X-ray output; secondly, the determination of the air volume of which the ionization is being measured. The first has been treated by Behnken,[2] Glasser,[3] Duane,[4] and more recently by the author;[5] the second is effectively the object of the present paper.

Behnken[6] in a comparison of the r unit between the laboratories of Glasser, Duane, Grebe, Küstner, Holthusen, and the Physikalisch-Technische Reichsanstalt found a 4 per cent discrepancy between the different laboratories. In his publication of the results of this comparison no explanation is offered for the disagreement, it being assumed due to faulty experimental technique rather than to the theory of the experiment. In a study by the author[7] of the various measuring methods, a source of error sufficient to account for Behnken's results was traced to the measurement of the ionization current. However, it is recognized that even an agreement between two laboratories might arise from the errors present compensating each other, so that it is very desirable to study the possible errors in the various other controlling factors.

In practice the ionization is measured in several cubic centimeters and the ionization current divided by the corresponding air volume, the ionization throughout the entire volume being assumed uniform. However, this is not, in general, the case, and so we must determine the effective volume corresponding to uniform ionization. In some recent work Failla[8] has measured air ionization in a standard chamber, using widely varying diaphrams, and found that, according to the particular diaphram system used, there may be a considerable uncertainty in the determination of the air volume.

Behnken, Glasser, and Failla have used circular diaphragms of the order of 1 cm diameter, while Duane uses a rectangular slit system where his chamber diaphragm is 0.5 by 5.0 cm. Most of the observers have placed a screening diaphragm close to the tube to prevent radiation from the target stem entering the standard chamber. Depending upon its relative size and position with respect to the focal spot, this diaphragm may or may not have a direct bearing on the ionization readings.

It therefore seemed advisable to analyze the effects of the diaphragm system carefully so as to obtain some quantitative measure of the error introduced by certain assumptions regarding it. We shall, therefore, treat the problem first considering the focus as a

[2] H. Behnken and R. Jaeger, Zeit. f. Tech. Phys., **7**, p. 564; 1926.
[3] O. Glasser and U. V. Portmann, Am. J. Roent., **19**, p. 47; 1928.
[4] W. Duane and E. Lorenz, Am. J. Roent., **19**, p. 461; 1928.
[5] L. S. Taylor, B. S. Jour. Res., **2**, p. 771; 1929.
[6] H. Behnken, Strahlentherapie, **29**, p. 192; 1928.
[7] See footnote 5.
[8] G. Failla, Am. J. Roent., **21**, p. 47; 1929.

point source (Sec. II, 1); then as an extended source (Sec. II, 2); and finally show the experimental justification (or failure) for the assumption made (Sec. III, 2).

II. GEOMETRICAL ANALYSIS OF THE DIAPHRAGM SYSTEM

1. BEHNKEN'S ANALYSIS, ASSUMING A POINT SOURCE OF RADIATION

In this it is assumed that the focus is a point source of radiation, and that the X-ray flux density is uniform over the cross-sectional area of the beam in the ionization chamber. When the diaphragms are

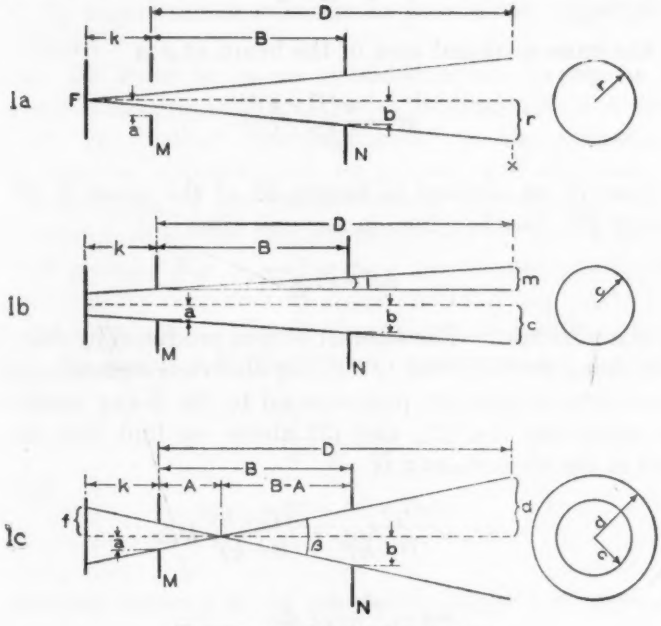

FIGURE 1.—*Diaphragm system*

very small compared with their separation, these two assumptions may be considered valid; but, in general, they are contradictory, since the radiation from a point source gives a flux density in the direction of the beam which is proportional to the cosine of the angle that the given ray makes with this axis.

In presenting Behnken's analysis,[9] we shall use for ease in the later development a nomenclature differing slightly from his. Referring to Figure 1(*a*), *F* is the focus of the X-ray tube, *M* the first diaphragm, radius *a;* *N* the ionization chamber diaphragm, radius *b;* and *x* a plane in the ionization chamber normal to the axis of the beam.

[9] H. Behnken, Strahlentherapie, **26**, p. 79; 1927.

The focus is assumed to be a point, the X-ray intensity of which is represented by a flux density of I_o at unit distance. Then on the axis of the beam at x, the intensity, or flux per unit area, is given by

$$I_x = \frac{I_o}{(D+k)^2} \tag{1}$$

provided, of course, that the radiation be sufficiently penetrating to permit loss by absorption in the length $(D+k)$ to be neglected. Letting r equal the radius of the cross section of the beam at x, we see that

$$\frac{r}{b} = \frac{D+k}{B+k}$$

so that the cross-sectional area of the beam at x is

$$\pi r^2 = \frac{\pi(D+k)^2 b^2}{(B+k)^2} \tag{2}$$

The volume of an element of length dx of the beam is $dV = \pi r^2 dx$. The energy dE absorbed therein per unit time is

$$dE = \kappa I_x dV \tag{3}$$

where κ is a constant. The number of ions produced by this absorbed radiation being proportional to dE, the electrical measurement of the ionization gives a quantity proportional to the X-ray intensity I_x.

From equations (1), (2), and (3) above we find that the energy absorbed in the element at x is

$$dE_1 = \frac{\kappa I_o}{(D+k)^2} \cdot \frac{\pi(D+k)^2}{(B+k)^2} b^2 dx \tag{4a}$$

$$= \kappa \frac{\pi b^2}{(B+k)^2} I_o dx \tag{4b}$$

Equation (4b) expresses, however, the energy absorbed in a volume of cross-sectional area πb^2 and thickness dx, located at a distance $(B+k)$ from the point source (that is, at the diaphragm N). Therefore, for any length L_o of the chamber. the total energy E_1 absorbed in the chamber is given by

$$E_1 = \frac{\kappa \pi b^2}{(B+k)^2} I_o L_o \tag{4c}$$

As a consequence we are justified in considering the effective air volume as having a radius b, a length equal to the effective length of the measuring electrode, and located at a distance $(B+k)$ from the

focus. The question as to what part of the ionized air volume the distance must be measured, in applying the inverse square law, is thus answered. In a previous paper the author has given the necessary electrical conditions to determine accurately this effective length L_0 of the air column from which the ionization is being measured.

2. ANALYSIS ASSUMING AN EXTENDED SOURCE OF RADIATION

(a) GENERAL TREATMENT

Mayneord [10] and others have considered the focus as an extended source, but exaggerated as shown below the importance of the error introduced by assuming a point source. To estimate this error another assumption will be made which, while not quite correct, is indicated by experimental evidence to be a closer approach to the true conditions.

Consider the focus to be an extended source having an area at least as great as the projected area of the diaphragm N upon the target. (Fig. 1(c).) Let further the "brightness" (in the optical sense) of the focal spot be uniform both as to area and direction viewed. Then over the plane x the distribution of flux density varies in a manner determined by the diaphragm system. There will be a *central area* of radius c (fig. 1(b)) having a nearly uniform distribution, and a surrounding *ring area* of outer radius d (fig. 1(c)) having a nonuniform distribution. Their dimensions are readily obtained.

To find the radius c of the central area, consider the system of Figure 1(b)

$$\frac{b-a}{c-a}=\frac{B}{D}$$

from which

$$c=\frac{Db-Da+Ba}{B} \tag{5}$$

For the outer radius d of the penumbra, Figure 1(c) gives,

$$\frac{a}{b}=\frac{A}{B-A} \text{ or } A=\frac{Ba}{a+b}$$

also

$$\frac{B-A}{b}=\frac{D-A}{d}$$

whence

$$d=\frac{D-A}{B-A}b$$

substituting the value of A above

$$d=\frac{Da+Db-Ba}{B} \tag{6}$$

[10] W. V. Mayneord, Brit. J. Rad., N. S., **1**, p. 125; 1928.

It is seen that the values of c and d are independent of the distance k from the focus to the first diaphragm M, and as experimentally demonstrated in Section III, 2 we are thus justified in considering the first diaphragm M, as the source of radiation, whose brightness is also, like that of the target, uniform with both direction and area for the small angles under consideration.

If now, the *aperture* of the system be defined as the solid angle β (fig. 1(*c*)) between the most divergent rays passing through the two diaphragms, we see that the first diaphragm may be considered as the source of radiation only if the actual area of the focal spot fills the aperture β of the system. This limiting condition is seen from Figure 1(*c*) where f is the radius of the focal spot. Its magnitude is taken from

$$\frac{f}{a}=\frac{A+k}{A}$$

from which

$$f=\frac{ka+kb+Ba}{B} \tag{7}$$

by substituting the value for A as derived in equation (6).

To determine the flux density at any point on the plane x due to the total emission from the focus, we may use the cosine law of emission and illumination as expressed by

$$dI_x=\frac{I_0 \cos^2\alpha \, da \, dc}{D_{ac}} \tag{8a}$$

where I_0 is the flux density at the target in the direction along the axis of the beam and likewise also the corresponding flux density through the area at M; dI_x is the flux density through an element of area dc in the plane x, and in a direction normal thereto; the angle which the line joining da and dc makes with the normal to these areas and D_{ac} the distance between the elements. The total flux I_x at any point on the plane is obtained by integrating the flux received from the various elements of the surface πa^2 of the diaphragm M. This has been evaluated by Foote [11] for the illumination from a radiating disk.

If β_0 is the angle between the axis and the most divergent ray, then referring to Figure 1 (*c*), for $\cos^2\beta_0=0.9950$, $\cos\beta_0$ can be assumed equal to unity without introducing an error greater than 0.5 per cent in the flux density at any point. This condition is true for the experimental arrangement of most observers. With a system such as used by Duane, however, it is not negligible.[12]

[11] P. D. Foote, B. S. Bulletin, **12** (No. 263), p. 583; 1916.

[12] It must be pointed out that the cosine law can not be applied rigorously to X-radiation. However, by considering the energy distribution about an X-ray tube target, we see that over small ranges the error introduced by assuming this law is very small. If we consider the change in flux density over a plane, from a point or extended source, as simply due to the change in distance from the source, we arrive at an equation identical with equation (8a).

In the case where $\cos^2 \beta_o = 0.9950$, we may assume the flux density I_x uniform over the central area (fig. 1 (*b*)) and given by

$$I_x = \frac{I_o}{D^2} \tag{8b}$$

where, since D is the distance from the plane x to the first diaphragm M, the effect at x is as if the source were located at the diaphragm M.

The energy dE_2 absorbed in the central volume element dv of cross sectional radius c and thickness dx is then

$$\begin{aligned} dE_2 &= \kappa I_x \, dv \\ &= \kappa \frac{I_o}{D^2} \, \pi \, c^2 \, dx \\ &= \frac{\kappa \pi \, (Db - Da + Ba)^2}{B^2} \cdot \frac{I_o}{D^2} \, dx \end{aligned} \tag{9a}$$

Like dE_1 in equation (4a) dE_2 is proportional to the ionization current measured. In the special case where the two diaphragms are equal $a = b$ and thus

$$dE'_2 = \frac{\kappa \, \pi b^2}{D^2} I_o \, dx \tag{9b}$$

It will be noticed that dE'_2 in equation (9b) has the same form as dE_1 in equation (4b), the only difference lying in the replacement of $(D+k)$ by D. It remains to determine the ionization in the penumbra, which may be neglected when using very small diaphragms very far apart, but not in general.

The ionization produced in a volume element of the surrounding ring area or penumbra of outer radius d can not be easily calculated, owing to the fact that from any given point on the ring only a fraction of the first diaphragm is visible. Thus, at the inner radius of the ring the X-ray flux density is equal to that of the inner area while at the outer edge it is zero.

(B) EFFECTIVE VOLUME OF AIR IONIZED

Having found the effect in the central area as above, one might proceed by using Foote's derivation to evaluate that in the penumbra, but a simpler and more direct method is suggested by the derivation above for the effect of a point source.

We proceed, therefore, to determine the total energy absorption within the chamber, regardless of its distribution. Since it is permissible to neglect the loss in flux arising from absorption along the path, it is obvious that the ionization in a length dx in any cross section of the beam at any plane x within the ionization chamber is proportional to the total flux through that cross section. This is given, however, by the total flux entering the diaphragm N. The

combined result along any length L of the beam in the ionization chamber is equal then to that of a beam having a cross section equal to that of the entrant diaphragm N and a total flux density equal to that at N. This gives for each element of length

$$dE_3 = \frac{\kappa\pi\ b^2\ I_o}{B^2}\ dx \tag{10}$$[13]

Summing up for the whole effective length L_o of the measuring electrode, we have

$$E_3 = \frac{\kappa\pi\ b^2\ I_o}{B^2}\ L_o \tag{11}$$

Equation (11) has the same form as that of Behnken, equation (4c), the difference being in the location of the effective source of the X-radiation at the diaphragm instead of the focus.

We have thus established that for either a point source (equation (4b)), or an extended source within fixed limits (equation (10)) the product of the area of the ionization chamber diaphragm by L determines the *effective air volume*; with the condition that in the first case the inverse square law is used with the source at the focus, while for the second it is used with the source considered at the first diaphragm M. The experimental justification for this is given in Section III.

Equation (11) should express actual conditions within experimental limits so long as $\cos^2 \beta_o$ differs from unity by less than the permissible experimental error. Having fixed the maximum permissible variation in flux density we may determine the range of magnitudes over which the equations above are valid. This, of course, depends upon the aperture of the system so that for any given system the region over which an accurate determination of the r unit is possible may be determined.

As indicated in Figure 1(*c*), the focal spot must fill the aperture if the assumptions made are valid; that is, from equation (7) we must have

$$f > \frac{ka + kb + Ba}{B} \tag{12a}$$

If in a particular case

$$f < \frac{ka + kb + Ba}{B} \tag{12b}$$

for a part of the range of B, then the inverse square law should be applied using the distance from diaphragm N to the focus instead of to M; the diaphragm M serving simply to reduce the radiation coming from points other than the focus. If we have a sufficiently small focal spot (one which never fills the aperture) and a diaphragm

[13] Equation (10) may also be obtained from equation (9a) by the process of decreasing D until it is equal to B, at which point the penumbra disappears with consequent simplification of the problem.

system such that $\cos^2 \beta_0 \geqq 0.995$, we can determine the volume of ionized air as accurately as the experimental precision warrants by assuming a point focus. These conditions have not been realized by all observers.

III. EXPERIMENTAL STUDY OF DIAPHRAGM SYSTEM

1. TYPE OF DIAPHRAGMS USED

First, a study was made to determine if the form of the edge of the circular diaphragms used affected the measured magnitudes. One-quarter inch lead diaphragms having the same diameter (10 mm) were prepared, all having different edges. The first group were tapered ranging from 0° to 15°. The next group were beveled, leaving a half thickness of lead as an edge. In no case was a measurable difference produced in the ionization current. The diaphragms subsequently used were all of this beveled type.

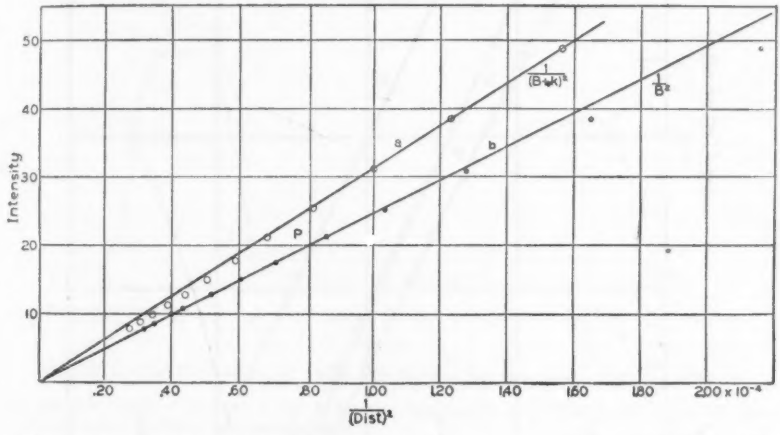

FIGURE 2.—*Intensity of measured ionization as a function of* $1/(\text{distance})^2$

2. TEST OF INVERSE SQUARE LAW

According to Section II, 2, so long as the aperture of the diaphragm system is filled (equation (12a)) by the extended focal area the distance B between diaphragms M and N should be used and the inverse square law applied thereto. When it is not filled, the distance $(B+k)$ from the focus should be used.

To test this the ionization chamber was mounted on a track of such length that the distance between focus and limiting diaphragm N could be varied from 40 to 200 cm; the radius of the diaphragm M could be varied from 2 to 6 mm and that of N from 2 to 10 mm. A null reading electrostatic system was used for measuring the ionization currents and a constant voltage generator for the X-ray tube.[14]

[14] See footnote 5, p. 808.

To align the system accurately, the ionization chamber track was leveled and approximately adjusted by sighting through the diaphragms at the target. A fine wire was then strung along the axis of the system and the track further adjusted until the wire remained in the center of the front and back chamber diaphragms for all positions of the chamber along the track. This was accomplished even more accurately by inserting in the diaphragms disks having very small holes in the center.

Curve b in Figure 2 gives (for $a=b=0.5$ cm, $k=12$ cm, and $f=$ about 0.62 cm) the observed X-ray intensity or ionization current i,

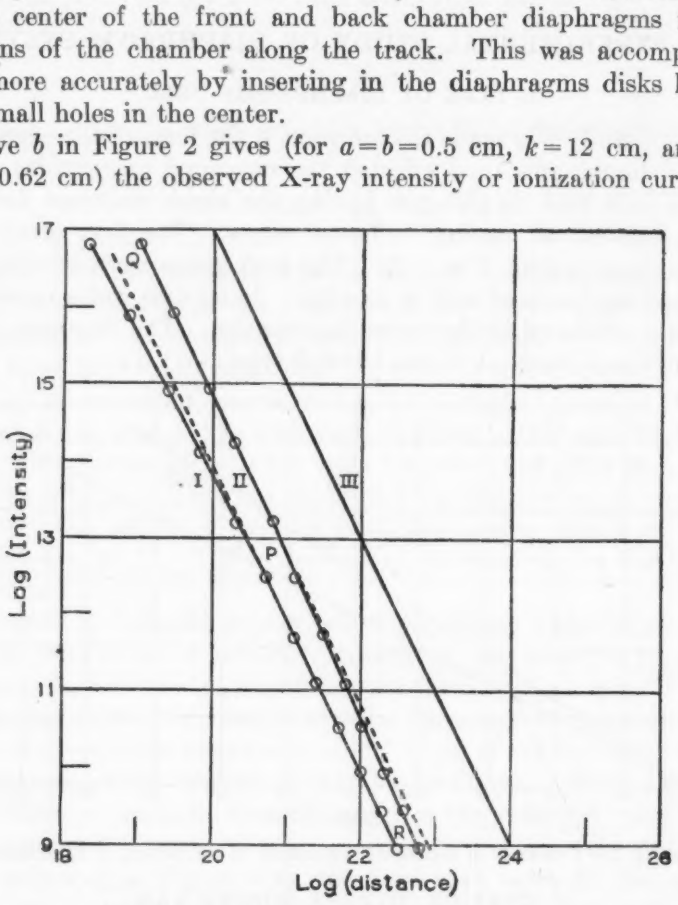

FIGURE 3.—*Validity of inverse square law*

plotted against the inverse square of the distance B between the tube focus and the ionization chamber diaphragm N. As should be expected, up to a certain value of $1/B^2$ corresponding to a distance $B=$ 105 cm, the intensity is found to be strictly proportional to $1/B^2$. According to equation (7), a break in this proportionality should occur when

$$\frac{ka+kb+Ba}{B}=0.62$$

Thus in this case the calculated value of f is 0.62 as compared with the observed value 0.61 obtained when the break occurred at $B=105$ cm.

Likewise if i is plotted against $1/(B+k)^2$ a break occurs at the point corresponding to $B=110$ cm (curve a) except that in this case the portion of the curve corresponding to distances near the tube obeys the inverse square law.

The inverse square law may be expressed as

$$\log i = \log c - 2 \log H \tag{13}$$

where c is a constant and H is the distance, either B or $(B+k)$ as the case may be. By plotting (fig. 3) the data, the log of the intensity (proportional to log i) against that of the distances B or $(B+k)$, as the case may be, the applicability of equation (13) is tested. For Curve *I*, H is taken as the distance B between diaphragms M and N; while in Curve *II*, H is taken as the distance $(B+k)$ between N and the focus. Curve *III* represents the slope (minus 2) which Curves *I* and *II* should have if the law expressed in equation (13)

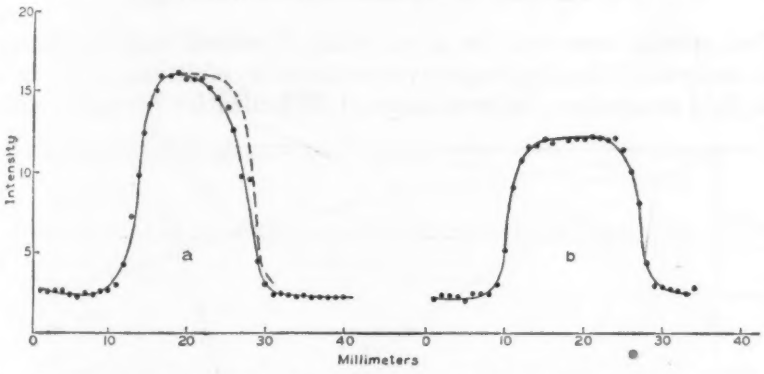

FIGURE 4.—*Distribution of intensity across the standard X-ray beam*

(The relative height of curves *a* and b has no significances.) Curve *a*, for displaced diaphragms; curve *b*, for properly aligned diaphragms.

is obeyed. It is to be seen that, of Curve *I*, the portion PR is parallel to *III*; while of Curve *II*, the portion PQ is parallel to *III*. Hence the experimental results bear out the conclusions that for distances within a certain range near the tube the inverse square law should be applied with the distance $(B+k)$; while over the range farther from the tube, the distance B is used instead.

It is thus clear that the assumption of neither a point source nor an extended source is valid under all conditions; hence, special care must be taken in any experimental set-up to decide which may be used.

3. UNIFORMITY OF X-RAY FLUX

To check if the flux obeyed the conditions assumed for deriving the equations of Section II, the uniformity of the flux over the cross section of the beam in the center of the ionization chamber was tested

by exposing photographic plates in this plane, the exposure being varied over wide limits of time. With a proper alignment of the diaphragm system, the distribution over the central area should be uniform. That this proved true is shown in Figure 4 (*b*) where the photographic density, obtained by measuring the resulting photographic plate with a Marten's photometer, is plotted against position across the beam. With the X-ray tube and first diaphragm displaced laterally about 0.5 cm. from the central position, a photographic plate exposed inside the ionization chamber, gave the distribution shown in Figure 4 (*a*)—the dotted line giving the expected density for a perfectly symmetrical beam. As expected, the densities were greater on the side toward which the source was shifted. The irregularity with which the observed curve fluctuates about the smooth curve can well be ascribed to the inhomogeneity of the photographic emulsion.

4. CHOICE OF OPERATING CONDITIONS

Two special cases may be given which illustrate how the geometrical analysis of the diaphragm system permits conditions to be chosen that yield an accurate determination of the ionization per unit volume.

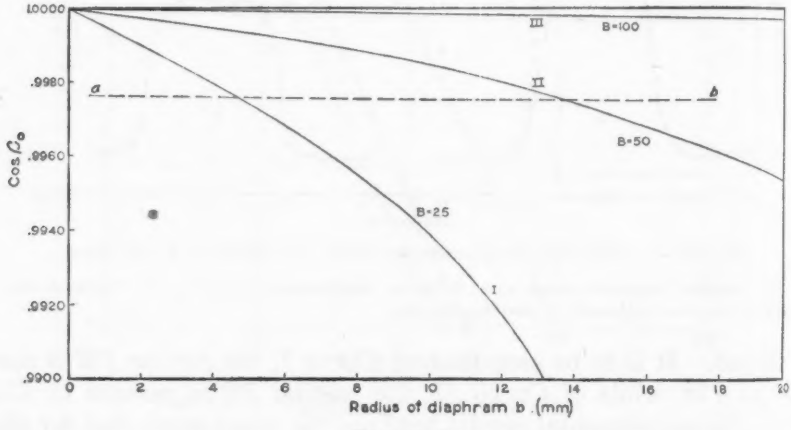

FIGURE 5

Letting β_0 be the maximum angle of divergence between the axis and the rays passing through the diaphragm system, then Curves I, II, and III (fig. 5) give the values of cos β_o plotted against the radial position in the ionization chamber for three cases where $B=25$, 50, and 100 cm, respectively, where $a=0.4$ cm. The values of cos β_o are obtained from the relation

$$\frac{\beta_o}{2}=\tan^{-1}\frac{a+b}{B}$$

from Figure 1 (*c*).

If we stipulate that $\cos^2 \beta_o=0.9950$ introduces the maximum permissible error—which means an error of less than 0.25 per cent in

r—it is seen that any physical conditions whereby $\cos \beta_o = 0.9975$ may be used. Thus the intersection of any curve in Figure 5 with the line $ab = 0.9975$, gives at once the upper limit within which our approximations would be valid. In Curve I for $B = 25$ cm it is seen that b must not exceed about 0.5 cm; in Curve II for $B = 50$ cm, b must not exceed 1.4 cm; while Curve III for $B = 100$ cm indicates that b may become extremely large before exceeding the given limit.

From equation (7) giving the radius of the focal spot necessary to fill the aperture, we may plot curves which indicate the diaphragms and distances which may be used and yet fulfill the condition that $f > (ka + kb + aB)/B$. If for instance, we have a focal spot

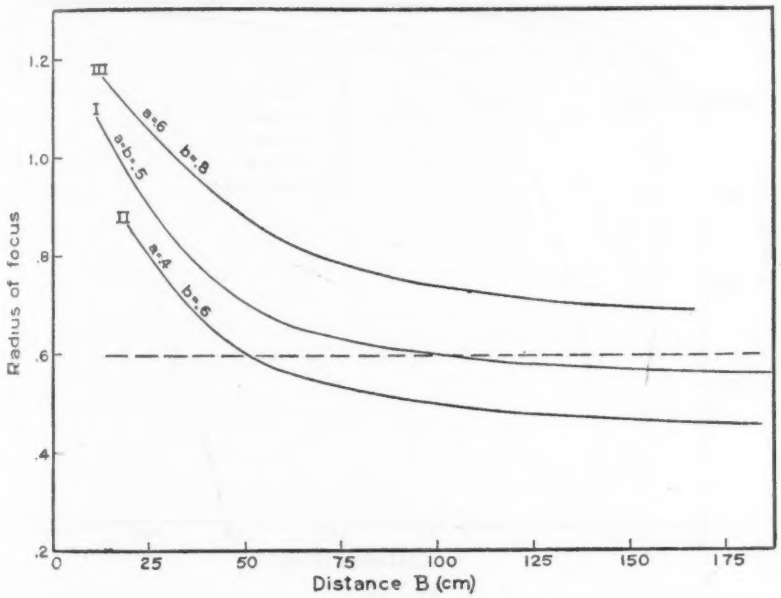

FIGURE 6

of radius 0.6 cm, any set of conditions composing the portion of the curve (fig. 6) below $f = 0.6$ may be used. Thus in Case I, where the diaphragms M and N have a radius of 0.5 cm each, the distance B must never be less than 100 cm. In Case II where $a = 0.4$ and $b = 0.6$ cm, B may be reduced to 50 cm; while for $a = 0.6$ and $b = 0.8$ cm no value of B whatever will suffice.

In the standardization equipments used by Behnken, Duane, and Glasser, each has a diaphragm corresponding to M. However, it is probable that their focal spots did not completely fill the aperture of the system, so that for the purpose of indicating the allowable deviation in each, we may consider the aperture as determined by the radii of the focal spot and diaphragm N and the distance $(B + k)$. We

may then compute cos β_o as a function of $(B+k)$ for different radii of the diaphragm N and so determine the range over which the allowable error in measuring the air volume is not exceeded. A set of these relations are plotted in Figure 7. All conditions falling on the curves above the line at cos $\beta_o = 0.9975$ may then be used without introducing more than the stipulated error.

Consider now three of the well-known X-ray standardization equipments:

I. Behnken.[15] (Physikalische Technischen-Reichsanstalt). $(B+k)$= 105 cm; the radius of the focal spot f and diaphragm N are about the same and equal to 0.35 cm making cos β_o fall between Curves *I*

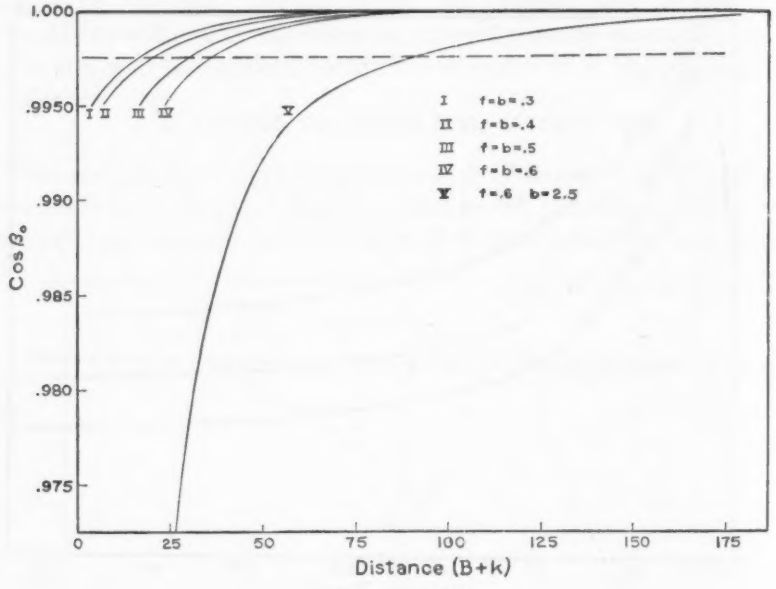

FIGURE 7

and *II* in Figure 7, thus indicating a very small error which may be neglected.

II. Glasser.[16] (Cleveland Clinic). $(B+k)=45$ cm and $f=b=0.4$ cm. The point fulfilling these conditions falls on Curve *II* well above cos $\beta_o = 0.9975$, also indicating a very small error.

In the two cases above, the focal spot may be slightly greater than indicated, but, even so, the maximum error will be less than 0.5 per cent.

III. Duane.[17] (Harvard University). This system has for N a rectangular diaphragm 0.5 by 5.0 cm, and $(B+k)$ is approximately

[15] H. Behnken, Strahlentherapie, **70**, p. 26; 1927.
[16] O. Glasser and U. V. Portmann, Am. J. Roent., **19**, p. 47; 1928.
[17] W. Duane and E. Lorenz, Am. J. Roent., **19**, p. 461; 1928.

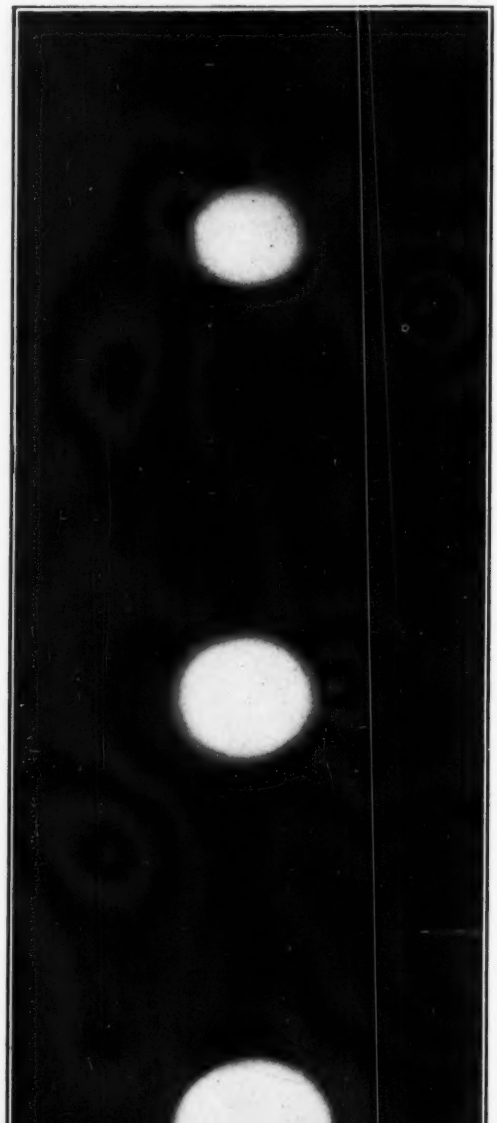

FIGURE 8.—*Pinhole photographs to indicate the magnitude of off-focus radiation*

60 cm. The energy distribution across the beam in the 0.5 cm direction will be uniform within the necessary limits. Along 5.0 cm direction, however, the variation in cos β_o with $(B+k)$ is shown in Curve *V*, whence it is seen that for $(B+k)=60$, the maximum error in $\cos^2 \beta_o$ is about 1.6 per cent and, therefore, can not be neglected. In order to reduce this error to within the prescribed limits, we must make $(B+k)=90$ cm.

IV. INFLUENCE OF "OFF-FOCUS" RADIATION

Off-focus radiation may be defined as that *radiation from an X-ray tube which originates from points on the target face other than the sharply defined focal spot.* If a diaphragm *M* be used which is sufficiently small, "off-focus radiation" does not enter. In this radiation lies another possible source of error in standardization measurements, and on account of the difficulty in accurately measuring its magnitude most observers have avoided a quantitative study of the question. Glasser [18] has indicated the importance of screening the ionization chamber diaphragm (*N*) from radiation coming from the stem and the body of the target other than the face. Likewise, Behnken,[19] Failla,[20] Duane [21] and most others have taken similar precautions, although in every case the method was entirely arbitrary.

A pinhole photograph of the target taken through the diaphragm system will indicate any source of off-focus radiation. Especial care, however, must be used in making such photographs, since an underexposed plate may apparently indicate a good focal spot and little off-focus radiation; an overexposure indicates general radiation from the whole face; whereas an exposure commensurate with the limiting error would give some indication of the actual off-focus radiation in proper proportion to the focal spot radiation. These three cases are shown, respectively, in Figures 8 (*a*), (*b*), and (*c*). While the amount of off-focus radiation will usually be but a small percentage of the focal spot radiation, it may at times be of too great a magnitude to be neglected.

To measure the off-focus radiation, the diaphragm *N* was fixed and the ionization chamber placed at a fixed distance from the tube such that the aperture of the diaphragm system did not introduce more than 0.5 per cent maximum deviation in the flux density across a plane within the chamber. Ionization current readings were made as the diaphragm *M* was varied from a diameter of 0.4 to 1.2 cm. The curve in Figure 9 shows the intensity (α to ionization current)

[18] See footnote 16, p. 820.
[19] See footnote 15, p. 820.
[20] See footnote 8, p. 808.
[21] See footnote 17, p. 820.

plotted against a^2 (α to area of M) for a 200 k. v. Coolidge tube having a focus of radius about 0.4 cm. It is seen that the intensity increases very rapidly up to a point P which corresponds to the condition where the sharply defined focus just fills the aperture, while beyond this point the ionization increases very slowly and somewhat irregularly. Nevertheless, a continual increase is evident and no saturation value of the X-ray flux was indicated over the range studied. It is thus seen that for this particular tube and diaphragm system, the magnitude of this off-focus radiation can not be neglected.

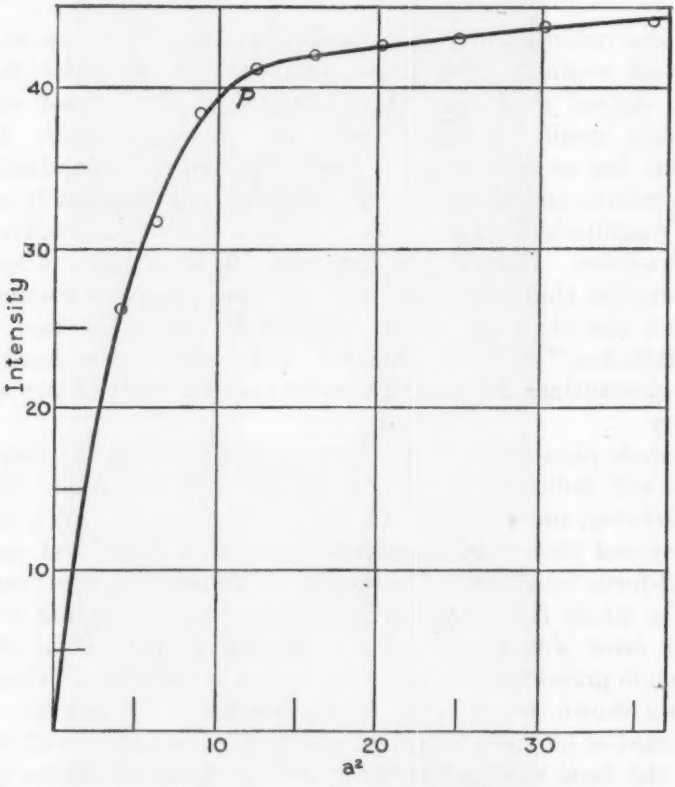

FIGURE 9.—*Measure of the proportion of off-focus radiation to focal spot radiation for a particular tube*

It is probable that if two observers were to use, respectively, diaphragms M of 0.9 and 1.5 cm diameter for such a tube that some correction would have to be applied to make their measured r units agree. Similar curves obtained for two other tubes showed differences in their respective off-focus radiation.

Referring to Curve *II* in Figure 5, showing the validity of the inverse-square law, we have seen that the upper portion PQ gave

the nearest approach to the proper slope of -2. However, there is a very slight but definite divergence which may probably be attributed to the off-focus radiation, since the quantity of this radiation entering the ionization chamber varies with the distance B. Over the lower part PR of Curve I the slope is exactly -2 indicating good agreement with the universe square law. (Equation (13).)

Behnken and Glasser have diaphragms M of 15 and 12.5 mm diameter, respectively, placed in each case about 15 cm from the target. Their X-ray tubes have focal spots of different size. It is therefore evident that both may have quite a different ratio of on-focus to off-focus energy, and thus introduce discrepancies between their r units. Again, Failla has no diaphragm close to his X-ray tube, but restricts his scattered radiation by a diaphragm some 30 cm away from the focus. He has given a detailed discussion [22] of the changes in ionization due to varying the size and positions of his diaphragms. These differences in experimental technique require that proper allowance be made for off-focus radiation or else it must be completely shielded from entering the ionization chamber, which may be accomplished by using a diaphragm system wherein the focus always fills the aperture.

V. ERRORS DUE TO ENERGY DISTRIBUTION ABOUT THE TARGET

In three cases noted above (Failla's, Behnken's, and Glasser's) the radiation is taken off the target face at an angle of 45°, and at 90° to the cathode stream. Duane's diaphragm system is similar to that of Behnken and Glasser, except in being rectangular. However, it is dissimilar in that the radiation is taken off the target at a small angle of some 10° to 15°, and, consequently, it is important to determine whether there is any possible error due to the uneven distribution of energy with angular direction about the focus.

The energy distribution about a massive target has been studied by Kaye,[23] Coolidge,[24] and others and is shown in Figure 10 for a 45° angle between cathode stream and normal to the target; the data being taken from the paper by Coolidge and Kearsley and replotted on polar instead of rectangular coordinates. Figure 11 likewise shows the energy distribution about the focus in a plane perpendicular to the cathode stream. It is seen from the curves in Figure 10 that the distribution is nearly uniform in the direction used by Behnken, Glasser, and the Bureau of Standards. This is the direction in which radiation is usually taken in practice. At glancing angles to the

[22] See footnote 8, p. 808.

[23] G. W. C. Kaye, Proc. Roy. Soc. (London), **83**, p. 189; 1910. Kaye found that as the angle between normal and cathode stream changed the distribution about the normal did not vary very much.

[24] W. D. Coolidge and W. K. Kearsley, Am. J. Roent., **9**, p. 77; 1922.

target, however, the change in distribution is very rapid, so that the flux density across a plane x as considered in Section II should decrease appreciably in passing from one side of the beam to the other.

In Duane's case, where long rectangular slits are used, we should expect, therefore, an appreciable change in the flux density across the beam. Of course, if the diaphragms are sufficiently small such a change would be very small and could be neglected. A photographic determination of this effect was easily obtained. A rec-

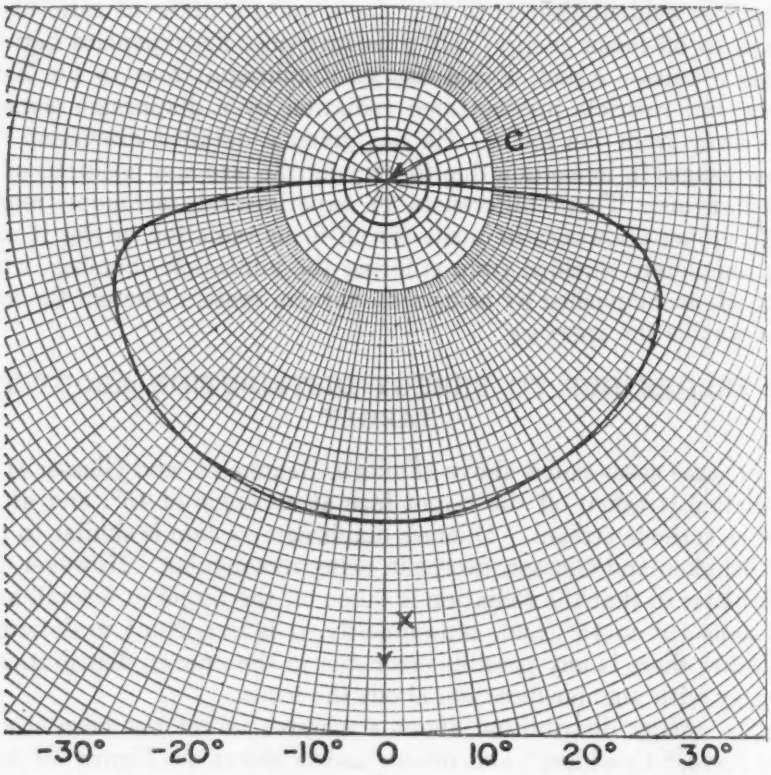

FIGURE 10.—*Distribution of energy about 200 k. v. deep therapy X-ray tube target in a plane normal to the tube axis*

tangular diaphragm system was set up and carefully aligned so as to correspond to that used by Duane, the tube tilted to an angle of about 35° and rotated about +70° to 75° from its normal position, and the cross section of the beam photographed behind the second diaphragm. The resulting plate densities are indicated in Figure 12, curve *a* being taken lengthwise of the rectangular diaphragm, and curve *b* crosswise. As should be expected, the lower part of the field is more intense than the upper and likewise the right side more intense than the left. These inequalities were obtained likewise in

the opposite direction when the tube was rotated through −70° to 75°.

The variation in flux density here considered is entirely independent of that due to the cosine law; it is, however, possible that the two may be present at the same time. In an accurate comparison of the r unit between two laboratories care must be taken that such errors are small enough to be neglected. An ideal standardization

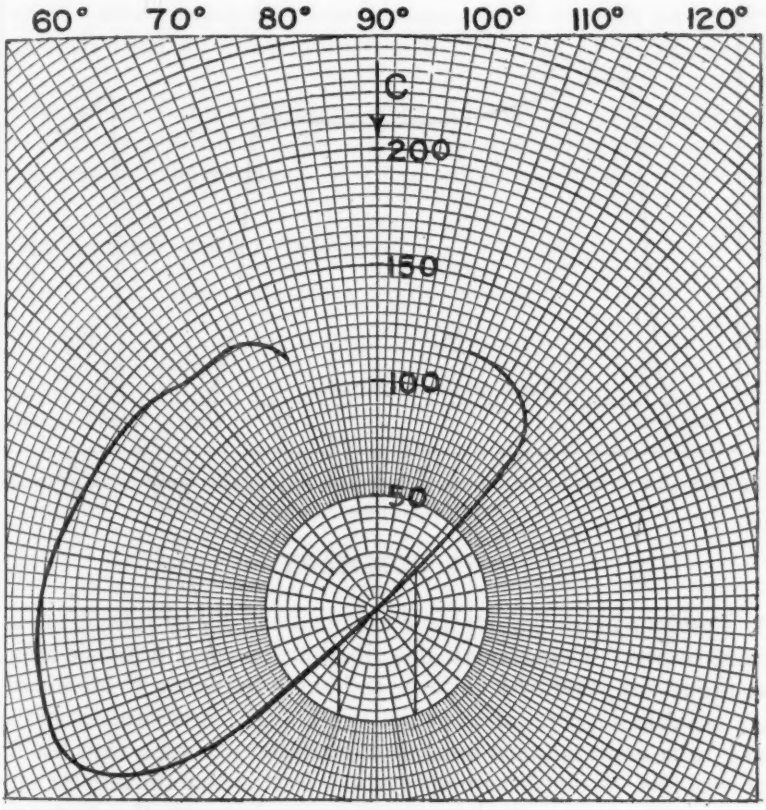

FIGURE 11.—*Distribution of energy about target in a plane through the tube axis and the normal to the target face*

equipment would have the X-ray tube so constructed that the radiation is taken normally from the target.

In the author's first paper,[25] a careful study was made of the several methods used in measuring air ionization with particular reference to the accuracy of each method. As a consequence of the differences found, an improved method was tested and found to be satisfactory. In the present paper, the methods for obtaining the

[25] L. S. Taylor, B. S. Jour. Research, **2**, p. 771; 1929.

effective volume of air ionized, have been analyzed; the results being summarized below. The next logical problem is that of analyzing the methods used in the comparison of the r unit between the different laboratories having a standard ionization chamber. This problem is being undertaken at present at the Bureau of Standards.

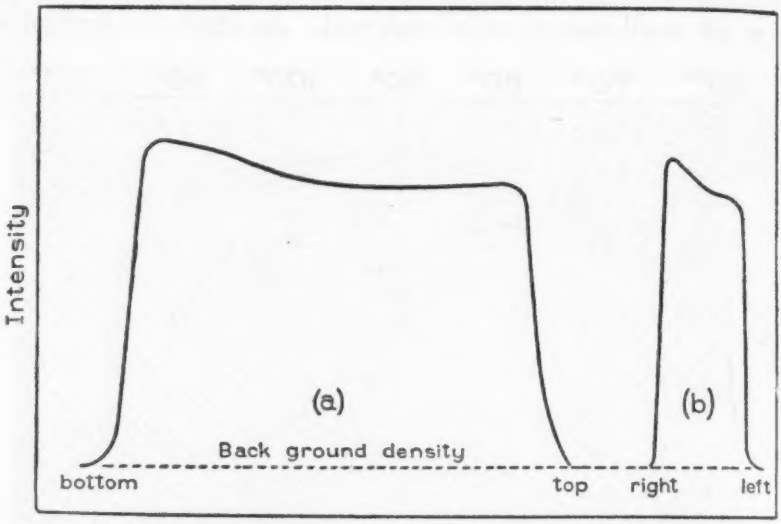

FIGURE 12.—*Distribution of energy across a rectangular beam taken from the target at a glancing angle*

VI. SUMMARY

1. Previous investigators have assumed the X-ray tube focus to be a point source. Experiments described in the present article indicate that the assumption of a uniform and extended focus yields instead a more reliable determination of the r unit when the distances between X-ray tube and standard ionization chamber are such that the focal spot area fills the diaphragm aperture. In this case the inverse square law is valid when applied to the distance between the X-ray tube diaphragm and the entrant diaphragm of the ionization chamber.

When the X-ray tube diaphragm is not filled the inverse square law should be used with the distance between the target and the entrant diaphragm of the ionization chamber. Off-focus radiation may impair, however, the accuracy of the results in this case.

2. The use of a limiting diaphragm close to the X-ray tube may introduce an error in the measurement of the ionization in the effective volume, this being due to the off-focus radiation entering the chamber. Such error may introduce discrepancies between the r unit as established in various laboratories.

3. By having incorrect alignment of the diaphragm system serious error may be introduced in measuring the effective volume.

4. Due to nonuniform energy distribution about the target, the use of narrow rectangular diaphragms is inadvisable except under carefully determined conditions.

5. Using diaphragms of the same size, but having edges beveled at different angles introduces no measurable difference in the ionization.

6. The discrepancy in measurements of the air volume under the conditions used by other observers is shown to lie within expected error.

Discussion of these problems with the various investigators cited has been very helpful. Recognition is due G. Singer and C. G. Malmberg, of the bureau, for their assistance in the experimental work.

WASHINGTON, April 1, 1929.